

**FUNCTIONAL CHARACTERIZATION OF  
 $\beta$ -GLUCOSIDASES AND  $\beta$ -GLUCAN  
EXOXYDROLASE FROM RICE AND BARLEY**

**Sukanya Luang**

**A Thesis Submitted in Partial Fulfillment of the Requirements for the  
Degree of Doctor of Philosophy in Biochemistry  
Suranaree University of Technology  
Academic Year 2010**

การทำงานของเอนไซม์บีตากลูโคซิเดสและบีตากลูแคนเอกโซไฮโดรเลสจาก  
ข้าวและบาเลย์

นางสาวสุกัญญา เลือง

วิทยานิพนธ์นี้เป็นส่วนหนึ่งของการศึกษาตามหลักสูตรปริญญาวิทยาศาสตรดุษฎีบัณฑิต  
สาขาวิชาชีวเคมี  
มหาวิทยาลัยเทคโนโลยีสุรนารี  
ปีการศึกษา 2553

สำคัญงาน เลื่อง : การทำงานของเอนไซม์บีตาไกลูโคซิเดสและบีตาไกลูแคนเอกโซไฮโดรเลสจากข้าว และบาร์เลย์ (FUNCTIONAL CHARACTERIZATION OF  $\beta$ -GLUCOSIDASES AND  $\beta$ -GLUCAN EXOHYDROLASE FROM RICE AND BARLEY) อาจารย์ที่ปรึกษา : รองศาสตราจารย์ ดร.เจมส์ เกตุทัต-คาร์นส์, 183 หน้า.

พบความหลากหลายต่อความจำเพาะในการย่อยสับสเตรตของเอนไซม์บีตาไกลูโคซิเดสตระกูล Glycoside hydrolase family 1 (GH1) ในข้าวจากการพิสูจน์ด้วยการผลิตเอนไซม์สายผสม Os7BGlu26 และ Os9BGlu31 และการแสดงลักษณะเฉพาะของเอนไซม์ทั้งสองชนิดนี้ Os7BGlu26 เป็นเอนไซม์บีตาไกลูโคซิเดส/แมนโนซิเดสที่มีลำดับกรดอะมิโนและความจำเพาะต่อการย่อยสับสเตรตคล้ายกับเอนไซม์บีตาไกลูโคซิเดส rHvBII ของข้าวบาร์เลย์ คือมีประสิทธิภาพในการย่อยสลาย 4-nitrophenyl- $\beta$ -D-mannopyranoside ดีกว่าการย่อยสลาย 4-nitrophenyl- $\beta$ -D-glucopyranoside (4NPGlc) และสามารถย่อยสลาย  $\beta$ -(1,4)-manno-oligosaccharides ได้ แต่แตกต่างจาก rHvBII ตรงที่ Os7BGlu26 ย่อยสลาย cellobiose ได้ไม่ดีซึ่งไปคล้ายกับสมบัติของเอนไซม์บีตาไกลูโคซิเดส Os3BGlu7 ของข้าว ส่วนเอนไซม์ Os9BGlu31 ที่ถึงแม้มีลำดับกรดอะมิโนคล้ายคลึงกับเอนไซม์ hydroxyisourate hydrolase (HIUHase) ซึ่งประกอบไปด้วยช่วงลำดับของกรดอะมิโน TVNEP และ IHENG ที่อยู่รอบ ๆ catalytic acid/base และ nucleophile เหมือนกัน แต่ Os9BGlu31 ไม่สามารถย่อยสลายสับสเตรตของ HIUHase ได้ Os9BGlu31 ย่อยสลาย 4NPGlc ได้ช้า ( $k_{cat}/K_M$  เท่ากับ  $0.02 \pm 0.001 \text{ mM}^{-1} \cdot \text{s}^{-1}$ ) และสามารถย่อยสลาย dhurrin ซึ่งเป็น cyanogenic glucoside ได้เร็วกว่าการย่อยสลาย 4NPGlc 10 เท่า glucono  $\delta$ -lactone และ 2,4-dinitrophenyl- $\beta$ -D-2-deoxy-2-fluoro-glucopyranoside ไม่สามารถยับยั้งการทำงานของ Os9BGlu31 ได้ ซึ่งแตกต่างจากเอนไซม์บีตาไกลูโคซิเดสโดยทั่วไป จากการศึกษาการทำงานของ Os7BGlu26 และ Os9BGlu31 แสดงให้เห็นว่าความคล้ายคลึงของลำดับกรดอะมิโนอาจนำมาใช้คาดเดาความจำเพาะต่อการย่อยสับสเตรตของเอนไซม์ที่ไม่ทราบการทำงานได้บ้าง แต่เอนไซม์ที่แม้จะอยู่ในตระกูล GH1 เหมือนกันอาจมีการทำงานที่แตกต่างกันอย่างสิ้นเชิง

ในทางตรงกันข้ามกลับพบว่าเอนไซม์บีตาไกลูแคนเอกโซไฮโดรเลสไฮโอเอนไซม์ที่หนึ่ง (HvExoI) ในตระกูล Glycoside hydrolase family 3 (GH3) ของข้าวบาร์เลย์สามารถย่อยสลายสับสเตรตของ  $\beta$ -linked gluco-oligosaccharides ได้เช่นเดียวกับเอนไซม์ Os7BGlu26 และเอนไซม์บีตาไกลูโคซิเดสใน GH1 อื่น ๆ ได้ผลิตเอนไซม์สายผสม HvExoI (rHvExoI) ใน *Pichia pastoris* ให้ได้โปรตีนที่แตกต่างจาก HvExoI ดั้งเดิม โดยมีกรดอะมิโนเพิ่มขึ้นมา 11 ตัว (AHHHHHHHAA) เชื่อมต่อที่

ปลายอะมิโนของสายโปรตีนและชนิดของน้ำตาลที่ต่อกับแอสพาราจีน 3 ตำแหน่ง (Asn221 Asn498 และ Asn600) rHvExoI มีความจำเพาะต่อการย่อยสับสเตรตได้หลากหลายและสามารถย่อยสลาย (1,2)- (1,3)- (1,4)- และ (1,6)- $\beta$ -linked gluco-oligosaccharides และพอลิแซคคาไรด์ laminarin และ barley (1,3;1,4)- $\beta$ -D-glucan ของบาร์เลย์ได้เหมือนกับ HvExoI ดั้งเดิม ยิ่งไปกว่านั้น โครงสร้างสามมิติของ rHvExoI น่าจะเหมือนกันอีกด้วย เนื่องจากผลึกของ rHvExoI สามารถกำเนิดจากผลึกขนาดเล็กของ HvExoI ดั้งเดิมในสารละลายที่ใช้ในการตกผลึกของ HvExoI และในสารละลายที่มีความเข้มข้นของเกลือแอมโมเนียม ซัลเฟต 1.8 M หรือ 2.2 M ใน malate-MES-Tris, pH 5.0 โดยปราศจากผลึกของ HvExoI

กรดอะมิโนที่พบว่ามีความสำคัญในตำแหน่งเร่งปฏิกิริยาในโครงสร้างของ HvExoI ได้ถูกเปลี่ยนเป็นกรดอะมิโนชนิดอื่นใน rHvExoI ดังนี้ D95A D95N R158A E161A E161Q K206V E220A E220Q D285A D285N W286A W434A E491A E491Q และ R158A/E161A ถึงแม้เอนไซม์กลายพันธุ์ส่วนใหญ่จะสูญเสียการทำงาน แต่การเปลี่ยนกรดอะมิโน W434 ด้วยอะลานีนทำให้เอนไซม์สูญเสียความสามารถในการย่อยสลาย  $\beta$ -(1,2)  $\beta$ -(1,4) และ  $\beta$ -(1,6)-oligosaccharides การแทนที่กรดอะมิโน E220 เป็นอะลานีนทำให้อัตราเร็วในการย่อยสลายสับสเตรตและค่า  $k_{cat}$  ลดลงโดยเฉพาะต่อ cellobiose และ 4NPGlc และยังทำให้ค่า  $K_i$  ต่อ glucono  $\delta$ -lactone เพิ่มขึ้น เอนไซม์กลายพันธุ์ทั้งสองชนิดได้สูญเสียความสามารถในการย่อยสลายพอลิแซคคาไรด์ จากการศึกษาเหล่านี้ยืนยันความสำคัญของ catalytic nucleophile D285 catalytic acid/base E491 และกรดอะมิโนที่อยู่รอบ ๆ และ W434 ที่อยู่ +1 subsite มีความสำคัญต่อการเร่งปฏิกิริยาและความจำเพาะในการย่อยสับสเตรตของเอนไซม์ rHvExoI

สาขาวิชาชีวเคมี

ปีการศึกษา 2553

ลายมือชื่อนักศึกษา \_\_\_\_\_

ลายมือชื่ออาจารย์ที่ปรึกษา \_\_\_\_\_

ลายมือชื่ออาจารย์ที่ปรึกษาร่วม \_\_\_\_\_

SUKANYA LUANG : FUNCTIONAL CHARACTERIZATION OF  
β-GLUCOSIDASES AND β-GLUCAN EXOHYDROLASE FROM RICE AND  
BARLEY. THESIS ADVISOR : ASSOC. PROF. JAMES R. KETUDAT-CAIRNS,  
Ph.D. 183 PP.

β-GLUCOSIASE/β-MANNOSIDASE/BARLEY β-GLUCAN EXOHYDROLASE/  
SUBSTRATE SPECIFICITY/MUTAGENESIS

Diverse substrate specificity has been found in rice glycoside hydrolase family 1 (GH1) β-glucosidases, as demonstrated by the recombinant expression and characterization of two GH1 enzymes, Os7BGlu26 and Os9BGlu31. Os7BGlu26 is a β-glucosidase/β-mannosidase that shares amino acid sequence and substrate specificity similarity with barley rHvBII, in terms of hydrolysing 4-nitrophenyl-β-D-mannopyranoside more efficiently than 4-nitrophenyl-β-D-glucopyranoside (4NPGlc) and hydrolysing β-(1,4)-manno-oligosaccharides. However, unlike HvBII, Os7BGlu26 hydrolyses cellobiose poorly, similar to rice Os3BGlu7 β-glucosidase. In contrast, despite sequence similarity to hydroxyisourate hydrolase (HIUHase) and having the same TVNEP and IHENG sequences around the catalytic acid/base and nucleophile, respectively, rice Os9BGlu31 β-glucosidase has no HIUHase activity. Os9BGlu31 hydrolyses 4NPGlc slowly ( $k_{cat}/K_M$  of  $0.02 \pm 0.001 \text{ mM}^{-1} \cdot \text{s}^{-1}$ ) and the cyanogenic glucoside dhurrin with 10-fold higher relative activity than 4NPGlc. The activity of Os9BGlu31 was not inhibited by glucono δ-lactone and 2,4-dinitrophenyl-β-D-2-deoxy-2-fluoro-glucopyranoside, unlike most other β-glucosidases. Based on these observations of the GH1 β-glucosidases Os7BGlu26 and Os9BGlu31, sequence similarity can sometimes be used to predict the substrate specificity of unknown proteins, but sometimes similar GH1 enzymes have completely different activities.

On the other hand, it was found that the GH3 barley β-D-glucan exohydrolase I

(HvExoI) acts similar to Os7BGlu26 and similar GH1  $\beta$ -glucosidases in terms of its hydrolysis of  $\beta$ -linked gluco-oligosaccharides. Recombinant HvExoI (rHvExoI), was expressed in *Pichia pastoris*, to produce a protein different from native HvExoI in the presence of an extra 11 residues (AHHHHHHHHAA) at the N-terminus and in the type of sugar attached at the three N-glycosylation sites of native HvExoI (Asn221, Asn498 and Asn600). The rHvExoI exhibited broad substrate specificity and was able to hydrolyse (1,2)-, (1,3)-, (1,4)-, and (1,6)- $\beta$ -linked gluco-oligosaccharides, and the polysaccharides laminarin, and barley (1,3;1,4)- $\beta$ -D-glucan, similar to native HvExoI. Moreover, the structure of rHvExoI is likely to also be nearly identical, since tetragonal crystals of rHvExoI grew in the same conditions used for crystallisation of native HvExoI by macroseeding with native crystal seeds and in the conditions of 1.8 M and 2.2 M ammonium sulfate in malate-MES-Tris buffer, pH 5.0, without seeds.

Amino acid residues that appeared to be essential to the active site, based on the HvExoI structure, were mutated in rHvExoI as follows: D95A, D95N, R158A, E161A, E161Q, K206V, E220A, E220Q, D285A, D285N, W286A, W434A, E491A, E491Q and R158A/E161A. Although most of these mutations resulted in lack of detectable activity, the substitution of W434 by alanine led to an active enzyme that lost its ability to hydrolyse  $\beta$ -(1,2),  $\beta$ -(1,4), and  $\beta$ -(1,6)-oligosaccharides. Another mutation, E220A, decreased the hydrolytic rate and the  $k_{cat}$  values, especially for cellobiose and 4NPGlc, and increased the  $K_i$  constant value of glucono  $\delta$ -lactone. Both mutants lost the ability to hydrolyse polysaccharides. These studies confirm the importance of the catalytic nucleophile, D285, the catalytic acid-base, E491, and the surrounding amino acids and suggest that W434, which helps form the +1 subsite of rHvExoI is critical to substrate specificity.

School of Biochemistry

Student's signature \_\_\_\_\_

Academic Year 2010

Advisor's signature \_\_\_\_\_

Co-advisor's signature \_\_\_\_\_

## **ACKNOWLEDGEMENTS**

I would like to express my deepest gratitude to my advisor, Assoc. Prof. Dr. James R. Ketudat-Cairns for kind supervision, valuable advice, unconditional support, and providing me the opportunity to study toward my Ph.D. degree in Biochemistry. I am deeply grateful to my co-advisor, Asst. Prof. Dr. Rodjana Opassiri for advice in the first academic year and teaching me molecular cloning and biochemical techniques. I would like to express my deepest gratitude to Assoc. Prof. Dr. Maria Hrmova for her warm encouragement and thoughtful guidance for experiments during my lab work at the University of Adelaide, Australia. I am very grateful to Assoc. Prof. Wipa Suginta for teaching me one of the most challenging subjects, Enzymology. I am also grateful to Prof. Dr. Peter A. Tipton to help testing for HIHUase activity assay. I am equally grateful to all my committee for their constructive comments on my thesis. Special thanks are extended to all friends for their help in the Biochemistry Lab.

The Thailand Research Fund (TRF) is thanked for providing the Royal Golden Jubilee Ph.D. Scholarship for my study in Suranaree University of Technology.

Finally, my graduation would not be achieved without my family's love, understanding and encouragement, which was the best I could wish for.

Sukanya Luang

# CONTENT

|  | <b>Page</b> |
|--|-------------|
| ABSTRACT IN THAI .....   | I           |
| ABSTRACT IN ENGLISH.....   | III         |
| ACKNOWLEDGEMENT .....  | V           |
| CONTENTS .....   | VI          |
| LIST OF TABLES .....   | XIV         |
| LIST OF FIGURES.....   | XVI         |
| LIST OF ABBREVIATIONS .....  | XXI         |
| <b>CHAPTER</b>   |             |
| <b>I INTRODUCTION.....</b>   | <b>1</b>    |
| 1.1 Glycoside hydrolases .....   | 1           |
| 1.1.1 Glycoside hydrolase mechanism.....   | 2           |
| 1.1.1.1 Retaining glycosidases .....   | 2           |
| 1.1.1.2 Inverting glycosidases .....   | 3           |
| 1.1.2 Substrate distortion during the enzymatic hydrolysis of glycosides .....                   | 4           |
| 1.2 $\beta$ -D-Glucosidases in glycosyl hydrolase family 1 .....                                 | 6           |
| 1.2.1 $\beta$ -D-Mannosidases and $\beta$ -D-glucosidases in family 1.....                       | 8           |
| 1.3 $\beta$ -Glucan exohydrolases and $\beta$ -glucosidases in glycoside hydrolase family 3..... | 9           |
| 1.3.1 Broad substrate specificity of barley $\beta$ -D-glucan exohydrolase I.....                | 11          |
| 1.3.2 Catalytic mechanism of barley $\beta$ -D-glucan exohydrolase I.....                        | 14          |
| 1.4 Significance of study .....  | 16          |
| 1.5 Research objectives .....  | 17          |

## CONTENTS (Continued)

|  | <b>Page</b> |
|--|-------------|
| 1.6 References .....   | 17          |
| <br><b>II COMPLIMENTARY DNA CLONING, PROTEIN EXPRESSION</b>  |             |
| <b>AND CHARACTERIZATION OF RICE Os7BGlu26 <math>\beta</math>-GLUCOSIDASE.....</b>  | <b>24</b>   |
| Abstract .....   | 24          |
| 2.1 Introduction .....   | 25          |
| 2.2 Materials and methods.....   | 30          |
| 2.2.1 Plasmids, bacterial strains and plant .....  | 30          |
| 2.2.2 General methods .....  | 31          |
| 2.2.2.1 Preparation of competent <i>Escherichia coli</i> Strain DH5 $\alpha$<br>and Origami(DE3) and DNA transformation..... | 31          |
| 2.2.2.2 Isolation of recombinant plasmid by alkaline lysis.....  | 32          |
| 2.2.2.2 Protein analysis by sodium dodecyl sulfate polyacrylamide<br>gel electrophoresis (SDS-PAGE).....                     | 32          |
| 2.2.3 Molecular cloning, expression, purification and characterization<br>of rice $\beta$ -glucosidase Os7BGlu26 .....       | 33          |
| 2.2.3.1 RNA isolation .....  | 33          |
| 2.2.3.2 cDNA synthesis by reverse transcriptase.....   | 34          |
| 2.2.3.3 DNA cloning of mature Os7BGlu26 .....  | 35          |
| 2.2.3.4 Expression of Os7BGlu26 .....  | 36          |
| 2.2.3.5 Purification of Os7BGlu26 .....  | 37          |
| 2.2.3.6 Determination of the optimal pH and temperature for<br>Os7BGlu26 .....   | 38          |

## CONTENTS (Continued)

|   | <b>Page</b> |
|---|-------------|
| 2.2.3.7 Substrate specificity of Os7BGlu26.....                               | 38          |
| 2.2.3.8 Kinetic parameter determination of Os7BGlu26 .....                    | 39          |
| 2.3 Results .....   | 39          |
| 2.3.1 Cloning and expression of Os7BGlu26 $\beta$ -glucosidase .....          | 39          |
| 2.3.2 Purification of Os7BGlu26 $\beta$ -glucosidase .....                    | 46          |
| 2.3.3 Characterization of Os7BGlu26 $\beta$ -glucosidase.....                 | 50          |
| 2.3.3.1 Optimum pH and temperature profile of Os7BGlu26 .....                 | 50          |
| 2.3.3.2 Substrate specificity of Os7BGlu26.....                               | 52          |
| 2.3.3.3 Kinetic parameters of Os7BGlu26.....                                  | 52          |
| 2.4 Discussion.....   | 59          |
| 2.4.1 Sequence analysis of Os7BGlu26.....                                     | 59          |
| 2.4.2 Protein purification of Os7BGlu26.....                                  | 59          |
| 2.4.3 Characterization of Os7BGlu26.....                                      | 60          |
| 2.5 Conclusions .....   | 61          |
| 2.6 References .....  | 62          |
| <b>III RECOMBINANT PROTEIN EXPRESSION AND</b>                                 |             |
| <b>CHARACTERIZATION OF RICE Os9BGlu31 <math>\beta</math>-GLUCOSIDASE.....</b> | <b>64</b>   |
| Abstract.....   | 64          |
| 3.1 Introduction .....  | 65          |
| 3.2 Materials and methods.....  | 67          |
| 3.2.1 Plasmids and bacterial strains .....                                    | 67          |
| 3.2.2 Molecular cloning and expression .....                                  | 67          |
| 3.2.2.1 Cloning of DNA encoding mature Os9BGlu31 .....                        | 67          |

## CONTENTS (Continued)

|  | <b>Page</b> |
|--|-------------|
| 3.2.2.2 The protein expression of Os9BGlu31 .....                                  | 67          |
| 3.2.2.3 The purification of Os9BGlu31 .....  | 68          |
| 3.2.2.4 Enzymatic characterization of Os9BGlu31 .....                              | 68          |
| 3.3 Results .....  | 69          |
| 3.3.1 Cloning and expression of Os9BGlu31 .....                                    | 69          |
| 3.3.2 Purification of Os9BGlu31 .....  | 73          |
| 3.3.3 Characterization of Os9BGlu31 .....  | 76          |
| 3.3.3.1 Optimum pH and temperature profile of Os9BGlu31 .....                      | 76          |
| 3.3.3.2 Substrate specificity and kinetic parameters<br>of Os9BGlu31 .....         | 78          |
| 3.3.3.3 Effects of EDTA, metal salts and inhibitors<br>on Os9BGlu31 activity ..... | 81          |
| 3.4 Discussion.....  | 82          |
| 3.5 Conclusions .....  | 85          |
| 3.6 References .....   | 85          |
| <br><b>IV DNA CLONING, PROTEIN EXPRESSION AND</b>                                  |             |
| <br><b>CHARACTERIZATION OF RECOMBINANT BARLEY GLUCAN</b>                           |             |
| <b>GLUCOHYDROLASE ISOENZYME I.....</b>   | <b>88</b>   |
| Abstract.....  | 88          |
| 4.1 Introduction .....   | 89          |
| 4.2 Materials and methods.....   | 92          |
| 4.2.1 Plasmids, bacterial and yeast strains .....                                  | 92          |

## CONTENTS (Continued)

|   | Page |
|---|------|
| 4.2.2 Molecular cloning, expression, purification<br>and characterization of barley exohydrolase I (HvExoI) ..... | 92   |
| 4.2.2.1 DNA cloning of native HvExoI cDNA from barley seedlings .....   | 92   |
| 4.2.2.2 DNA subcloning of the optimized HvExoI cDNA .....   | 93   |
| 4.2.2.3 Recombinant protein expression in <i>E. coli</i> .....  | 95   |
| 4.2.2.4 Protein refolding by iFOLD protein refolding system 2 kit.....  | 95   |
| 4.2.2.5 Protein refolding of rHvExoI by dialysis.....   | 96   |
| 4.2.2.6 Preparation of competent <i>Pichia pastoris</i> strains Y11430 and<br>SMD1168H.....                       | 97   |
| 4.2.2.7 DNA preparation for electroporation.....  | 97   |
| 4.2.2.8 Expression of recombinant HvExoI in <i>P. pastoris</i> .....  | 98   |
| 4.2.2.9 Purification of recombinant HvExoI.....   | 99   |
| 4.2.2.10 Determination of the optimal pH and thermostability<br>for recombinant HvExoI .....                      | 100  |
| 4.2.2.11 Substrate specificity of recombinant HvExoI .....  | 100  |
| 4.2.2.12 Determination of glucosyltransferase activity of rHvExoI.....  | 101  |
| 4.2.2.13 Determination of kinetic parameters and inhibition .....   | 102  |
| 4.2.2.14 Immunoblot analysis .....  | 102  |
| 4.2.2.15 Tryptic mapping of rHvExoI by MALDI-ToF/ToF<br>spectrometry.....   | 103  |
| 4.2.2.16 Molecular mass determination of rHvExoI via<br>MALDI spectrometry .....                                  | 104  |
| 4.3 Results.....  | 105  |

## CONTENTS (Continued)

|  | <b>Page</b> |
|--|-------------|
| 4.3.1 Expression of HvExoI.....  | .105        |
| 4.3.2 Protein purification and tryptic mapping of optimized rHvExoI.....                             | .112        |
| 4.3.3 Characterization of wild type rHvExoI.....   | .118        |
| 4.3.3.1 Effect of pH and temperature on rHvExoI enzyme activity .....                                | .118        |
| 4.3.3.2 Substrate specificity of rHvExoI.....  | .121        |
| 4.3.3.3 Kinetic parameters of rHvExoI.....   | .123        |
| 4.3.3.4 Transglycosylation products of rHvExoI.....  | .125        |
| 4.3.3.5 Inhibition of rHvExoI.....   | .128        |
| 4.4 Discussion.....  | .129        |
| 4.4.1 Sequence analysis of normal and optimized rHvExoI.....   | .129        |
| 4.4.2 Development of an expression system for active rHvExoI .....                                   | .131        |
| 4.4.3 Catalytic properties of rHvExoI.....   | .132        |
| 4.5 Conclusions .....  | .134        |
| 4.6 References .....   | .135        |
| <b>V STRUCTURE-FUNCTION STUDIES OF RECOMBINANT</b>   |             |
| <b>BARLEY <math>\beta</math>-D-GLUCAN HYDROLASE I .....</b>  | <b>.141</b> |
| Abstract.....  | .141        |
| 5.1 Introduction .....   | .142        |
| 5.2 Materials and methods .....  | .143        |
| 5.2.1 Plasmids and bacterial strains .....   | .143        |
| 5.2.2 Mutation of the optimized HvExoI cDNA by the QuikChange®<br>Site-Directed Mutagenesis Kit..... | .143        |
| 5.2.3 Protein expression and purification of rHvExoI mutants .....                                   | .146        |

## CONTENTS (Continued)

|  | <b>Page</b> |
|--|-------------|
| 5.2.4 Protein characterization of rHvExoI mutants.....   | .146        |
| 5.3 Results .....  | .147        |
| 5.3.1 Protein expression and purification of mutants .....   | .147        |
| 5.3.2 Effect of pH and temperature on rHvExoI mutant enzyme activities.....                                      | .150        |
| 5.3.3 Substrate specificity and kinetic analysis of mutant rHvExoI enzymes<br>compared to wild type rHvExoI..... | .153        |
| 5.3.4 Inhibition of rHvExoI mutants by inhibitors<br>of wild type rHvExoI .....                                  | .156        |
| 5.4 Discussion.....  | .158        |
| 5.5 Conclusions .....  | .163        |
| 5.6 References .....   | .164        |
| <br><b>VI CRYSTALLISATION OF RECOMBINANT</b>   |             |
| <b>BARLEY <math>\beta</math>-D-GLUCAN EXOHYDROLASE I.....</b>  | <b>.166</b> |
| Abstract.....  | .166        |
| 6.1 Introduction .....   | .167        |
| 6.2 Materials and methods.....   | .168        |
| 6.2.1 Plasmid and yeast strains .....  | .168        |
| 6.2.2 Expression and purification of wild type rHvExoI and<br>rHvExoI E220A, W434A and R158A/E161A mutants ..... | .168        |
| 6.2.3 Preliminary protein crystallisation of wild type rHvExoI .....   | .169        |
| 6.2.3.1 Protein solution preparation.....  | .169        |

## CONTENTS (Continued)

|  | <b>Page</b> |
|--|-------------|
| 6.2.3.2 Initial screening of wild type rHvExoI for crystallization conditions by microbatch and sitting-drop vapour-diffusion techniques ..... | .169        |
| 6.2.3.3 rHvExoI crystallisation by macroseeding with native HvExoI seed .....  | .170        |
| 6.3 Results .....  | .171        |
| 6.3.1 Protein purification of rHvExoI .....  | .171        |
| 6.3.2 rHvExoI crystallisation .....  | .172        |
| 6.3.2.1 Initial screening for crystallisation of rHvExoI by microbatch and sitting-drop vapour-diffusion techniques .....                      | .172        |
| 6.3.2.2 Crystallisation of wild type rHvExoI by macroseeding with native HvExoI .....  | .175        |
| 6.4 Discussion.....  | .176        |
| 6.5 Conclusions .....  | .177        |
| 6.6 References .....   | .177        |
| <b>VII CONCLUSION</b> .....  | <b>.180</b> |
| 7.1 Rice $\beta$ -glucosidases .....   | .180        |
| 7.2 Barley $\beta$ -D-glucan exohydrolase I .....  | .181        |
| <b>CURRICULUM VITAE</b> .....  | <b>.183</b> |

## LIST OF TABLES

| <b>Table</b>  | <b>Page</b> |
|---|-------------|
| 2.1 Recombinant plasmids used for Os7BGlu26 cloning and expression.....   | 30          |
| 2.2 Bacterial strains.....  | 30          |
| 2.3 Primers for Os7BGlu26 amplification.....  | 35          |
| 2.4 Cycling parameters for Os7BGlu26 amplification.....   | 35          |
| 2.5 Comparison of the relative activities of Os7BGlu26, rHvBII and Os3BGlu7 on<br>aryl glycosides and oligosaccharides.....                             | 53          |
| 2.6 Hydrolysis of natural glycosides by Os7BGlu26.....  | 66          |
| 2.7 Kinetic parameters of rHvBII, Os3BGlu7 and Os7BGlu26 hydrolysis of 4NPGlc,<br>4NPMAN, cello-oligosaccharides, laminaribiose and laminaritriose..... | 58          |
| 3.1 Relative activities of Os9BGlu31 to 4NP-glycosides and dhurrin.....   | 78          |
| 3.2 Hydrolysis of natural glycosides by Os9BGlu31.....  | 80          |
| 3.3 Effect of EDTA, metal salts and inhibitors on Os9BGlu31 activity.....   | 81          |
| 4.1 Yeast strain.....   | 92          |
| 4.2 Primers for HvExoI amplification.....   | 94          |
| 4.3 Cycling parameters for HvExoI amplification.....  | 94          |
| 4.4 Enzyme yields during purification of rHvExoI.....   | 116         |
| 4.5 Amino acid sequences of tryptic fragments of rHvExoI identified by<br>MALDI-ToF/ToF.....  | 118         |
| 4.6 Relative activities of rHvExoI on polysaccharides, oligosaccharides<br>and synthetic substrates.....  | 122         |

## LIST OF TABLES (Continued)

| <b>Table</b>  | <b>Page</b> |
|---|-------------|
| 4.8 Inhibition parameters of rHvExoI with methyl-O-thio-gentiobiose, glucono $\delta$ -lactone and 2,4-dinitrophenyl 2-fluoro-2-deoxy- $\beta$ -D-glucopyranoside ....  | .128        |
| 4.9 The codon usage of <i>Pichai pastoris</i> .....   | .130        |
| 5.1 Cycling parameters for mutation of the optimized HvExoI by the QuikChange® Site-Directed Mutagenesis method .....   | .144        |
| 5.2 The mutagenic oligonucleotide primers for optimized HvExoI. ....  | .145        |
| 5.3 Enzyme yields during purification of the rHvExoI E220A mutant .....   | .148        |
| 5.4 Enzyme yields during purification of the rHvExoI W434A mutant.....  | .148        |
| 5.5 Activities of glycosylated rHvExoI E220A and W434A to synthetic and natural substrates.....   | .154        |
| 5.6 Kinetic parameters of the rHvExoI E220A and W434A mutants compared with wild type rHvExoI .....   | .155        |
| 5.7 Inhibition parameters of rHvExoI E220A and W434A mutants with methyl-O-thio-gentiobiose, glucono $\delta$ -lactone and 2,4-dinitrophenyl 2-fluoro-2-deoxy- $\beta$ -D-glucopyranoside compared with wild type rHvExoI ..... | .157        |
| 6.1 Conditions yielding crystallisation of wild type rHvExoI in microbatch and sitting-drop vapour-diffusion screening .....  | .173        |

## LIST OF FIGURES

| Figure   | Page |
|--|------|
| 1.1 Mechanism for retaining and inverting glycosidases .....   | 3    |
| 1.2 Structure of the oxocarbenium ion-like transition state formed during<br>the glycosylation step of the ‘classical’ retaining mechanism and possible<br>transition state conformations employed during glycoside hydrolysis ..... | 5    |
| 1.3 Stereo-representation of cyclohexitol and 2-deoxy-2-fluoro- $\alpha$ -D-glucopyranoside<br>bound in the active site of barley $\beta$ -D-glucan exohydrolase I .....   | 11   |
| 1.4 Hydrogen bonding interactions of sophorose, S-laminaribiose, S-cellobiose<br>and gentiobiose in the active site of barley $\beta$ -D-glucan exohydrolase I .....   | 12   |
| 1.5 Positions of G2OG, S-laminaribiose, S-cellobiose and G6OG in the active site<br>of the barley $\beta$ -D-glucan exohydrolase I with respect to the two tryptophan residues<br>that constitute binding subsite +1 .....           | 13   |
| 1.6 Hydrogen bonding interactions of PheGlcIm and AmGlcIm with<br>barley $\beta$ -D-glucan exohydrolase I.....   | 15   |
| 2.1 Relationship between rice and other plant GH1 protein sequences described<br>by a phylogenetic tree rooted by Os11BGlu36 .....   | 27   |
| 2.2 Phylogenetic tree of plant $\beta$ -D-mannosidases with rHvBII, Os1BGlu1,<br>Os3BGlu7, Os3BGlu8 and Os7BGlu26 rice $\beta$ -D-glucosidases .....   | 29   |
| 2.3 Alignment of the AK068499 and Os7BGlu26 cDNA sequences.....  | 42   |
| 2.4 The mature Os7BGlu26 PCR product.....  | 43   |
| 2.5 Amino acid sequence alignment of Os7BGlu26 with AK068499 .....   | 44   |

## LIST OF FIGURES (Continued)

| Figure   | Page |
|--|------|
| 2.6 Amino acid sequence alignment of Os7BGlu26, barley rHvBII, rice Os1BGlu1, and Os3BGlu7, Os3BGlu8, <i>Arabidopsis</i> BGLU44 $\beta$ -glucosidase and tomato $\beta$ -mannosidase ..... | 45   |
| 2.7 SDS-PAGE analysis of Os7BGlu26 purified by immobilized Ni <sup>2+</sup> affinity chromatography .....  | 46   |
| 2.8 SDS-PAGE analysis of Os7BGlu26 purified by Q-sepharose anion exchange chromatography .....   | 47   |
| 2.9 SDS-PAGE analysis of Os7BGlu26 purified by S200 gel filtration chromatography .....  | 48   |
| 2.10 SDS PAGE analysis of Os7BGlu26 purification for kinetic analyses .....  | 49   |
| 2.11 pH profile of Os7BGlu26 at pH range of 3.0-10.0 .....   | 50   |
| 2.12 Activity profile of Os7BGlu26 over the temperature range 10-80°C .....  | 51   |
| 2.13 Thin layer chromatography of products of manno-oligosaccharide (DP 2-6) hydrolysis by rHvBII and Os7BGlu26 .....  | 54   |
| 2.14 Structures of plant substrates tested for hydrolysis by Os7BGlu26 .....   | 55   |
| 2.15 Thin layer chromatogram of hydrolysis of <i>p</i> -coumarol glucoside, sambunigrin, D-amydalin, and quercetin-3-glucoside with Os7BGlu26. ....  | 57   |
| 3.1 The nucleotide and amino acid sequences of Os9BGlu31, indicating the sequence that was amplified by the AK121679F and AK121679R primers.....   | 70   |
| 3.2 SDS-PAGE analysis of soluble expressed Os9BGlu31 protein in the <i>E. coli</i> Origami(DE3) with induction with 0.1-0.4 mM IPTG and varied times of expression.....                    | 71   |

## LIST OF FIGURES (Continued)

| Figure   | Page |
|--|------|
| 3.3 The ratio of 4-nitrophenol liberated from 4NPGlc hydrolysis per cell density (OD <sub>600</sub> ) of Os9BGlu31 expressed in <i>E. coli</i> Origami(DE3) at different IPTG inducer concentrations and induction times ..... | 72   |
| 3.4 SDS-PAGE analysis of Os9BGlu31 purified by IMAC.....   | 73   |
| 3.5 SDS-PAGE analysis of Os9BGlu31 purified by Q-sepharose anion exchange chromatography .....   | 74   |
| 3.6 SDS-PAGE analysis of Os9BGlu31 without fusion tag purified by subtractive IMAC after enterokinase cleavage.....  | 75   |
| 3.7 Activity versus pH profile of Os9BGlu31 over a pH range of 3.5-10.0.....   | 76   |
| 3.8 Activity profile of Os9BGlu31 over the temperature range 10-80°C .....   | 77   |
| 3.9 TLC chromatogram of hydrolysis of phlorizin with Os9BGlu31 .....   | 79   |
| 3.10 Protein sequence alignment of rice Os9BGlu31, Os3BGlu7, <i>Zea mays</i> $\beta$ -glucosidase, sorghum $\beta$ -glucosidase dhurrinase-1 and <i>Glycine max</i> hydroxyisourate hydrolase.....                             | 83   |
| 4.1 Alignment of the nucleotide sequences of the native and optimized HvExoI cDNA .....  | 108  |
| 4.2 Plasmid constructs of the pPICZ $\alpha$ BNH <sub>8</sub> -HvExoI plasmid.....   | 109  |
| 4.3 Protein production of optimized rHvExoI detected by western immunoblot analysis .....  | 110  |
| 4.4 Time course of $\beta$ -glucosidase activity in media from <i>P. pastoris</i> transformed with empty plasmid control, optimized and native expression vectors .....  | 111  |

## LIST OF FIGURES (Continued)

| Figure  | Page |
|---|------|
| 4.5 SDS-PAGE of rHvExoI from crude broth, and purified via SP-Sepharose chromatography, the 1 <sup>st</sup> IMAC step, and the 2 <sup>nd</sup> IMAC step, after deglycosylation with endoglycosidase H..... | .113 |
| 4.6 SDS-PAGE analysis of rHvExoI purified by 1 <sup>st</sup> IMAC step.....   | .114 |
| 4.7 SDS-PAGE analysis of rHvExoI purified by a 2 <sup>nd</sup> round of IMAC.....   | .115 |
| 4.8 MALDI-ToF spectra of N-deglycosylated and glycosylated rHvExoI .....  | .117 |
| 4.9 pH activity profiles of glycosylated and N-deglycosylated rHvExoI.....  | .119 |
| 4.10 Thermostability of glycosylated and N-deglycosylated rHvExoI at temperatures ranging from 0-80°C.....  | .120 |
| 4.11 TLC chromatogram of hydrolysis and transglycosylation products formed by glycosylated rHvExoI with 4NPGlc as a substrate.....  | .126 |
| 4.12 TLC chromatogram of hydrolysis and transglycosylation products formed by glycosylated rHvExoI with barley (1,3;1,4)-β-D-glucan as a substrate.....   | .127 |
| 5.1 Purification of glycosylated forms of wild type and E220A and W434A mutants rHvExoI by IMAC.....  | .149 |
| 5.2 pH profiles of activity for wild type and mutant rHvExoI enzymes .....  | .151 |
| 5.3 Thermostability of glycosylated forms of wild type and mutant rHvExoI enzymes .....   | .152 |
| 5.4 Alignment of the regions of GH3 protein sequences containing amino acid residues at the -1 and +1 subsites.....   | .159 |
| 5.5 Hydrogen bonding between glucose, amino acid residues and water molecules around the -1 subsite of HvExoI.....  | .160 |

## LIST OF FIGURES (Continued)

| <b>Figure</b>   | <b>Page</b> |
|---|-------------|
| 5.6 Superimposition of the HvExoI complexes with S-laminaribiose and S-cellobiose and the relative orientations of S-lamaribiose and S-cellobiose at the -1 and +1 subsites ..... | .161        |
| 6.1 N-deglycosylated wild type and mutant forms of rHvExoI after BioGel-P100 size-exclusion chromatography .....  | .171        |
| 6.2 Crystals of wild type rHvExoI from the initial microbatch and sitting-drop vapour-diffusion screening .....   | .174        |
| 6.3 Microcrystals of native HvExoI were used for growing wild type rHvExoI and rHvExoI E220A mutant crystals.....   | .175        |

## LIST OF ABBREVIATIONS

|                   |  |
|-------------------|--|
| A                 | absorbance   |
| Å                 | Ångstrom   |
| °C                | degrees Celsius  |
| bis-acrylamide    | N,N-methylene-bis-acrylamide                           |
| BSA               | bovine serum albumin                                   |
| CaCl <sub>2</sub> | calcium chloride                                       |
| cDNA              | complementary deoxynucleic acid                        |
| CV                | column volumes   |
| DNA               | deoxyribonucleic acid                                  |
| DNaseI            | deoxyribonuclease I                                    |
| DP                | degree of polymerization                               |
| DTT               | 1,4-dithio-DL-threitol                                 |
| EDTA              | ethylene diamine tetraacetic acid                      |
| 2F-DNPGlc         | 2,4-dinitrophenyl 2-fluoro-2-deoxy-β-D-glucopyranoside |
| (n/μ/m)g          | (nano, micro, milli) gram                              |
| h                 | hour   |
| HEPES             | 4-(2-hydroxyethyl)-1-piperazineethanesulfonic acid     |
| HvExoI            | native barley β-D-glucan exohydrolase I                |
| IMAC              | immobilized metal-affinity chromatography              |
| IPTG              | isopropyl β-D-thioglucopyranoside                      |
| K                 | Kelvin   |
| (k)bp             | (kilo) base pair                                       |

**LIST OF ABBREVIATIONS (Continued)**

|                   |  |
|-------------------|--|
| kDa               | kilodalton   |
| ( $\mu$ /m)l      | (micro, milli) liter                                       |
| ( $\mu$ /m)M      | (micro, milli) molar                                       |
| MALDI-ToF         | matrix-assisted laser-desorption ionization-time of flight |
| MgCl <sub>2</sub> | magnesium chloride   |
| min               | minute   |
| NaCl              | sodium chloride  |
| NaOH              | sodium hydroxide   |
| PCR               | Polymerase chain reaction                                  |
| PGO               | peroxidase-glucose oxidase                                 |
| PMSF              | phenylmethylsulfonylfluoride                               |
| 4NPGlc            | 4-nitrophenyl $\beta$ -D-glucopyranoside                   |
| 4NPMAN            | 4-nitrophenyl $\beta$ -D-mannopyranoside                   |
| 4NP               | 4-nitrophenol  |
| PAGE              | polyacrylamide gel electrophoresis                         |
| PEG               | polyethyleneglycol   |
| rHvBII            | recombinant barley $\beta$ -glucosidase                    |
| rHvExoI           | recombinant barley $\beta$ -D-glucan exohydrolase I        |
| SDS               | sodium dodecyl sulfate                                     |
| s                 | second   |
| Tris              | tris-(hydroxymethyl)-aminomethane                          |
| T <sub>m</sub>    | melting temperature  |
| TEMED             | N, N, N', N'-Tetramethylethylenediamine                    |

**LIST OF ABBREVIATIONS (Continued)**

|       |   |
|-------|---|
| TLC   | thin layer chromatography                               |
| $V_0$ | initial velocity  |
| v/v   | volume by volume  |
| w/v   | weight by volume  |
| x g   | relative centrifugal force (times the force of gravity) |

# CHAPTER I

## INTRODUCTION

### 1.1 Glycoside hydrolases

Glycoside hydrolases (GH) are present in all kingdoms of living organisms, and can catalyze the hydrolysis of O-, N- and S-linked glycosides. The Enzyme Commission (EC) classification nomenclature assigns enzymes systematic names and EC numbers based on the reaction they catalyze and their substrate specificity. Glycoside hydrolases are given the code EC 3.2.1.X, in which the first three digits indicate enzymes hydrolysing O-glycosyl linkages and X represents the substrate specificity. The EC classification is the simplest, but it is not appropriate for enzymes showing broad specificity and does not reflect the structural and mechanistic features of the enzyme. For example, certain endoglucanases are considered to be cellulases, but they are also active on xylan,  $\beta$ -glucan (Henrissat and Davies, 1997).

A classification of glycoside hydrolases in families based on amino acid sequence similarities has been proposed, by which the relationship between sequence and folding similarities can be deduced directly. This classification is available to predict substrate specificity, molecular mechanism and three-dimension structure for uncharacterized enzymes by comparing with a member of the same family that is known. Many of the sequence-based families are polyspecific, they contain enzymes of different substrate specificities, suggesting an evolutionary divergence. The existence of a number of polyspecific families indicates that the acquisition of new specificities by glycosyl hydrolases is a common evolutionary event. Sometimes, enzymes with similar specificities are found in different families, which raises the possibility of convergent evolution

(Henrissat, 1991; Henrissat and Bairoch, 1993; Henrissat and Davies, 1997).

### **1.1.1 Glycoside hydrolase mechanism**

Many GH enzymes catalyze glycosidic bond hydrolysis by direct catalytic involvement of two amino acid residues, which are a general acid/base and a nucleophile residue (Zechel and Withers, 2000). The two most commonly employed mechanisms used by glycosidases are distinguished by whether glycosidic bond cleavage occurs with overall inversion or retention of anomeric stereochemistry (Figure 1.1).

#### **1.1.1.1 Retaining glycosidases**

Retaining glycosidases achieve hydrolysis of the glycosidic bond via a double displacement mechanism involving a glycosyl-enzyme intermediate (Figure 1.1a). Two carboxylic acid residues located on opposite sides of the glycosidic bond at the active site, and are approximately 5.5 Å apart (Koshland, 1953; Zechel and Withers, 2000). In the first step, a general acid/base protonates the glycosidic oxygen, while a general nucleophile attacks the anomeric carbon to form a covalent glycosyl-enzyme intermediate, thereby cleaving the C-O bond at the anomeric carbon to displace the aglycone group. In the second step, a general acid/base deprotonates the incoming water molecule which attacks the anomeric center and displaces the sugar.

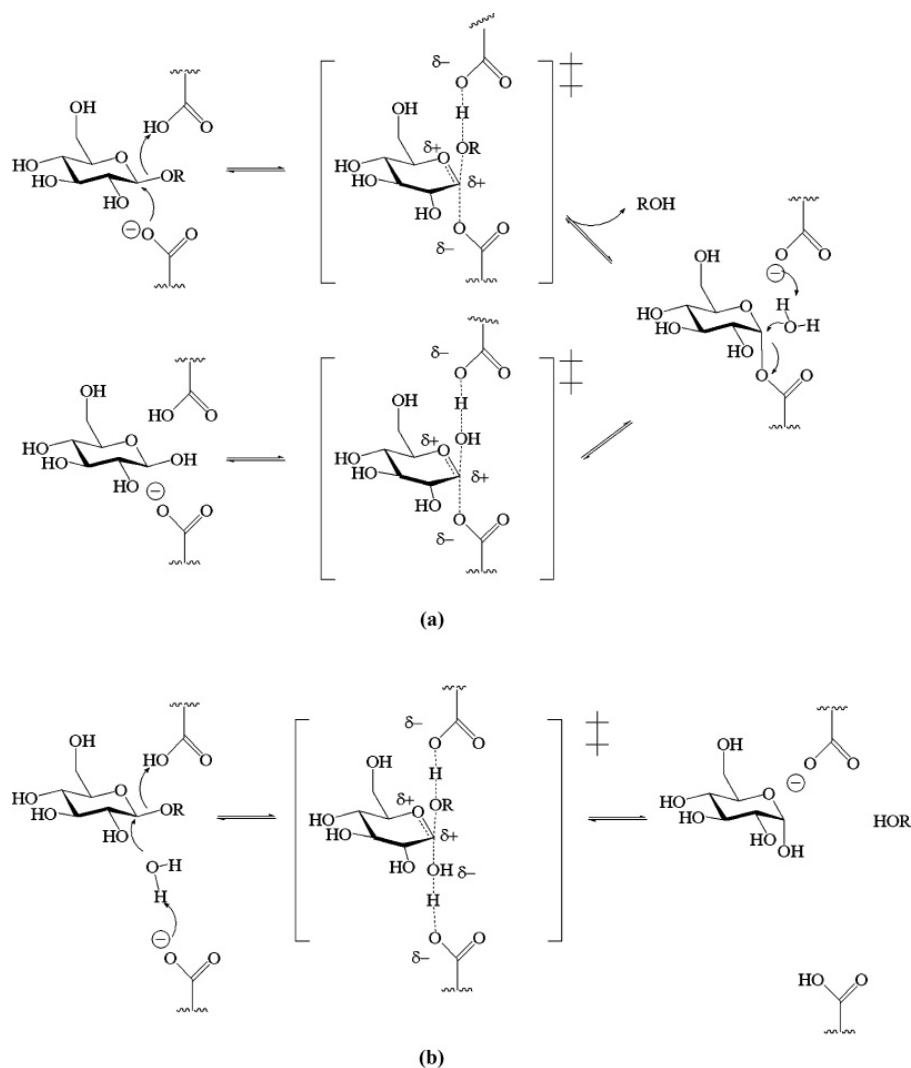


**Figure 1.1** Mechanism for retaining (a) and inverting (b) glycosidases. O-R is the alkyl or aryl group that acts as the leaving group (Rempel and Withers, 2008).

### 1.1.1.2 Inverting glycosidases

With inverting glycosidases, hydrolysis occurs via a single-displacement mechanism involving an oxocarbenium ion-like transition state (Figure 1.1b). Two carboxylic groups act as general acid and general nucleophilic catalysts located, and are at least 10 Å apart on opposite sides of the active site (Koshland, 1953). The general nucleophile removes a proton from the water molecule during its attack at the anomeric carbon, while the general acid protonates the departing aglycone oxygen atom, thus assisting in its departure from the anomeric center. The retaining mechanism differs from

the inverting mechanism by the formation of a covalently bound glycosyl-enzyme intermediate and in its proceeding through two oxocarbenium ion-like transition states instead of one.

### 1.1.2 Substrate distortion during the enzymatic hydrolysis of glycosides

An important aspect of  $\beta$ -GH mechanism is the conformational itinerary that the substrate follows during the reaction, in which substrate distortion is induced upon binding to the enzymes. The way to trap the enzyme/substrate couple by X-ray crystallography normally relies either on the use of inhibitors (Sulzenbacher *et al.*, 1996) or enzyme mutants (Guerin *et al.*, 2002). Pauling first postulated in the 1940s that the highest affinity inhibitors of an enzyme were likely to be those that mimicked the structure of a ‘strained activated complex’ (i.e. transition state) (Pauling, 1946; 1948). In the case of glycoside hydrolysis, the short-lived transition state possesses substantial oxocarbenium character (Figure 1.2a); it contains partially formed or broken bonds between anomeric carbon and the attacking nucleophile and the glycosidic oxygen of the leaving group. Under these conditions the anomeric carbon possesses trigonal character, which is caused by  $sp^2$  hybridisation due to electron delocalization predominantly along the bond between the anomeric carbon and endocyclic oxygen. The double bond character imposed on the pyranose ring means there is distortion from a relaxed chair conformation typical of the substrate, since the C1, C2, O5 and C5 to lie in a plane for this double bond to form, and to take a more energetically unfavorable half chair or boat conformation at the transition state (Figure 1.2b) (Vocadlo and Davies, 2008; Davies *et al.*, 2003). There is also a considerable build-up of positive charge on the pyranose ring at the transition state, which is delocalized along the bond between the anomeric carbon and endocyclic oxygen.

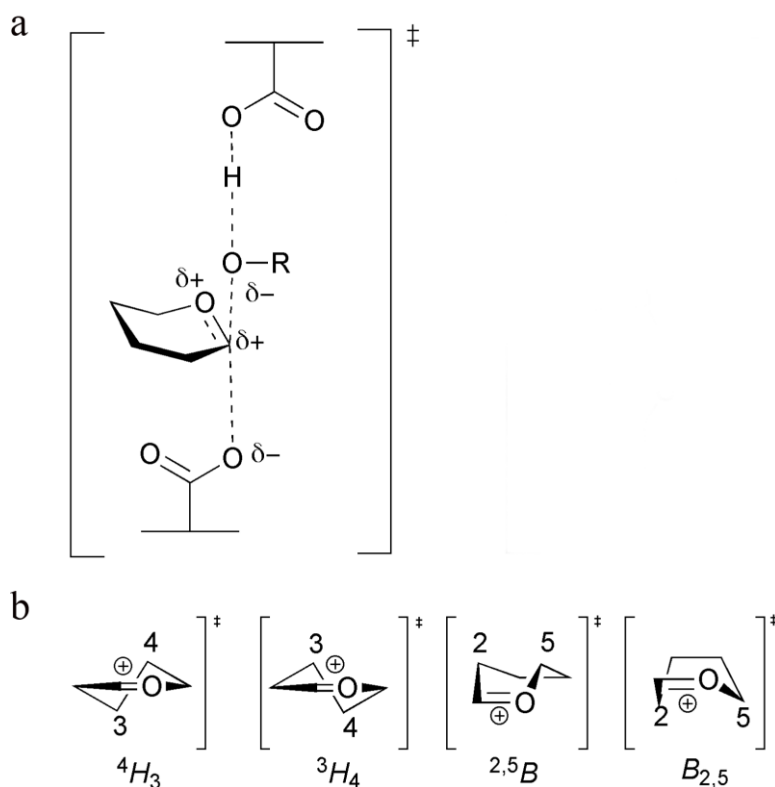


**Figure 1.2** Structure of the oxocarbenium ion-like transition state formed during the glycosylation step of the ‘classical’ retaining mechanism (a); R is the leaving group. Possible transition state conformations employed during glycoside hydrolysis (b); half chair ( ${}^4H_3$  or  ${}^3H_4$ ) or boat ( ${}^{2,5}B$  and  $B_{2,5}$ ) conformation (Gloster and Davies, 2010).

In the complex of endoglucanase *Cel5A* from *Bacillus agaradbaerens* with 2,4-dinitrophenyl-2-deoxy-2-fluoro- $\beta$ -D-cellobioside (Davies *et al.*, 1998), the *gluco*-configured substrate adopted a distorted  ${}^1S_3$  conformation for the Michaelis complex. In this configuration the position in of the glycosidic bond pseudo-axially will orient the *trans* C(2)OH group pseudo-axially as well. The reorientation of the C(2)OH group is associated with a stronger destabilization of oxobarbenium cation. The destabilization is alleviated in the transition state by a hydrogen bond from C(2)OH to the catalytic nucleophile, corresponding to a partial deprotonation of C(2)OH (Winkler and Holan, 1989).

The GH26  $\beta$ -mannanase from *Cellvibrio japonicas* and GH2  $\beta$ -mannosidase from *Bacteroides thetaiotaomicron* revealed a  ${}^1S_5$  conformation for the mannoside (Ducros *et al.*,

2002; Offen *et al.*, 2009). The  ${}^1S_5$  conformation with a *manno*-configured ligand likewise allows in-line nucleophilic attack with an axial leaving group orientation and has the added benefit of placing the *manno*-O-2 pseudo-equatorial. The  ${}^1S_5$  conformation can be coupled to the  ${}^0S_2$  conformation for the intermediate via a  $B_{2,5}$  transition-state conformation for the glycosylation step of glycoside hydrolysis (Tailford *et al.*, 2008).

## 1.2 $\beta$ -D-glucosidases in glycosyl hydrolase family 1

Glycoside hydrolase family 1 (GH1) enzymes hydrolyse glycoside bonds to release  $\beta$ -D-glucose,  $\beta$ -D-galactose,  $\beta$ -D-mannose,  $\beta$ -D-fucose, phospho- $\beta$ -D-galactose, and modified  $\beta$ -D-glucose residues from a carbohydrate or lipid or other aglycone (CAZy database at <http://www.cazy.org/GH1.html>).  $\beta$ -glucosidases ( $\beta$ -D-glucoside glucohydrolases; EC 3.2.1.21), one type of glycosyl hydrolase according to their activity, are members of glycoside hydrolase families 1, 3, 5, 9 and 30 (GH1, GH3, GH5, GH9 and GH30, respectively), based on their amino acid sequences (Cantarel *et al.*, 2009; Ketudat Cairns and Esen, 2010). The  $\beta$ -glucosidases that have been characterized from plants fall primarily in GH families 1 (GH1) and 3 (GH3). GH1, GH3, GH5 and GH30  $\beta$ -glucosidases hydrolyse O-glycosidic bonds at the nonreducing end of carbohydrates with retention of the anomeric configuration and hydrolyse a variety of glycosides, including aryl- and alkyl- $\beta$ -D-glycosides. In higher plants,  $\beta$ -glucosidases are involved in the defense against pests, phytohormone activation, lignification and hydrolysis of cell wall-derived oligosacchrides during germination degradation. The primary structures of GH1  $\beta$ -glucosidases contain the conserved peptide motifs Thr-(Phe/Leu)-Asn-Glu-Pro, T(F/L)NEP, which includes the catalytic acid/base, and (Ile/Val)-Thr-Glu-Asn-Gly, (I/V)TENG, which includes the catalytic nucleophile residue (Czjzek *et al.*, 2000). The three-dimensional structures of GH1  $\beta$ -glucosidases are  $(\beta/\alpha)_8$  barrels, with the catalytic

acid/base and nucleophile located at the C-terminus of the  $\beta$ -barrel strands  $\beta$ 4 and  $\beta$ 7, respectively. The residues of the conserved peptide motifs or their equivalents were found to form part of a pocket or crater-shaped active site (Davies and Henrissat, 1995).

Plant  $\beta$ -glucosidases have been shown to hydrolyse their natural  $\beta$ -glucosidase substrate, such as cassava linamarase and linamarin (Hughes *et al.*, 1992), Thai rosewood  $\beta$ -glucosidase and dalcochinin  $\beta$ -glucoside (Svasti *et al.*, 1999), maize  $\beta$ -glucosidase and DIMBOA- $\beta$ -glucoside (2,4-dihydroxy-7-methoxy-1,4-benzoxazin-3-one-glucoside; Babcock and Esen, 1994), sorghum  $\beta$ -glucosidase and dhurrin (Hösel *et al.*, 1987), *Polygonum tinctorium*  $\beta$ -glucosidase and indoxyl- $\beta$ -glucoside (Minami *et al.*, 1996), walnut  $\beta$ -glucosidase and hydrojuglone- $\beta$ -glucoside (Duroux *et al.*, 1998), and rice cell wall-bound  $\beta$ -glucosidase and oligosaccharides (Akiyama *et al.*, 1998).

There are many reports about the different efficiency of  $\beta$ -glucosidases to hydrolyse different substrates. For example, maize  $\beta$ -glucosidase isoenzymes ZmGlu1 and ZmGlu2 hydrolyse DIMBOAGlc (their natural substrate), but the efficiency of ZmGlu2 to hydrolyse artificial substrates is lower than ZmGlu1 (Bandaranayake and Esen, 1996). For the sorghum  $\beta$ -glucosidases SbDhr1 and SbDhr2, SbDhr1 hydrolyses only dhurrin (its natural substrate), whereas SbDhr2 hydrolyses dhurrin and artificial substrates (Cicek *et al.*, 2000). So, the substrate specificity of  $\beta$ -glucosidases varies, and apparently depends upon the amino acids within the active site. In addition, the C-terminal ends of the  $\beta$ -strands in the  $(\beta/\alpha)_8$  barrel contain sites that are necessary for aglycone recognition and binding (Singh *et al.*, 1995; Barrett *et al.*, 1995; Burmeister *et al.*, 1997; Sanz-Aparicio *et al.*, 1998; Chi *et al.*, 1999).

### 1.2.1 $\beta$ -D-mannosidases and $\beta$ -D-glucosidases in family 1

Tomato  $\beta$ -mannosidase (EC 3.2.1.25) participates in the degradation of galactomannans, by hydrolysing oligomannan products of (1,4)- $\beta$ -mannan endohydrolase.  $\beta$ -mannosidase activity was found to be higher in the lateral endosperm than in the micropylar endosperm. The enzyme hydrolysed 4NP- $\beta$ -D-mannopyranoside with a  $K_M$  of 0.55 mM (Mo and Bewley, 2002).

A barley (*Hordeum vulgare* L.)  $\beta$ -glucosidase isoenzyme (BGQ60) of GH1 was purified from seed and characterized (Leah *et al.*, 1995). BGQ60 had  $\beta$ -glucosidase and  $\beta$ -mannosidase activities, and it hydrolysed  $\beta$ -linked oligosaccharides composed of glucose or mannose. BGQ60 hydrolysed 4NP- $\beta$ -D-mannopyranoside (4NPMan) faster than 4NP- $\beta$ -D-glucoopyranoside (4NPGlc). It also had cellobiase activity with better hydrolysis of cellobiose than cellotriose. Barley  $\beta$ -D-glucosidase isoenzyme II (HvBII) was purified from the endosperm of germinated seeds and found to be homologous to BGQ60 (Hrmova *et al.*, 1996). HvBII had activity similar to the BGQ60, in that it hydrolysed 4NPMan more rapidly than 4NPGlc and could hydrolyse  $\beta$ -(1,2)-,  $\beta$ -(1,3)-,  $\beta$ -(1,4)-gluco-oligosaccharides. HvBII was later shown to be primarily a  $\beta$ -mannosidase with the capability of releasing mannose from oligosaccharides generated from  $\beta$ -mannans by barley  $\beta$ -mannanase (Hrmova *et al.*, 2006).

An enzyme similar to these  $\beta$ -glucosidase/ $\beta$ -mannosidases was also investigated in *Arabidopsis thaliana* and its substrate specificity characterized (Xu *et al.*, 2004). BGLU 44  $\beta$ -glucosidase preferred to hydrolyse 4NPMan, for which it had a  $K_M$  of 0.43 mM and  $V_{max}$  of 94.7 nkatal/mg protein, and it could also hydrolyse  $\beta$ -(1,4)-D-manno-oligosaccharides.

### 1.3 $\beta$ -glucan exohydrolases and $\beta$ -glucosidases in glycoside hydrolase family 3

Glycoside hydrolase family 3 (GH3) enzymes remove successive  $\beta$ -D-glucose,  $\beta$ -D-xylose and  $\beta$ -N-acetylglucosamine residues from the nonreducing end of homodisaccharides, oligosaccharides,  $\beta$ -(1,3) or (1,4) and (1,3-1,4)-glucans or glucosides (CAZy database at <http://afmb.cnrs-mrs.fr/CAZy/index.html>). Many GH3 enzymes exhibit a combination of different activities, for example  $\beta$ -glucosidase and  $\beta$ -xylosidase activities were found in *salA* from *Azospirillum irakense* KBC1 and *bgxA* from *Erwinia chrysanthemi* D1 (Faure *et al.*, 1999; Vroemen *et al.*, 1995). Functions of GH3s include the assimilation of plant polymer products by bacteria and fungi, recycling of cell wall components, and modification of toxic plant compounds.

Barley  $\beta$ -D-glucan exohydrolase I (HvExoI, EC 3.2.1.-) is a member of GH3 that was purified from *Hordeum vulgare* L., cv. Clipper seedlings (Hrmova *et al.*, 1996). HvExoI preferred to hydrolyse (1,3)- $\beta$ -D-gluco-oligosaccharides and also hydrolysed (1,2)-, (1,4)-, and (1,6)- $\beta$ -D-gluco-oligosaccharides and (1,3; 1,6)-, and (1,3;1,4)- $\beta$ -D-glucans (Hrmova *et al.*, 1998). HvExoI appears to be involved in cell wall degradation and expression of the gene was found in the scutellum of germinated grain, elongating coleoptiles, and young roots and leaves (Harvey *et al.*, 2001). The three-dimensional structure of HvExoI consists of a  $(\beta/\alpha)_8$  barrel in domain 1 and an  $(\alpha/\beta)_6$  sheet in domain 2, which contains five parallel  $\beta$  strands and one anti-parallel strand, with three helices on either side of it (Varghese *et al.*, 1999). The catalytic nucleophile of HvExoI (D285) was identified by its covalent modification with conduritol B epoxide (1, 2-anhydro-*myo*-inositol) and 2-deoxy-2-fluoro- $\alpha$ -D-glucopyranoside (Figure 1.3) (Hrmova *et al.*, 2001). The glutamate at the position 491 is likely to be the catalytic acid/base, since in the complexes of HvExoI with thio-substrate analogs, the distance between the S atom of the

glycosyl substrate analogs and Oε<sub>2491</sub> of E491 was 2.75 Å. The active site of HvExoI is between the 2 domains, with the catalytic nucleophile located in domain 1 and the catalytic acid/base located in domain 2 (Hrmova *et al.*, 2002). It was shown kinetically and structurally that this active site contains two to three subsites for oligosaccharide glycosyl residue binding (Hrmova *et al.*, 1996; 2002).

Most β-glucosidases in GH3 can hydrolyse many aryl-glycosides and (1,2)-, (1,3)-, (1,4)- and (1,6)-β-D-gluco-oligosaccharides. However, β-glucosidases cannot hydrolyse β-glucan. Recently, the structure of *Thermotoga neapolitana* β-glucosidase has been solved (Pozzo *et al.*, 2010). *T. neapolitana* β-glucosidase is composed of 3 domains. The first domain is a (β/α)<sub>8</sub> triose phosphate isomerase (TIM) barrel, which is followed by the five-stranded α/β sandwich fold of the second domain. The catalytic nucleophile (D242) and catalytic acid/base (E458) residues are in the domain 1 and domain 2, respectively. Domain 2 of β-glucosidase is different from domain 2 of HvExoI in that it is missing one β-strand (βk, in HvExoI), which is replaced with an α-helix (αK1, in *T. neapolitana* β-glucosidase). Domain 2 has a long flexible loop between αK1 and αK2 that extends far from domain 2 toward domain 1. Domain 3 has a fibronectin type III (FnIII) fold, which consists of a β-sandwich structure with three strands (A, B and E) on one side and four strands (C, D, F and G) on the other, and this domain has unknown function. *T. neapolitana* β-glucosidase only shows 21% amino acid sequence identity to HvExoI. However, the amino acid residues involved in the binding of glucose at the active site of β-glucosidase (D58, R130, K163, H164, Y210 and E458) are conserved with the corresponding amino acid residues of HvExoI (D95, R158, K206, H207, Y253 and E491).

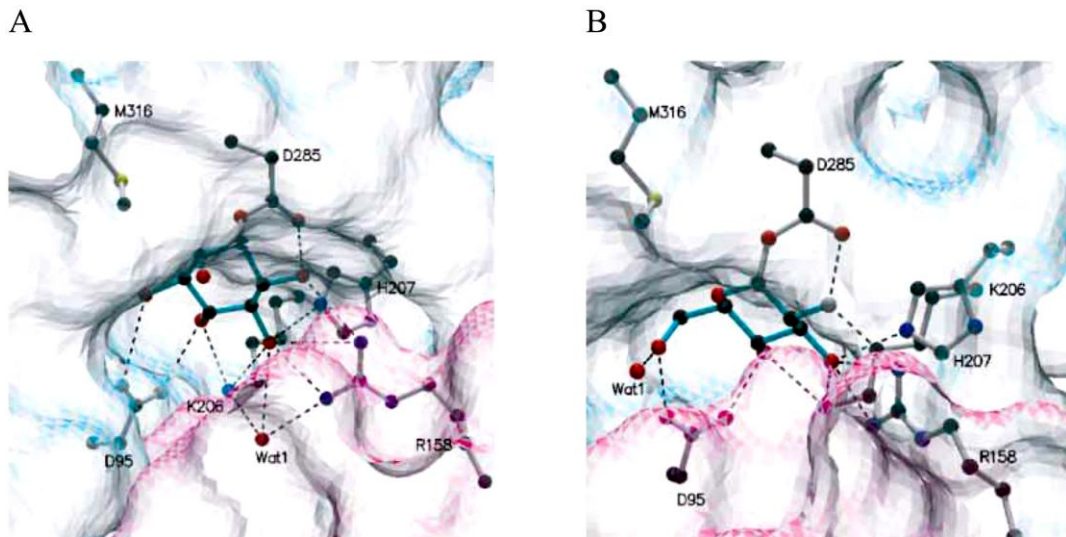


**Figure 1.3** Stereo-representation of cyclohexitol ring (A) and 2-deoxy-2-fluoro- $\alpha$ -D-glucopyranoside (B) bound in the active site of barley  $\beta$ -D-glucan exohydrolase I. Ligands are colored in cyan and the molecular surfaces of domains 1 and 2 are represented by transparent cyan and magenta surfaces, respectively. Black, red, blue, yellow, and gray spheres represent carbon, oxygen, nitrogen, sulfur and fluorine atoms, respectively, and Wat indicates water molecule, (Hrmova *et al.*, 2001).

### 1.3.1 Broad substrate specificity of barley $\beta$ -D-glucan exohydrolase I

The availability of procedures to crystallise HvExoI allowed the structural basis for its broad specificity to be examined. The HvExoI complexes with the nonhydrolysable S-glycoside substrate analogs of laminaribiose (G3SG) and cellobiose (G3SG) were determined by X-ray crystallography, and the molecular modeling of sophorose (G2OG) and gentiobiose (G6OG) were done to complete the range of linkages hydrolysed by HvExoI (Hrmova *et al.*, 2001). As shown in Figure 1.4, nine amino acid residues in the active site are positioned to interact with several  $\beta$ -linked disaccharides in order to fix the nonreducing glucosyl residue at the -1 subsite. The positions of these groups and their interactions with the nonreducing glucosyl group are nearly identical, with only distance of hydrogen bonding between OH groups and D95 and K206 differing a little. In contrast, the

reducing end glucosyl residues of the S-laminaribiose and S-cellobiose moieties, which occupy subsite +1 located between two tryptophan residues (W286 and W434), are significantly different in their positions. These tryptophan residues are at the entrance of the substrate binding pocket of HvExoI, so they might also play a role in the binding of acceptor molecules in transglycosylation reactions (Hrmova *et al.*, 2002).

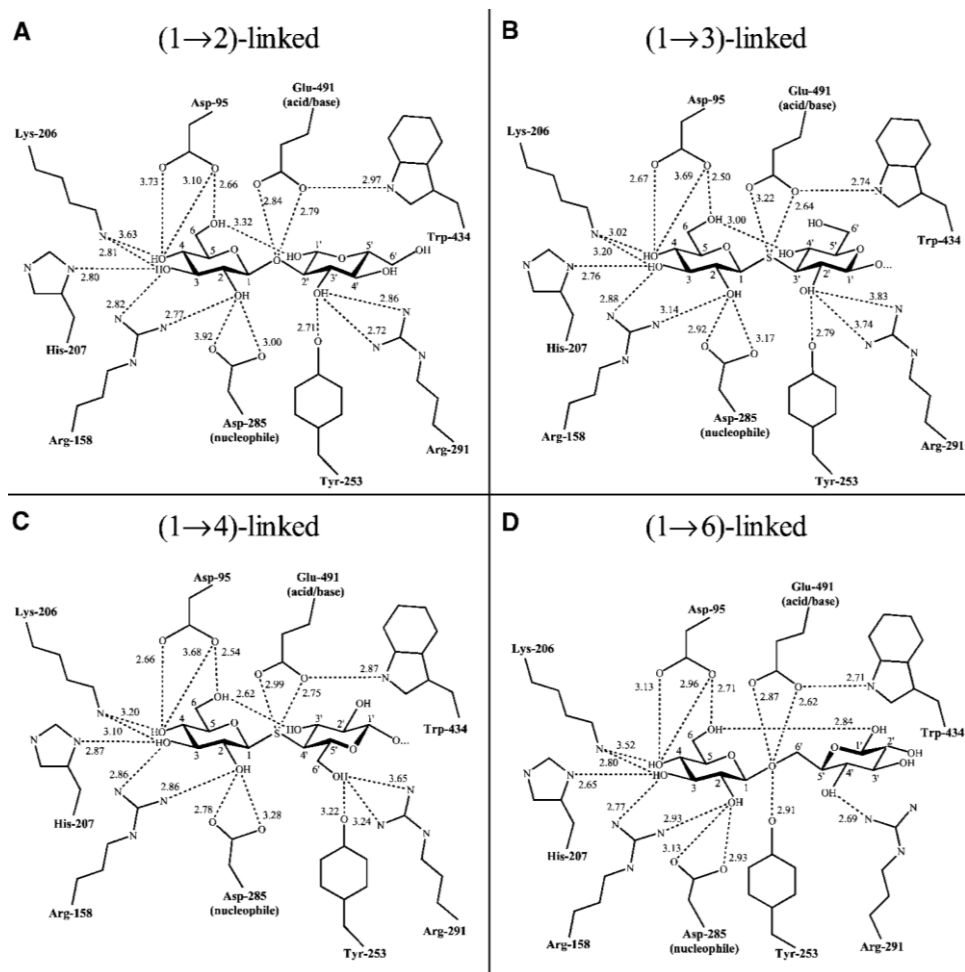


**Figure 1.4** Hydrogen bonding interactions (dash line) of sophorose (A), S-laminaribiose (B), S-cellobiose (C) and gentiobiose (D) in the active site of barley  $\beta$ -D-glucan exohydrolase I (Hrmova *et al.*, 2002).

The broad specificity of the enzyme for  $\beta$ -D-glucoside substrates requires a degree of positional flexibility at the +1 subsite which is achieved by hydrophobic  $\pi$ -stacking interactions of the substrates with W268 and W434. The glucosyl residue in the +1 subsite can be rotated and translated partially yet still remain located between the indole moieties of the two tryptophan residues (Figure 1.5). The flexibility in binding positions at the +1 subsite presumably is allowed because the glucosyl residue is  $\sim 3$  Å wide, whereas the indole moiety of the tryptophan residues is  $\sim 5$  Å wide (Hrmova *et al.*, 2002).

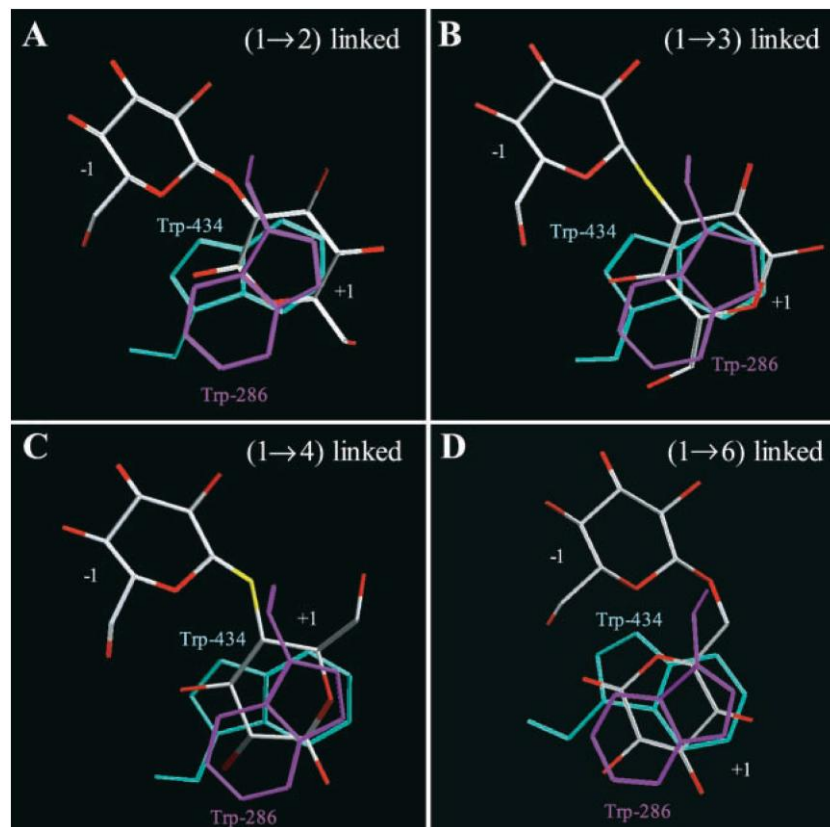


**Figure 1.5** Positions of G2OG (A), S-laminaribiose (B), S-cellobiose (C) and G6OG (D) in the active site of the barley  $\beta$ -D-glucan exohydrolase I with respect to the two tryptophan residues that constitute binding subsite +1. Bound carbohydrates moieties are shown in carbon atom (gray), oxygen atom (red), sulfur atom (yellow), and the stacked W286 (magenta) and W343 (cyan) residues at the +1 subsite are rotated to the positions where their pyrrole (W286) and phenyl (W434) portions overlap (Hrmova *et al.*, 2002).

### 1.3.2 Catalytic mechanism of barley $\beta$ -D-glucan exohydrolase I

The interactions of a transition state mimic with inhibitors of anilinomehyl glucoimidazole (AmGlcIm) result in a  $K_i$  constant of  $1.7 \times 10^{-9}$  M and phenyl glucoimidazole (PheGlcIm) result in a  $K_i$  constant of  $0.6 \times 10^{-9}$  M. Both of the inhibitors could protrude into the +1 subsite of the active site for additional interactions that may increase their strength of binding (Figure 1.6) (Hrmova *et al.*, 2005). AmGlcIm binds 3 times more tightly to the HvExoI than PheGlcIm, likely reflecting the differences in these +1 site interaction. The active sites of both inhibitor/enzyme complexes contain seven water molecules, five of which are associated with the catalytic acid/base (E491) and E220. E220 binds to the glucoimidazole inhibitors through water-mediated hydrogen bonds and coordinates water molecules around the catalytic acid/base residue. The AmGlcIm/enzyme complex showed a network of seven hydrogen bonds between the enzyme's catalytic pocket residues K206, H207, Y253, D285 and E491 and the atoms of the glucoimidazoles are shorter by 0.15-0.53 Å, compared with distances of corresponding H-bonds in the S-cellobiose/enzyme (Figure 1.4). The enzyme complex with S-cellobiose showed the reducing glucosyl residues at the +1 subsite adopted a distorted  ${}^4C_1$  conformation. The conformations of sugar components of PheGlcIm and AmGlcIm at the -1 subsite are likely to represent a transition state with a distorted  ${}^4H_3$  conformation, which is close to the  ${}^4E$  conformation with the coplanar C8, C9, C10, N1 and C5 atoms.

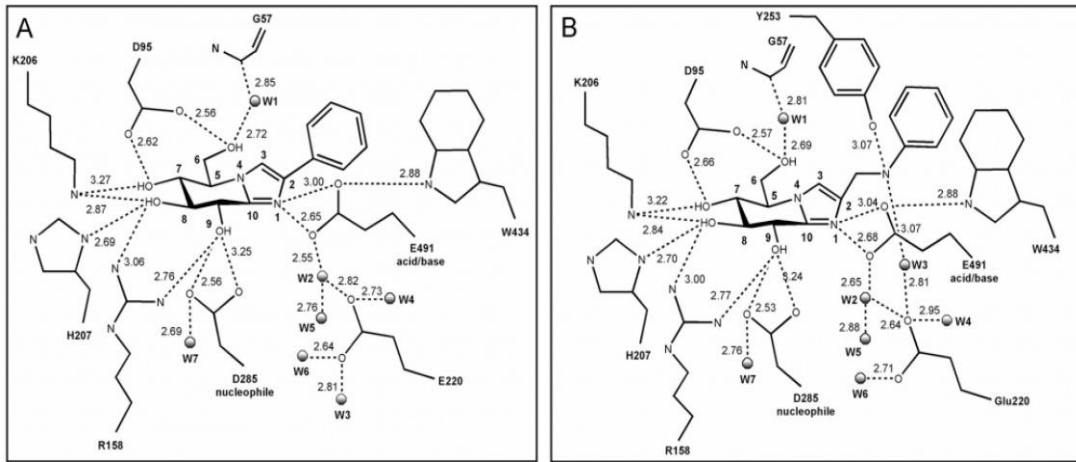


**Figure 1.6** Hydrogen bonding interactions of PheGlcIm (A) and AmGlcIm (B) with barley  $\beta$ -D-glucan exohydrolase I. PheGlcIm is shown in the  ${}^4H_3$  conformation with atomic numbering of the carbon atoms of the tetrahydroimidazopyridine moiety. The dashed lines represent hydrogen bonding interactions among the ligand, water molecules, and amino acid residues (Hrmova *et al.*, 2005).

## 1.4 Significance of study

The mode of enzyme action can be reflected in substrate specificity. GH1  $\beta$ -glucosidases and GH3  $\beta$ -glucan exohydrolases are exo-hydrolase enzymes that can hydrolyse glucoside substrates, including several  $\beta$ -linked oligosaccharides, to release glucose from the nonreducing end with retention of anomeric stereochemistry. GH1 and GH3 enzymes are divided into different families according to their different sequences and structural folding, but have similar substrate specificities which reflect a convergent evolution. On the other hand, members of each family have different substrate specificities, although they share a common evolutionary origin. The specificities of enzymes can be adapted to different substrates, depending on the dimensions of the active site tunnel or on the geometry of the substrate-binding site.

Forty members of rice GH1  $\beta$ -glucosidases have been identified from rice genome sequences (Opassiri *et al.*, 2006), and their localization was predicted and their sequences compared with those of other plant GH1 enzymes to try to elucidate the roles of rice GH1  $\beta$ -glucosidases. In order to understand the precise roles of these  $\beta$ -glucosidases, their substrate specificities and biochemical properties must be determined. Once the substrate specificities are known, the structural basis of this divergent set of specificities can be studied in order to understand the biochemical basis of protein functional divergence. Although some of the rice GH1 isoenzymes were previously characterized (Opassiri *et al.*, 2003, 2004, 2006; Seshadri *et al.*, 2009; Kuntothom *et al.*, 2009), the work presented here represents the first characterization of a rice  $\beta$ -mannosidase and a representative of the phylogenetic clade closely related to *Glycine max* hydroxyisourate hydrolase.

Barley  $\beta$ -D-glucan exohydrolase isoenzyme I is the only GH3 enzyme that has been characterized in detail in terms of its structure, enzymatic mechanism, and substrate specificity. The roles of amino acid residues at the active site have been investigated by X-ray crystallographic structural analysis of inhibitor/enzyme and substrate

analogue/enzyme complexes, but were yet to be studied by site-directed mutagenesis at the start of this study. Characterization of mutants (around the active site), in terms of substrate specificity and biochemical properties, are more precisely identified the roles of two active site amino acid residues and confirmed that several others are critical for barley  $\beta$ -D-glucan exohydrolase I activity.

### 1.5 Research objectives

1. To clone and express active recombinant rice  $\beta$ -glucosidases (Os7BGlu26 and Os9BGlu31) and barley  $\beta$ -D-glucan exohydrolase I (rHvExoI).
2. To purify the recombinant Os7BGlu26, Os9Glu31 and rHvExoI in order to characterize the activities of each specific enzyme in terms of its substrate specificity and biochemical properties.
3. To determine the amino acids critical to the substrate specificity and catalytic mechanism of rHvExoI by site-directed mutagenesis.
4. To screen the conditions for recombinant HvExoI crystallization.

### 1.6 References

- Akiyama, T., Kaku, H., and Shibuya, N. (1998). A cell-wall bound  $\beta$ -glucosidase from germinated rice: Purification and properties. **Phytochemistry** 48: 49-54.
- Babcock, G.D., and Esen, A. (1994). Substrate specificity of maize  $\beta$ -glucosidase. **Plant Sci.** 101: 31-39.
- Bandaranayake, H., and Esen, A. (1996). Nucleotide sequence of a  $\beta$ -glucosidase (*glu2*) cDNA from maize (*Zea mays* L.). **Plant Physiol.** 110: 1048.

- Barrett, T., Suresh, C.G., Tolley, S.P., Dodson, E.J., and Hughes, M.A. (1995). The crystal structure of a cyanogenic  $\beta$ -glucosidase from white clover, a family 1 glycosyl hydrolase. **Structure** 3: 951-960.
- Burmeister, W.P., Cottaz, S., Driguez, H., Iori, R., Palmieri, S., and Henrissat, B. (1997). The crystal structures of *Sinapis alba* myrosinase and a covalent glycosyl-enzyme intermediate provide insights into the substrate recognition and active-site machinery of an S-glycosidase. **Structure** 5: 663-675.
- Cantarel, B.L., Coutinho, P.M., Rancurel, C., Bernard, T., Lombard, V., and Henrissat, B. (2009). The Carbohydrate-Active EnZymes database (CAZy): an expert resource for glycogenomics. **Nucleic Acids. Res.** 37: D233-D238.
- Chi, Y.I., Martinez-Cruz, L.A., Jancarik, J., Swanson, R.V., Robertson, D.E., and Kim, S.H. (1999). Crystal structure of the  $\beta$ -glucosidase from the hyperthermophile *Thermosphaera aggregans*: insights into its activity and thermostability. **FEBS Lett.** 445: 375-383.
- Cicek, M., Blanchard, D., Bevan, D.R., and Esen, A. (2000). The aglycone specificity-determining sites are different in 2,4-dihydroxy-7-methoxy-1,4-benzoxazin-3-one (DIMBOA)-glucosidase (maize  $\beta$ -glucosidases) and dhurrinase (sorghum  $\beta$ -glucosidases). **J. Biol. Chem.** 275: 20002-20011.
- Czjzek, M., Cicek, M., Zamboni, V., Bevan, D.R., Henrissat, B., and Esen, A. (2000). The mechanism of substrate (aglycone) specificity in  $\beta$ -glucosidases is revealed by crystal structures of mutant maize  $\beta$ -glucosidase-DIMBOA, -DIMBOAGlc, and -dhurrin complexes. **Proc. Nat. Acad. Sci., USA.** 97: 13555-13560.
- Davies, G., and Henrissat, B. (1995) Structures and mechanisms of glycosyl hydrolases. **Structure** 3: 853-859.

- Davies, G.J., Mackenzie, L., Varrot, A., Dauter, M., Brzozowski, A.M., Schülein, M., and Withers, S.G. (1998). Snapshots along an enzymatic reaction coordinate: analysis of a retaining  $\beta$ -glycoside hydrolase. **Biochemistry** 37: 11707-11713.
- Davies, G.J., Ducros, V.M.A., Varrot, A., and Zechel, D.L. (2003). Mapping the conformational itinerary of  $\beta$ -glycosidases by X-ray crystallography. **Biochem. Soc. Trans.** 31: 523-527.
- Duroux, L., Delmotte, F.M., Lancelin, J.M., Keravis, G., and Jay-Allemand, C. (1998). Insight into naphthoquinone metabolism:  $\beta$ -glucosidase-catalysed hydrolysis of hydrojuglone  $\beta$ -D-glucopyranoside. **Biochem J.** 333: 275-283.
- Ducros, V.M.A., Zechel, D.L., Murshudov, G.N., Gilbert, H.J., Szabo, L., Stoll, D., Withers, S.G., and Davies, G.J. (2002). Substrate distortion by a  $\beta$ -mannanase: snapshots of the Michaelis and covalent intermediate complexes suggest a  $B_{2,5}$  conformation for the transition-state. **Angew. Chem. Int. Ed.** 41: 2824-2827.
- Faure, D., Desair, J., Veijers, V., Bekri, M.A., Proost, P., Henrissat, B., and Vanderleyden, J. (1999). Growth of *Azospirillum irakense* KBCI on the aryl  $\beta$ -glucoside, salicin, requires either SalA or SalB. **J. Bacteriol.** 181: 3003-3009.
- Gloster, T.M., and Davies, G. (2010). Glycosidase inhibition: assessing mimicry of the transition state. **Org. Biomol. Chem.** 8: 305-320.
- Guerin, D.M., Lascombe, M.B., Costabel, M., Souchon, H., Lamzin, V., Beguin, P., and Alzari, P.M. (2002). Atomic (0.94 Å) resolution structure of an inverting glycosidase in complex with substrate. **J. Mol. Biol.** 316: 1061-1069.
- Harvey, A.J., Hrmova, M., and Fincher, G.B. (2001). Regulation of genes encoding  $\beta$ -D-glucan glucohydrolases in barley (*Hordeum vulgare* L.). **Physiol. Plant** 113: 108-120.
- Henrissat, B. (1991). A classification of glycosyl hydrolases based on amino acid sequence similarities. **Biochem. J.** 280: 309-316.

- Henrissat, B., and Bairoch, A. (1993). New families in the classification of glycosyl hydrolases based on amino acid sequence similarities. **Biochem. J.** 293: 781-788.
- Henrissat, B., and Davies, G. (1997). Structural and sequence-based classification of glycoside hydrolases. **Curr. Opin. Struct. Biol.** 7: 637-644.
- Hösel, W., Surholt, E., and Borgmann, E. (1978). Characterization of  $\beta$ -glucosidase isoenzymes possibly involved in lignifications from chick pea (*Cicer arietinum* L.) cell suspension culture. **Eur. J. Biochem.** 84: 487-492.
- Hrmova, M., Harvey, A.J., Wang, J., Shirley, N.J., Jones, G.P., Stone, B.A., Høj, P.B., and Fincher, G.B. (1996). Barley  $\beta$ -D-glucan exohydrolases with  $\beta$ -D-glucosidase activity: purification, characterization, and determination of primary structure from a cDNA clone. **J. Biol. Chem.** 271: 5277-5286.
- Hrmova, M., and Fincher, G.B. (1998). Barley  $\beta$ -D-glucan exohydrolases. Substrate specificity and kinetic properties. **Carbohydr. Res.** 305: 209-221.
- Hrmova, M., Varghese, J.N., Gori, R.D., Smith, B.J., Driguez, H., and Fincher, G.B. (2001). Catalytic mechanisms and reaction intermediates along the hydrolytic pathway of a plant  $\beta$ -D-glucan glucohydrolase. **Structure** 9: 1005-1016.
- Hrmova, M., Gori, R.D., Smith, B.J., Fairweather, J.K., Driguez, H., Varghese, J.N., and Fincher, G.B. (2002). Structural basis for broad substrate specificity in higher plant  $\beta$ -D-glucan glucohydrolases. **Plant Cell** 14: 1033-1052.
- Hrmova, M., Streltsov, V.A., Smith, B.J., Vasella, A., Varghese, J.N., and Fincher G.B. (2005). Structural rationale for low-nanomolar binding of transition state mimics to a family GH3  $\beta$ -D-glucan glucohydrolase from barley. **Biochemistry** 44: 16529-16539.
- Hrmova, M., Burton, R.A., Biely, P., Lahnstein, J., and Fincher, G.B. (2006). Hydrolysis of (1,4)- $\beta$ -D-mannans in barley (*Hordeum vulgare* L.) is mediated by the concerted

- action of (1,4)- $\beta$ -D-mannan endohydrolase and  $\beta$ -D-mannosidase. **Biochem. J.** 399: 77-90.
- Hughes, M.A, Brown, K., Pancoro, A., Murray, B.S., Oxtoby, E., and Hughes, J. (1992). A molecular and biochemical analysis of the structure of the cyanogenic  $\beta$ -glucosidase (linamarase) from cassava (*Manihot esculenta* Cranz.) **Arch Biochem Biophys.** 295: 273-279.
- Ketudat Cairns, J.R., and Esen, A. (2010).  $\beta$ -glucosidases. **Cell. Mol. Life Sci.** DOI 10.1007/s00018-010-0399-2.
- Koshland, D.E. (1953). Stereochemistry and the mechanism of enzymatic reactions. **Biol. Rev. Camb. Philos. Soc.** 28: 416-436.
- Kuntothom, T., Luang, S., Harvey, A.J., Fincher, G.B., Opassiri, R., Hrmova, M., and Ketudat Cairns, J.R. (2009). Rice family GH1 glycoside hydrolases with  $\beta$ -D-glucosidase and  $\beta$ -D-mannosidase activities. **Arch. Biochem. Biophys.** 491: 85-95.
- Leah, R., Kigel, J., Svendsen, I.B., and Mundy, J. (1995). Biochemical and molecular characterization of a barley seed  $\beta$ -glucosidase. **J. Biol. Chem.** 270: 15789-15797.
- Minami, Y., Kanafuji, T., and Miura, K. (1996). Purification and characterization of a  $\beta$ -glucosidase from *Polygonum tinctorium*, which catalyzes preferentially the hydrolysis of indican. **Biosci. Biotechnol. Biochem.** 60: 147-149.
- Mo, B., and Bewley, J.D. (2002).  $\beta$ -mannosidase (EC 3.2.1.25) activity during and following germination of tomato (*Lycopersicon esculentum* Mill.) seeds. Purification, cloning and characterization. **Planta.** 215: 141-152.
- Offen, W.A., Zechel, D.L., Withers, S.G., Gilbert, H.J., and Davies, G.J. (2009). Structure of the Michaelis complex of  $\beta$ -mannosidase, Man2A, provides insight into the conformational itinerary of mannoside hydrolysis. **Chem. Commun.** 14: 2484-2486

- Opassiri, R., Ketudat Cairns, J.R., Akiyama, T., Wara-Aswapati, O., Svasti, J., and Esen, A. (2003). Characterization of a rice  $\beta$ -glucosidase highly expressed in flower and germinating shoot. **Plant Sci.** 165: 627-638.
- Opassiri, R., Hua, Y., Wara-aswapati, O., Akiyama, T., Svasti, J., Esen, A., and Ketudat Cairns, J.R. (2004).  $\beta$ -glucosidase, exo- $\beta$ -glucanase and pyridoxine transglucosylase activities of rice BGlu1. **Biochem. J.** 379: 125-131.
- Opassiri, R., Pomthong, B., Onkoksoong, T., Akiyama, T., Esen, A., and Ketudat Cairns, J.R. (2006). Analysis of rice glycosyl hydrolase family 1 and expression of Os4bglu12  $\beta$ -glucosidase. **BMC Plant Biol.** 6.
- Pauling, L. (1946). Molecular architecture and biological reactions. **Chem. Eng. New.** 24: 1375-1377.
- Pauling, L. (1948). The nature of forces between large molecules of biological interest. **Nature** 161: 707-709.
- Pozzo, T., Pasten, J.L., Karlsson, E.N., and Logan, D.T. (2010). Structural and functional analyses of  $\beta$ -glucosidase 3B from *Thermotoga neapolitana*: A thermostable three-domain representative of glycoside hydrolase 3. **J. Mol. Biol.** 397: 724-739.
- Rempel, B.P., and Withers, S.G. (2008). Covalent inhibitors of glycosidases and their applications in biochemistry and biology. **Glycobiology** 18: 570-586.
- Sanz-Aparicio, J., Hermoso, J.A., Martínez-Ripoll, M., Lequerica, J.L., and Polaina, J. (1998). Crystal structure of  $\beta$ -glucosidase A from *Bacillus polymyxa*: insights into the catalytic activity in family 1 glycosyl hydrolases. **J. Mol. Biol.** 275: 491-502.
- Singh, A., Hayashi, K., Hoa, T.T., Kashiwagi, Y., and Tokuyasu, K. (1995). Research communication: construction and characterization of a chimeric  $\beta$ -glucosidase. **Biochem J.** 305: 715-719.
- Sulzenbacher, G., Driguez, H., Henrissat, B., Schülein, M., and Davies, G.J. (1996). Structure of the *Fusarium oxysporum* endoglucanase I with a nonhydrolyzable

- substrate analogue: substrate distortion gives rise to the preferred axial orientation for the leaving group. **Biochemistry** 35: 15280-15287.
- Svasti, J., Srisomsap, C., Techasakul, S., and Surarit, R. (1999). Dalcochinin-8-O- $\beta$ -D-glucoside and its  $\beta$ -glucosidase enzyme from *Dalbergia cochinchinensis*. **Phytochemistry** 50: 739-743.
- Tailford, L.E., Offen, W.A., Smith, N.L., Dumon, C., Morland, C., Gratien, J., Heck, M.P., Stick, R.V., Bleriot, Y., and Vassela, A. (2008). Structural and biochemical evidence for a boat-like transition state in  $\beta$ -mannosidases. **Nat. Chem. Biol.** 4: 306-312.
- Varghese, J.N., Hrmova, M., and Fincher, G.B. (1999). Three-dimensional structure of a barley  $\beta$ -D-glucan exohydrolase, a family 3 glycosyl hydrolase. **Structure** 7: 179-190.
- Vocadlo, D.J., and Davies, G.J. (2008). Mechanistic insights into glycosidase chemistry. **Curr. Opin. Chem. Biol.** 12: 539-555.
- Vroemen, S., Heldens, J., Boyd, C., Henrissat, B., and Keen, N.T. (1995). Cloning and characterization of the *bgxA* gene from *Erwinia chrysanthemi* D1 which encodes a  $\beta$ -glucosidase/xylosidase enzyme. **Mol. Gen. Genet.** 246: 465-477.
- Winkler, D.A. and Holan, G. (1989). Design of potential anti-HIV agents.1. Mannosidase inhibitors. **J. Med. Chem.** 32: 2084-2089.
- Xu, Z., Escamilla-Trevino, L.L., Zeng, L., Lalgondar, M., Bevan, D.R., Winkel, B.S.J., Mohamed, A., Cheng, C.L., Shih, M.C., Poulton, J.E., and Esen, A. (2004). Functional genomic analysis of *Arabidopsis thaliana* glycoside hydrolase family 1. **Plant Mol. Biol.** 55: 343-367.
- Zechel, D.L., and Withers, S.G. (2000). Glycosidase mechanisms: anatomy of a finely tuned catalyst. Glycosidase mechanisms: anatomy of a finely tuned catalyst. **Acc. Chem. Res.** 33: 11-18.

# CHAPTER II

## COMPLIMENTARY DNA CLONING, PROTEIN EXPRESSION AND CHARACTERIZATION OF RICE Os7BGlu26 $\beta$ -GLUCOSIDASE

### Abstract

Os7BGlu26 is a member of glycosyl hydrolase family 1 which is a  $\beta$ -glucosidase/ $\beta$ -mannosidase. Os7BGlu26 has 82% amino acid sequence identity to rHvBII  $\beta$ -glucosidase/ $\beta$ -mannosidase from barley, and they have exactly the same sequences at the conserved motifs TFNEP at the catalytic acid/base and LSENG at the catalytic nucleophile. Substrate specificity studies were conducted on Os7BGlu26 with synthetic and natural substrates. Os7BGlu26 hydrolysed 4NP- $\beta$ -D-mannopyranoside approximately 3-fold more rapidly than 4NP- $\beta$ -D-glucopyranoside. It is able to hydrolyse  $\beta$ -(1,4)-manno-oligosaccharides, and  $\beta$ -(1,2)-,  $\beta$ -(1,3)-,  $\beta$ -(1,4)-gluco-oligosaccharides, similar to rHvBII. However the activity of Os7BGlu26 to cellobiose was low, similar to Os3BGlu7 and not rHvBII. Os7BGlu26 also hydrolyses many important natural glycoside substrates including: the cyanogenic glucosides dhurrin, sambunigrin, D-amygdalin and prunasin; a monolignol glucoside, *p*-coumaryl alcohol glucoside; and a flavonol glucoside, quercetin-3-glucoside. Based on the natural substrates it hydrolyses, Os7BGlu26 functions may include cell wall degradation, lignification, secondary metabolite hydrolysis and defense.

## 2.1 Introduction

In rice (*Oryza sativa* L.), there are around 40 members of glycosyl hydrolase family 1 (GH1) (Opassiri *et al.*, 2006). When their protein sequences were aligned with other plant GH1 members to predict their properties, such as substrate specificity, the rice GH1 genes Os1BGlu1, Os3BGlu7, Os3BGlu8, Os7BGlu26 and Os12BGlu38 were in the cluster of  $\beta$ -mannosidases, including tomato  $\beta$ -mannosidase, and barley  $\beta$ -glucosidase/ $\beta$ -mannosidase (BGQ60, HvBII), as shown in Figure 2.1. Tomato  $\beta$ -mannosidase (EC 3.2.1.25) is highly expressed in the lateral and micropylar endosperm of germination seed. It is involved in the hydrolysis of galactomannans from the cell walls of the seed endosperm by hydrolysis of the oligomannans released by  $\beta$ -(1,4)-mannan endohydrolase (EC 3.2.1.78) (Mo and Bewley, 2002). Barley  $\beta$ -glucosidase (BGQ60, EC 3.2.1.21) from barley seeds (*Hordeum vulgare* L.) could hydrolyse 4NP- $\beta$ -D-mannopyranoside (4NPM) and 4NP- $\beta$ -D-glucopyranoside (4NPGlc), with relative activities of 55% and 47%, respectively, compared to cellobiose (Leah *et al.*, 1995). It also hydrolysed  $\beta$ -(1,2)-,  $\beta$ -(1,3)-, and  $\beta$ -(1,4)-gluco-oligosaccharides. Hrmova *et al.* (1996) also purified a barley  $\beta$ -glucosidase designated isoenzyme  $\beta$ II (HvBII) from germinated barley the N-terminal amino acid sequence of which was nearly identical to BGQ60. The substrate specificity of HvBII was similar to BGQ60 for  $\beta$ -(1,2)-,  $\beta$ -(1,3)-, and  $\beta$ -(1,4)-gluco-oligosaccharides hydrolysis (Hrmova *et al.*, 1996). In addition, HvBII hydrolysed 4NPM approximately 3-fold faster than 4NPGlc and also hydrolysed  $\beta$ -(1,4)-manno-oligosaccharides with degree of polymerization (DP) 2 to 6 (Hrmova *et al.*, 2006). Xu *et al.* (2004) reported that the *Arabidopsis thaliana*  $\beta$ -glucosidase BGLU44 also prefers to hydrolyse 4NPM approximately 2.5-fold more rapidly than 4NPGlc, and also hydrolyses  $\beta$ -(1,4)-manno-oligosaccharides (DP 2-6). Os3BGlu7 is the rice  $\beta$ -glucosidase in this group for which the most information is known, including gene expression (Opassiri *et al.*, 2003), biochemical properties (Opassiri *et al.*, 2003 and 2004) and the X-ray crystal structure (Chuenchor *et al.*,

2008). The Os3BGlu7 protein sequence shares 65% identity with HvBII, but they still have different substrate specificities, in that Os3BGlu7 prefers to hydrolyse 4NPGlc more than 4NPMan and prefers to hydrolyse cellotriose to cellobiose, in contrast to HvBII. Both enzymes also hydrolyse short chain laminari-oligosaccharides and long chain cello-oligosaccharides (Opassiri *et al.*, 2003 and 2004). Although Os3BGlu7 hydrolysed 4NPMan at one-tenth the rate of 4NPGlc, it can also release mannose from  $\beta$ -(1,4)-oligosaccharides (Kuntothom *et al.*, 2009). Previously Kuntothom *et al.* (2009) cloned a cDNA corresponding to HvBII (Hrmova *et al.*, 1998) from germinating barley seeds and expressed it in the *E.coli*. This recombinant protein sequence was more similar to HvBII than BGQ60 and was designed as rHvBII. rHvBII preferred to hydrolyse 4NPMan more than 4NPGlc. Its rate of hydrolysis of manno-oligosaccharides was higher than that of Os3BGlu7 (Kuntothom *et al.*, 2009). The preference of rHvBII was similar to Os3BGlu7 for laminari-oligosaccharides, but different for cello-oligosaccharides, in that it hydrolysed cellobiose better than cellotriose.

Kuntothom *et al.* (2009) re-analysed the phylogenetic tree of GH1 members in the  $\beta$ -mannosidase-like cluster to tomato  $\beta$ -mannosidase, barley rHvBII, BGLU43 and BGLU44  $\beta$ -glucosidases from *Arabidopsis thaliana* in Figure 2.2. Os7BGlu26 is a rice family 1 glycoside hydrolase more similar to rHvBII than to Os3BGlu7, and was predicted to have substrate specificity more similar to rHvBII than to Os3BGlu7. In this study, DNA cloning, protein expression and characterization of recombinant Os7BGlu26 expressed in *E. coli* is described.



**Figure 2.1** Relationship between rice and other plant GH1 protein sequences described by a phylogenetic tree rooted by Os11Bglu36. The tree was produced by the neighbor joining method and analysed with 1000 bootstrap replicates. The internal branches supported by a maximum parsimony tree made from the same sequences are shown as bold lines. The sequences other than rice include: ME AAB71381, *Manihot esculenta* linamarase; RSMYr BAB17226, *Raphanus sativus* myrosinase; BJMYr AAG54074, *Brassica juncea* myrosinase; BN CAA57913, *Brassica napus* zeatin-O-glucoside-degrading  $\beta$ -glucosidase; HB AAO49267, *Hevea brasiliensis* rubber tree  $\beta$ -glucosidase; CS BAA11831, *Costus speciosus* furostanol glycoside 26-O- $\beta$ -glucosidase (F26G); PS AAL39079 *Prunus serotina*

prunasin hydrolase isoform PH B precursor; PA AAA91166, *Prunus avium* ripening fruit  $\beta$ -glucosidase; TR CAA40057, *Trifolium repens* white clover linamarase; CA CAC08209, *Cicer arietinum* epicotyl  $\beta$ -glucosidase with expression modified by osmotic stress; DC AAF04007, *Dalbergia cochinchinensis* dalcochinin 8'-O- $\beta$ -glucoside  $\beta$ -glucosidase; PT BAA78708, *Polygonum tinctorium*  $\beta$ -glucosidase; DL CAB38854, *Digitalis lanata* cardenolide 16-O-glucohydrolase; OE AAL93619, *Olea europaea* subsp. *europaea*  $\beta$ -glucosidase; CR AAF28800, *Catharanthus roseus* strictosidine  $\beta$ -glucosidase; RS AAF03675, *Rauvolfia serpentina* raucaffricine-O- $\beta$ -D-glucosidase; CP AAG25897, *Cucurbita pepo* silverleaf whitefly induced protein 3; AS CAA55196, *Avena sativa*  $\beta$ -glucosidase; SC AAG00614, *Secale cereale*  $\beta$ -glucosidase; ZM AAB03266, *Zea mays* cytokinin  $\beta$ -glucosidase; ZM AAD09850, *Zea mays*  $\beta$ -glucosidase; SB AAC49177, *Sorghum bicolor* dhurrinase; LE AAL37714, *Lycopersicon esculentum*  $\beta$ -mannosidase; HV AAA87339, barley BGQ60  $\beta$ -glucosidase; HB AAP51059, *Hevea brasiliensis* latex cyanogenic  $\beta$ -glucosidase; PC AAC69619 *Pinus contorta* coniferin  $\beta$ -glucosidase; GM AAL92115, *Glycine max* hydroxyisourate hydrolase; CS BAC78656, *Camellia sinensis*  $\beta$ -primeverosidase (Opassiri *et al.*, 2006).

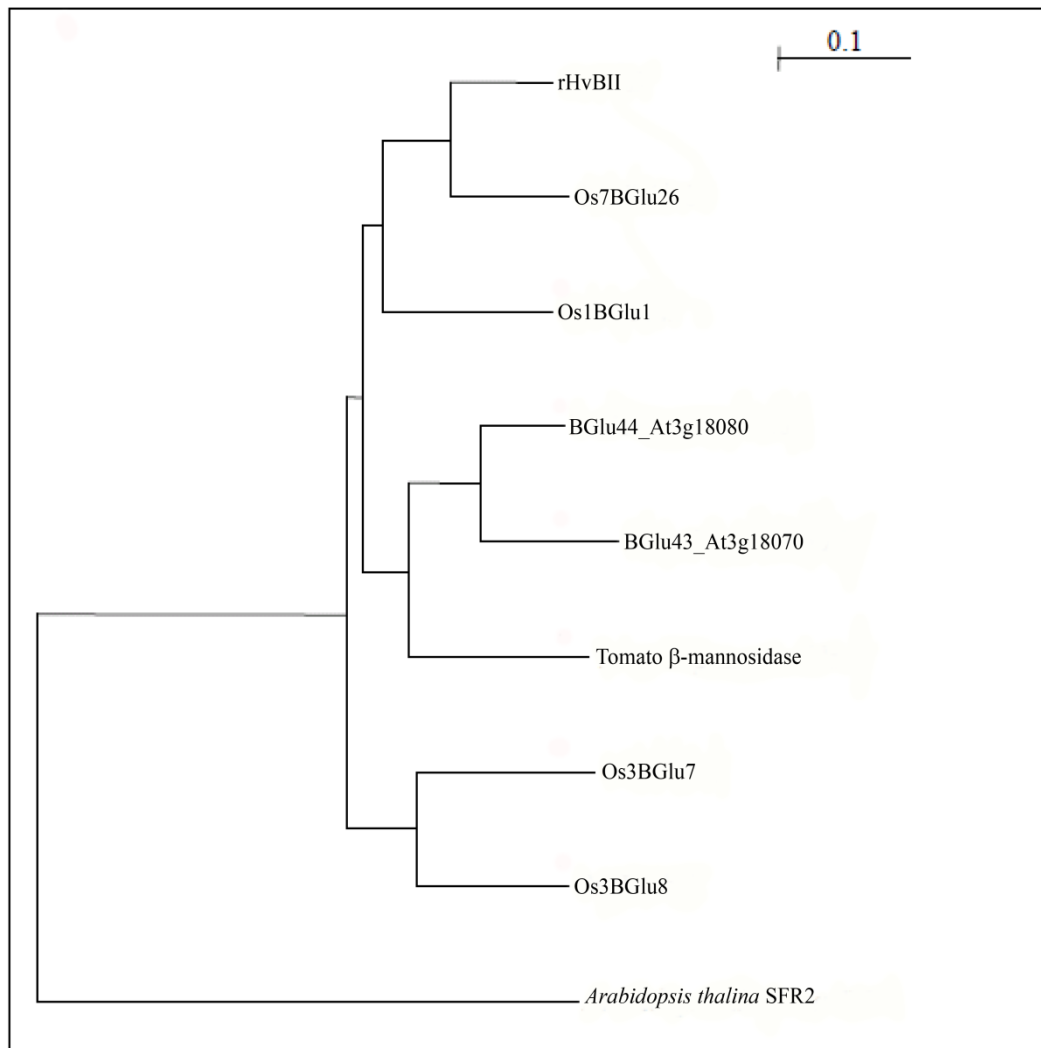


**Figure 2.2** Phylogenetic tree of plant  $\beta$ -D-mannosidases with rHvBII (GenBank AC EU807965), Os1BGlu1 (AC AK069177), Os3BGlu7 (AC U28047), Os3BGlu8 (AC AK120790), and Os7BGlu26 (AC AK068499) rice  $\beta$ -D-glucosidases from Kuntothom *et al.* (2009). *Arabidopsis thaliana* SFR2 (AC At3g06510) is included as an outgroup. Plant  $\beta$ -D-mannosidases include *Arabidopsis* BGlu44 and its sister isozyme BGlu43, and tomato  $\beta$ -D-mannosidase (AC AAL37714).

## 2.2 Materials and methods

### 2.2.1 Plasmids, bacterial strains and plant

Plasmids for this works included pENTR<sup>TM</sup>/D-TOPO (Invitrogen) for cloning, and pET32a(+)/DEST for expression plasmid (Opassiri *et al.*, 2006). The *E. coli* cell strains used included DH5 $\alpha$  and TOP10 for cloning, and Origami(DE3) as an expression host cell. Rice (*Oryza sativa* L., cv. KDML 105) was used as a source of Os7BGlu26 mRNA.

**Table 2.1** Recombinant plasmids used for Os7BGlu26 cloning and expression.

| Recombinant Plasmid DNA | Antibiotic resistance      | Total size (kb) |
|-------------------------|----------------------------|-----------------|
| pENTR/D-TOPO            | Kanamycin (50 $\mu$ g/ml)  | ~2.6            |
| pET32a/DEST             | Ampicillin (50 $\mu$ g/ml) | ~6.0            |

**Table 2.2** Bacteria strain.

| Bacteria strain | Antibiotic resistance                                       | Genotype   |
|-----------------|---|--|
| TOP10           | none  | F <sup>-</sup> <i>mcrA</i> $\Delta$ ( <i>mrr-hsdRMS-mcrBC</i> ) $\Phi$ 80 <i>lacZ</i> $\Delta$ M15 $\Delta$ <i>lacX74</i> <i>recA1</i> <i>araD139</i> $\Delta$ ( <i>araleu</i> )7697 <i>galU</i> <i>galK</i> <i>rpsL</i> (Str <sup>R</sup> ) <i>endA1</i> <i>nupG</i> $\lambda$ -  |
| DH5 $\alpha$    | none  | F <sup>-</sup> <i>endA1</i> <i>glnV44</i> <i>thi-1</i> <i>recA1</i> <i>relA1</i> <i>gyrA96</i> <i>deoR</i> <i>nupG</i> 80 <i>dlacZ</i> $\Delta$ M15 $\Delta$ ( <i>lacZYA-argF</i> )U169, <i>hsdR17</i> (r <sub>K</sub> <sup>-</sup> m <sub>K</sub> <sup>+</sup> ) $\lambda$ -  |
| Origami(DE3)    | Kanamycin (15 $\mu$ g/ml),<br>Tetracyclin (12.5 $\mu$ g/ml) | $\Delta$ ( <i>ara-leu</i> )7697 $\Delta$ <i>lacX74</i> $\Delta$ <i>phoA</i> <i>PvuII</i> <i>phoR</i> <i>araD139</i> <i>ahpC</i> <i>galE</i> <i>galK</i> <i>rpsL</i> F'[ <i>lac+</i> <i>lacIq</i> <i>pro</i> ] (DE3) <i>gor522::Tn10</i> <i>trxB</i> pLacI (Cam <sup>R</sup> , Kan <sup>R</sup> , Str <sup>R</sup> , Tet <sup>R</sup> ) |

## 2.2.2 General methods

### 2.2.2.1 Preparation of competent *Escherichia coli* strain DH5 $\alpha$ and Origami(DE3) and DNA transformation

Bacteria glycerol stock was streaked onto a Lennox broth (LB, 10 g/l tryptone, 5 g/l yeast extract, 5 g/l sodium chloride) agar plate. A single colony was picked into 5 ml LB media containing 15  $\mu$ g/ml kanamycin and 12.5  $\mu$ g/ml tetracycline for Origami(DE3) or without antibiotic for DH5 $\alpha$ . The cells were grown at 37°C for 16 to 18 h with shaking at 220 rpm. Then, 0.5 ml of starter culture was inoculated into 50 ml LB in a 250 ml flask and incubated at 37°C with shaking until the OD<sub>600</sub> reached 0.3-0.4. The culture was cooled on ice for 15 min, then transferred to pre-cooled centrifuge tubes, and the cells were collected by centrifugation at 1500xg for 5 min. Cells were gently and slowly resuspended with 20 ml of cold 0.1 M CaCl<sub>2</sub> and placed on ice for 15 min. The cells were centrifuged as before and resuspended once again in cold 0.1 M CaCl<sub>2</sub> for 15 min. Finally, the cells were resuspended with 0.5 ml of cold 0.1 M CaCl<sub>2</sub> containing 15% glycerol, and placed on ice for 1 h. Then, they were dispensed in 50  $\mu$ l aliquots in cold microcentrifuge tubes and stored at -80°C.

Circular plasmid DNA (50 ng) was added into the 50  $\mu$ l of competent cells, mixed by tapping and immediately place on ice for 30 min. The cells were heat shocked at 42°C for exactly 45 second and then immediately put on ice for 2-3 min. LB medium was added into the cell mixture and the tube was incubated in a 37°C shaker for 1 h. Fifty to two hundred microlitres of the cells were spread on a LB plate containing antibiotic and incubated at 37°C overnight.

### **2.2.2.2 Isolation of recombinant plasmid by alkaline lysis**

The cell pellet in sterile microcentrifuge tube was resuspended with 100  $\mu$ l of lysis buffer (0.05 M Tris-HCl pH 8.0, 0.01 M EDTA, and 0.05 M glucose) by vortexing. Two hundred microlitres of fresh 1% SDS/0.2 M NaOH solution was added into the resuspended solution and gently mixed by inverting. Then, 150  $\mu$ l of cold 3 M potassium acetate, pH 4.8, was added and mixed in by inverting briefly. The cell lysate was incubated on ice for 3-5 min. The mixture was centrifuged at 12,000xg, 4°C for 5 min. The supernatant was transferred into a new sterile microcentrifuge tube and 600  $\mu$ l absolute ethanol was added to precipitate the DNA at 4°C for 10 min. The precipitated DNA was centrifuged at 12,000xg, 4°C for 5 min. The DNA pellet was washed with 500  $\mu$ l of 70% ethanol and centrifuged at 12,000xg, 4°C for 5 min. All the solution was removed by pipetting and the DNA was dried by incubating it at 37°C for 10 min. The pellet was dissolved with 100  $\mu$ l of TE buffer (10 mM Tris-HCl, 1 mM EDTA, pH 8.0) containing 20  $\mu$ g/ml RNase A and incubated at 37°C for 10 min. The plasmid DNA was precipitated with 70  $\mu$ l of 20% (w/v) PEG 6000/2.5 M NaCl solution and incubated on ice for 1 h. Then, the precipitated plasmid was centrifuged at 12,000xg, 4°C for 5 min. The pellet was washed with 500  $\mu$ l of 70% ethanol and centrifuged at 12,000xg, 4°C for 5 min. The DNA was dried as described above and dissolved with 20  $\mu$ l of TE buffer.

### **2.2.2.3 Protein analysis by sodium dodecyl sulfate polyacrylamide gel electrophoresis (SDS-PAGE)**

Protein was separated by size with SDS-PAGE according to the method of Laemmli (1970). The 12% separating gel was prepared by mixing of 3.3 ml of distilled water, 2.5 ml of 1.5 M Tris-HCl, pH 8.8, 4 ml of 30% acrylamide/bisacrylamide solution, 100  $\mu$ l of 10% (w/v) SDS, 100  $\mu$ l of 10% (w/v) ammonium persulfate, and 4  $\mu$ l TEMED. The 5% stacking gel was prepared by mixing of 3.4 ml of distilled water, 0.63 ml of 0.5 M Tris-

HCl, pH 6.8, 0.83 ml of 30% acrylamide/bisacrylamide solution, 50  $\mu$ l of 10% (w/v) SDS, 50  $\mu$ l of 10% (w/v) ammonium persulfate, and 5  $\mu$ l of TEMED. Sixteen microlitres of protein sample was mixed with 4  $\mu$ l of 5x denaturing and reducing sample buffer (2.5 M Tris-HCl pH 6.8, 10% SDS, 50% glycerol, 0.5% bromophenol blue, 4% 2-mercaptoethanol) and boiled at 100°C for 5 min. The sample was centrifuged at 10,000xg for 5 min to separate the insoluble protein. Soluble protein was loaded onto the gel under running buffer (25 mM Tris, 192 mM glycine, 0.1% SDS, pH 7.5) and placed in an electric field at 150 volt for 1 h 30 min. The protein bands were detected with Coomassie brilliant blue staining solution (0.1% Coomassie brilliant blue R-250, 40% methanol, 10% glacial acetic acid, 50% distilled water) and the blue background washed out with destaining solution (40% methanol, 10% glacial acetic acid, 50% distilled water). The migration distance of the protein band was compared to the low molecular weight calibration electrophoresis standards (GE Healthcare).

### **2.2.3 Molecular cloning, expression, purification and characterization of rice $\beta$ -glucosidase Os7BGlu26.**

#### **2.2.3.1 RNA isolation**

Total mRNA was extracted with the Spectrum<sup>TM</sup> Plant Total RNA Kit (Sigma). Seven-day-old rice (*O. sativa* L., cv. KDML105) seedlings were ground to a fine power in liquid nitrogen using a mortar and pestle. Approximately 100 mg of tissue powder was quickly put into a 2 ml microcentrifuge tube. The tissue was lysed by adding 500  $\mu$ l of lysis solution/2-mercaptoethanol mixture, vortexing immediately and incubating at room temperature for 3-5 min. The supernatant was collected by centrifugation at 12,000xg for 3 min. The lysate supernatant was pipetted into a filtration column and centrifuged at 12,000xg for 1 min. Five hundred microlitres of binding solution was added to the filtered lysate and mixed immediately and thoroughly by vortexing. Then 700  $\mu$ l of the mixture was pipetted into a binding column and centrifuged at 12,000xg for 1 min. The flow-through

liquid was discarded and the binding column was centrifuged at 12,000xg for 1 min again. The column was washed with wash solution 1, wash solution 2 and the diluted wash solution 2, respectively. After that the column was transferred to a new collection tube and 50 µl of elution solution was added at the center of the column, which was then left to sit for 1 min at room temperature. Total RNA was collected by centrifuged at 12,000xg for 1 min and stored at -80°C or used immediately for reverse transcription and polymerase chain reaction (RT-PCR).

#### **2.2.3.2 cDNA synthesis by reverse transcriptase**

First-stand cDNA was synthesized with the SuperScript™ III First-Strand Synthesis System for RT-PCR (Invitrogen). First 2-5 µg of total RNA was treated with DNase in a reaction containing 1 µl DNase and 1 µl 10X buffer, adjusted to a final volume of 10 µl with DEPC-treated water, at 37°C for 30 min. DNase was inactivated by adding 1 µl DNase buffer stop and incubating at 65°C for 10 min. Next, 1 µl of 50 µM Oligo(dT)<sub>20</sub> primer and 1 µl of 10 mM dNTP mix were added to the DNase-treated RNA solution, which was then incubated at 65°C for 5 min and immediately placed on ice at least 1 min. Then, 2 µl of 10X RT buffer, 4 µl of 25 mM MgCl<sub>2</sub>, 2 µl of 0.1 M DTT, 1 µl of 40 U/µl RNase OUT and 1 µl of 200 U/µl SuperScript III RT were added into the RNA primer mixture and incubated at 50°C for 50 min to synthesize cDNA. To terminate the process, the reaction was incubated at 85°C for 5 min and then transferred to ice. After that, the mRNA template was digested with 1 µl of RNase H at 37°C for 20 min. The cDNA synthesis reaction was immediately used for PCR.

### 2.2.3.3 DNA cloning of mature Os7BGlu26

The full-length Os7BGlu26 cDNA was amplified from the RT product with the AK068499Nter and AK068499 3'UTRr primers and *Pfu* DNA polymerase using the temperature cycling shown in Table 2.3. The cDNA encoding the predicted mature Os7BGlu26 isoenzyme was amplified from the initial PCR product with the AK068499MatNf and AK068499 3'UTRr primers and *Pfu* DNA polymerase using the temperature cycling shown in Table 2.4.

**Table 2.3** Primers for Os7BGlu26 amplification.

| Primer          | sequence (5'→3')       | T <sub>m</sub> (°C) |
|-----------------|------------------------|---------------------|
| AK068499Nter    | ACATGAGGAAATTCATAGCAGC | 70                  |
| AK068499MatNf   | CACCTACTGGCTCAACCCGGAG | 60                  |
| AK068499 3'UTRr | TAGTCCCTTCTGTCAGCTC    | 56                  |

**Table 2.4** Cycling parameters for Os7BGlu26 amplification.

| Segment | Cycles | Temperature            | Time   |
|---------|--------|------------------------|--------|
| 1       | 1      | 95°C                   | 4 min  |
| 2       | 30     | 95°C                   | 30 sec |
|         |        | Annealing temperature* | 30 sec |
|         |        | 72°C                   | 4 min  |
| 3       | 1      | 72°C                   | 7 min  |

\* The annealing temperatures for amplification of the full-length and mature protein coding regions of the Os7BGlu26 gene cDNA were 53.8°C and 62.7°C, respectively.

The PCR product was analysed on a 1% agarose gel. The expected band (1.5 kb) was purified from the agarose gel by the Perfectprep Gel Cleanup Kit (Eppendorf). Purified PCR product was cloned into pENTR<sup>TM</sup>/D-TOPO Gateway® entry vector (Invitrogen) by mixing 5 ng PCR product per 1 µl of 15-20 ng vector and incubating at 22-23°C for 16-18 h. The reaction (2.5 µl) was transformed into TOP10 competent cells (Invitrogen) and selected on a 15 µg/ml kanamycin LB agar plate. The entry clone size (~4.3 kb) was cut checked with *EcoRI* restriction endonuclease enzyme. Then, the Os7BGlu26 cDNA was recombined into the pET32a/DEST destination vector with Gateway® LR clonase (Invitrogen) using 75 ng entry clone per 150 ng destination vector, and the reaction was incubated at 25°C for 18 h. A 2.5 µl aliquot of the reaction was transformed into DH5α competent cells and plasmid-containing cells were selected on a 50 µg/ml ampicillin LB agar plate. The recombinant expression vector (~8 kb) was cut checked within the insert gene and the plasmid with *PstI* restriction endonuclease and DNA sequencing was done at Macrogen (Korea).

#### **2.2.3.4 Expression of Os7BGlu26**

The circular recombinant pET3a/DEST plasmid containing the Os7BGlu26 cDNA (pET3a/DEST/Os7BGlu26) was transformed into *E. coli* Origami(DE3) competent cells by heat shock and the cells were selected on an LB plate containing 15 µg/ml kanamycin, 12.5 µg/ml tetracycline and 50 µg/ml ampicillin at 37°C overnight. One colony of transformed cells, was picked into 5 ml LB liquid media containing the same antibiotics and grown at 37°C overnight. The starter culture was added to a 1:100 dilution to a large scale culture medium and grown continuously at 37°C with shaking at 220 rpm until the OD<sub>600</sub> reached 0.6. Protein expression was induced with 0.4 mM IPTG (final concentration) at 20°C for 16-18 h. Cells were collected by centrifugation at 4800xg for 10 min at 4°C and the pellet was stored at -80°C.

### 2.2.3.5 Purification of Os7BGlu26

The frozen pellet was thawed at room temperature. Cells were resuspended with extraction buffer (20 mM Tris-HCl, pH 8.0, 200 µg/ml lysozyme, 1% Triton-X100, 1 mM phenylmethylsulfonylfluoride (PMSF), 0.25 mg/ml DNase I and 0.1 mg/ml soybean trypsin inhibitor) and incubated at room temperature for 30 min. Soluble protein was separated from cell debris by centrifugation at 12,000xg for 10 min at 4°C. Recombinant Os7BGlu26 was purified with 3 steps. First, crude protein was immediately mixed with pre-equilibrated Ni<sup>2+</sup> (IMAC) resin with equilibration buffer (20 mM Tris-HCl, pH 8.0, and 150 mM NaCl) at 4°C for 30 min. Then the resin with crude protein was loaded into a column and unbound proteins were washed out with 10 column volumes (CV) of wash buffer 1 (10 mM imidazole in equilibration buffer) and 5 CV of wash buffer 2 (20 mM imidazole in equilibration buffer), respectively. Finally recombinant protein was eluted with elution buffer (250 mM imidazole in equilibration buffer). The fractions with activity were pooled and imidazole removed by dialysis with 50 mM Tris-HCl, pH 8.0, at 4°C. Next, the recombinant protein was loaded onto a Q-sepharose column (2 ml) pre-equilibrated with 50 mM Tris-HCl, pH 8.0, with a flow rate of 0.5 ml/min and unbound protein was washed from the column with 10 CV of 50 mM Tris-HCl, pH 8.0. Recombinant Os7BGlu26 was eluted with a linear gradient of 0-0.3 M NaCl in 50 mM Tris-HCl, pH 8.0, with the same flow rate. The fractions containing activity to hydrolyse 4NPGlc were pooled and concentrated with a 30 kDa molecular-weight cutoff ultrafiltration membrane. Then, 0.5-1 ml of concentrated protein was loaded onto an S200 gel filtration column, run at a flow rate of 0.3 ml/min and eluted with 50 mM Tris-HCl, pH 8.0, containing 150 mM NaCl. Finally, protein fractions were pooled and kept on ice.

### **2.2.3.6 Determination of the optimal pH and temperature for Os7BGlu26**

The optimum pH of Os7BGlu26 was determined in 140  $\mu$ l of reaction volume containing 1 mM 4NPGlc substrate in 50 mM buffers with pH in the range between 3.0 to 10.0 (citrate buffer, pH 3.0-4.5, sodium acetate buffer, pH 4.5-7.0, and Tris-HCl buffer, pH 7.0-10.0). The reaction was incubated at 30°C for 30 min and then 100  $\mu$ l of 2 M sodium carbonate was added to stop the reaction. Enzyme activity was measured as 4-nitrophenol (4NP) released, based on the absorbance at 405 nm. The optimum temperature was determined at various temperatures from 10°C to 80°C. The enzyme activity was assayed against 1 mM 4NPGlc in the 50 mM sodium acetate, pH 4.5, for 30 min. Then the reaction was stopped by adding 100  $\mu$ l of 2 M sodium carbonate and the 4-nitrophenol released was measured as described above.

### **2.2.3.7 Substrate specificity of Os7BGlu26**

The substrate specificity of Os7BGlu26 was determined by testing hydrolysis of natural and synthetic substrates. The reaction was set in volumes of 140  $\mu$ l for synthetic substrates and 50  $\mu$ l for natural substrates, including 1 mM substrates in 50 mM sodium acetate, pH 4.5, at 30°C. The hydrolysis of synthetic substrates was detected as 4NP release (as in section 2.2.3.6). The reactions with natural substrates were stopped by boiling at 100°C for 5 min. The hydrolysis of natural substrate was detected by thin layer chromatography (TLC) or the glucose oxidase/peroxidase (PGO) coupled assay. For thin layer chromatography, the reactions were dried by speed vac and each redissolved with 5  $\mu$ l of methanol. Two to five microlitres of dissolved reaction was spotted on a silica gel-coated F<sub>254</sub> aluminium plates and developed in the solvent of ethyl acetate: acetic acid: water (3:2:1). The TLC plate was coated with 10% sulfuric in methanol and heated at 120°C until the product spot was observed. For the PGO assay, 50  $\mu$ l of reaction was transferred to a

microtiter plate well containing 50  $\mu$ l of 1 mg/ml 2,2'-azinobis(3-ethylbenzthiazolinesulfonic acid) (ABTS), and 100  $\mu$ l of PGO enzyme. The PGO reaction assay was incubated at 37°C for 30 min. The glucose release was measured as the absorbance at 405 nm.

#### **2.2.3.8 Kinetic parameter determination of Os7BGlu26**

Kinetic parameters of Os7BGlu26 were determined with 4NPGlc, 4NPMAN, cello-oligosaccharides (DP 2-6) and laminari-oligosaccharides (DP 2-3). The initial velocity ( $V_o$ ) was determined by measuring the enzyme activity at different time points for 10 to 60 min, depending on the individual substrates used. The amount of Os7BGlu26 used was between 1.64  $\mu$ mole and 5.2  $\mu$ mole and the substrate concentrations ranged from approximately  $1/3 K_M$  to  $3 K_M$ . The  $K_M$  and  $V_{max}$  values were calculated by fitting the rate of product formation and substrate concentrations in nonlinear regression of the Michaelis-Menten curves with Grafit 5.0 (Erithacus Software, Horley, Surrey, UK). The  $k_{cat}$  was calculated by dividing the maximum velocity ( $V_{max}$ ) by the total amount of enzyme.

### **2.3 Results**

#### **2.3.1 Cloning and expression of Os7BGlu26 $\beta$ -glucosidase**

In the National Center for Biotechnology Information (NCBI), a cDNA (1897 bases) of rice (*Oryza sativa* L. ssp. Japonica cv. Nipponbare) similar to barley HvBII  $\beta$ -mannosidase has been assigned the GenBank Accession No. AK068499. The AK068499 cDNA contains an intron, as shown in Figure 2.3, and could not be used to express protein in *E. coli* or *P. pastoris* (data not shown). Thus, the cDNA without the intron was amplified by RT-PCR from total mRNA of 7-day-old rice (*Oryza sativa* L., cv. KDML105) seedlings with primers designed from the AK068499 cDNA sequence. First, a cDNA encoding the Os7BGlu26 precursor was amplified with the AK068499Nter and AK068499 3'UTRr

primers, and then this cDNA was used as the template to amplify the Os7BGlu26 cDNA encoding the predicted mature protein with the AK068499MatNf and AK068499 3'UTRr primers, as shown in Figure 2.4. This cDNA lacked the intron found in the AK068499 sequence and was otherwise different from AK068499 at two nucleotides (Figure 2.3), which led to an amino acid difference at one position (Figure 2.5). Since this gave a contiguous protein-coding region, it could be used to produce protein that was similar to GH1  $\beta$ -mannosidases (Figure 2.6).

The cDNA encoding mature Os7BGlu26 (GenBank Accession No. EU835514) containing part of the 3' untranslated region (bases 1452-1709, which were incubated simply for ease of cloning) was inserted into the pET32a/DEST expression vector to express in the *E. coli* strain Origami(DE3). The cell containing this construct produced Os7BGlu26 as thioredoxin and 6xhistidine-tag fusion protein when induced with 0.4 mM IPTG at 20°C for 16 h. The protein expression pattern was analysed by SDS-PAGE.

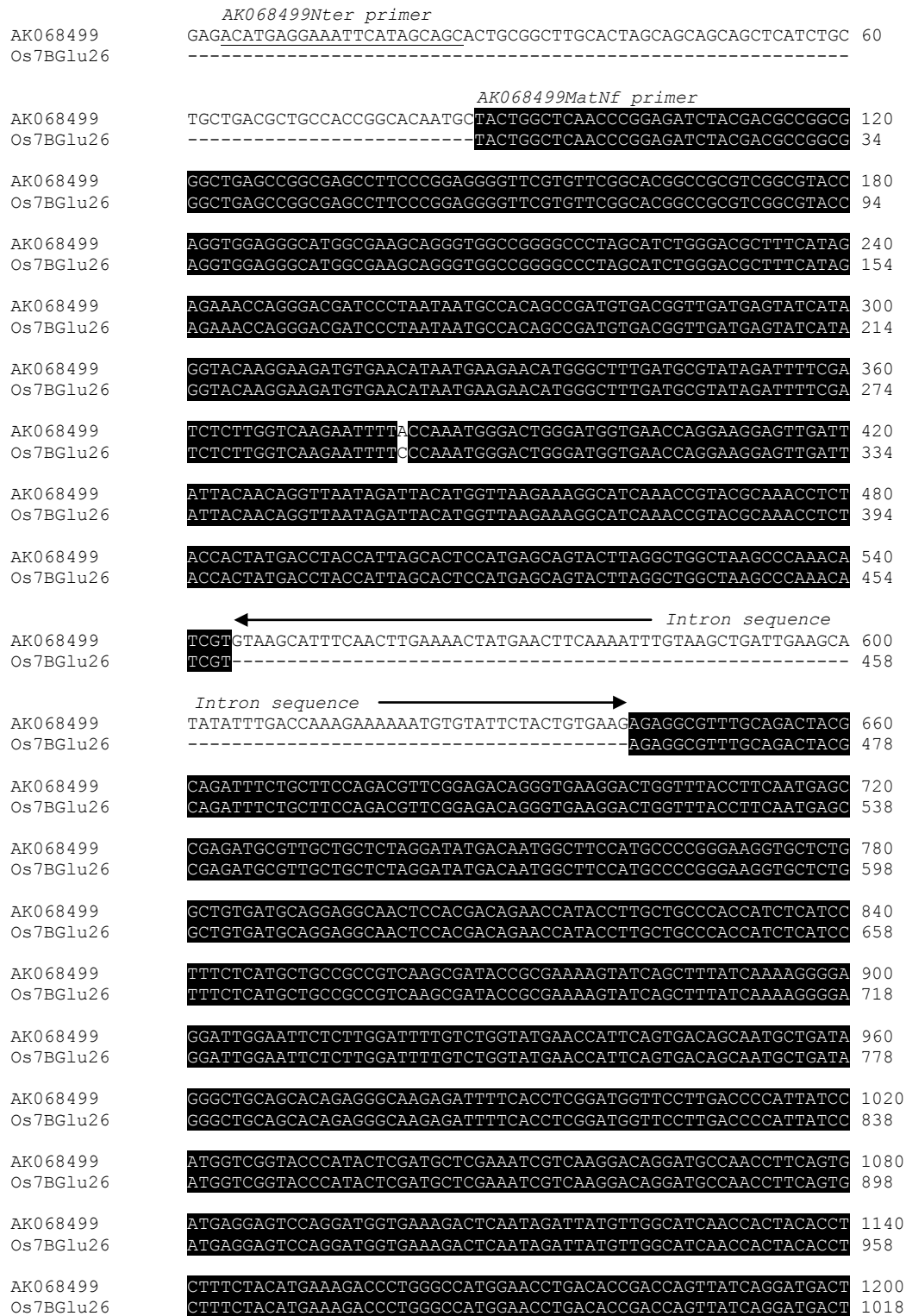


**Figure 2.3** Alignment of the AK068499 and Os7BGlu26 cDNA sequences. Primers designed for Os7BGlu26 amplification are indicated as underlined characters, the intron region in AK068499 is indicated between the arrows. The cDNA encoding the mature Os7BGlu26 protein is indicated in black highlight where the sequences are identical. They are different by 2 nucleotides.

|           |  |      |
|-----------|--|------|
| AK068499  | <b>GGCATGTTGGGTTTGCCTATGAACGAAACGGCGTGCCCATGGAGCTCAAGCAAACCTCT</b>           | 1260 |
| Os7BGlu26 | <b>GGCATGTTGGGTTTGCCTATGAACGAAACGGCGTGCCCATGGAGCTCAAGCAAACCTCT</b>           | 1078 |
| AK068499  | <b>ACTGGCTTTACATTGTGCCATGGGGAATCAACAAGGCTGTGACCTATGTAAAGGAAACAT</b>          | 1320 |
| Os7BGlu26 | <b>ACTGGCTTTACATTGTGCCATGGGGAATCAACAAGGCTGTGACCTATGTAAAGGAAACAT</b>          | 1138 |
| AK068499  | <b>ATGGAACCCCTACAATGATCCTTTCTGAAAATGGTATGGACCAACCTGGCAACGTCAGTA</b>          | 1380 |
| Os7BGlu26 | <b>ATGGAACCCCTACAATGATCCTTTCTGAAAATGGTATGGACCAACCTGGCAACGTCAGTA</b>          | 1198 |
| AK068499  | <b>TCACTCAGGGTGTGCATGATACAGTAAGAATCAGATACTACAGAACTACATCACTGAGC</b>           | 1440 |
| Os7BGlu26 | <b>TCACTCAGGGTGTGCATGATACAGTAAGAATCAGATACTACAGAACTACATCACTGAGC</b>           | 1258 |
| AK068499  | <b>TCAAGAAGCGGATAGACGATGGTGCCAAAGTGATTGGATACTTTGCTTGCTCATTGCTTG</b>          | 1500 |
| Os7BGlu26 | <b>TCAAGAAGCGGATAGACGATGGTGCCAAAGTGATTGGATACTTTGCTTGCTCATTGCTTG</b>          | 1318 |
| AK068499  | <b>ACAACCTTCGAGTGGAGGCTCGGGTACACTTCCCCTTTTGGCATCGTCTACGTGGACTACA</b>         | 1560 |
| Os7BGlu26 | <b>ACAACCTTCGAGTGGAGGCTCGGGTACACTTCCCCTTTTGGCATCGTCTACGTGGACTACA</b>         | 1378 |
| AK068499  | <b>AGACGCTAAAGAGGTACCCCAAGGACTCA</b> <u>AGCTTTCTGGTTCAAGAACATGCTCTCCAGTA</u> | 1620 |
| Os7BGlu26 | <b>AGACGCTAAAGAGGTACCCCAAGGACTCA</b> <u>AGCTTTCTGGTTCAAGAACATGCTCTCCAGTA</u> | 1438 |
| AK068499  | <b>AGAAGAGGAACTAA</b> <u>AGTATGCAGACAAAAGGATCAAGCTGTGAAAGCCTCAAAGGCTTCC</u>  | 1680 |
| Os7BGlu26 | <b>AGAAGAGGAACTAA</b> <u>AGTATGCAGACAAAAGGATCAAGCTGTGAAAGCCTCAAAGGCTTCC</u>  | 1498 |
| AK068499  | ACTGTCAGATTTCAGAACAAGCTAACTCTAGCGTATGCTCATCGTAGCGGTTAGTTTA                   | 1740 |
| Os7BGlu26 | ACTGTCAGATTTCAGAACAAGCTAACTCTAGCGTATGCTCATCTTAGCACGTTAGCCTA                  | 1558 |
| AK068499  | GCTTTAGTTATATGTGAAAAACAACCAATGTGGAGATTGGTAGCTTCACTAGCTTCTGCA                 | 1800 |
| Os7BGlu26 | GCTTTAGTTATATGTGAAAAACAACCAATGTGGAGATTGGTAGCTTCACTAGCTTCTGCA                 | 1618 |
| AK068499  | ACAGAAGGAGAAATAAATGGATTGAACTTCAATACAGATTTGTTTCATCAGAACCGTAGGC                | 1860 |
| Os7BGlu26 | ACAG---GAGAAATAAATGGATTGAACTTCAATACAGATTTGTTTCATCAGAACCGTAGGC                | 1675 |
|           | <i>AK068499 3'UTRr primer</i>  |      |
| AK068499  | TATTTGTACAATAAAGAGCTGACAGAAGGGACTATTC  | 1897 |
| Os7BGlu26 | TATTTGTACAATGAAGAGCTGACAGAAGGGACTA---  | 1709 |

**Figure 2.3** (Continued) Alignment of the AK068499 and Os7BGlu26 cDNA sequences.

Primers designed for Os7BGlu26 amplification are indicated as underlined characters, the intron region in AK068499 is indicated between the arrows. The cDNA encoding the mature Os7BGlu26 protein is indicated in black highlight where the sequences are identical. They are different by 2 nucleotides.

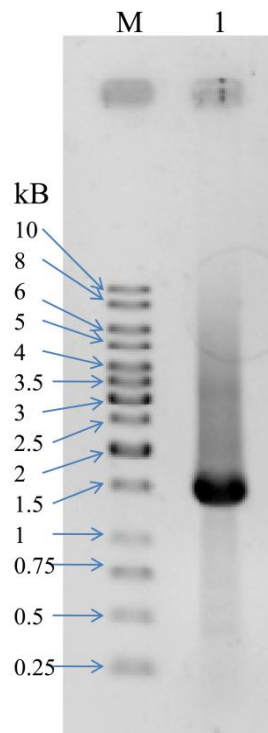


**Figure 2.4** The mature Os7BGlu26 PCR product. The product was separated on 1% agarose electrophoresis and stained with ethidium bromide. Lane M, 1 kb DNA ladder (Bio-Rad); Lane 1, PCR product of Os7BGlu26 with the AK068499MatNf and AK068499 3'UTRr primers.

```

Os7BGlu26      -----YWLNPEIYDAGGLSRRAPPEGFVFGTAASAYQVEG
AK068499      MRKFIAALALAAAAHLLTLPPAQCYWLNPEIYDAGGLSRRAPPEGFVFGTAASAYQVEG
                                     ↑

Os7BGlu26      MAKQGGRGPSIWDAFIEKPGTIPNNATADVTVDEYHRYKEDVNIMKNMGFDAYRFSISWS
AK068499      MAKQGGRGPSIWDAFIEKPGTIPNNATADVTVDEYHRYKEDVNIMKNMGFDAYRFSISWS

Os7BGlu26      RIFPNGTGMVNQEGVDYYNRLIDYMVKKGKIPYANLYHYDLPALHEQYLGWLSPNIV--
AK068499      RILPNGTGMVNQEGVDYYNRLIDYMVKKGKIPYANLYHYDLPALHEQYLGWLSPNIV*A
                                     ←

Os7BGlu26      -----EAFADYADFCFQTFGDRVKDWFTEFNEPRCV
AK068499      FQLENYELQNL*AD*SIYLTKEKMCILL*REAFADYADFCFQTFGDRVKDWFTEFNEPRCV
      Intron sequence →

Os7BGlu26      AALGYDNGFHAPGRCSGCDAGGNSTTEPYLAAHHLILSHAAAVKRYREKYQLYQKGRIGI
AK068499      AALGYDNGFHAPGRCSGCDAGGNSTTEPYLAAHHLILSHAAAVKRYREKYQLYQKGRIGI

Os7BGlu26      LLDFVWYEPFSDSNADRAAAQRARDFHLGWFLDPIIHGRYPYSMLEIVKDRMPTFSDEES
AK068499      LLDFVWYEPFSDSNADRAAAQRARDFHLGWFLDPIIHGRYPYSMLEIVKDRMPTFSDEES

Os7BGlu26      RMVKDSIDYVGINHYTSFYMKDPGPWNLTPTSYQDDWHVGFAYERNGVPIGAQANSYWLY
AK068499      RMVKDSIDYVGINHYTSFYMKDPGPWNLTPTSYQDDWHVGFAYERNGVPIGAQANSYWLY

Os7BGlu26      IVPWGINKAVTYVKEYTYGNPTMILSENGMDQPGNVSI TQGVHDTVRIYYRNYITELKKA
AK068499      IVPWGINKAVTYVKEYTYGNPTMILSENGMDQPGNVSI TQGVHDTVRIYYRNYITELKKA

Os7BGlu26      IDDGAKVIGYFAWSSLDNFEWRLGYTSRFGIVYVDYKTLKRYPKDSAFWFKNMLSSKRN
AK068499      IDDGAKVIGYFAWSSLDNFEWRLGYTSRFGIVYVDYKTLKRYPKDSAFWFKNMLSSKRN

```

**Figure 2.5** Amino acid sequence alignment of Os7BGlu26 with AK068499. The translated AK068499 sequence was predicted to contain an N-terminal secretory signal peptide of 25 residues by SignalP (Bendtsen *et al.*, 2004). There is one amino acid residue of Os7BGlu26 (Phenylalanine98) different from AK068499 (Leucine).

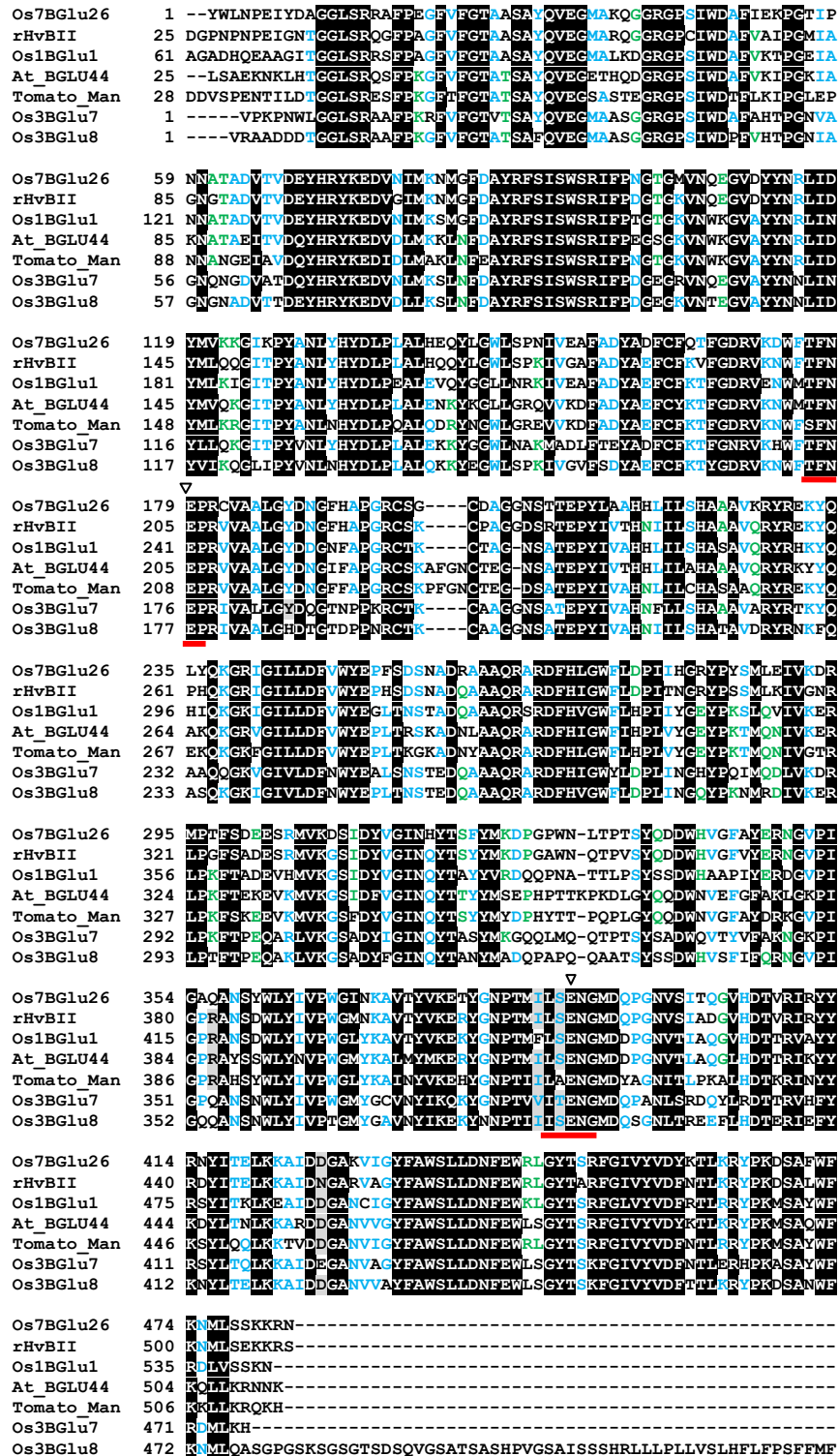


**Figure 2.6** Amino acid sequence alignment of Os7BGlu26, barley rHvBII, rice Os1BGlu1, and Os3BGlu7, Os3BGlu8, *Arabidopsis* BGLU44 β-glucosidase and tomato β-mannosidase. The conserved TFNEP and L(S/A)ENG sequence are underlined and the catalytic acid/base and nucleophile residues indicated by triangles.

### 2.3.2 Purification of Os7BGlu26 $\beta$ -glucosidase

Recombinant Os7BGlu26 containing thioredoxin and 6xhistidine-tag was purified and concentrated from host proteins by  $\text{Ni}^{2+}$  IMAC (Figure 2.7). The fractions containing activity were pooled. Os7BGlu26 was further purified by Q-sepharose anion exchange chromatography, which could eliminate some contaminating proteins between 66 kDa and 20 kDa (Figure 2.8). The fractions containing activity were analysed on SDS-PAGE and concentrated in a 30 kDa molecular-weight cutoff ultrafiltration membrane. Finally, Os7BGlu26 was purified over an S200 gel filtration column. The fractions containing activity were analysed on SDS-PAGE (Figure 2.9). At the beginning of the S200 peak, the Os7BGlu26 fractions were separated from a 20 kDa band, the elution of which overlapped the Os7BGlu26 protein in the fractions at the end of the peak. A comparison of protein purity at each step of the purification is shown in Figure 2.10.

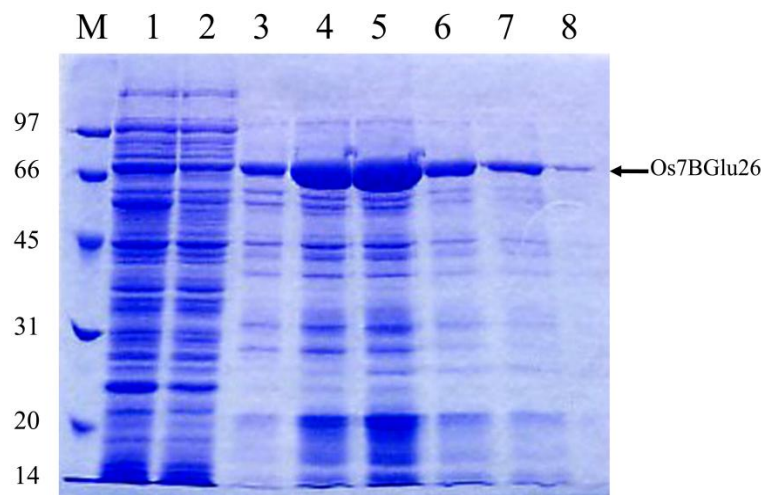


**Figure 2.7** SDS-PAGE analysis of Os7BGlu26 purified by immobilized  $\text{Ni}^{2+}$  affinity chromatography (IMAC). Lane M, Bio-Rad low molecular weight markers; lane 1, crude protein extract of induced Origami(DE3) cells; lane 2, flow-through fraction of proteins that passed through the  $\text{Ni}^{2+}$  column; lanes 3-8, purified Os7BGlu26 in the IMAC elution fractions 4-9, respectively.

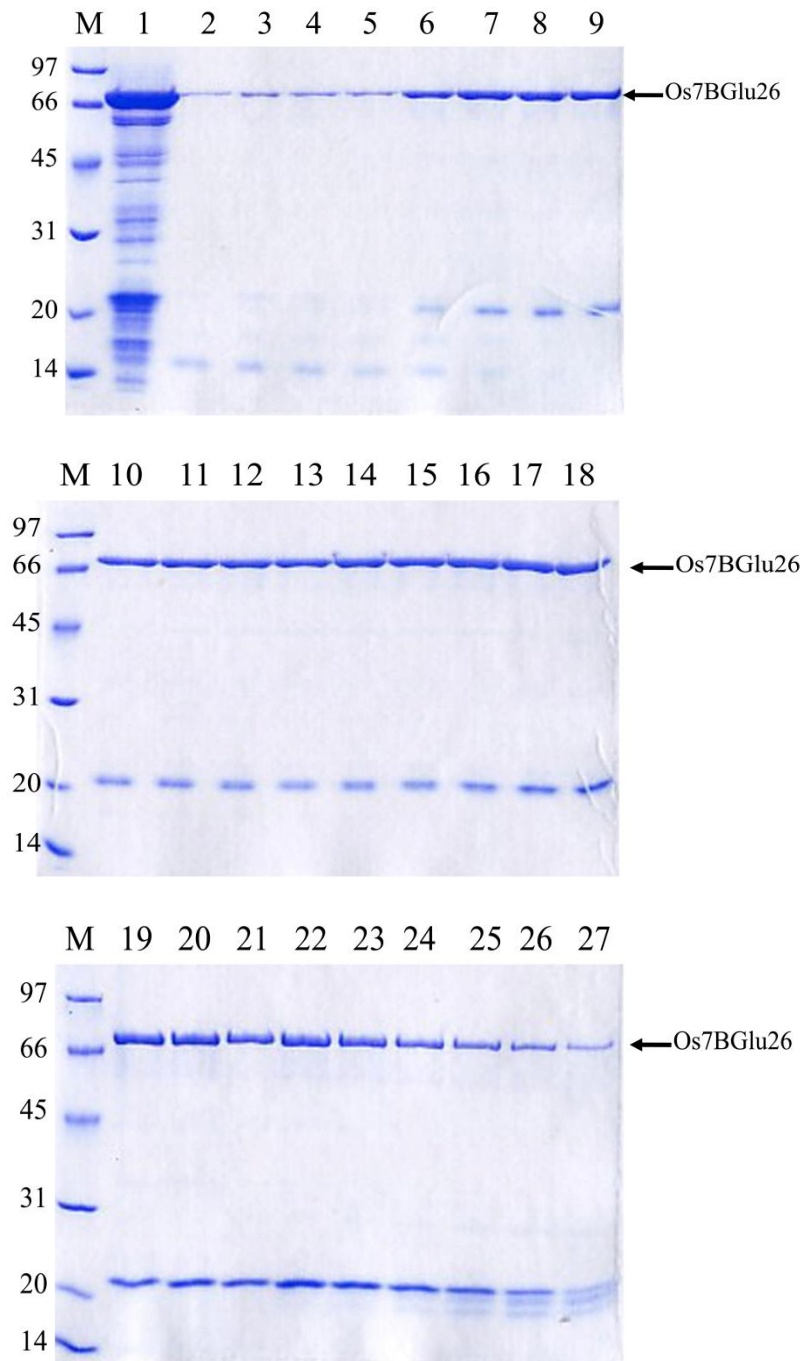


**Figure 2.8** SDS-PAGE analysis of Os7BGlu26 purified by Q-sepharose anion exchange chromatography. Lane M, Bio-Rad low molecular weight markers; lane 1, pooled fractions from  $\text{Ni}^{2+}$  (IMAC) affinity chromatography; lanes 2-27, Q-sepharose fractions 36-61, respectively, which contained activity to hydrolyse 1 mM 4NPGlc.

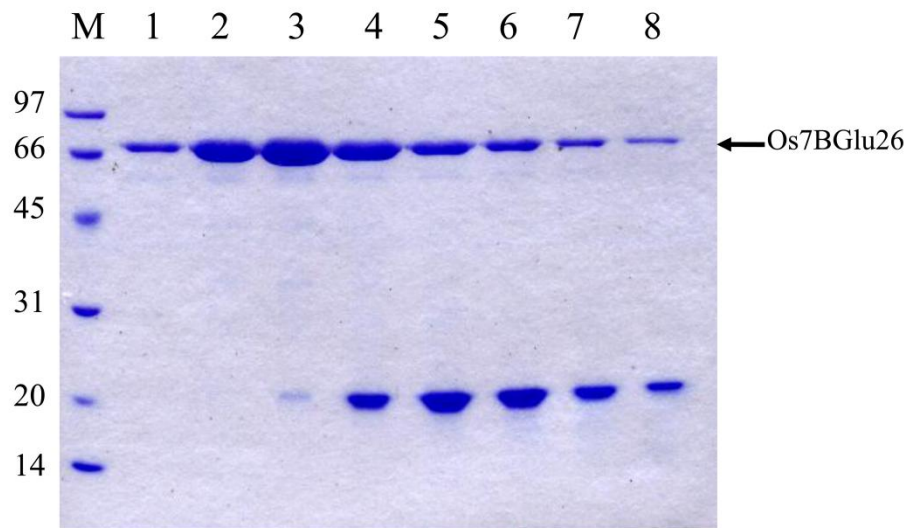


**Figure 2.9** SDS-PAGE analysis of Os7BGlu26 purified by S200 gel filtration chromatography. Lane M, Bio-Rad low molecular weight markers; lanes 2-8, fractions 18-25, which contained activity to 1 mM 4NPGlc. Fractions 18-20 were pooled for kinetic analyses.

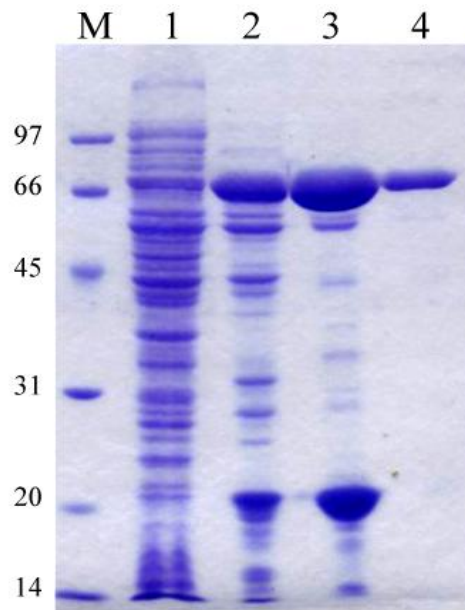


**Figure 2.10** SDS PAGE analysis of Os7BGlu26 purification for kinetic analysis.

Lane M, Bio-Rad low molecular weight markers.

Lane 1, crude protein extract of induced Origami(DE3) cell.

Lane 2, Os7BGlu26 fusion protein from IMAC purification.

Lane 3, Os7BGlu26 after Q-sepharose chromatography.

Lane 4, Os7BGlu26 after S200 gel filtration chromatography.

### 2.3.3 Characterization of Os7BGlu26 $\beta$ -glucosidase

#### 2.3.3.1 Optimum pH and temperature profile of Os7BGlu26

Os7BGlu26 activity against 1 mM 4NPGlc in buffers with pH that varied from 3.0-10.0 was assayed. The pH profile was a bell-shaped, with the activity increasing slowly from pH 3.0 to 4.5, where it reached the maximum and rapidly decreasing from pH 5.0 to 5.5. Os7BGlu26 was not significantly active in the pH 6.0-10.0 range. Os7BGlu26 was projected to have 50% activity at pH 3.7 and 5.3. The activity of Os7BGlu26 at temperatures between 10 and 80°C was determined at pH 4.5. As shown in Figure 2.12, Os7BGlu26 activity increased from 10-30°C and the highest activity was observed at 40°C. At higher temperatures, it decreased slowly to less than 10% at 80°C.

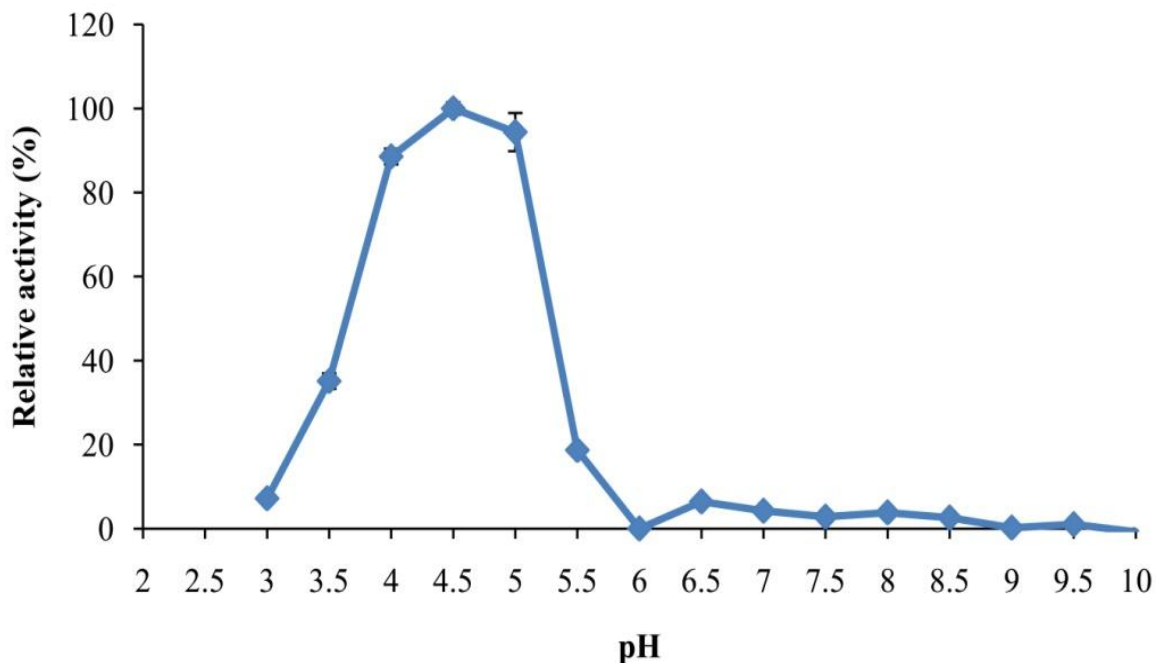


**Figure 2.11** pH profile of Os7BGlu26 at pH range of 3.0-10.0 against 1 mM 4NPGlc at 30°C for 30 min.

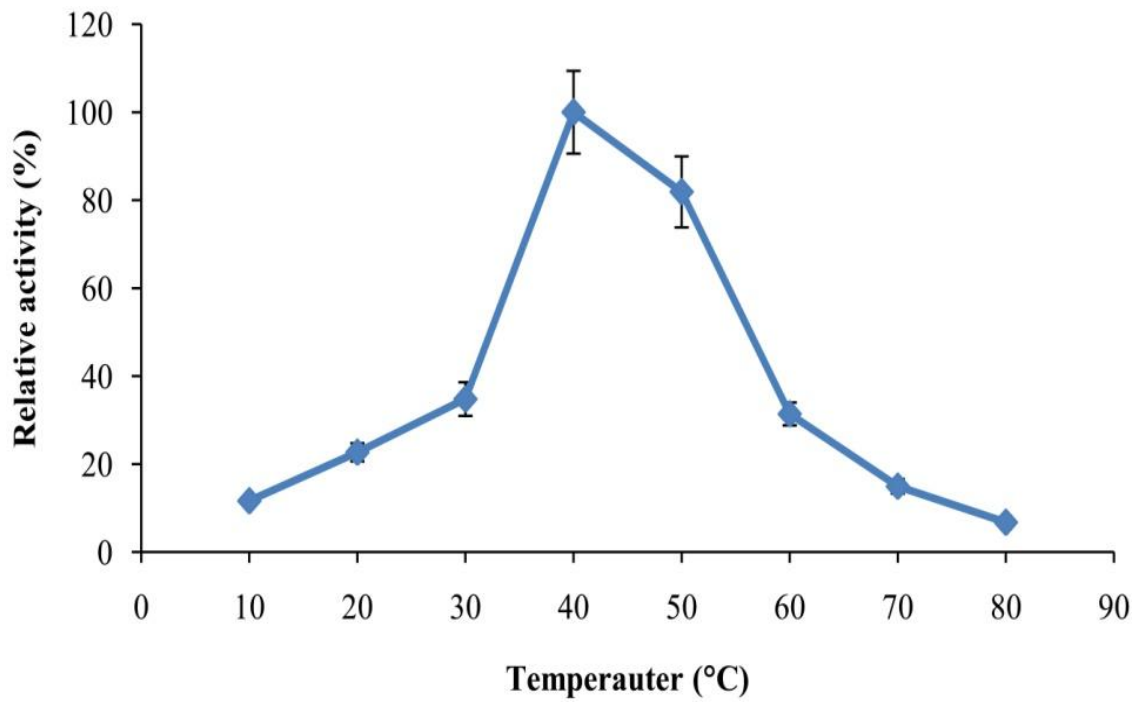


**Figure 2.12** Activity profile of Os7BGlu26 over the temperature range 10-80°C. Activity was measured against 1 mM 4NPGlc in 50 mM sodium acetate, pH 4.5, for 30 min.

### 2.3.3.2 Substrate specificity of Os7BGlu26

The glycone (sugar) specificity of Os7BGlu26 was determined by hydrolysis of 4NP-glycoside substrates. Os7BGlu26 hydrolysed  $\beta$ -D-glucoside,  $\beta$ -D-mannoside, and  $\beta$ -D-fucoside well and had low activity to  $\beta$ -D-galactoside,  $\beta$ -D-xyloside and  $\alpha$ -L-arabinoside, as shown in Table 2.5. Os7BGlu26 could hydrolyse different  $\beta$ -(1,2)-, (1,3)-, and (1,4)-linked gluco-oligosaccharides, but could not hydrolyse the  $\beta$ -(1,6)-linked disaccharide gentiobiose. Os7BGlu26 could hydrolyse 4NPMan with higher activity than 4NPGlc and also hydrolysed  $\beta$ -(1,4)-manno-oligosaccharides with DP 2 to 6, similar to rHvBII. Os7BGlu26 appeared to have low activity toward  $\beta$ -(1,4)-mannobiose, but higher activity toward mannotriose, mannotetraose, mannopentaose, and mannohexaose. The aglycone specificity of Os7BGlu26 hydrolysis was determined with the plant glucosides shown in Figure 2.14. Of these, it hydrolysed *p*-coumaryl alcohol glucoside, sambunigrin, dhurrin, D-amydalin, prunasin, and quercetin-3-glucoside (Figure 2.15).

### 2.3.3.3 Kinetic parameters of Os7BGlu26

The Os7BGlu26, had a catalytic efficiency value ( $k_{cat}/K_M$ ) for 4NPMan that was 3.3-fold higher than that for 4NPGlc. Os7BGlu26 hydrolysed cello-oligosaccharides with increasing efficiency as the DP increased from 2 to 6, with the  $k_{cat}/K_M$  values of 0.026, 1.27, 10.9, 18.5, and 29  $\text{mM}^{-1}\text{s}^{-1}$ , respectively. However the hydrolysis of laminari-oligosaccharides was opposite to cello-oligosaccharides in that it hydrolysed laminaribiose better than the laminaritriose.

**Table 2.5** Comparison of the relative activities of Os7BGlu26, rHvBII and Os3BGlu7 on aryl glycosides and oligosaccharides. Os7BGlu26 activity was assayed with 1 mM synthetic substrates and gluco-oligosaccharides, including the  $\beta$ -(1,2) disaccharide sophorose,  $\beta$ -(1,3) laminari-oligosaccharides (DP 2-3),  $\beta$ -(1,4) cello-oligosaccharides (DP 2-6), and the  $\beta$ -(1,6) disaccharide gentiobiose.

| Substrate                          | Relative activity (%) |                |                       |
|------------------------------------|-----------------------|----------------|-----------------------|
|                                    | rHvBII <sup>a</sup>   | Os7BGlu26      | Os3BGlu7 <sup>b</sup> |
| <i>Synthetic substrates</i>        |                       |                |                       |
| 4NP- $\beta$ -D-glucofuranoside    | 100 $\pm$ 3           | 100 $\pm$ 4    | 100                   |
| 4NP- $\beta$ -D-mannopyranoside    | 238 $\pm$ 12          | 302 $\pm$ 4    | 10                    |
| 4NP- $\beta$ -D-fucopyranoside     | 129 $\pm$ 10          | 128 $\pm$ 8    | 180                   |
| 4NP- $\beta$ -D-galactopyranoside  | 17 $\pm$ 3            | 12.6 $\pm$ 1.7 | 27                    |
| 4NP- $\beta$ -D-xylopyranoside     | 3.1 $\pm$ 1.9         | 6.4 $\pm$ 1.5  | nd <sup>c</sup>       |
| 4NP- $\alpha$ -L-arabinopyranoside | 16 $\pm$ 3            | 9 $\pm$ 3      | nd                    |
| <i>Oligosaccharides</i>            |                       |                |                       |
| Sophorose                          | 15 $\pm$ 4            | 25 $\pm$ 4     | nd                    |
| Laminaribiose                      | 13 $\pm$ 4            | 158 $\pm$ 13   | 95                    |
| Laminaritriose                     | 2.8 $\pm$ 1.1         | 23 $\pm$ 5     | 25                    |
| Laminaritetraose                   | -                     | -              | -                     |
| Laminaripentaose                   | -                     | -              | -                     |
| Laminarihexaose                    | -                     | -              | nd                    |
| Laminariheptaose                   | -                     | -              | nd                    |
| Cellobiose                         | 33 $\pm$ 7            | 21 $\pm$ 5     | 1.5                   |
| Cellotriose                        | 19 $\pm$ 8            | 124 $\pm$ 18   | 34                    |
| Cellotetraose                      | 52 $\pm$ 9            | 194 $\pm$ 11   | 58                    |
| Cellopentaose                      | 225 $\pm$ 15          | 403 $\pm$ 17   | nd                    |
| Cellohexaose                       | 303 $\pm$ 12          | 472 $\pm$ 12   | nd                    |
| Gentiobiose                        | -                     | -              | 0.3                   |

<sup>a</sup> Relative activity of rHvBII from Kuntothom *et al.*, 2009.

<sup>b</sup> Relative activity of Os3BGlu7 from Opassiri *et al.*, 2003.

<sup>c</sup> 'nd' indicated 'not determined'.

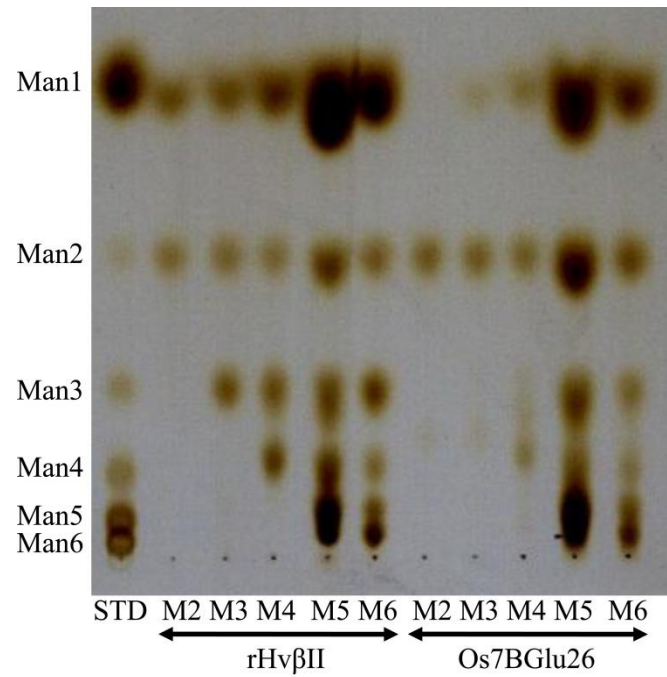


**Figure 2.13** Thin layer chromatography of products of manno-oligosaccharide (DP 2-6) hydrolysis by rHvBII and Os7BGlu26.

Lane STD, mannose to mannohexaose (Man1-Man6) standards.

Lanes M2-M6, mannobiose to mannohexaose hydrolysis by rHvBII and Os7BGlu26, respectively.

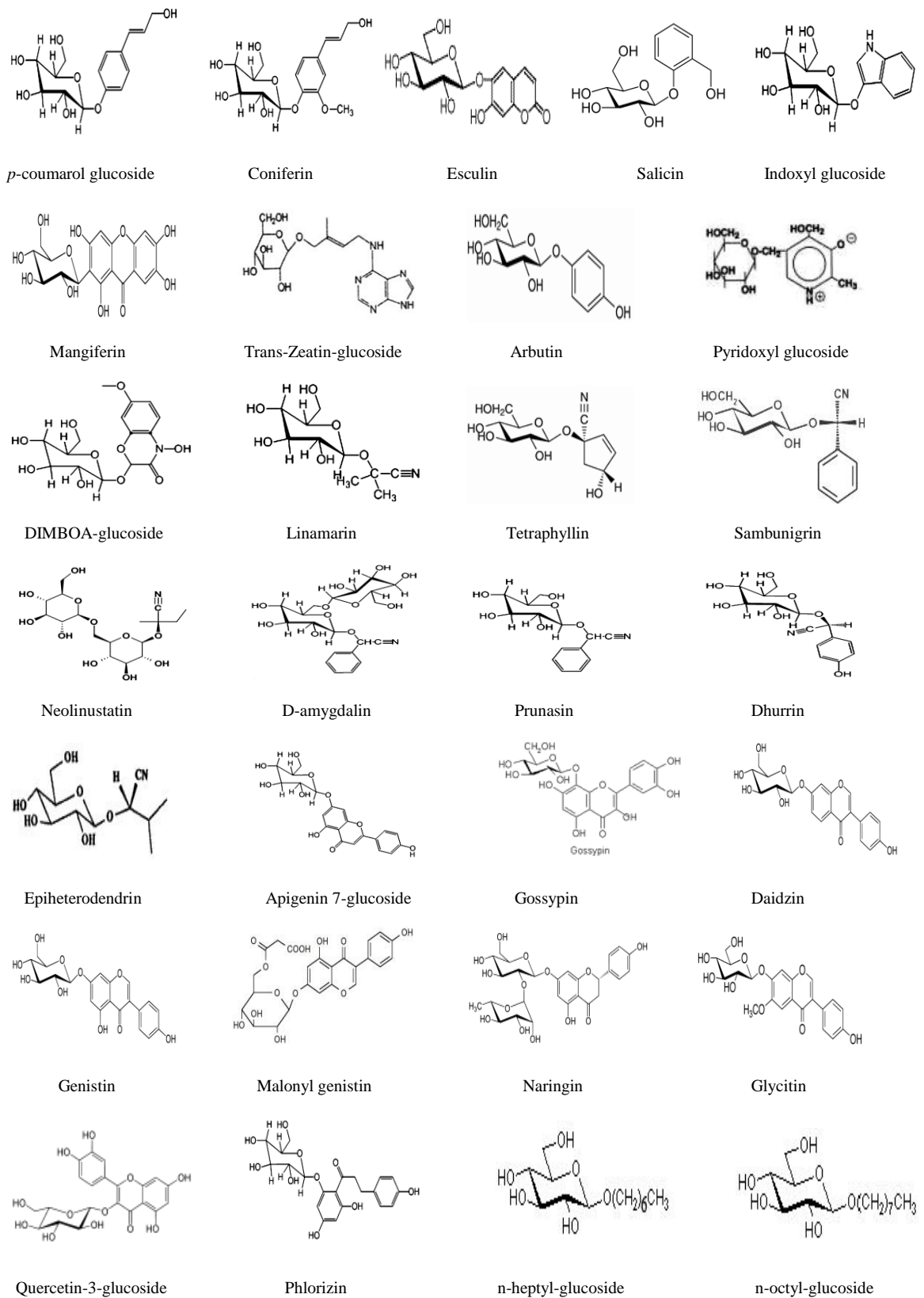


**Figure 2.14** Structures of plant substrates tested for hydrolysis by Os7BGlu26.

**Table 2.6** Hydrolysis of natural glycosides by Os7BGlu26.

| Substrate                            | Os7BGlu26 |
|--------------------------------------|-----------|
| <i>p</i> -coumaryl alcohol glucoside | +         |
| Coniferin                            | -         |
| Salicin                              | -         |
| Esculin                              | -         |
| Indoxyl glucoside                    | -         |
| Mangiferin                           | -         |
| Trans-Zeatin glucoside               | -         |
| Arbutin                              | -         |
| Pyridoxine glucoside                 | -         |
| DIMBOA-glucoside                     | -         |
| Linamarin                            | -         |
| Tetraphylin                          | -         |
| Sambunigrin                          | +         |
| Neolinustatin                        | -         |
| D-amydalin                           | +         |
| Prunasin                             | +         |
| Dhurrin                              | +         |
| Epiheterodendrin                     | -         |
| Apigenin                             | -         |
| Gossypin                             | -         |
| Daidzin                              | -         |
| Genistin                             | -         |
| Malonyl genistin                     | -         |
| Glycitin                             | -         |
| Naringin                             | -         |
| Quercetin-3-glucoside                | +         |
| Phlorizin                            | -         |

\*The activity of Os7BGlu26 was detected by thin layer chromatography.

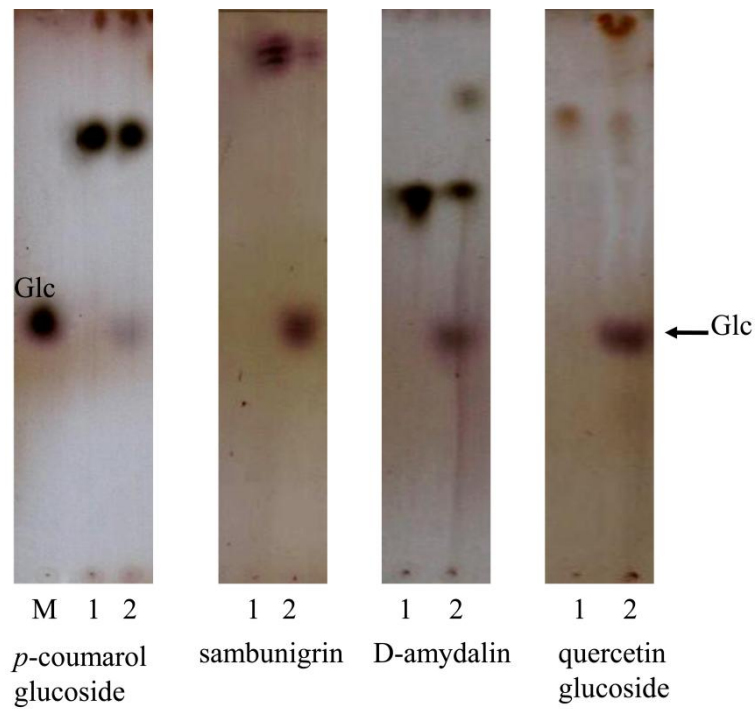


**Figure 2.15** Thin layer chromatogram of hydrolysis of *p*-coumarol glucoside, sambunigrin, D-amydalin, and quercetin-3-glucoside with Os7BGlu26. Lane M; glucose; lane 1, substrate blank; and lane 2, hydrolysis products of Os7BGlu26.

**Table 2.7** Kinetic parameters of rHvBII, Os3BGlu7 and Os7BGlu26 hydrolysis of 4NPGlc, 4NPMAN, cello-oligosaccharides, laminaribiose and laminaritriose.

| Substrate   | rHvBII <sup>a</sup> | Os7BGlu26         | Os3BGlu7 <sup>b</sup> |
|---|---------------------|-------------------|-----------------------|
| <b>4NPGlc</b>                                     |                     |                   |                       |
| $K_M$ (mM)  | $0.50 \pm 0.03$     | $0.27 \pm 0.02$   | $0.23 \pm 0.02$       |
| $k_{cat}$ (s <sup>-1</sup> )                      | $0.50 \pm 0.07$     | $0.16 \pm 0.003$  | $7.93 \pm 0.37$       |
| $k_{cat}/K_M$ (s <sup>-1</sup> mM <sup>-1</sup> ) | $1.00 \pm 0.05$     | $0.63 \pm 0.003$  | $34.70 \pm 1.40$      |
| <b>4NPMAN</b>                                     |                     |                   |                       |
| $K_M$ (mM)  | $0.25 \pm 0.01$     | $0.52 \pm 0.04$   | $1.27 \pm 0.10$       |
| $k_{cat}$ (s <sup>-1</sup> )                      | $3.06 \pm 0.02$     | $1.10 \pm 0.03$   | $1.32 \pm 0.05$       |
| $k_{cat}/K_M$ (s <sup>-1</sup> mM <sup>-1</sup> ) | $12.67 \pm 0.17$    | $2.11 \pm 0.20$   | $1.01 \pm 0.02$       |
| <b>Cellobiose</b>                                 |                     |                   |                       |
| $K_M$ (mM)  | $2.76 \pm 0.10$     | $19.6 \pm 1.9$    | $31.50 \pm 1.60$      |
| $k_{cat}$ (s <sup>-1</sup> )                      | $16.08 \pm 0.15$    | $0.52 \pm 0.03$   | $1.52 \pm 0.13$       |
| $k_{cat}/K_M$ (s <sup>-1</sup> mM <sup>-1</sup> ) | $5.84 \pm 0.23$     | $0.026 \pm 0.001$ | $0.05 \pm 0.01$       |
| <b>Cellotriose</b>                                |                     |                   |                       |
| $K_M$ (mM)  | $0.74 \pm 0.06$     | $0.52 \pm 0.05$   | $0.72 \pm 0.02$       |
| $k_{cat}$ (s <sup>-1</sup> )                      | $2.97 \pm 0.39$     | $0.67 \pm 0.03$   | $18.13 \pm 0.35$      |
| $k_{cat}/K_M$ (s <sup>-1</sup> mM <sup>-1</sup> ) | $3.45 \pm 0.084$    | $1.27 \pm 0.03$   | $25.4 \pm 0.04$       |
| <b>Cellotetraose</b>                              |                     |                   |                       |
| $K_M$ (mM)  | $1.03 \pm 0.02$     | $0.09 \pm 0.01$   | $0.28 \pm 0.01$       |
| $k_{cat}$ (s <sup>-1</sup> )                      | $9.57 \pm 0.40$     | $0.97 \pm 0.02$   | $17.34 \pm 0.63$      |
| $k_{cat}/K_M$ (s <sup>-1</sup> mM <sup>-1</sup> ) | $9.34 \pm 0.53$     | $10.9 \pm 0.4$    | $61.10 \pm 0.40$      |
| <b>Cellopentaose</b>                              |                     |                   |                       |
| $K_M$ (mM)  | $0.33 \pm 0.02$     | $0.06 \pm 0.01$   | $0.24 \pm 0.01$       |
| $k_{cat}$ (s <sup>-1</sup> )                      | $12.87 \pm 0.35$    | $1.07 \pm 0.03$   | $16.90 \pm 0.06$      |
| $k_{cat}/K_M$ (s <sup>-1</sup> mM <sup>-1</sup> ) | $40.20 \pm 0.80$    | $18.5 \pm 0.4$    | $71.50 \pm 2.20$      |
| <b>Cellohexaose</b>                               |                     |                   |                       |
| $K_M$ (mM)  | $0.23 \pm 0.01$     | $0.05 \pm 0.01$   | $0.22 \pm 0.01$       |
| $k_{cat}$ (s <sup>-1</sup> )                      | $13.10 \pm 0.08$    | $1.31 \pm 0.04$   | $16.93 \pm 0.32$      |
| $k_{cat}/K_M$ (s <sup>-1</sup> mM <sup>-1</sup> ) | $54.24 \pm 1.59$    | $29 \pm 3$        | $152.9 \pm 0.50$      |
| <b>Laminaribiose</b>                              |                     |                   |                       |
| $K_M$ (mM)  | $5.00 \pm 0.00$     | $0.86 \pm 0.07$   | $2.05 \pm 0.01$       |
| $k_{cat}$ (s <sup>-1</sup> )                      | $11.28 \pm 0.03$    | $0.61 \pm 0.02$   | $31.90 \pm 3.10$      |
| $k_{cat}/K_M$ (s <sup>-1</sup> mM <sup>-1</sup> ) | $2.30 \pm 0.06$     | $0.70 \pm 0.06$   | $15.70 \pm 1.90$      |
| <b>Laminaritriose</b>                             |                     |                   |                       |
| $K_M$ (mM)  | $2.77 \pm 0.17$     | $8.7 \pm 0.9$     | $1.92 \pm 0.04$       |
| $k_{cat}$ (s <sup>-1</sup> )                      | $2.33 \pm 0.17$     | $2.4 \pm 0.1$     | $21.20 \pm 0.20$      |
| $k_{cat}/K_M$ (s <sup>-1</sup> mM <sup>-1</sup> ) | $0.84 \pm 0.01$     | $0.28 \pm 0.006$  | $11.0 \pm 0.2$        |

<sup>a</sup> Kinetics constants from Kuntothom *et al.*, 2009.

<sup>b</sup> Kinetics constants from Opassiri *et al.*, 2004.

## 2.4 Discussion

### 2.4.1 Sequence analysis of Os7BGlu26

The Os7BGlu26 DNA sequence (1709 bases) was free of the intron between bases 545-640 in the AK068499 sequence, had 2 nucleotides bases mismatched with it and had 3 gaps at positions 1623-1625 which are different from the AK068499 sequence. The Os7BGlu26 cDNA translates to a mature protein containing 483 amino acid residues with residue 98 being phenylalanine which is the same as in rHvBII and Os3BGlu7, but different from the original AK068499 cDNA translation. In the phylogenetic tree of the plant GH1  $\beta$ -glucosidase/ $\beta$ -mannosidase cluster, the Os7BGlu26 amino acid sequence groups with that of rHvBII  $\beta$ -mannosidase, with which it shares 82% identity and it is more distant and shares only 63% identity with Os3BGlu7  $\beta$ -glucosidase. The putative catalytic glutamate residues were embedded in the highly conserved regions of TFNEP and LSENG of Os7BGlu26, which are the same as rHvBII, but different from the TFNEP and ITENG sequence of Os3BGlu7.

### 2.4.2 Protein purification of Os7BGlu26

Os7BGlu26 cDNA could be used to express the active Os7BGlu26 thioredoxin and His<sub>6</sub>-tag fusion protein in *E. coli* at 20°C. The predicted molecular weight and isoelectric point (pI) of the Os7BGlu26 fusion protein were approximately 75 kDa and 6.1, respectively. Os7BGlu26 was purified from crude protein with IMAC on Ni<sup>2+</sup> resin. Based on the calculated pI, it was surmised that Os7BGlu26 could be purified with Q-sepharose strong anion exchange chromatography at pH 8.0, and the protein was obtained in higher purity after it was passed through S200 gel filtration chromatography.

### 2.4.3 Characterization of Os7BGlu26

The properties of Os7BGlu26 were more similar to rHvBII than to Os3BGlu7. Os7BGlu26 had optimal pH at 4.5 and temperature at 40°C, which are different from the optima of pH 4.0 and 30°C for rHvBII (Kuntothom *et al.*, 2009) and pH 5.0 and 30°C for Os3BGlu7 (Opassiri *et al.*, 2003). The hydrolysis of synthetic substrates by Os7BGlu26 was more similar to rHvBII, especially in that it hydrolysed 4NPMan better than 4NPGlc. Os7BGlu26 could hydrolyse only  $\beta$ -(1,2)-,  $\beta$ -(1,3)- and  $\beta$ -(1,4)-linked gluco-oligosaccharides, and could not hydrolyse the  $\beta$ -(1,6) linkage, the same as rHvBII. However, the rate of hydrolysis of  $\beta$ -(1,4)-cello-oligosaccharides DP 2 to 6 increased in order from cellobiose to cellohexaose, similar to Os3BGlu7. In addition, the hydrolysis of laminari-oligosaccharides by Os7BGlu26 was similar to rHvBII and Os3BGlu7, which hydrolysed laminaribiose approximately 2.5-fold more rapidly than laminaritriose, while laminaribiose was hydrolysed approximately 2.7-fold more rapidly than laminaritriose by rHvBII. For  $\beta$ -(1,4)-manno-oligosaccharides DP 2 to 6, Os7BGlu26 had poor activity to mannobiose, but higher activity to mannotriose to mannohexaose. In comparison, rHvBII appeared to have higher manno-oligosaccharide hydrolysis activity than Os7BGlu26, especially to mannobiose.

*Arabidopsis thaliana* BGLU44  $\beta$ -glucosidase is in the  $\beta$ -glucosidase/ $\beta$ -mannosidase cluster and shares 73% identity with tomato  $\beta$ -mannosidase (Xu *et al.*, 2004) and 66% identity with Os7BGlu26. Os7BGlu26 and BGLU44 had pH optima at 4.5 and act as  $\beta$ -mannosidases to hydrolyse 4NPMan approximately 3 fold and 2.4 fold more rapidly than 4NPGlc for Os7BGlu26 and BGLU44, respectively. Both  $\beta$ -mannosidase/ $\beta$ -glucosidases hydrolyse manno-oligosaccharides (DP 2-6). The presence of the conserved L(S/A)ENG motif in rHvBII, BGLU44 and Os7BGlu26 might be predicative of  $\beta$ -mannosidase activity for this cluster (Xu *et al.*, 2004).

Os7BGlu26 could hydrolyse a monolignol glucoside (*p*-coumaryl alcohol glucoside), cyanogenic glucosides (sambunigrin, D-amygdalin, prunasin, dhurrin) and a flavonol glycoside (quercetin-3-glucoside). Opassiri *et al.* (2006) analysed the expression of AK068499 and found it expressed in many parts of rice, including shoot, leaf (2 weeks), flowering panicle, ripening panicle, and infected leaf (3 weeks). Thus the biological function of Os7BGlu26 might be to act in cell wall degradation, lignification, and/or defense.

## 2.5 Conclusions

Os7BGlu26 is a  $\beta$ -D-mannosidase/ $\beta$ -D-glucosidase with the motifs TFNEP and LSENG around its catalytic amino acids, and shares 82% amino acid sequence identity with barley rHvBII. The biochemical properties of Os7BGlu26 are similar to rHvBII, which also hydrolysed  $\beta$ -(1,2)-,  $\beta$ -(1,3)- and  $\beta$ -(1,4)-gluco-oligosaccharides, and preferred to hydrolyse 4NPMan to 4NPGlc. Both could also hydrolyse manno-oligosaccharides. On the other hand, Os7BGlu26 has a cello-oligosaccharides hydrolysis pattern similar to Os3BGlu7, in that it hydrolyses cellotriose better than cellobiose, which is different from rHvBII.

## 2.6 References

- Bendtsen, J.D., Nielsen, H., von Heijne, G., and Brunak, S. (2004). Improved prediction of signal peptides: SignalP 3.0. **J. Mol. Biol.** 340: 783-795.
- Chuenchor, W., Pengthaisong, S., Yuvanayama, J., Opassiri, R., Svasti, J., and Ketudat Cairns, J.R. (2006). Purification, crystallization and preliminary X-ray analysis of rice BGl1  $\beta$ -glucosidase with and without 2-deoxy-2-fluoro- $\beta$ -D-glucoside. **Acta Cryst.** F62: 798-801.
- Hrmova, M., Harvey, A.J., Wang, J., Shirley, N.J., Jones, G.P., Stone, B.A., Høj, P.B., and Fincher, G.B. (1996). Barley  $\beta$ -D-glucan exohydrolases with  $\beta$ -D-glucosidase activity: purification, characterization, and determination of primary structure from a cDNA clone. **J. Biol. Chem.** 271: 5277-5286.
- Hrmova, M., MacGregor, E.A., Biely, P., Stewart, R.J., and Fincher, G.B. (1998). Substrate binding and catalytic mechanism of a barley  $\beta$ -D-glucosidase/(1,4)- $\beta$ -D-glucan exohydrolase. **J. Biol. Chem.** 273: 11134-11143.
- Hrmova, M., Burton, R.A., Biely, P., Lahnstein, J., and Fincher, G.B. (2006). Hydrolysis of (1,4)- $\beta$ -D-mannans in barley (*Hordeum vulgare* L.) is mediated by the concerted action of (1,4)- $\beta$ -D-mannan endohydrolase and  $\beta$ -D-mannosidase. **Biochem. J.** 399: 77-90.
- Kuntothom, T., Luang, S., Harvey, A.J., Fincher, G.B., Opassiri, R., Hrmova, M., and Ketudat Cairns, J.R. (2009). Rice family GH1 glycoside hydrolases with  $\beta$ -D-glucosidase and  $\beta$ -D-mannosidase activities. **Arch. Biochem. Biophys.** 491: 85-95.
- Leah, R., Kigel, J., Svendsen, I.B., and Mundy, J. (1995). Biochemical and molecular characterization of a barley seed  $\beta$ -glucosidase. **J. Biol. Chem.** 270: 15789-15797.
- Laemmli. (1970). Cleavage of structural proteins during assembly of head of bacteriophage-T<sub>4</sub>. **Nature** 227: 680-685.

- Mo, B., and Bewley, J.D. (2002).  $\beta$ -mannosidase (EC 3.2.1.25) activity during and following germination of tomato (*Lycopersicon esculentum* Mill.) seeds. Purification, cloning and characterization. **Planta**. 215: 141-152.
- Opassiri, R., Ketudat Cairns, J.R., Akiyama, T., Wara-Aswapati, O., Svasti, J., and Esen, A. (2003). Characterization of a rice  $\beta$ -glucosidase highly expressed in flower and germinating shoot. **Plant Science** 165: 627-638.
- Opassiri, R., Hua, Y., Wara-aswapati, O., Akiyama, T., Svasti, J., Esen, A., and Ketudat Cairns, J.R. (2004).  $\beta$ -glucosidase, exo- $\beta$ -glucanase and pyridoxine transglucosylase activities of rice BGlu1. **Biochem. J.** 379: 125-131.
- Opassiri, R., Pomthong, B., Onkoksoong, T., Akiyama, T., Esen, A., and Ketudat Cairns, J.R. (2006). Analysis of rice glycosyl hydrolase family 1 and expression of Os4bglu12  $\beta$ -glucosidase. **BMC Plant Biol.** 6.
- Xu, Z., Escamilla-Trevino, L.L., Zeng, L., Lalgondar, M., Bevan, D.R., Winkel, B.S.J., Mohamed, A., Cheng, C.L., Shih, M.C., Poulton, J.E., and Esen, A. (2004). Functional genomic analysis of *Arabidopsis thaliana* glycoside hydrolase family 1. **Plant Mol. Biol.** 55: 343-367.

# CHAPTER III

## RECOMBINANT PROTEIN EXPRESSION AND CHARACTERIZATION OF RICE Os9BGlu31 β-GLUCOSIDASE

### Abstract

Os9BGlu31 β-glucosidase is a member of glycosyl hydrolase family 1 (GH1) from rice (*Oryza sativa*) which is similar to hydroxyisourate hydrolase and has the sequence IHENG around its conserved nucleophile residue, instead of the I(V/T)ENG sequence more commonly found in GH1 β-glucosidases. Os9BGlu31 was expressed as an N-terminal thioredoxin and His<sub>6</sub>-tag fusion protein in *E. coli* Origami(DE3) and then purified by immobilized metal affinity and ion exchange chromatography. The optimum pH of Os9BGlu31 was 4.5 and its optimum temperature was 40°C. Os9BGlu31 was found to hydrolyse the synthetic substrate of 4-nitrophenyl-β-D-glucopyranoside (4NPGlc) at  $k_{cat}/K_M$  was  $0.02 \pm 0.001 \text{ mM}^{-1}\cdot\text{s}^{-1}$ . Among natural glycosides, Os9BGlu31 preferred to hydrolyse dhurrin and had low activity to phlorizin. It could not hydrolyse any β-linked gluco-oligosaccharides and other alkyl β-glucosides tested. Os9BGlu31 was sensitive to inhibition by 1 mM HgCl<sub>2</sub> (90% inhibition), and slightly inhibited by FeCl<sub>3</sub> and CuSO<sub>4</sub>, but showed little sensitivity to other metal salts, glucono δ-lactone, and 2,4-dinitrophenyl-β-D-2-fluoroglucoside.

### 3.1 Introduction

$\beta$ -glucosidases hydrolyse O-glycosidic bonds of  $\beta$ -D-glucosyl residues at the nonreducing end of carbohydrates and hydrolyse a variety of glycosides, including aryl- and alkyl- $\beta$ -D-glycosides.  $\beta$ -glucosidases have many roles in fundamental biological and biotechnological processes (Ketudat Cairns and Esen 2010). Plant  $\beta$ -glucosidases are involved in the defense against pests, phytohormone activation, lignification and cell wall degradation. Many  $\beta$ -glucosidases belong to glycosyl hydrolase family 1 (GH1) and they contain highly conserved amino acid sequences of T(F/L)NEP at the catalytic acid/base and (I/V)TENG at the catalytic nucleophile.

Maize  $\beta$ -glucosidases [2-O- $\beta$ -D-glucopyranosyl-4-hydroxy-7-methoxy-1,4-benzoxazin-3-one (DIMBOAGlc)-hydrolase] isoenzymes ZmGlu1 and ZmGlu2 share 90% sequence identity (Bandaranayake and Esen, 1996). They hydrolyse a broad range of synthetic and natural substrates, including their natural substrate DIMBOAGlc. The efficiency of hydrolysis of synthetic substrates by ZmGlu2 was lower than ZmGlu1. Czjzek *et al.* (2000) identified amino acid residues within the active site of ZmGlu1 which are involved in glucose binding and aglycone binding of ZmGlu1. The cyanogenic  $\beta$ -glucosidases dhurrinase-1 (Dhr1) and dhurrinase-2 (Dhr2) were purified from sorghum seedlings (*Sorghum bicolor* L. Moench) by Hösel *et al.* (1987). Dhr1 and Dhr2 hydrolysed dhurrin (their substrate) with similar catalytic efficiencies, but Dhr2 was able to hydrolyse the synthetic substrates 4-methylumbelliferyl- $\beta$ -D-glucopyranoside and 4NP- $\beta$ -D-glucopyranoside (4NPGlc), while Dhr1 was not. The Dhr1 protein sequence showed 70% identity to ZmGlu1 (Cicek and Esen, 1998) and the amino acid residues at the C-terminus of these two enzymes are important for their substrate specificity.

The gene encoding hydroxyisourate hydrolase (HIUHase) had been cloned from soybean (*Glycine max*; Raychaudhuri and Tipton, 2002). HIUHase is involved in allantoin biogenesis or urate degradation, in which it converts 5-hydroxyisourate to 2-oxo-4-

hydroxy-4-carboxy-5-ureidoimidazoline, which can be used as a nitrogen source when the preferred nitrogen sources are exhausted (Sarma *et al.*, 1999). HIUHase is also in GH1 and had conserved glutamates at the positions of the acid/base and nucleophile residues of GH1  $\beta$ -glucosidases, but has a slightly different sequence surround around the catalytic nucleophile (IHENG). The amino acid sequence of HIUHase has 33% identical to that of ZmGlu1. The glutamate residues in the conserved TVNEP and IHENG motifs, corresponding to the GH1 catalytic acid/base and nucleophile, respectively, are critical to its activity (Raychaudhuri and Tipton, 2002).

Opassiri *et al.* (2006) analysed protein sequences of rice (*Oryza sativa*) GH1 with other plant enzymes. The protein sequence in the phylogenetic cluster containing rice Os1BGlu2, Os1BGlu3, Os1BGlu5, Os5BGlu19, Os5BGlu20, Os5BGlu21, Os5BGlu22, Os5BGlu23, Os9BGlu31, Os9BGlu32 and Os9BGlu33 were more closely related to HIUHase than to previously characterized  $\beta$ -glucosidases, but only Os9BGlu31, Os9BGlu32 and Os9BGlu33 have the same IHENG sequence around the catalytic nucleophile. Here the Os9BGlu31 cDNA was cloned, its protein expressed in *E. coli* and its enzymatic activity characterized.

## **3.2 Materials and methods**

### **3.2.1 Plasmids and bacterial strains**

The plasmid constructs containing the full-length cDNA encoding the rice Os9BGlu31  $\beta$ -glucosidase (GenBank Accession number AK121679) was acquired from the Rice Genome Resource Center, Tsukuba, Japan (<http://www.rgrc.dna.affrc.go.jp/>) (Kikuchi *et al.*, 2003). The cloning and expression vectors and bacteria for this work were described in section 2.2.1.

### **3.2.2 Molecular cloning and expression**

#### **3.2.2.1 Cloning of DNA encoding mature Os9BGlu31**

The cDNA fragment encoding mature Os9BGlu31 was amplified with the AK121679F primer (5' CACCATGGCGGCGGGGATCACCAG 3') and AK121679R primer (5' CTCGAGAACCTTGATCACTGGGAGTAGGCTC 3') by *Pfu* DNA polymerase with clone (AK121679) plasmid as template. The Os9BGlu31 cDNA fragment was amplified with 30 cycles according to the manufacturer's instructions with an annealing temperature of 63.5°C. The PCR product (~1.5 kb) was purified from the agarose gel, and cloned into pENTR/D-TOPO and then recombined into the pET32a/DEST expression vector, as described for Os7BGlu26 in section 2.2.3.3.

#### **3.2.2.2 The protein expression of Os9BGlu31**

The pET32a/DEST expression vector containing Os9BGlu31 was transformed into the *E. coli* strain Origami(DE3) and the protein expressed as described for the Os7BGlu26 isoenzyme in section and 2.2.3.4.

### 3.2.2.3 The purification of Os9BGlu31

The induced bacterial cells were collected by centrifugation, frozen and lysed with extraction buffer and purified with immobilized Ni<sup>2+</sup> affinity chromatography (IMAC), and Q-sepharose chromatography by the same procedures described for Os7BGlu26 in section 2.2.3.5. After the active fractions from anion exchange chromatography were pooled, the thioredoxin and 6xhistidine tag at the N-terminus of Os9BGlu31 was removed by digestion with enterokinase (New England BioLabs) at a ratio of 1 µl of enterokinase per 1 mg of recombinant protein, incubated at 23°C for 18 h. Then, the fusion tag was adsorbed from the protein with IMAC. Finally, Os9BGlu31 was stored in 50 mM Tris-HCl, pH 8.0, containing 150 ml NaCl.

### 3.2.2.4 Enzymatic characterization of Os9BGlu31

The optimum pH of Os9BGlu31 was determined with 5 mM 4NPGlc in 50 mM buffers with pH in the range between 3.5 to 10.0, as described for Os7BGlu26 in section 2.2.3.6. The optimum temperature was determined at the various temperatures from 10°C to 80°C with 5 mM 4NPGlc in 50 mM sodium acetate, pH 4.5.

Substrate hydrolysis by Os9BGlu31 was assayed by monitoring the release of 4-nitrophenol or glucose from synthetic and natural substrates, as described for Os7BGlu26 in section 2.2.3.7. Kinetic parameters for 4NPGlc by Os9BGlu31 were obtained from untransformed data by nonlinear least-square regression using Grafit 5.0 (Erithacus Software, Horley, surrey, UK).

In addition, the effect of EDTA, metal salts and inhibitors on Os9BGlu31 activity was studied. Os9BGlu31 was pre-incubated with 1 mM concentration of EDTA and metal ions, 20 µM and 40 µM of 2,4-dinitrophenyl-β-D-2-deoxy-2-fluoro-glucofuranoside, and 1 mM and 5 mM of glucono δ-lactone inhibitors in 50 mM sodium acetate, pH 4.5 at

30°C for 10 min, and then enzyme activity to hydrolyse 5 mM 4NPGlc at 30°C in 1 h was determined. The enzyme activity was detected as described in section 2.2.3.7.

### **3.3 Results**

#### **3.3.1 Cloning and expression of Os9BGlu31**

The full-length cDNA sequence of Os9BGlu31 (GenBank Accession number AK121679) consists of 1875 nucleotides. From this cDNA, a 1491 nucleotide uninterrupted reading frame (URF) encoding the mature protein of 497 amino acid residues, as shown in Figure 3.1, was cloned into the pET32a/DEST expression vector for expression in *E. coli* strain Origami(DE3). The mature protein had a predicted molecular weight of 56 kDa and predicted pI of 5.3.

The optimum conditions for expression of Os9BGlu31 as a thioredoxin fusion protein from pET32a/DEST in *E. coli* strain Origami(DE3) were determined at 20°C by varying the IPTG concentration and time of induction. The optimum expression conditions for Os9BGlu31 were induction with 0.3 mM IPTG for 16 h, as illustrated in Figures 3.2 and 3.3.

|   | AK121679F |  |
|---|-----------|--|
| ATGACGCCGGCGAGGGTGGTGGTTCATCTGCTGCGTTGTTCTGCTCGCCGCCGCCGCCGGCGCGCTCGTCTCGACGGCGCGGGG      | 87        |  |
| ·M·T·P·A·R·V·V·F·I·C·C·V·V·L·L·A·A·A·A·A·A·S·S·S·T·A·A·G·                                 |           |  |
| <u>primer</u>   |           |  |
| ATCACCAGGGCCGACTTCCCGCCGAGTTTCATCTTCGGCCCGGCTCCTCCGCTTATCAGGTTGAAGTGCATTTGCAGAGGATGGA     | 174       |  |
| ·I·T·R·A·D·F·P·P·E·F·I·F·G·A·G·S·S·A·Y·Q·V·V·E·G·A·F·A·E·D·D·G·                           |           |  |
| AGAAAGCCTAGTATCTGGGACACGTTTTTCGCACTCAGGCTATTCTGTTGATGGAGCAACCGGTGATGTAAGTGCAGATCAGTATCAT  | 261       |  |
| ·R·K·P·S·I·W·D·T·F·S·H·S·G·Y·S·V·D·G·A·T·G·D·V·T·A·D·Q·Y·H·                               |           |  |
| AAGTACAAGGAAGATGTAAGCTTTTGAAGACATGGGCGTTGACGCGTACAGGATGTCCATTTCTTGGTCTCGGCTTATTCCTGAT     | 348       |  |
| ·K·Y·K·E·D·V·K·L·L·Q·D·M·G·V·D·A·Y·R·M·S·I·S·W·S·R·L·I·P·D·                               |           |  |
| GGGCGAGGAGCTGTCAATCCGAAGGGACTGGAATACATAACAACCTGATTGATGAAGTCTGAGCCATGGAATCCAACCTCACGTA     | 435       |  |
| ·G·R·G·A·V·N·P·K·G·L·E·Y·Y·N·N·L·I·D·E·L·L·S·H·G·I·Q·P·H·V·                               |           |  |
| ACGATATATCATTTTCGATTTTCCTCAGGCTCTCCAAGATGAATACAATGGGATACTTAGTCCTAGATTTGTAGAGGACTTACAGCA   | 522       |  |
| ·T·I·Y·H·F·D·F·P·Q·A·L·Q·D·E·Y·N·G·I·L·S·P·R·F·V·E·D·F·T·A·                               |           |  |
| TACGCGGATGTCTGCTTCAAGAAGTCTTGGTGTAGAGTGAAGCACTGGAGCACTGTCAATGAGCCTAACATCGAGCCGATGGCGGA    | 609       |  |
| ·Y·A·D·V·C·F·K·N·F·G·D·R·V·K·H·W·S·T·V·N·E·P·N·I·E·P·I·G·G·                               |           |  |
| TACGATCAAGGAATCCCTCCGCCACGGCGATGTCTATCCCTTTGGTGTCTCAGTTGTGACAATGGCAACTCTACCACAGAGCCA      | 696       |  |
| ·Y·D·Q·G·I·L·P·P·R·R·C·S·F·P·F·G·V·L·S·C·D·N·G·N·S·T·T·E·P·                               |           |  |
| TACATAGTAGCACATCATCTTCTTTCGCACATTCCTCAGCAGTGTCCCTTACAGAGAGAAGTACCAGGCCACTCAAGGAGGACAA     | 783       |  |
| ·Y·I·V·A·H·H·L·L·L·A·H·S·S·A·V·S·L·Y·R·E·K·Y·Q·A·T·Q·G·G·Q·                               |           |  |
| ATTGGGCTCACATTGCTCGGTTGGTGGTACGAGCCCGGACGCAAGATCCTGAAGATGTAGCAGCAGCTGCAAGGATGAATGATTTTC   | 870       |  |
| ·I·G·L·T·L·L·G·W·W·Y·E·P·G·T·D·D·P·E·D·V·A·A·A·A·R·M·N·D·F·                               |           |  |
| CACATTGGATGGTACATGCATCCTTTGGTGTACGGTACTACCTCCGGTAATGAGGAAGAATGTTGGGTCCAGGCTACCATCTTTC     | 957       |  |
| ·H·I·G·W·Y·M·H·P·L·V·Y·G·D·Y·P·P·V·M·R·K·N·V·G·S·R·L·P·S·F·                               |           |  |
| ACAGCTGAAGAATCAAAGAGTACTTGAATCCTATGATTTTGTGCGGATTTAACCATATGTCCGCAATTTTGTGAGAGCCGACCTT     | 1044      |  |
| ·T·A·E·E·S·K·R·V·L·E·S·Y·D·F·V·G·F·N·H·Y·V·A·I·F·V·R·A·D·L·                               |           |  |
| AGCAAAGTGTAGAGCCCTCAGAGATTACATGGGCGATGCAGCTGTCAAAATATGACCTCCCATTCTGAAATCAAATAATGAGTTTC    | 1131      |  |
| ·S·K·L·D·Q·S·L·R·D·Y·M·G·D·A·A·V·K·Y·D·L·P·F·L·K·S·N·N·E·F·                               |           |  |
| CCACTCGGTTGACGAGTACTTTCATGACGTCGACCCATGGGCTCTGAAGAAGATGCTCAATCATCTCCAAGAGAAGTACAAGAAC     | 1218      |  |
| ·P·L·G·L·T·S·D·F·M·T·S·T·P·W·A·L·K·K·M·L·N·H·L·Q·E·K·Y·K·N·                               |           |  |
| CCTATTGTATGATCCATGAGAATGGAGCCGCTGGGCGAGCTGACCTTCAGGCGGAAACACCTACGACGACGATTTTCAGGTGCGCAA   | 1305      |  |
| ·P·I·V·M·I·H·E·N·G·A·A·G·Q·P·D·P·S·G·G·N·T·Y·D·D·D·F·R·S·Q·                               |           |  |
| TATCTGCAGGATTACATCGAGGCCACACTTCAATCCATCAGGAACGGGTGCAACGTGCAGGGCTACTTCGTGTGGTCTTCTGGAC     | 1392      |  |
| ·Y·L·Q·D·Y·I·E·A·T·L·Q·S·I·R·N·G·S·N·V·Q·G·Y·F·V·W·S·F·L·D·                               |           |  |
| GTGTTTCGAGTACCTGTTCCGGCTACCGCTCCGCTTCGGCCTCCTACGGCGTCGACTTCGCCTCGCCGGAGAGGACCAGGTACCAGAGG | 1479      |  |
| ·V·F·E·Y·L·F·G·Y·R·L·R·F·G·L·Y·G·V·D·F·A·S·P·E·R·T·R·Y·Q·R·                               |           |  |
| <i>AK121679R</i>  |           |  |
| CACTCGGCGGGTGGTACGCGGCTTCCCTCCGCGGCGGAGCTCCGCGCGGCGGCGGCGCTGGCCGGCGGCGGAGCCTACTCC         | 1566      |  |
| ·H·S·A·R·W·Y·A·G·F·L·R·G·G·E·L·R·P·A·A·A·A·L·A·G·G·G·A·Y·S·                               |           |  |
| <u>primer</u>   |           |  |
| CAGTGATCAAGGTTCTCAGTCTTCCCTCGCAGCTTTTCATCTCGCAAGAACAGGACAGGACGGGACAATAAAATTTACCTGGATAG    | 1653      |  |
| ·Q·*·*  |           |  |
| ATACAGAAGAATTATACAGTTTATGGAAGTTGATCTTTTGAATAGGGTCTTAGAATGAATGGTCTCTTCTTCCCTGGTTTTT        | 1740      |  |
| GGTCTTCTGTTTACAGACCAATGATGGTCAATGTCAGTCAAATGTGTGATTTAGATCAATGGGTCAAAGTGTATGATGTGATTG      | 1827      |  |
| TGTAATTGTGTCGATTATATATAAAATTTGAAGTCTCTCGTAGTTTG   | 1875      |  |

**Figure 3.1** The nucleotide and amino acid sequences of Os9BGl31, indicating the sequence that was amplified by the AK121679F and AK121679R primers (underlined).

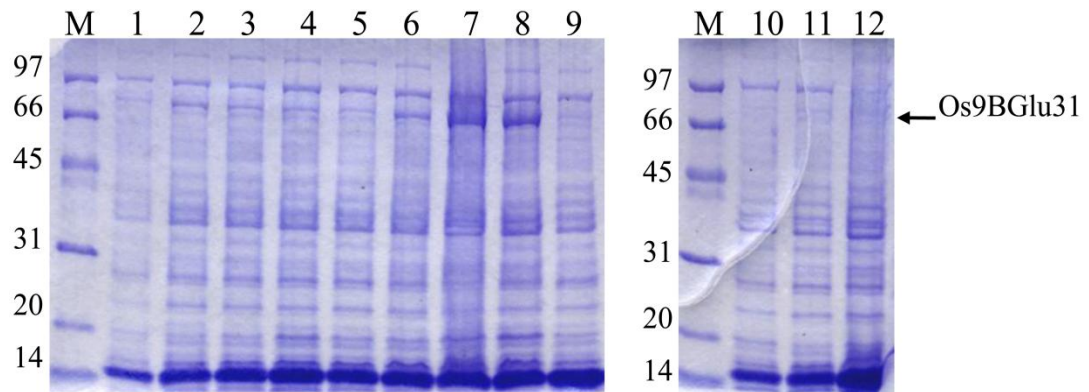


**Figure 3.2** SDS-PAGE analysis of soluble expressed Os9BGlu31 protein in the *E. coli* Origami(DE3) with induction with 0.1-0.4 mM IPTG and varied times of expression.

Lane M, Bio-Rad molecular weight markers.

Lanes 1-3, induced proteins with 0.1 mM IPTG for 8, 16 and 24 h, respectively.

Lanes 4-6, induced proteins with 0.2 mM IPTG for 8, 16 and 24 h, respectively.

Lanes 7-9, induced proteins with 0.3 mM IPTG for 8, 16 and 24 h, respectively.

Lanes 10-12, induced proteins with 0.4 mM IPTG for 8, 16 and 24 h, respectively.

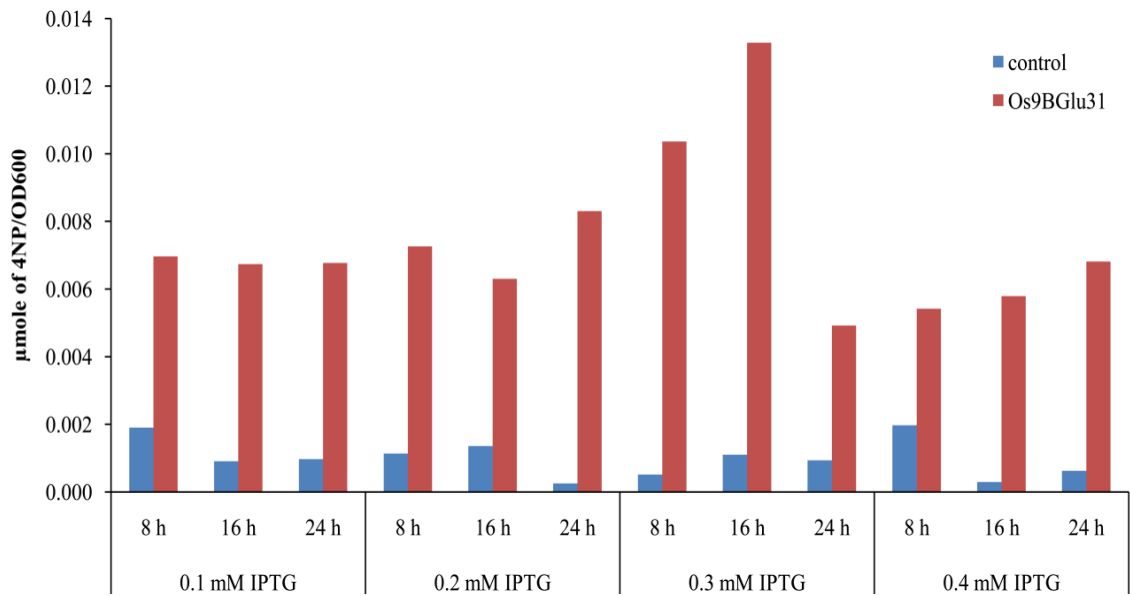


**Figure 3.3** The ratio of 4-nitrophenol (4NP) liberated from the 4NPGlc hydrolysis per cell density ( $OD_{600}$ ) of Os9BGlu31 expressed in *E. coli* Origami(DE3) at different IPTG inducer concentrations and induction times.

### 3.3.2 Purification of Os9BGlu31

The recombinant Os9BGlu31 containing 6xhistidine-tag at its N-terminus could be purified by IMAC and anion exchange chromatography. Analysis of the IMAC fractions by SDS-PAGE, indicated a strong band of fusion protein at the predicted size of approximately 70 kDa, but many other proteins were also found in the same elutions fractions (Figure 3.4). The Q-sepharose anion exchange chromatography could remove most of the contaminating proteins from the IMAC purified Os9BGlu31 (Figure 3.5). The Os9BGlu31 fusion protein was further digested with enterokinase and passed through an IMAC column again to remove the cleaved tag, in order to produce highly purified protein for kinetic analyses.

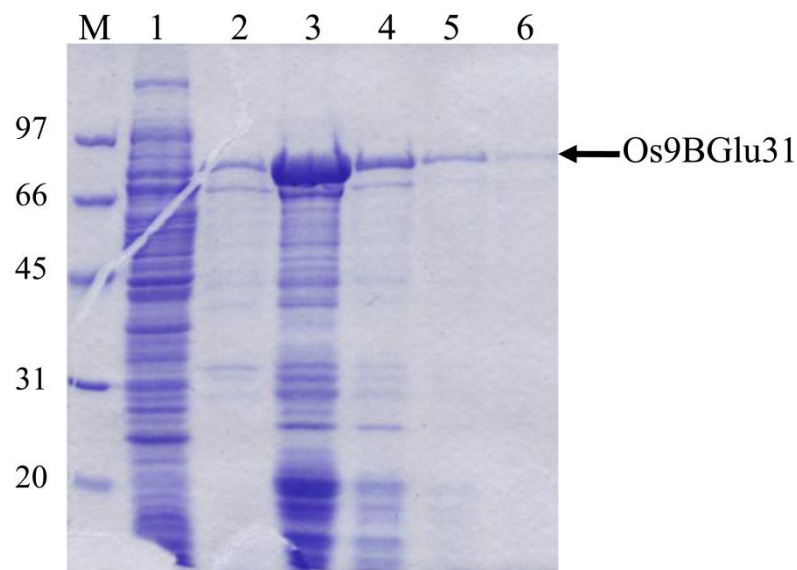


**Figure 3.4** SDS-PAGE analysis of Os9BGlu31 purified by IMAC. Lane M, Bio-Rad low molecular weight markers; lane 1, crude protein extract of induced Origami(DE3) cells; lanes 2-6, the IMAC elution fractions 4-8, respectively.

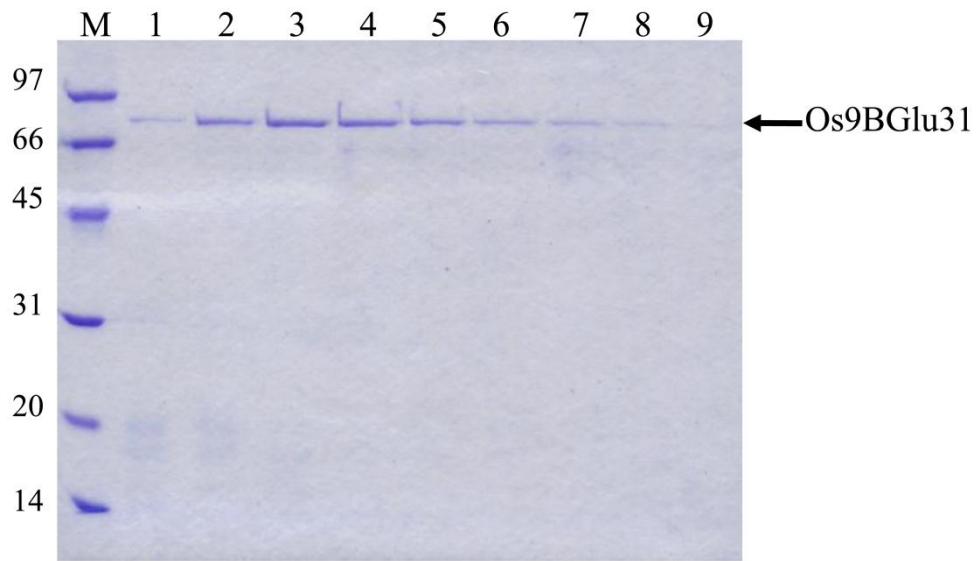


**Figure 3.5** SDS-PAGE analysis of Os9BGlu31 purified by Q-sepharose anion exchange chromatography. Lane M, Bio-Rad low molecular weight markers; lanes 1-9, fractions 25-33, which contained activity to hydrolyse 5 mM 4NPGlc.

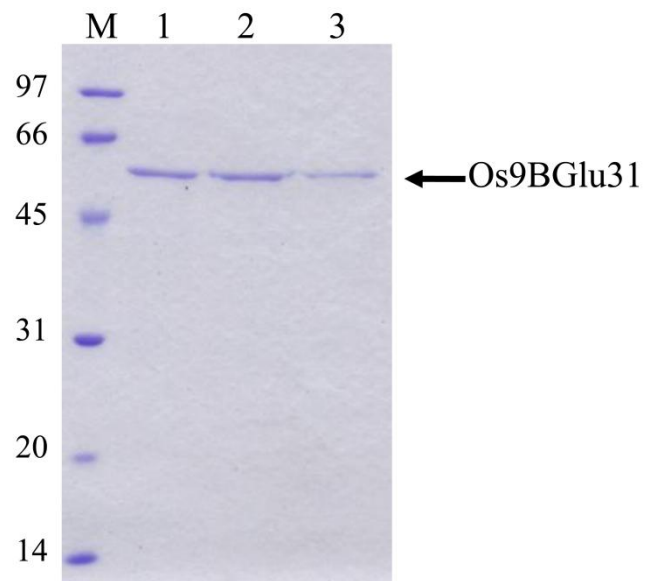


**Figure 3.6** SDS-PAGE analysis of Os9BGlu31 without fusion tag purified by subtractive IMAC after enterokinase cleavage. Lane M, Bio-Rad low molecular weight markers; lane 1, flow-through of Os9BGlu31 that passed through the  $\text{Ni}^{2+}$  column; lanes 2 and 3, purified Os9BGlu31 fractions 1 and 2, which eluted in the IMAC equilibration buffer wash, respectively.

### 3.3.3 Characterization of Os9BGlu31

#### 3.3.3.1 Optimum pH and temperature profile of Os9BGlu31

The effects of pH on the hydrolytic activity of Os9BGlu31 toward 4NPGlc were tested in buffers with pH 3.5-10. Maximal activity was observed at pH 4.5, and the activity rapidly decreased to approximately 40% maximal at pH 5.5, then slowly decreased to negligible as the pH was raised to pH 8.5. A similar rapid decrease in activity was seen as the pH was lowered to 3.5. The protein was projected to have 50% maximal activity at approximately pH 4.0 and 5.3. At temperatures ranging from 10 to 80°C, the enzyme activity increased steadily from 10 to 40°C, the maximum activity was observed at 40°C, and then activity decreased at higher temperatures to be negligible at 80°C.

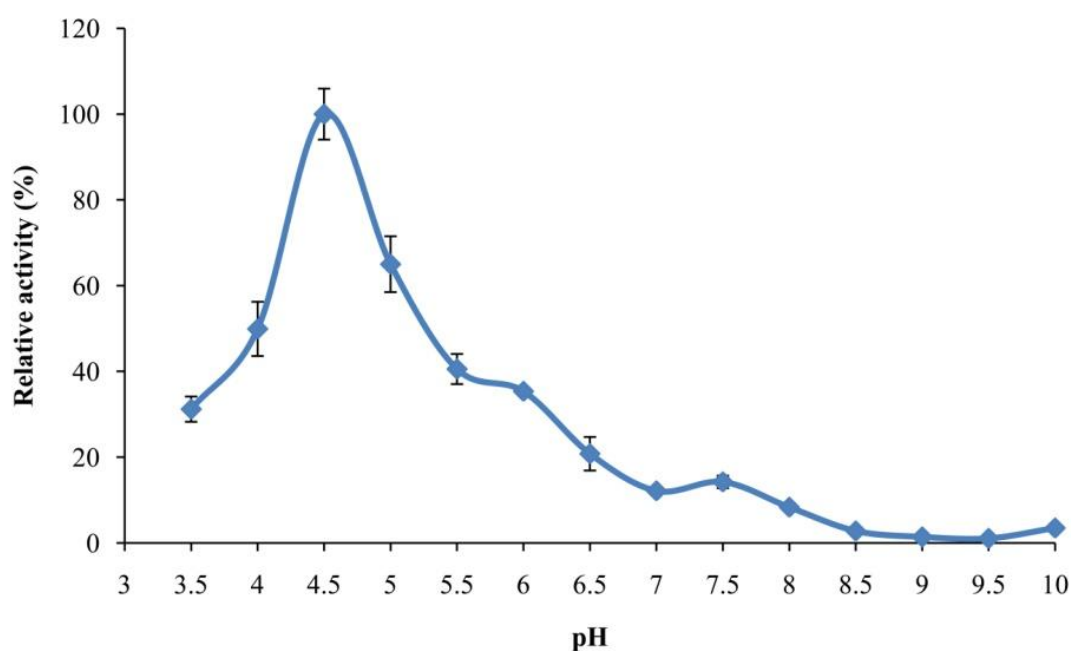


**Figure 3.7** Activity versus pH profile of Os9BGlu31 over a pH range of 3.5-10.0. Os9BGlu31 was assayed for hydrolysis of 5 mM 4NPGlc at 30°C for 60 min. The specific activity for ‘100% relative activity’ equals to 0.03 units/mg protein.

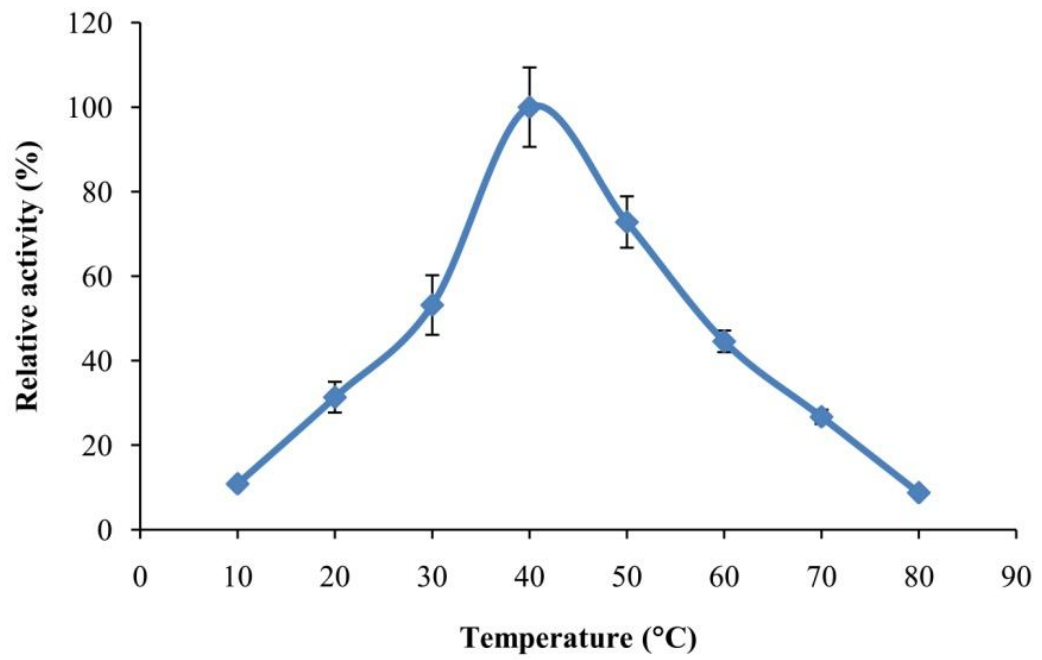


**Figure 3.8** Activity profile of Os9BGlu31 over the temperature range 10-80°C. Os9BGlu31 was assayed with 5 mM 4NPGlc in 50 mM sodium acetate, pH 4.5, for 30 min.

### 3.3.3.2 Substrate specificity and kinetic parameters of Os9BGlu31

Table 3.1 shows the hydrolytic activity of Os9BGlu31 for 4NP-glycosides and the cyanogenic glucoside dhurrin. 4NPGlc was the best synthetic substrate of Os9BGlu31, which also showed approximately 20% relative activity for  $\beta$ -D-galactoside,  $\beta$ -D-fucoside, and  $\beta$ -D-xyloside. Os9BGlu31 also hydrolysed dhurrin with approximately 11 fold higher activity than 4NPGlc. In addition, Os9BGlu31 able to slowly hydrolyse phlorizin, which could be observed by TLC (Figure. 3.9). No enzyme activity could be observed to gluco-oligosaccharides with  $\beta$ -(1,2),  $\beta$ -(1,3),  $\beta$ -(1,4) and  $\beta$ -(1,6)-linkages, and the other substrates as listed in Table 3.2. Os9BGlu31 had a  $K_M$  value of  $15.3 \pm 0.9$  mM, and  $k_{cat}$  of  $0.4 \pm 0.03$  s<sup>-1</sup> for 4NPGlc.

**Table 3.1** Relative activities of Os9BGlu31 to 5 mM substrates in 50 mM sodium acetate, pH 4.5, incubated at 30°C for 15 min.

| Substrates                         | Relative activity (%)      |
|------------------------------------|----------------------------|
| 4NP- $\beta$ -D-glucopyranoside    | 100 $\pm$ 3.6 <sup>a</sup> |
| 4NP- $\beta$ -D-mannopyranoside    | nd <sup>b</sup>            |
| 4NP- $\beta$ -D-galactopyranoside  | 20.3 $\pm$ 1.7             |
| 4NP- $\beta$ -D-fucopyranoside     | 21.9 $\pm$ 2.0             |
| 4NP- $\alpha$ -L-arabinopyranoside | nd                         |
| 4NP- $\beta$ -D-xylopyranoside     | 19.9 $\pm$ 1.4             |
| Dhurrin <sup>c</sup>               | 1065 $\pm$ 93              |

<sup>a</sup> The specific activity that correlates to 100% equals 0.03 units/mg protein.

<sup>b</sup> 'nd' indicated 'not detectable'.

<sup>c</sup> Dhurrin hydrolysis was determined by measuring glucose (the second product of the reaction) while the activity toward 4NP-glycosides were determined by measuring 4NP (the first product of the reaction), so they are only approximately equivalent.

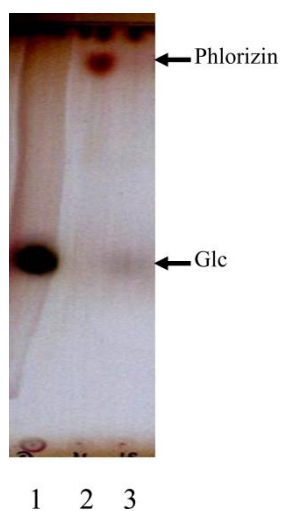


**Figure 3.9** TLC chromatogram of hydrolysis of phlorizin with Os9BGlu31. The reaction was assayed with 5 mM substrate in 10 mM sodium acetate, pH 4.5, at 30°C for 16 h. The hydrolysis products were separated on silica gel F<sub>254</sub> TLC using ethyl acetate: acetic acid: water (3:2:1). Lane 1; glucose, lane 2; phlorizin, and lane 3; product of hydrolysis by Os9BGlu31, respectively.

**Table 3.2** Hydrolysis of natural glycosides by Os9BGlu31.

| Substrate                            | Os9BGlu31 |
|--------------------------------------|-----------|
| <i>p</i> -coumaryl alcohol glucoside | -         |
| Coniferin                            | -         |
| Salicin                              | -         |
| Esculin                              | -         |
| Indoxyl glucoside                    | -         |
| Mangiferin                           | -         |
| Trans-Zeatin glucoside               | -         |
| Arbutin                              | -         |
| Pyridoxine glucoside                 | -         |
| DIMBOA                               | -         |
| Linamarin                            | -         |
| Tetraphylin                          | -         |
| Sambunigrin                          | -         |
| Neolinustatin                        | -         |
| D-amydalin                           | -         |
| Prunasin                             | -         |
| Epiheterodendrin                     | -         |
| Apigenin                             | -         |
| Gossypin                             | -         |
| Daidzin                              | -         |
| Genistin                             | -         |
| Malonyl genistin                     | -         |
| Glycitin                             | -         |
| Naringin                             | -         |
| Quercetin-3-glucoside                | -         |
| Phlorizin                            | +         |
| sophorose                            | -         |
| gentiobiose                          | -         |

\*The activity of Os9BGlu31 was detected by thin layer chromatography.

### 3.3.3.3 Effects of EDTA, metal salts and inhibitors on Os9BGlu31 activity

The effects of several metal ions and EDTA, 2,4-dinitrophenyl- $\beta$ -D-2-deoxy-2-fluoro-glucoside, glucono  $\delta$ -lactone and gibberellins (GA3) on Os9BGlu31 activity are shown in Table 3.4. No or little inhibition of EDTA, Ni<sup>2+</sup> and Zn<sup>2+</sup> was seen on Os9BGlu31 activity. The enzyme activity was decreased 10-13% by 1 mM Mg<sup>2+</sup>, Mn<sup>2+</sup>, Co<sup>2+</sup> and Ca<sup>2+</sup>, while Fe<sup>3+</sup> and Cu<sup>2+</sup> decreased the activity by 25% and 34%, respectively. Hg<sup>2+</sup> had a greater effect on Os9BGlu31, decreasing activity by approximately 90% at 1 mM. Surprisingly, concentration of 2,4-dinitrophenyl- $\beta$ -D-2-deoxy-2-fluoro-glucopyranoside and glucono  $\delta$ -lactone that would completely inhibit many  $\beta$ -glucosidases had no significant effect on Os9BGlu31 activity. The enzyme did not appear to be a gibberellin  $\beta$ -glucosidase, since gibberellins (GA3) had no effect on activity.

**Table 3.3** Effect of EDTA, metal salts and inhibitors on Os9BGlu31 activity.

| Metal ions/inhibitors  | concentration | Relative activity (%) |
|--|---------------|-----------------------|
| control  | -             | 100 $\pm$ 5.5         |
| EDTA   | 1 mM          | 93.8 $\pm$ 8.6        |
| HgCl <sub>2</sub>  | 1 mM          | 10.7 $\pm$ 1.0        |
| MgCl <sub>2</sub>  | 1 mM          | 90.2 $\pm$ 7.4        |
| MnCl <sub>2</sub>  | 1 mM          | 90.8 $\pm$ 1.7        |
| FeCl <sub>3</sub>  | 1 mM          | 65.9 $\pm$ 0.6        |
| NiSO <sub>4</sub>  | 1 mM          | 103.9 $\pm$ 5.3       |
| ZnSO <sub>4</sub>  | 1 mM          | 97.0 $\pm$ 4.7        |
| CuSO <sub>4</sub>  | 1 mM          | 74.8 $\pm$ 3.6        |
| CoCl <sub>2</sub>  | 1 mM          | 88.8 $\pm$ 7.4        |
| CaCl <sub>2</sub>  | 1 mM          | 87.7 $\pm$ 3.6        |
| 2,4-dinitrophenyl- $\beta$ -D-2-deoxy-2-fluoro-glucopyranoside | 20 $\mu$ M    | 98.4 $\pm$ 1.7        |
|  | 40 $\mu$ M    | 97.9 $\pm$ 3.1        |
| Glucono $\delta$ -lactone                                      | 1 mM          | 100.9 $\pm$ 1.8       |
|  | 5 mM          | 98.2 $\pm$ 1.7        |

### 3.4 Discussion

The amino acid sequence alignment of Os9BGlu31 was 44% identical to hydroxyisourate hydrolase (*Glycine max*), 43% to rice Os3BGlu7  $\beta$ -glucosidase, 40% to sorghum  $\beta$ -glucosidase and 38% to *Zea mays*  $\beta$ -glucosidase, respectively. The sequence around the catalytic acid/base was TVNEP and that around the catalytic nucleophile was IHENG for both Os9BGlu31 and HIUHase (Figure 3.10). The sequences of Os9BGlu31 and HIUHase are different in that the Os9BGlu31 sequence contains the conserved residues involved in glucose binding in GH1  $\beta$ -glucosidases, but HIUHase does not.

Os9BGlu31 was found to have  $\beta$ -glucosidase activity for 4NPGlc, although with very low catalytic efficiency ( $k_{\text{cat}}/K_M$  of  $0.02 \pm 0.001 \text{ mM}\cdot\text{s}^{-1}$ ), and also hydrolysis of  $\beta$ -D-galactoside,  $\beta$ -D-fucoside, and  $\beta$ -D-xyloside, which were hydrolysed at rate approximately 5-fold lower than 4NPGlc. Os9BGlu31 could not hydrolyse any  $\beta$ -linked gluco-oligosaccharides and had no HIUHase activity (Raychandhuri and Tipton, personal communication). Os9BGlu31 could hydrolyse the natural glycosides dhurrin and phlorizin. The aglycone specificity of sorghum  $\beta$ -glucosidase (Dhr1), which hydrolysed only dhurrin, had been analysed with ZmGlu1 that showed 70% sequence identity and hydrolysed many substrates, but could not hydrolyse dhurrin (Cicek *et al.*, 2000; Verdoucq *et al.*, 2003). They reported the peptide of  $^{466}\text{FAGFTERY}^{473}$  at the C-terminal domain of ZmGlu1 that is homologous to  $^{462}\text{SSGYTERF}^{469}$  of Dhr1, is important for dhurrin hydrolysis. ZmGlu1 could hydrolyse dhurrin with about 3% of the activity of Dhr1 for the mutations of F466S and F466S/A467S, and 10% for the Y473F mutant. Os9BGlu31 shares 40% sequence identity with Dhr1 and the peptide  $^{443}\text{LFGYRLRF}^{450}$  is homologous to  $^{462}\text{SSGYTERF}^{469}$  of Dhr1, which includes Os9BGlu31 residues G445, Y446, R449 and F450 that are conserved with Dhr1. The last position, F450, is especially interesting, since it is identical at the position where changing to phenylalanine gave dhurrinase activity to ZmGlu1.

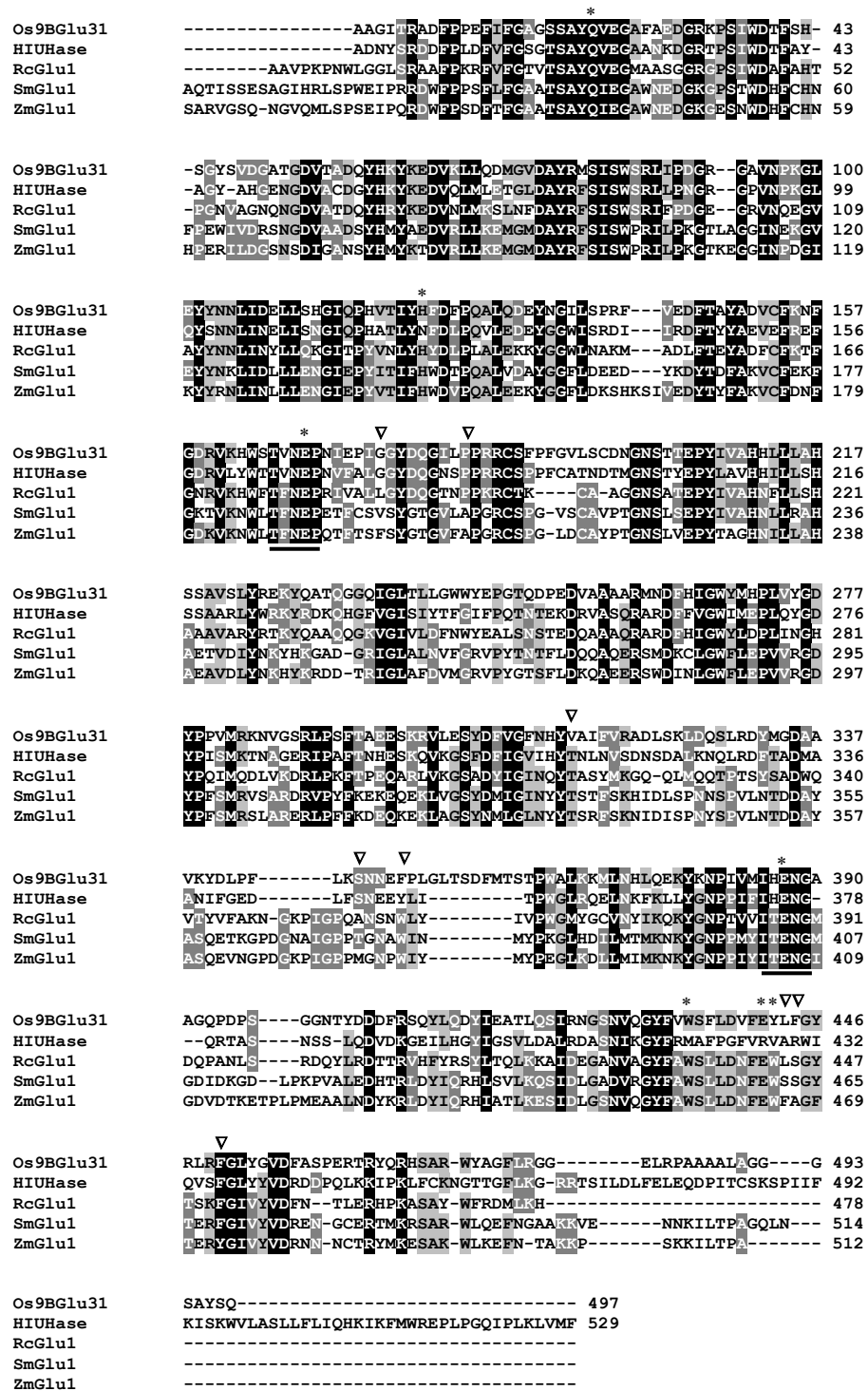


**Figure 3.10** Protein sequence alignment of rice Os9BGlu31, Os3BGlu7 (Rc\_BGlu1), *Zea mays*  $\beta$ -glucosidase (Zm\_Glu1), sorghum  $\beta$ -glucosidase dhurrinase-1 (Sm\_BGlu1) and *Glycine max* hydroxyisourate hydrolase (HIUHase). The sites indicated by Czizek *et al.* (2000) as interacting with the glycone (\*) or aglycone ( $\nabla$ ) of maize  $\beta$ -glucosidase are marked and the catalytic acid/base and nucleophile consensus sequences are underlined.

Note that the glycone binding residues are not conserved in HIUHase, but are found in Os9BGlu31.

The expression of the Os9BGlu31 gene had been analysed by Opassiri *et al.* (2006), the gene was expressed in immature seed, shoot, leaf, root seedling, panicle or flower and under stress conditions, including treatment with naphthaleneacetic acid, benzyl amino purine, or cadmium, histone deacetylase overexpression, *Acidovorax avenae* infection, and lesion mimics. Although the gene was expressed in many plant tissues, a natural rice substrate for Os9BGlu31 could not be observed when it was incubated with crude extracts from immature seed and seedling shoots and roots (data not shown). The induction of its activity in *Acidovorax avenae* infection and in other stresses, together with its hydrolysis of a cyanogenic glucoside, suggest it may act in defense.

The activity of Os9BGlu31 was inhibited with  $\text{Hg}^{2+}$ , which is a strong inhibitor for other  $\beta$ -glucosidases (Esen A., 1992; Srisomsap *et al.*, 1996; Odoux *et al.*, 2003). Glucono  $\delta$ -lactone is an analogue of the oxocarbenium ion-like transition state that could inhibit  $\beta$ -glucosidase activity of other enzymes, such as rice Os3BGlu7  $\beta$ -glucosidase (Opassiri *et al.*, 2003) and dhurrinase (Hösel *et al.*, 1987), but did not inhibit Os9BGlu31. Additionally, Os9BGlu31 activity was not affected by 2,4-dinitrophenyl- $\beta$ -D-2-deoxy-2-fluoro-glucopyranoside, which is generally a strong inhibitor because electron withdrawal by the 2-fluoro group destabilizes the oxocarbenium ion-like transition state (Withers *et al.*, 1987; Williams and Withers, 2000; Rempel and Withers, 2008), the 2,4-dinitrophenolate is a good leaving group that allows the glycosylation step to proceed, resulting in a stable covalent intermediate. Some  $\beta$ -glucosidases were strongly inhibited at 0.1-1 mM concentration of glucono  $\delta$ -lactone (Akiyama *et al.*, 1998; Hsieh and Graham, 2001; Opassiri *et al.*, 2003) and 50-100  $\mu\text{M}$  concentration of 2,4-dinitrophenyl- $\beta$ -D-2-deoxy-2-fluoro-glucopyranoside

(Hommalai *et al.*, 2005), at which the remaining activity was lower than 5% of the uninhibited activity.

### 3.5 Conclusions

The amino acid sequence of Os9BGlu31 exhibits 43% or less identity to plant  $\beta$ -glucosidases (rice, maize, and sorghum). However, the recombinant Os9BGlu31 expressed in *E. coli* hydrolysed the cyanogenic glycoside dhurrin, the substrate of sorghum  $\beta$ -glucosidase and had low activity to the flavonoid of phlorizin. The induction of Os9BGlu31 gene expression in rice plants under biotic and abiotic stress and the hydrolysis of a cyanogenic glycoside suggest that Os9BGlu31 might have a defensive function in response to pathogen infection.

### 3.6 References

- Akiyama, T., Kaku, H., and Shibuya, N. (1998). A cell wall-bound  $\beta$ -glucosidase from germinated rice: purification and properties. **Phytochemistry** 48: 49-54.
- Bandaranayake, H., and Esen, A. (1996). Nucleotide sequence of a  $\beta$ -glucosidase (*glu2*) cDNA from maize (*Zea mays* L.). **Plant Physiol.** 110: 1048.
- Cicek, M., and Esen, A. (1998). Structure and expression of a dhurrinase ( $\beta$ -glucosidase) from sorghum. **Plant Physiol.** 116: 1469-1478.
- Cicek, M., Blanchard, D., Bevan, D.R., and Esen, A. (2000). The aglycone specificity-determining sites are different in 2,4-dihydroxy-7-methoxy-1,4-benzoxazin-3-one (DIMBOA)-glucosidase (maize  $\beta$ -glucosidase) and dhurrinase (sorghum  $\beta$ -glucosidase). **J. Biol. Chem.** 275: 20002-20011.
- Czjzek, M., Cicek, M., Zamboni, V., Bevan, D.R., Henrissat, B., and Esen, A. (2000). The mechanism of substrate (aglycone) specificity in  $\beta$ -glucosidases is revealed by

- crystal structures of mutant maize  $\beta$ -glucosidase-DIMBOA, -DIMBOAGlc, and -dhurrin complexes. **Proc. Nat. Acad. Sci., USA.** 97: 13555-13560.
- Esen, A. (1992). Purification and partial characterization of maize (*Zea mays* L.)  $\beta$ -glucosidase. **Plant Physiol.** 98; 174-182.
- Hommelai, G., Chaiyen, P., and Svasti, J. (2005). Studies on the transglucosylation reactions of cassava and Thai rosewood  $\beta$ -glucosidases using 2-deoxy-2-fluoroglycosyl-enzyme intermediates. **Arch. Biochem. Biophys.** 442: 11-20.
- Hösel, W., Tober, I., Eklund, S.H., and Conn, E.E. (1987). Characterization of  $\beta$ -glucosidase with high specificity for the cyanogenic glucoside dhurrin in *Sorghum bicolor* (L.) Moench seedlings. **Arch. Biochem. Biophys.** 252: 152-162.
- Hsieh, M.C., and Graham, T. (2001). Partial purification and characterization of a soybean  $\beta$ -glucosidase with high specific activity towards isoflavone conjugates. **Phytochemistry** 58: 995-1005.
- Ketudat Cairns, J.R., and Esen, A. (2010).  $\beta$ -glucosidases. **Cell. Mol. Life Sci.** DOI 10.1007/s00018-010-0399-2.
- Kikuchi, S., Sotoh, K., Nagata, T., Kawagashira, N., Doi, K., Kishimoto, N., Yazaki, J., Ishikawa, M., and Yamada, H. (2003). Collection, mapping, and annotation of over 28,000 cDNA clones from *Japonica* rice. **Science** 301: 376-379.
- Odoux, E., Chauwin, A., and Brillouet, J.M. (2003). Purification and characterization of vanilla bean (*Vanilla planifolia* Andrews)  $\beta$ -D-glucosidase. **J. Agric. Food Chem.** 51; 3168-3173.
- Opassiri, R., Ketudat Cairns, J.R., Akiyama, T., Wara-Aswapati, O., Svasti, J., and Esen, A. (2003). Characterization of a rice  $\beta$ -glucosidase highly expressed in flower and germinating shoot. **Plant Science** 165: 627-638.

- Opassiri, R., Pomthong, B., Onkoksoong, T., Akiyama, T., Esen, A., and Ketudat Cairns, J.R. (2006). Analysis of rice glycosyl hydrolase family 1 and expression of Os4bglu12  $\beta$ -glucosidase. **BMC Plant Biol.** 6.
- Raychaudhuri, A., and Tipton, P.A. (2002). Cloning and expression of the gene for soybean hydroxyisourate hydrolase. Localization and implications for function and mechanism. **Plant Physiol.** 130: 2061-2068.
- Rempel, B.P., and Withers, S.G. (2008). Covalent inhibitors of glycosidases and their applications in biochemistry and biology. **Glycobiology** 18: 570-586.
- Sarma, A.D., Serfozo, P., Kahn, K., and Tipton, P.A. (1999). Identification and purification of hydroxyisourate hydrolase, a novel ureide-metabolizing enzyme. **J. Biol. Chem.** 274: 33863-33865.
- Srisomsap, C., Svasti, J., Surarit, R., Champattanachai, V., Sawangareetrakul, P., Boonpuan, K., Subhasitanont, P., and Chokchaichamnankit, D. (1996). Isolation and characterization of an enzyme with  $\beta$ -glucosidase and  $\beta$ -fucosidase activities from *Dalbergia cochinchinensis* Pierre. **J. Biochem.** 119: 585-590.
- Withers, S.G., Street, I.P., Bird, P., and Dolphin, D.H. (1987). 2-Deoxy-2-fluoroglucosides. A novel class of mechanism-based glucosidase inhibitors. **J. Am. Chem. Soc.** 109: 7530-7531.
- Williams, S.J. and Withers, S.G. (2000). Glycosyl fluorides in enzymatic reactions. **Carbohydr. Res.** 327: 27-46.



# CHAPTER IV

## DNA CLONING, PROTEIN EXPRESSION AND CHARACTERIZATION OF RECOMBINANT BARLEY GLUCAN GLUCOHYDROLASE ISOENZYME I

### Abstract

The native  $\beta$ -D-glucan exohydrolase isoenzyme ExoI from barley seedlings, designated HvExoI, was the first GH3 glycoside hydrolase for which a crystal structure was determined. A precise understanding of relationships between structure and function in this enzyme has been gained by structural and enzymatic studies. To allow testing of hypotheses gained from these studies, an efficient system for expression of HvExoI in *Pichia pastoris* was developed using a codon-optimized cDNA. Protein expression at a temperature of 20°C yielded a recombinant enzyme, designated rHvExoI, which had molecular masses of 70-110 kDa due to heavy glycosylation at Asn 221, Asn498 and Asn600, the three sites of N-glycosylation in native HvExoI. Most of the N-linked carbohydrate could be removed from rHvExoI, resulting in N-deglycosylated rHvExoI with a substantially decreased molecular mass of 67 kDa. rHvExoI was able to hydrolyse barley (1,3;1,4)- $\beta$ -D-glucan, laminarin and lichenans. The catalytic efficiency value,  $k_{cat}/K_M$ , of rHvExoI with barley (1,3;1,4)- $\beta$ -D-glucan was similar to that reported for native HvExoI. Further, laminaribiose, cellobiose and gentiobiose were formed through transglycosylation reactions with 4-nitrophenyl  $\beta$ -D-glucoside and barley (1,3;1,4)- $\beta$ -D-glucan. Overall, the biochemical properties of rHvExoI were similar to those reported for native HvExoI, although differences were seen in thermostabilities and hydrolytic rate of certain  $\beta$ -linked glucosides.

## 4.1 Introduction

Glycoside hydrolases (EC 3.2.1.) are widely distributed in living organisms. These enzymes hydrolyse glycosidic linkages between two or more carbohydrates or between a carbohydrate and a non-carbohydrate moiety. Based on amino acid sequence similarities, catalytic mechanisms and structural features, the glycoside hydrolase family GH3 is one of 115 glycoside hydrolase families currently listed in the CAZy database (<http://www.cazy.org/>) (Cantarel *et al.*, 2009). The GH3 enzymes are more frequently represented in bacteria, plants and fungi, than in archaea and mammals. The GH3 family includes catalytic proteins with  $\beta$ -D-glucosidase (EC 3.2.1.21), xylan 1,4- $\beta$ -D-xylosidase (EC 3.2.1.37),  $\beta$ -N-acetylhexosaminidase (EC 3.2.1.52), exo- $\beta$ -D-glucanase (EC 3.2.1.-) and  $\alpha$ -L-arabinofuranosidase (EC 3.2.1.55) activities. The predicted functions of the GH3 enzymes involve: (i) the biodegradation and assimilation of oligo- and polysaccharides (Faure *et al.*, 1999; Tsujubo *et al.*, 2001; Shipkowski and Brenchley, 2005; Faure *et al.*, 2001), (ii) modification of bacterial macrolide antibiotics and other toxic plant compounds (Wulff-Strobe and Wilson, 1995; Quirós *et al.*, 1998), and (iii) turnover of cell wall components (Crombie *et al.*, 1989; Kotake *et al.*, 1997; Cheng *et al.*, 2000; Hrmova and Fincher, 2001; Hung *et al.*, 2001).

The biochemical and biophysical properties of various GH3 enzymes have previously been described (Breves *et al.*, 1997; Kawai *et al.*, 2004; Adelsberger *et al.*, 2004; Mayer *et al.*, 2006; Turner *et al.*, 2007). Some GH3 enzymes exhibit broad substrate specificity, such as the  $\beta$ -D-glucosidases BGL1 from *Pichia etchellsii* and *Saccharomycopsis fibuligera* (Machida *et al.*, 1998; Wallecha and Mishra, 2003), Gbg1 from *Agrobacterium tumefaciens* (Watt *et al.*, 1998), and bglB from *Thermotoga neapolitana* (Zverlov *et al.*, 1997) and enzymes with  $\alpha$ -L-arabinofuranosidase and  $\beta$ -D-xylosidase activities, such as ARA-I/XYL from barley (*Hordeum vulgare*), XarB from *Thermoanaerobacter ethanolicus* and MsXyl1 from alfalfa roots (Lee *et al.*, 2003; Mai *et al.*, 2000; Xiong *et al.*, 2007).

Therefore, the identification of natural substrates of GH3 enzymes based on their hydrolytic reactions, and assignments of the biological functions of these enzymes are often highly conjectural.

One of the most intensely studied enzymes in the GH3 family is a barley  $\beta$ -D-glucan exohydrolase, isoform I (Hrmova *et al.*, 1996), here designated as HvExoI. Based on substrate specificity and gene expression studies, it has been suggested that this enzyme might be involved in the turnover or modification of cell walls during the elongation of coleoptiles (Hrmova and Fincher, 2001 ; 2009). The enzyme is able to hydrolyse a variety  $\beta$ -D-glucosidic linkages (Hrmova *et al.*, 1996; Hrmova and Fincher, 1998). HvExoI was the first GH3 enzyme for which a crystal structure was determined (Varghese *et al.*, 1999). The 3D structure consists of an NH<sub>2</sub>-terminal  $(\beta/\alpha)_8$  barrel domain and a COOH-terminal  $(\alpha/\beta)_6$  sandwich domain (Varghese *et al.*, 1999). Two catalytic amino acid residues were identified in the active site and these are the catalytic nucleophile Asp285, located in the conserved SDW motif of the first domain, and the acid/base Glu491, positioned in the second domain (Hrmova *et al.*, 2001 ; 2004). The active site of HvExoI is located at the interface between the two domains and a glucose molecule was found at the -1 subsite in the native crystal structure, bound predominantly through hydrogen bonds to charged amino acid residues (Varghese *et al.*, 1999).

The catalytic mechanism and structural basis of substrate specificity of HvExoI have been investigated by kinetic and crystallographic studies with substrate analogues and inhibitors (Hrmova *et al.*, 2002; 2004; 2005; Hrmova and Fincher, 2007). Based on the premise that enzymes in the same family possess similar structures and catalytic mechanisms, HvExoI was also used as a structural model to predict the architectures of other GH3 members (Steenbakkers *et al.*, 2003). The catalytic mechanism of other GH3 enzymes has also been studied by site-directed mutagenesis with enzymes for which a crystal structure has yet to be determined, such as a  $\beta$ -D-glucosidase from *Flavobacterium*

*meningosepticum* (Chir and Chen, 2001; Li *et al.*, 2002). However, similar mutagenesis studies with HvExoI have yet to be conducted due to lack of an appropriate recombinant expression system. It is expected that the catalytic mechanism of HvExoI may be more precisely understood, if the roles of active site residues suggested from the structural studies could be confirmed by a site directed mutagenesis approach.

Although many plant glycoside hydrolases have been expressed in bacteria, not every glycoside hydrolase could be expressed in a prokaryotic system in an active form. The yeast *Pichia pastoris* has proven to be an effective eukaryotic host in many other instances (e.g. Juge *et al.*, 1996; Ferrares *et al.*, 1998). *P. pastoris* is a methylotrophic yeast, which can produce large amounts of recombinant proteins by methanol induction of the alcohol oxidase 1 (AOX) promoter, and has been shown to effectively synthesize eukaryotic post-translationally modified proteins (Cereghino *et al.*, 2000; Cregg *et al.*, 2009). *P. pastoris* has similar molecular genetics to *Saccharomyces cerevisiae*, but researchers have achieved much higher yields of plant glycoside hydrolases, such as barley  $\alpha$ -amylase (Juge *et al.*, 1996) and Thai rosewood  $\beta$ -D-glucosidase (Ketudat Cairns, 2000; Toonkool *et al.*, 2006), in *P. pastoris* than *S. cerevisiae*.

Here, we report the recombinant expression of the HvExoI isoenzyme (rHvExoI) from barley in various expression systems. This is the first successful recombinant expression of an active form of a plant enzyme from the GH3 family that as of April 2010 contains nearly 3,000 entries. We further describe the substrate specificity and biochemical properties of rHvExoI expressed in *P. pastoris*, and compare these characteristics with those of the native HvExoI isoenzyme.

## 4.2 Materials and methods

### 4.2.1 Plasmids, bacterial and yeast strains

Plasmids used for this work included pENTR<sup>TM</sup>/D-TOPO (Invitrogen), pET32a, pET32a/DEST (Opassiri *et al.*, 2006), pUC57 (GenScript), pPICZ $\alpha$ BNH<sub>8</sub>, and pPICZ $\alpha$ BNH<sub>8</sub>/DEST (Toonkool *et al.*, 2006). The bacteria used for DNA cloning were *E. coli* strains DH5 $\alpha$  and TOP10, while strain Origami(DE3) was used for expression. *Pichia pastoris* host strains used for expression in yeast were Y11430 and SMD1168H.

**Table 4.1** Yeast strains.

| strain   | Relevant Genotype   |
|----------|---|
| Y11430   | <i>MAT<math>\alpha</math> trp1-1 ura3-1 his3-11, 15 leu2-3, 112 ade2-1 can1-100</i> |
| SMD1168H | <i>pep4::URA3 his4 ura3</i>   |

### 4.2.2 Molecular cloning, expression, purification and characterization of barley exoglucanase I (HvExoI).

#### 4.2.2.1 DNA cloning of a native HvExoI cDNA from barley seedlings

A cDNA encoding the mature HvExoI protein (GenBank accession number AF102868) was amplified from cDNA reverse-transcribed from barley seedling RNA (Harvey *et al.*, 2001) with the ExoIMaF and ExoIstopR primers (Table 4.2) by *Pfu* DNA polymerase. The PCR product (~1.8 kb) was cloned into the pENTR<sup>TM</sup>/D-TOPO Gateway<sup>®</sup> system entry vector (Invitrogen) in *E. coli* strain TOP10 competent cells, selected on 50  $\mu$ g/ml kanamycin Lennox broth (LB). Then, the HvExoI gene was transferred from the entry vector to the pET32a/DEST expression vector for *E. coli* expression and pPICZ $\alpha$ B/DEST expression vector for *P. pastoris* expression by the LR

clonase recombination reaction (Invitrogen), as described in section 2.2.3.3. Reaction products were transformed into DH5 $\alpha$  competent cells and selected on 50  $\mu$ g/ml ampicillin LB plates for the pET32a/DEST derivative vector or 25 $\mu$ g/ml zeocin LB plates for the pPICZ $\alpha$ BNH<sub>8</sub>/DEST-derived vector. The recombinant pET32a/DEST\_HvExoI (~8 kb) and pPICZ $\alpha$ B/DEST\_HvExoI (~5 kb) were checked with *Hind*III and *Bam*HI restriction endonuclease digests, respectively. Then, the insert DNA was sequenced at Macrogen (Korea).

#### 4.2.2.2 DNA subcloning of the optimized HvExoI cDNA

An optimized HvExoI cDNA (GenBank accession number GU441535) was synthesized and inserted into the pUC57 vector by GenScript Corporation (Piscataway, NJ, USA). The optimized HvExoI cDNA was designed with the cloning restriction sites of *Pst*I and *Eco*RI at the 5' and 3' ends, respectively. The cDNA sequence was optimized by GenScript with their propriety software to maximize codon frequency in *Pichia pastoris*, while minimizing mRNA structures and repetitive sequences. The gene was amplified by *Pfu* DNA polymerase with the ExoIs\_Ntcor and M13 reverse primers (Table 4.2) which matched the 5' end of optimized HvExoI and M13 reverse promoter of the vector, respectively. The PCR product (~1.8 kb) and pPICZ $\alpha$ BNH<sub>8</sub> expression vector were digested with *Pst*I and *Eco*RI restriction endonucleases at 37°C overnight. The digested fragments were analysed on 1% agarose gel electrophoresis and purified from the gel by the Perfectprep® Gel Cleanup (Eppendorf). The optimized HvExoI cDNA and pPICZ $\alpha$ BNH<sub>8</sub> vector were ligated together with T4 ligase (Promega) and a ratio of 3:1 PCR product per plasmid, and the reaction was incubated at 14°C overnight. The reaction product was transformed into DH5 $\alpha$  competent cells and selected on a 25  $\mu$ g/ml zeocin LB plate. The recombinant expression vector was cut checked with *Pst*I and *Eco*RI restriction endonucleases and the DNA inserts and junctions sequenced at Macrogen (Korea).

**Table 4.2** Primers for HvExoI amplification.

| Primer      | sequence (5' -> 3')           | T <sub>m</sub> (°C) |
|-------------|-------------------------------|---------------------|
| ExoIMatF    | CACCGACTACGTGCTCTACAAGGA      | 70                  |
| ExoIstopR   | CTAGTACTTCTTCGTCGCGTTGGT      | 72                  |
| ExoIs_Ntcor | CACCGCTGCAGATTACGTTTTGTACAAGG | 88                  |
| M13 reverse | CAGGAAACAGCTATGAC             | 52                  |

**Table 4.3** Cycling parameters for HvExoI amplification.

| Segment | Cycles | Temperature            | Time   |
|---------|--------|------------------------|--|
| 1       | 1      | 95°C                   | 5 min  |
| 2       | 30     | 95°C                   | 45 sec   |
|         |        | Annealing temperature* | 45 sec   |
|         |        | 72°C                   | 4 min for native HvExoI,<br>5 min for optimized HvExoI |
| 3       | 1      | 72°C                   | 7 min  |

\* The annealing temperatures for amplification of the mature protein coding region of the native and optimized HvExoI gene cDNA were 65°C and 49°C, respectively.

#### **4.2.2.3 Recombinant protein expression in *E. coli***

The pET32a/DEST expression vector containing the native cDNA of HvExoI was transformed into *E. coli* strain Origami(DE3). Protein was induced with 0.4 mM IPTG at 20°C for 16 to 18 hours, and extracted as described in section 2.2.3.5. Protein expression was detected by measuring enzyme activity by release of 4-nitrophenol from 4NPGlc and analyzing the extract on SDS-PAGE.

#### **4.2.2.4 Protein refolding by iFOLD protein refolding system 2 kit**

Protein refolding of rHvExoI from the insoluble fraction was performed with the iFOLD protein refolding system 2 kit (Novagen). Five grams of induced cell pellet were resuspended in 50 ml of cell resuspension buffer (50 mM Tris-HCl, 50 mM NaCl, 1 mM Tris(2-carboxyethyl)phosphine hydrochloride (TCEP), 0.5 mM EDTA, 5% glycerol, pH 8.0). Then 100 µl of lysonase<sup>TM</sup> bioprocessing solution was added and stirred gently at room temperature for 15 min. The cell resuspensions were sonicated on ice 4 times with a Kegelspitze KE 76 probe with the amplitude set at 20% power for 30 s. After that, membrane components and contaminating proteins were removed by adding 5 ml of 1.5 M NDSB-201 and stirred slowly at room temperature for 15 min. Inclusion bodies were collected by centrifugation at 8000xg for 15 min at 10°C. The pellet was completely resuspended in 50 ml of 1X system2 IB wash buffer (50 mM Tris-HCl, 50 mM NaCl, 1 mM TCEP, 0.5 mM EDTA, 0.125 M NDSB-201, 5% glycerol, pH 8.0) and centrifuged at 8000xg for 15 min at 10°C. Residual NDSB-201 was removed from the pellet by resuspending the pellet 2 times in 50 ml of 1X cell resuspension buffer and collecting the pellet by centrifugation. Next, the inclusion body pellet was denatured by adding 25 ml iFOLD guanidine (GuHCl) denaturation buffer (50 mM Tris-HCl, 0.2 M NaCl, 2 mM EDTA, 7 M GuHCl, pH 8.0) and 250 µl 1 M TCEP, and stirring gently at 4°C until the solution became clear. The solution was centrifuged at 25,000xg for 15 min at 4°C and the

supernatant was passed through a 0.45  $\mu\text{m}$  syringe-tip filter. Finally, the protein was refolded by rapid dilution of 5  $\mu\text{l}$  of 5 mg/ml protein solution into 96 refolding conditions (<http://www.merck-chemicals.co.uk/life-science-research/ifold-system-2-plate-layout>) with volumes of 245  $\mu\text{l}$  each, and incubated at 4°C and 23°C with gentle shaking for 4 days. During protein refolding, the activity of rHvExoI to 4NPGlc was assayed every day.

#### **4.2.2.5 Protein refolding of rHvExoI by dialysis**

*E. coli* expression of rHvExoI was induced as in section 2.2.3.5. Four grams of cell pellet was resuspended with 30 ml of wash buffer (0.5% (v/v) TritonX-100, 100 mM NaCl, 0.1% (w/v) sodium azide, 50 mM Tris-HCl, pH 7.4) and the inclusion bodies were recovered by centrifugation at 12,000xg for 10 min at 4°C. This step was repeated 2 times, followed by a third time with wash buffer without TritonX-100. The inclusion bodies were solubilized in 20 ml of guanidine denaturation buffer (50 mM Tris-HCl, pH 7.4, 100 mM NaCl, 10 mM EDTA, 10 mM DTT, 6 M GuHCl) and gently stirred at 4°C overnight. The clear solution was obtained by centrifugation at 12,000xg for 15 min at 4°C. Refolding was performed with 0.16 mg/ml of solubilized inclusion bodies by dialysis into the refolding buffer with gradually decreasing concentrations from 6 M to 0.08 M of guanidine-HCl in 10 mM Tris-HCl, pH 7.4, 10% (v/v) glycerol, 1 mM reduced glutathione and 0.1 mM oxidized glutathione.

#### **4.2.2.6 Preparation of competent *Pichia pastoris* strains Y11430 and SMD1168H**

A glycerol stock of *P. pastoris* was streaked on a yeast extract peptone dextrose (YPD) plate without antibiotic, which was then incubated at 28°C for 2-3 days. A single colony was inoculated into 500 ml YPD broth in a 2 litres flask and grown at 28°C with 220 rpm shaking overnight until the OD<sub>600</sub> reached 1.3-1.5. The cells were collected by centrifugation at 1,500xg for 5 min at 4°C. The pellet was resuspended 2 times in 500 ml and 250 ml of ice-cold sterile water and collected by centrifugation at 1,500xg for 5 min at 4°C each time. Next, the pellet was resuspended with 20 ml of ice-cold 1 M sorbitol and centrifuged at 1,500xg for 5 min at 4°C. Finally, the pellet was resuspended and kept in 1 ml of ice-cold 1 M sorbitol.

#### **4.2.2.7 DNA preparation for electroporation**

Seven to ten micrograms of circular recombinant pPICZ $\alpha$ BNH<sub>8</sub> plasmid was linearized with *PmeI* in a 1.5 ml microcentrifuge tube and the reaction was incubated at 37°C overnight. Linearization of the plasmid was checked by electrophoresis 2  $\mu$ l of reaction on a 1% agarose gel. The restriction endonuclease was inactivated by heating at 65°C for 10 min. Linear DNA was precipitated by adding 0.1 volumes of 3 M sodium acetate, pH 5.2, and 2.5 volumes of 100% ethanol, and then incubating at -20°C for 30 min. Precipitated DNA was collected by centrifugation at 12,000xg for 10 min. The DNA pellet was washed with 500  $\mu$ l of 70% ethanol and centrifuged at 12,000xg for 10 min. All ethanol was removed by inverting the tube on tissue paper for 10 min. The DNA pellet was dissolved in 5-10  $\mu$ l of sterile deionized water.

Linearized pPICZ $\alpha$ BNH<sub>8</sub> vector (7  $\mu$ g) was added to a microcentrifuge tube containing 80  $\mu$ l of *P. pastoris* competent cells and mixed gently by pipetting. The cell mixture was transferred to a pre-cooled 0.2 cm electroporation cuvette. The cuvette with

the cells was incubated on ice for 5 min. The linearized vector was transformed into the *P. pastoris* by electroporation (Bio-Rad) with the parameters of 1.5 kV, 25  $\mu$ F and 400  $\Omega$ . After that, 1 ml of 1 M sorbitol was immediately added to the electroporated cells and they were incubated at 30°C for 1 h without shaking. Two hundred microlitres of cell solution was spread on a YPDS plate containing 100  $\mu$ g/ml zeocin antibiotic. The YPDS plate was incubated at 28°C for 3-5 days. Transformed cells were selected again on a YPD plate containing 500  $\mu$ g/ml zeocin.

#### **4.2.2.8 Expression of recombinant HvExoI in *P. pastoris***

A single colony that had been selected on a 500  $\mu$ g/ml zeocin YPD plate was inoculated into 500 ml of BMGY medium containing 100  $\mu$ g/ml zeocin and grown in a shaking incubator (220 rpm) at 28°C until the cell culture OD<sub>600</sub> reached 2-3. Cells were harvested by centrifugation at 3000xg for 5 min at 20°C and resuspended in 1000 ml BMMY medium at the final OD<sub>600</sub> of 1. Protein expression was induced by adding methanol to 1% (v/v) final concentration every 24 h for 7 days.

The expression conditions of native and optimized HvExoI constructs were varied in order to optimize protein production yield by using different *P. pastoris* strains (Y11430 and SMD1168H) and expression temperatures. The native gene was expressed in host strain Y11430 at 28°C under standard *Pichia* expression condition (*Pichia* manual, Invitrogen), and in strain SMD1168H at 20°C and 28°C, while the optimized gene was expressed in host strain SMD1168H at 20°C and 28°C.

#### 4.2.2.9 Purification of recombinant HvExoI

The culture broth with secreted rHvExoI was supplemented with PMSF to 1 mM and the pH was adjusted to 4.7 on ice with concentrated acetic acid. The protein solution was loaded onto a pre-equilibrated SP-Sepharose cation-exchange column at a flow rate 1.8 ml/min. The column was washed with 50 mM sodium acetate, pH 4.7, at a flow rate of 0.5 ml/min and protein was eluted with a linear gradient of 0-2 M NaCl in 50 mM sodium acetate, pH 4.7, at a flow rate 1 ml/min over 4 column volumes (CV). The active fractions were concentrated and resuspended in 50 mM sodium phosphate, pH 7.8, containing 300 mM NaCl (IMAC buffer). IMAC purification of rHvExoI was performed by mixing rHvExoI with Talon Co<sup>2+</sup>-bound IMAC resin at 4°C overnight, pouring into a column, washing with 10 CV of IMAC buffer, and eluting the enzyme with a 0-0.5 M imidazole gradient in the IMAC buffer at a flow rate of 0.5 ml/min over 8 CV. The active fractions were reconstituted in 20 mM sodium acetate buffer, pH 5.0, by centrifugal filtration (Vivaspin, 10 kDa exclusion limit). Protein was homogenized by passed through P100 gel filtration chromatography and eluted with 50 mM sodium acetate, pH 5.0, 1 mM DDT and 200 mM NaCl at a flow rate of 0.07 ml/min. The fractions containing activity were pooled and the buffer changed to 20 mM sodium acetate, pH 5.0, as described above.

Purified rHvExoI (60-100 µg) was deglycosylated by 500 U endoglycosidase H (New England BioLabs) in 50 mM sodium citrate buffer, pH 5.5. The mixture was incubated at 4°C for 3-4 days with gentle shaking. Finally, deglycosylated rHvExoI was purified through a 2<sup>nd</sup> IMAC column, as described above, to remove endoglycosidase H. After IMAC, imidazole was removed by centrifugal concentration and nearly homogenous rHvExoI was suspended in 20 mM sodium acetate, pH 5.25.

#### **4.2.2.10 Determination of the optimal pH and thermostability for recombinant HvExoI**

The optimal pH of rHvExoI was determined in 140  $\mu$ l of reaction containing 0.2% (w/v) 4NPGlc, 160  $\mu$ g/ml BSA in McIlvaine buffers with pH values in the range of 3.5-8.5 at 0.5 pH unit increments. The enzyme activity was assayed at 30°C for 15 min and the reaction stopped by adding 100  $\mu$ l of 2 M sodium carbonate. Enzyme activity was measured as 4-nitrophenol released, based on the absorbance at 405 nm.

The thermostability of rHvExoI was determined by pre-incubating enzyme in 0.1 M sodium acetate, pH 5.0 for glycosylated and pH 5.25 for N-deglycosylated rHvExoI, at temperatures between 0-80°C with and without 160  $\mu$ g/ml BSA for 15 min. Then, the enzyme was immediately cooled down on ice for 3 min. Enzyme activity was assayed in 140  $\mu$ l of the reaction containing 0.2% (w/v) 4NPGlc at 30°C for 15 min. The reaction was stopped with 100  $\mu$ l of 2 M sodium carbonate and the 4-nitrophenol released measured as the absorbance at 405 nm.

#### **4.2.2.11 Substrate specificity of recombinant HvExoI**

The rHvExoI activity was assayed with 0.2% (w/v) substrates, 160  $\mu$ g/ml BSA in 0.1 M sodium acetate at the optimum pH of 5.0 for glycosylated and 5.25 for N-deglycosylated rHvExoI, at 30°C for 15 min. The activity was tested for synthetic substrates, oligosaccharides and polysaccharides. The synthetic substrates consisted of 4NP- $\beta$ -D-glucopyranoside, 4NP- $\beta$ -D-galactopyranoside, 4NP- $\beta$ -D-xylopyranoside, 4NP- $\beta$ -D-fucopyranoside, 4NP- $\beta$ -D-lactopyranoside, 4NP- $\beta$ -D-glucosiduronic acid, 4NP- $\alpha$ -L-arabinopyranoside, 4NP-N-acetyl- $\beta$ -D-glucosaminide and 4NP- $\beta$ -D-cellobioside, which were assayed in 140  $\mu$ l reaction volumes, and the reactions stopped with 100  $\mu$ l of 2 M sodium carbonate. For the reaction of oligosaccharides (sophorose, laminarioligosaccharides DP 2-7, cellooligosaccharide DP 2-6 and gentiobiose) and

polysaccharides (laminarin from *Laminaria digitate*, curdlan from *Alcaligenes faecalis*, pachyman from *Poria cocos*, barley (1,3;1,4)- $\beta$ -D-glucan, CM-cellulose, CM-pachyman DS 0.23, schizophyllan M-2 from *Schizophyllum commune*, CM glucan from *Saccharomyces cerevisiae* and lichenan from *Cetraria islandica*) were assayed in 50  $\mu$ l reactions, which were stopped by boiling at 100°C for 5 min. Then 20  $\mu$ l of a reaction was placed in a microtiter plate well and 200  $\mu$ l of glucose diagnostic kit solution (4 mg of o-dianisidine dihydrochloride in 100 ml of glucose oxidase/peroxidase reagent, Sigma) was added. The reaction was incubated at 37°C for 30 min. The glucose liberated was measured from the absorbance at 450 nm compared to a glucose standard curve.

#### **4.2.2.12 Determination of glucosyltransferase activity of recombinant HvExoI**

One and a half nmoles of rHvExoI was assayed for glycosyltransferase activity in a 70  $\mu$ l reaction containing 20 mM 4NPGlc or 1% (w/v) barley (1,3;1,4)- $\beta$ -D-glucan in 5 mM sodium acetate, pH 5 for glycosylated and 5.25 for N-deglycosylated rHvExoI, at 30°C. The reactions with 20 mM 4NPGlc were stopped by boiling at 100°C for 5 min after incubating 0 min, 3 min, 4 h and 18 h. The reactions of 1% (w/v) barley (1,3;1,4)- $\beta$ -D-glucan were stopped at time points of 0, 4, 24 and 48 h. Then 10  $\mu$ l of the reactions were spotted on TLC silica gel 60 F<sub>254</sub> plates, which were developed in a solvent of ethyl acetate: acetic acid: water (3:2:1). The TLC plate was coated with 1% orcinol monohydrate in 10% (w/w) sulfuric acid, and heated at 150°C for a 2-3 min to visualize the carbohydrates.

#### 4.2.2.13 Determination of kinetic parameters and inhibition

Kinetic parameters were determined for hydrolysis of laminarin, barley (1,3;1,4)- $\beta$ -D-glucan, laminaribiose, cellobiose and 4NPGlc with 0.7-4.5 pmole of rHvExoI in 0.1 M sodium acetate containing 160  $\mu$ g/ml BSA. Reactions were incubated at 30°C for 30 min and stopped by boiling at 100°C for 5 min. Enzyme activity was calculated from the 4-nitrophenol or glucose liberated as described in section 4.2.2.11. The  $K_M$  and  $V_{max}$  values were calculated from non-linear-regression analysis of Michaelis-Menten plots with Grafit 5.0. The catalytic rate constant ( $k_{cat}$ ) was calculated by dividing the maximum velocity ( $V_{max}$ ) by the total amount of enzyme.

Inhibition of rHvExoI activity to 0.2% (w/v) 4NPGlc was determined with methyl-O-thio-gentiobiose (0-0.53  $\mu$ M G6sG-OMe), 2,4-dinitrophenyl 2-fluoro-2-deoxy- $\beta$ -D-glucoside (0-0.53  $\mu$ M 2F-DNPGlc), and glucono  $\delta$ -lactone (0-53  $\mu$ M GL) in 0.1 M sodium acetate containing 160  $\mu$ g/ml BSA. After incubation at 30°C for 15 min, the reaction was stopped by adding 100  $\mu$ l of 2 M sodium carbonate. The dissociation constants ( $K_i$ ) of enzyme-inhibitor complexes were determined by a proportional weighted fit, using a nonlinear regression analysis program based on Michaelis-Menten kinetics (Perella, 1988).

$$\frac{1}{v} = \frac{K_M + [S]}{V_{max} [S]} + [I] \frac{K_M/K_I}{V_{max} [S]}$$

#### 4.2.2.14 Immunoblot analysis

Two and a half micrograms of secreted proteins were separated on standard sodium dodecyl sulphate polyacrylamide gel electrophoresis (SDS-PAGE described in section 2.2.2.3). The protein in the gel was transferred onto a nitrocellulose membrane with transfer buffer (25 mM Tris-HCl pH 8.0, 190 mM glycine, and 20% (v/v) methanol) at 120 volts, 4°C for 100 min (Bio-Rad). The membrane was blocked with 5% non-fat dry milk in phosphate buffered saline (PBS) at room temperature for at least 60 min or at 4°C for

overnight. The membrane was washed 3 times for 5 min each with wash buffer (PBS containing 0.05% Tween 20). A mouse monoclonal anti-polyHistidine IgG2a isotype antibody (Sigma) was used as the primary antibody in 1:2000 dilution with PBS containing 1% bovine serum albumin (BSA), and incubated with the membrane for 2 h. The membrane was washed 3 times for 5 min each with wash buffer. The membrane was incubated with a 1:2000 dilution of peroxidase conjugated goat anti-mouse IgG (Sigma) as the secondary antibody in wash buffer for 1 h and then was washed 3 times for 5 min each with wash buffer. Finally, the membrane was developed with aminoethyl carbazole substrate kit (Sigma) for 30 min.

#### **4.2.2.15 Tryptic mapping of rHvExoI by MALDI-ToF/ToF spectrometry**

About 10 µg of rHvExoI were S-amidomethylated, digested with 100 ng sequencing grade trypsin (Promega) in 5 mM ammonium bicarbonate and concentrated to 5 µl. A 0.5 µl aliquot of the digest was applied to a 600 µm AnchorChip (Bruker Daltonik GmbH, Bremen, Germany) according to the  $\alpha$ -cyano-4-hydroxycinnamic acid (HCCA, Bruker Daltonik) thin-layer method. MALDI ToF mass spectra were acquired with a Bruker Ultraflex III MALDI ToF/ToF mass spectrometer (Bruker Daltonik GmbH) operating in reflectron mode under the control of FlexControl, version 3.0 (Bruker Daltonik GmbH). All spectrometry data were processed with FlexAnalysis, version 3.1 (Bruker Daltonik GmbH), and the spectra and mass lists were exported to BioTools (Bruker Daltonik GmbH). The MS and corresponding MS/MS spectra were combined and submitted to a Mascot database-search.

#### **4.2.2.16 Molecular mass determination of rHvExoI via MALDI**

##### **spectrometry**

Samples of 1-3  $\mu\text{l}$  of glycosylated and N-deglycosylated rHvExoI were mixed with 1  $\mu\text{l}$  matrix solution (10 mg/ml sinipinic acid in 90% acetonitrile/0.1% trifluoroacetic acid) and applied to a 600 mm AnchorChip target plate (Bruker Daltonik GmbH, Bremen, Germany). MALDI ToF mass spectra were acquired on a Bruker Ultraflex III MALDI ToF/ToF mass spectrometer (Bruker Daltonik GmbH) operating in linear mode under the control of the FlexControl software (Version 3.0, Bruker Daltonik GmbH). External calibration was performed with a mix of ClinProt Protein Calibration Standard and Protein Calibration Standards 2 (Bruker Daltonik GmbH) over a range of 1 to 25 kDa that were analysed under the same conditions. Spectra were obtained at various locations over the surface of the matrix spot.

## 4.3 Results

### 4.3.1 Expression of HvExoI

A construct in which the HvExoI cDNA was inserted in pET32a/DEST was first used to express an NH<sub>2</sub>-terminal thioredoxin-His<sub>6</sub>-tagged fusion protein in *Escherichia coli* strain Origami(DE3) cells, as this system has been successfully used for expression of other plant glycoside hydrolases (Opassiri *et al.*, 2003; 2006; Chantarangsee *et al.*, 2007; Kuntothom *et al.*, 2009; Seshadri *et al.*, 2009). Under the conditions tested, the rHvExoI protein was observed only in the insoluble fraction upon cell extraction and no enzyme activity was detected. Therefore, refolding of rHvExoI was attempted after solubilisation in guanidine-HCl, but again the enzyme was found to be inactive under any refolding conditions tested.

Expression of rHvExoI in yeast was attempted by inserting the native cDNA into the pPICZ $\alpha$ BNH<sub>8</sub>/DEST expression vector, to produce a protein fused to the  $\alpha$ -factor prepropeptide for secretion (Figure 4.2). *P. pastoris* strain Y11430 was tested as a host to produce rHvExoI. No increase in  $\beta$ -D-glucosidase (with 4-nitrophenyl  $\beta$ -D-glucopyranoside, 4NPGlc) or exoglucanase (with barley (1,3;1,4)- $\beta$ -D-glucan) activities were observed and the protein could not be detected on Coomassie-stained SDS-PAGE gels in the predicted mass range. Since this construct contains an eight-histidine tag at the NH<sub>2</sub>-terminus of rHvExoI (AHHHHHHHHAA) after the secretory peptide cleavage site, the rHvExoI could be detected by immunoblot analysis with anti-polyhistidine antibody. Here, a 43 kDa band was detected, which could be correlated to the size of domain 1 of rHvExoI (data not shown). This analysis indicated that either rHvExoI was produced as a full-length protein and then proteolytically degraded by an unspecified protease from the host, or that premature termination of translation occurred near the end of domain 1, possibly because the native barley cDNA contained codons of low usage in *P. pastoris*. To avoid the problems of proteolysis and poor codon usage for protein synthesis in *P. pastoris*, the

HvExoI cDNA was codon-optimized and expressed in the protease-deficient *P. pastoris* strain SMD1168H.

The native and codon-optimized rHvExoI cDNA fusions were transformed into *P. pastoris* strain SMD1168H and protein expression was induced at a temperature of 20°C. High levels of HvExoI activity, measured with 4NPGlc, were detected from the codon-optimized rHvExoI cDNA fusion and a series of bands from 75 to 85 kDa were detected by immunoblot analysis with anti-polyhistidine antibody (Figure 4.3). The activity in the media slowly increased until 4 days of induction, after which it did not change (Figure 4.4). However, little increase in rHvExoI activity and protein production (as determined by SDS-PAGE and Coomassie-staining) were observed from the cDNA fusions containing codon-optimized HvExoI that were induced at a temperature of 28°C, or from a construct containing the native HvExoI cDNA induced at any temperature.

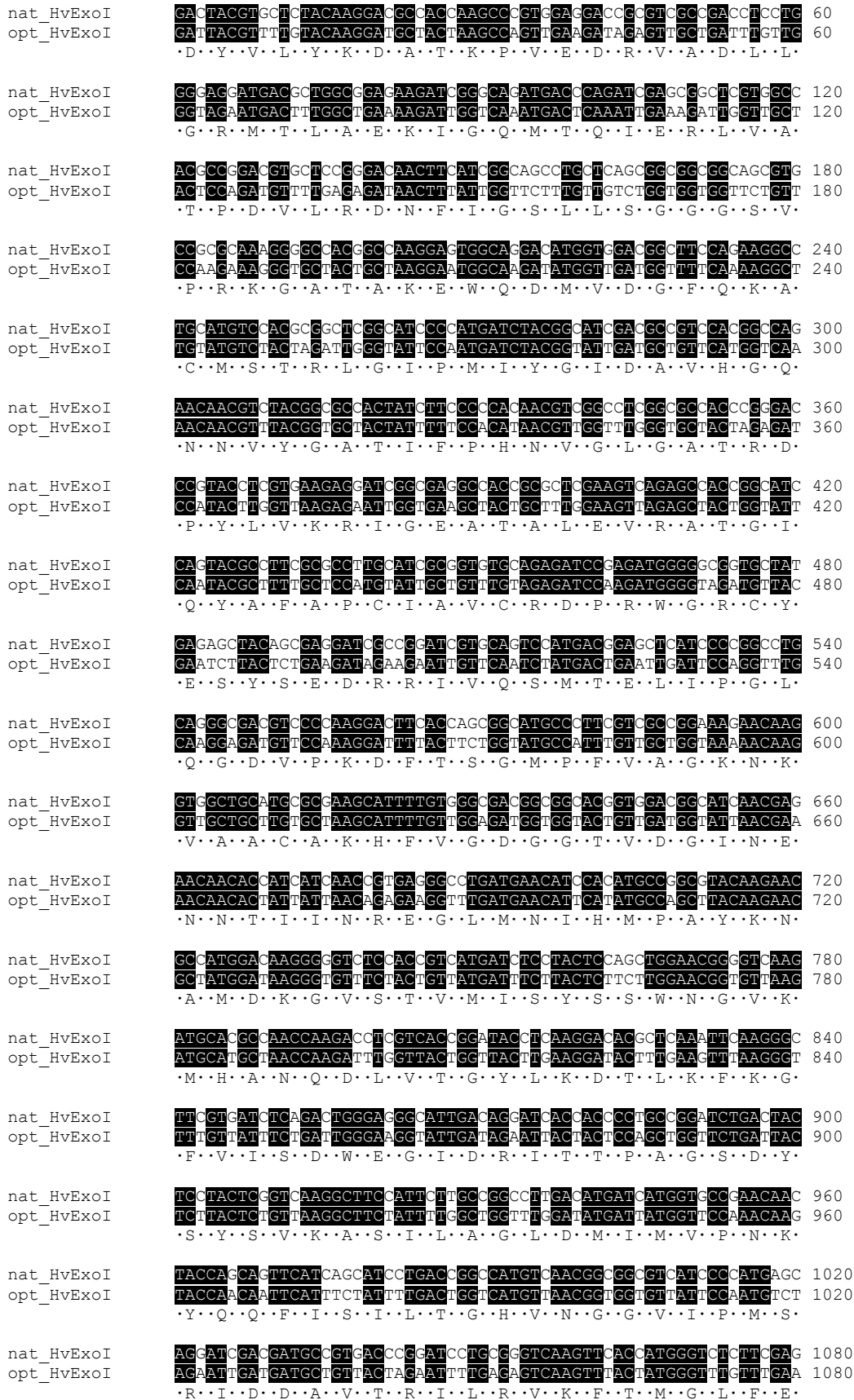


**Figure 4.1** Alignment of the nucleotide sequences of the native (upper) and optimized (lower) HvExoI cDNA. Both sequences encode the same 605 amino acid residues.

```

nat_HvExoI      AACCCCTACGCTGACCCCTGCATGGCCGACCCAGCTAGGAAAGCAGCAGCAAGGATTTG 1140
opt_HvExoI      AACCCATACGCTGATCCAAGCTATGGCTGACAATTCGGTAAACAAGACATAGAGATTTG 1140
                ·N·P·Y·A·D·P·A·M·A·E·Q·L·G·K·Q·E·H·R·D·L·

nat_HvExoI      GCGAGGGAAGGGCCAGGAAGTCGCTGGTCTGCTGAAGAACGGCAAGACTTCGACCGAC 1200
opt_HvExoI      GCTAGAGAAGCTGCTAGAAAGTCCTGGTCTTGGTTGTTGAAGAACGGTAAACTTCTACTGAT 1200
                ·A·R·E·A·A·R·K·S·L·V·L·L·K·N·G·K·T·S·T·D·

nat_HvExoI      GCGCCGCTTCTGCCGCTGCCAAGAAGGCCCCCAAGATCTGGTCCCGGAGCACAAGCC 1260
opt_HvExoI      GCTCCATTTGTGCCATTGCCAAAGAAGGCCCAAGATTTGGTTGCTGGTCTCTCATGCT 1260
                ·A·P·L·L·P·L·P·K·K·A·P·K·I·L·V·A·G·S·H·A·

nat_HvExoI      GACAACTGGGCTACCAAGTCGGCGGCTGGACATCGAGTGGCAAGCGACAGGCCCGC 1320
opt_HvExoI      GATAACTGGGTTACCAATGCTGGTGGTTGGACTATCGAATGGCAAGGAGATACTGGTAGA 1320
                ·D·N·L·G·Y·Q·C·G·G·W·T·I·E·W·Q·G·D·T·G·R·

nat_HvExoI      ACCACCGTGGCACCCACCATCCGGAGGGGCTGAAGGCCGCCGTGACCCCTCGACGGTC 1380
opt_HvExoI      ACTACTGTGGTACTACTATTTGGAAAGCTGTTAAGGCTGCTGTGATCCCTCTACTGTT 1380
                ·T·T·V·G·T·T·I·L·E·A·V·K·A·A·V·D·P·S·T·V·

nat_HvExoI      GTGCTGTTCCCGAACAACCCGACCGGGAATTCGTCAAGAGCGGCGGCTTCTCAGCC 1440
opt_HvExoI      GTTCTTTGCTGAACAACCCGATGCTGAATTTGTTAAGTCTGGTGGTCTTCTCAGCC 1440
                ·V·V·F·A·E·N·P·D·A·E·F·V·K·S·G·G·F·S·Y·A·

nat_HvExoI      ATCGTTGCCCTGGCGAGCACCCCTACACGAGACCAAGGGCGACAACCTGAACCTGAC 1500
opt_HvExoI      ATTGTGCTCTGCTGAACATCCAATACACTGAAACTAAGGGAATAACTGAACCTGACT 1500
                ·I·V·A·V·G·E·H·P·Y·T·E·T·K·G·D·N·L·N·L·T·

nat_HvExoI      ATCCGGGACCCGGCCAGCACCCTGAGCACCCTGCAAGCGGCTGTGCGGGCGTGCCTGCGGACG 1560
opt_HvExoI      ATTCAAGAACCAAGGTTGTCTACTCTCAAGCTGTGTGTTGGTGGTGTAGATGTGCTACT 1560
                ·I·P·E·P·G·L·S·T·V·Q·A·V·C·G·G·V·R·C·A·T·

nat_HvExoI      GTGCTCATCAGCGGCGGCCCGTGTGGTGCAGCCGCTGTGTCGGCCGCTCCGACCGCTG 1620
opt_HvExoI      GTTTTGATTTCTGGTAGCAAGTGTGTGTTCAACCATGTGTCGGCTGCTCATGCTTTG 1620
                ·V·L·I·S·G·R·P·V·V·V·Q·P·L·L·A·A·S·D·A·L·

nat_HvExoI      GTGCGGGCTGGCTCCCGGCTCGGAGGGCGAGGGAAGTACCGACCGGCTGTTTGGCGAC 1680
opt_HvExoI      GTTGGTGGTGGTTGCCAGCTTCTCAAGTCAAGCTGTACTGATGGTTTGGTTGAGAT 1680
                ·V·A·A·W·L·P·G·S·E·G·Q·G·V·T·D·A·L·F·G·D·

nat_HvExoI      TTCGGGTTACCGGAGGCTGCCGCGGACTGGTTCAAGTCGGTGGACCACTGCCGATG 1740
opt_HvExoI      TTTGGTTTACTGGTAGATGGCCAAAGACTTGGTTTAAAGTCTGTGATCAATGGCAATG 1740
                ·F·G·F·T·G·R·L·P·R·T·W·F·K·S·V·D·Q·L·P·M·

nat_HvExoI      AACGTCGGCGACCGCCACTACGACCCGCTCTTCCGCTCGATACGGCCCTCACACCAAC 1800
opt_HvExoI      AACGTTGGAGATGCTCATTACGATCCATTCGTTAGATTGGTTACGGTTTCACTACTAAC 1800
                ·N·V·G·D·A·H·Y·D·P·L·F·R·L·G·Y·G·L·T·T·N·

nat_HvExoI      GCGACGAAGAAGTACTAG 1818
opt_HvExoI      GCTACTAAGAAGTACTAG 1818
                ·A·T·K·K·Y·*·*·

```

**Figure 4.1** (Continued) Alignment of the nucleotide sequences of the native (upper) and optimized (lower) HvExoI cDNA. Both sequences encode the same 605 amino acid residues.

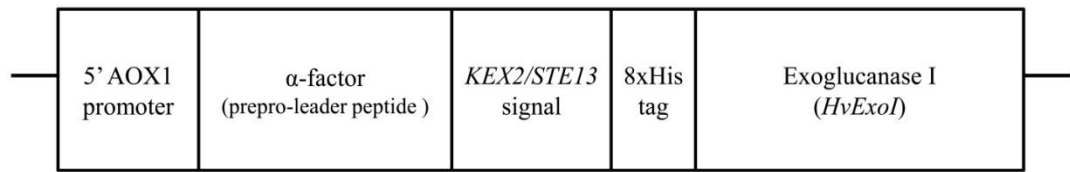


**Figure 4.2** Plasmid constructs of the pPICZ $\alpha$ BNH<sub>8</sub>-HvExoI plasmid. The plasmid provides alcohol oxidase 1 (AOX1) promoter-controlled expression of rHvExoI in *P. pastoris*. rHvExoI was produced as an N-terminal prepro- $\alpha$ -factor-8xHis-tagged fusion protein, containing the KEX2/STE13 cleavage signal (Glu Lys Arg \* Glu Ala \* Glu Ala \*). The *kex2* gene product cleaves between Arg and Glu and the *ste13* gene product cleaves after the Glu-Ala repeats, with the cleavage site indicated by asterisks in the sequence above.

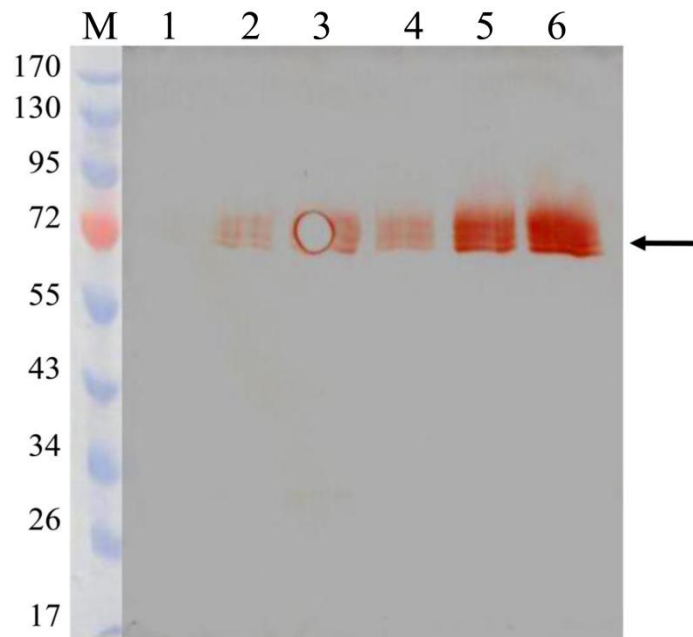


**Figure 4.3** Protein production of optimized rHvExoI detected by western immunoblot analysis with a mouse monoclonal anti-polyHistidine IgG2a isotype antibody and peroxidase conjugated goat anti-mouse IgG. Levels of rHvExoI production after 1, 2, and 3 days of colony 1 (lanes 1-3) and colony 2 (lanes 4-6). Lane M is a prestained protein marker.

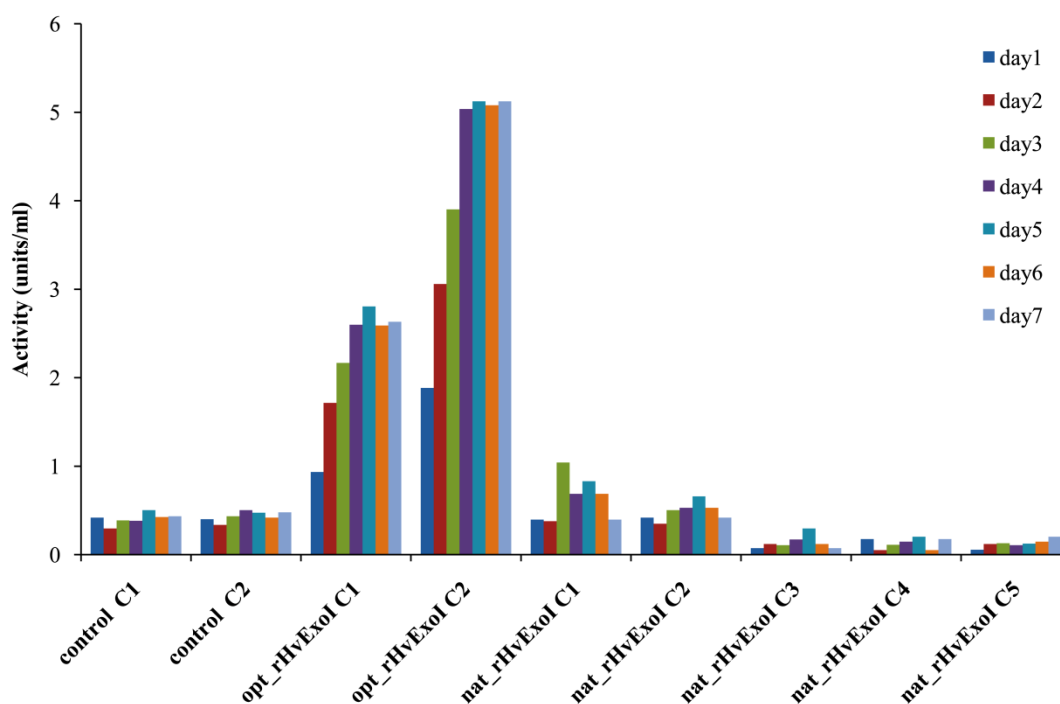


**Figure 4.4** Time course of  $\beta$ -glucosidase activity in media from *P. pastoris* transformed with empty plasmid control (control C1 and C2), optimized (opt\_rHvExoI C1 and C2) and native (nat\_rHvExoI C1-C5) expression vectors. rHvExoI activity in *P. pastoris* strain SMD1168H media upon induction of expression at 20°C, was measured as the 405 nm absorbance of 4NP released from 4NPGlc in the standard assay.

### 4.3.2 Protein purification and tryptic mapping of optimized rHvExoI

After rHvExoI was expressed in *P. pastoris* from the codon-optimized cDNA at 20°C for 4 days, a set of major protein bands, with apparent masses corresponding to the molecular mass of rHvExoI and higher, was detected by SDS-PAGE with Coomassie staining (Figure 4.5). This protein was purified from the culture media by SP-Sepharose chromatography. Protein was eluted with 1.2 M NaCl in 50 mM sodium acetate, pH 4.7. The fractions containing narrow ranges of activity near the Gaussian peak (based on activity, absorbance at 280 and SDS-PAGE profiles) were concentrated and purified by IMAC, which bound rHvExoI containing the His<sub>8</sub>-tag. A portion of the activity passed through the column, which may be attributed to rHvExoI that had lost its His-tag to proteolysis and a native *P. pastoris* (1,3)- $\beta$ -D-glucan exohydrolase (Xu *et al.*, 2006). Nevertheless, most of the expressed rHvExoI was eluted from the column with 250 mM imidazole (Figure 4.6) and the specific activity of rHvExoI was increased by about 4-fold after IMAC purification (Table 4.4). It has been reported that native HvExoI has three N-glycosylation sites at Asn221, Asn498 and Asn600 (Varghese *et al.*, 1999). To test whether the bands detected in the range between 80 and 100 kDa (Figure 4.5) were due to the presence of over-N-glycosylated forms of rHvExoI, and whether these N-glycosylation sites could affect enzyme properties, the N-linked carbohydrate was removed by endoglycosidase H. After N-deglycosylated rHvExoI was purified by a second round of IMAC (Figure 4.7), the specific activity remained more-or-less unchanged. The amino acid sequence of N-deglycosylated rHvExoI was confirmed by mass spectrometry (Figure 4.8 and Table 4.5).

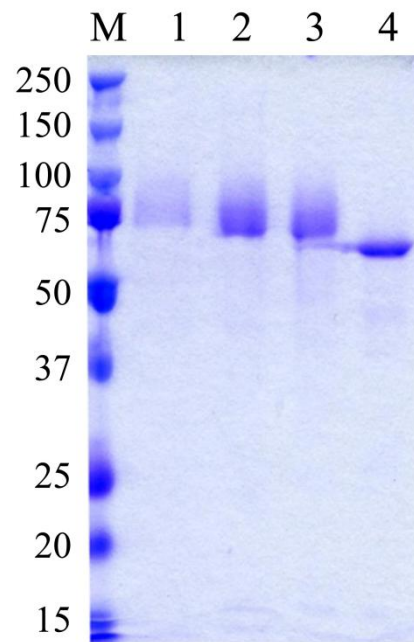


**Figure 4.5** SDS-PAGE of rHvExoI from crude broth (lane1), and purified via SP-Sepharose chromatography (lane 2), the 1<sup>st</sup> IMAC step (lane 3), and the 2<sup>nd</sup> IMAC step, after deglycosylation with endoglycosidase H (lane 4) compared with a prestained protein marker (lane M).

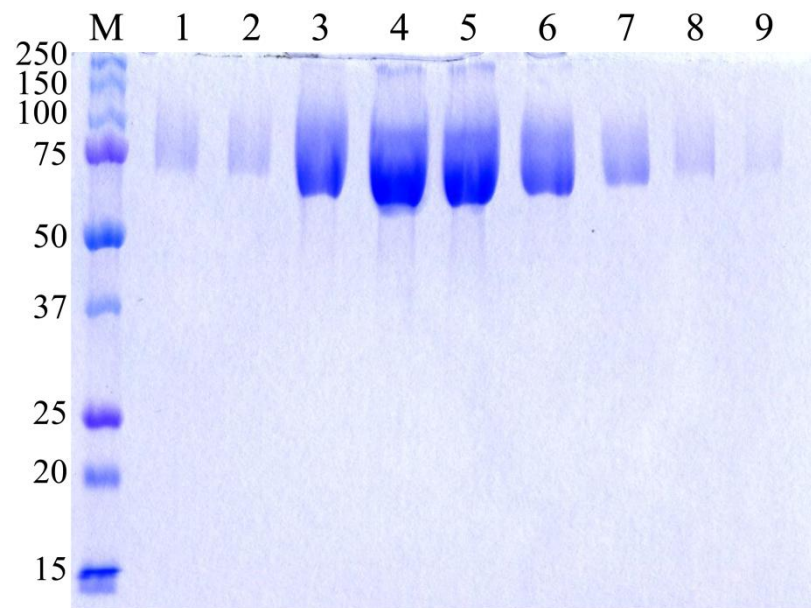


**Figure 4.6** SDS-PAGE analysis of rHvExoI purified by 1<sup>st</sup> IMAC step. Lane M, Prestained protein markers; lanes 1-9, elution fractions 8-16, which contained activity to hydrolyse 1 mM 4NPGlc.

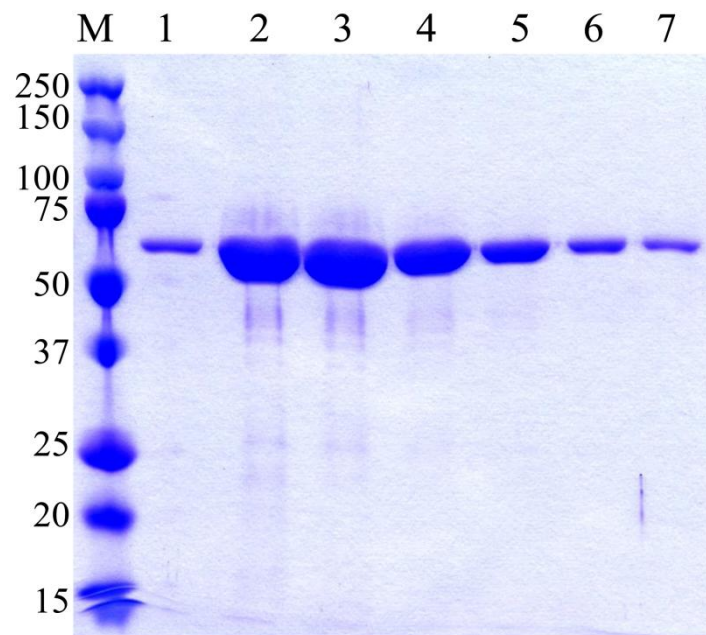


**Figure 4.7** SDS-PAGE analysis of rHvExoI purified by a 2<sup>nd</sup> round of IMAC after N-deglycosylation with endoglycosidase H. Lane M, Prestained protein markers; lanes 1-7, elution fractions 5-11, respectively, which contained activity to hydrolyse 1 mM 4NPGlc.

**Table 4.4** Enzyme yields during purification of rHvExoI.

| Purification step    | Yield     |                       | Specific activity            | Recovery <sup>b</sup> | Purification Factor <sup>b</sup> |
|----------------------|-----------|-----------------------|------------------------------|-----------------------|----------------------------------|
|                      | Protein   | Activity <sup>a</sup> |                              |                       |                                  |
|                      | <i>mg</i> | <i>units</i>          | <i>units·mg<sup>-1</sup></i> | <i>%</i>              | <i>fold</i>                      |
| Crude protein        | 119       | 98.7                  | 0.8                          | 100                   | 1                                |
| SP-Sepharose         | 18.9      | 41.3                  | 2.2                          | 41.9                  | 2.6                              |
| 1 <sup>st</sup> IMAC | 3.3       | 11.7                  | 3.5                          | 11.8                  | 4.2                              |
| 2 <sup>st</sup> IMAC | 2.9       | 9.0                   | 3.1                          | 9.1                   | 3.7                              |

<sup>a</sup> Recovered enzyme units assayed on 4NPGlc.

<sup>b</sup> Recoveries are expressed as percentage of enzyme activity in the crude protein, and purification factors are calculated on the basis of specific activities.

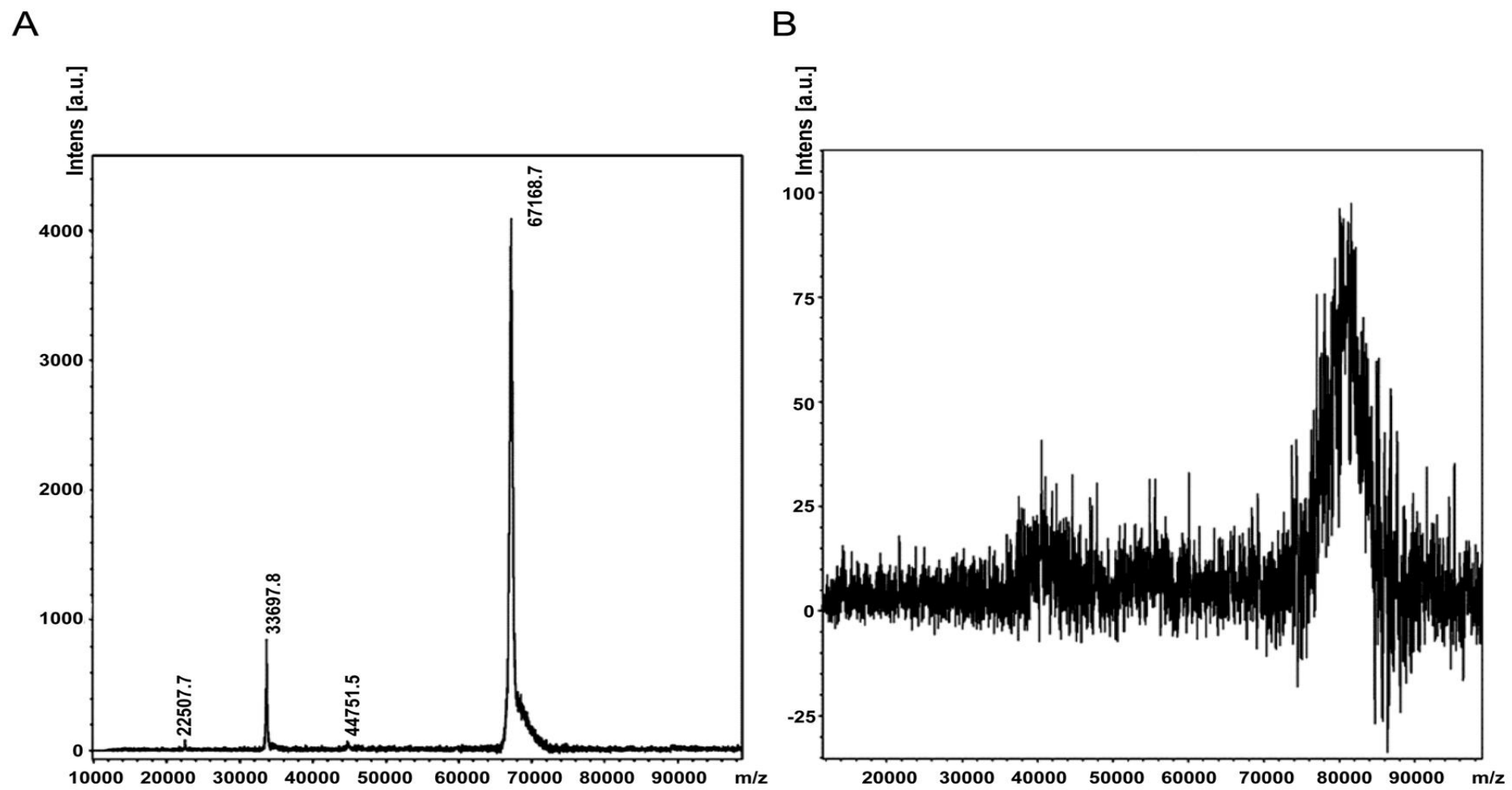


**Figure 4.8** MALDI-ToF spectra of N-deglycosylated (A) and glycosylated (B) rHvExoI.

**Table 4.5** Amino acid sequences of tryptic fragments of rHvExoI identified by MALDI-ToF/ToF.

| Tryptic fragments <sup>a</sup> |   |
|--------------------------------|---|
| 1.                             | MTLAEKIGQMTQIERLVATPDVLRDNFIGSLLSGGGSVPR  |
| 2.                             | GATAKEWQDMVDGFQK  |
| 3.                             | RIGEATALEVRATGIQYAFAPCIAVCR   |
| 4.                             | RIVQSMTELIPGLQGDVPKDFTS GMPFVAGK  |
| 5.                             | HFVGDGGTVDGINEN <u>N</u> TIINREGLMNIHMPAYKNAMDKG<br>VSTVMISYSSWNGVKMHANQDLVTGYLKDTLKFKGFVISD<br>WEGIDRITTPAGSDYSYSVKASILAGLDMIMVPNK |
| 6.                             | RVKFTMGLFENPYADPAMAEQLGK  |
| 7.                             | NGKTSTDAPLLPLPK   |
| 8.                             | TTVGTTILEAVKAAVDPSTVVVFAENPDAEFVKSGGFSYAI<br>VAVGEHPYTETKGDNL <u>N</u> LTIPEPGLSTVQAVCGGVR  |
| 9.                             | SVDQLPMNVGDAHYDPLFRLGYGLTT <u>N</u> ATK   |

<sup>a</sup>The underlined letters indicate N-glycosylated Asn (N) residues.

### 4.3.3 Characterization of wild type rHvExoI

#### 4.3.3.1 Effect of pH and temperature on rHvExoI enzyme activity

The pH optima of the glycosylated and N-deglycosylated forms of rHvExoI were determined in McIlvaine buffer over the pH range of 3.5-8.5 at 30°C (Figure 4.9). The pH profiles were bell-shaped, and the highest activities of glycosylated and N-deglycosylated rHvExoI occurred at pH 5.0 and 5.25, respectively. As for the temperature stability of rHvExoI, the activities were assayed after incubation at temperatures over the range between 0 and 80°C for 15 min (Figure 4.10). While glycosylated rHvExoI was stable at the temperature range between 10°C to 20°C, N-deglycosylated rHvExoI was stable in the range between 10°C to 30°C. Above these temperature ranges, the activities of both rHvExoI forms decreased substantially. The temperatures at which 50% inactivation of the glycosylated and N-deglycosylated rHvExoI forms were observed were at 34°C and 39°C, respectively. Both rHvExoI forms were denatured at 50°C and no activity was

detected at higher temperatures. Upon addition of BSA, the enzyme activity was approximately 2-fold higher than with no BSA in the reaction, which indicated that BSA could stabilize and protect the rHvExoI protein against heat inactivation by increasing the temperatures of 50% inactivation of glycosylated and N-deglycosylated rHvExoI forms to 39°C and 42.5°C, respectively. The BSA may also be preventing loss of enzyme by nonspecific binding to the tube.

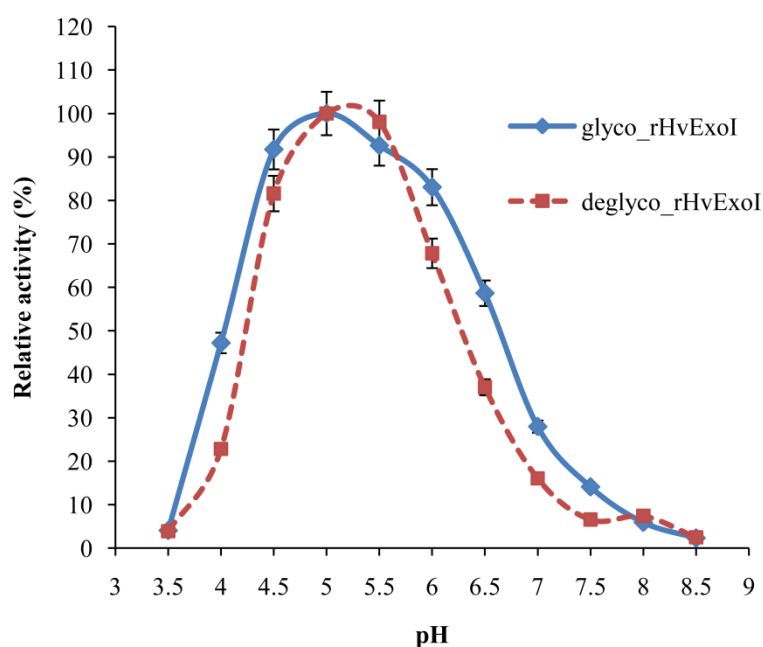


**Figure 4.9** pH activity profiles of glycosylated and N-deglycosylated rHvExoI. The proteins were assayed for hydrolysis of 0.2% (w/v) 4NPGlc at 30°C for 15 min.

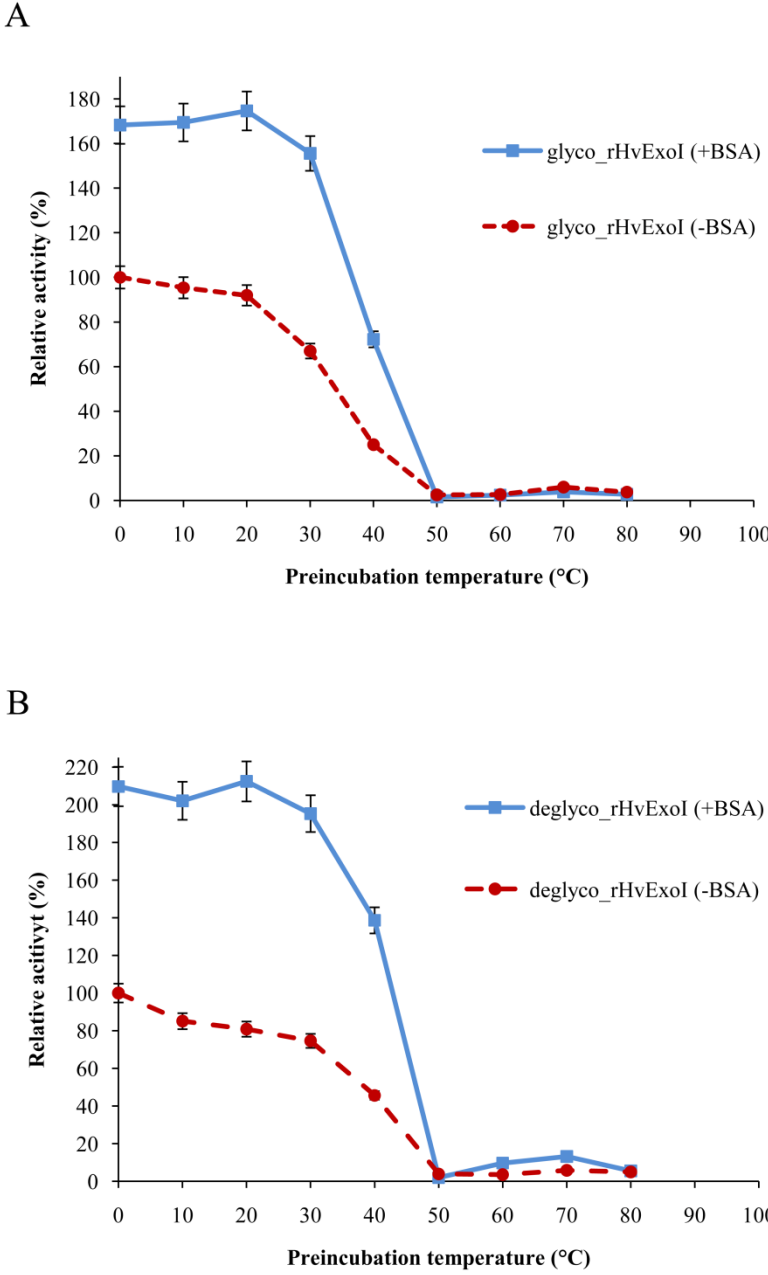


**Figure 4.10** Thermostability of glycosylated (A) and N-deglycosylated (B) rHvExoI at temperatures ranging from 0-80°C with and without 160 µg/ml BSA.

#### 4.3.3.2 Substrate specificity of rHvExoI

The glycosylated form of rHvExoI was tested for hydrolysis of polysaccharides, oligosaccharides and synthetic substrates, as shown in Table 4.6. Glycosylated rHvExoI hydrolysed glucoside substrates including 4NPGlc and 4NP  $\beta$ -D-cellobioside, but could not hydrolyse  $\beta$ -D-galactoside,  $\beta$ -D-xyloside,  $\beta$ -D-fucoside,  $\beta$ -D-lactoside,  $\beta$ -D-glucosiduronic acid, N-acetyl- $\beta$ -D-glucosaminide and  $\alpha$ -L-arabinoside. It was able to hydrolyse  $\beta$ -(1,2),  $\beta$ -(1,3),  $\beta$ -(1,4), and  $\beta$ -(1,6)-linked disaccharides and polysaccharides, including barley (1,3;1,4)- $\beta$ -D-glucan and laminarin. The glycosylated rHvExoI also slowly hydrolysed  $\beta$ -(1,3;1,4) lichenans from the *C. islandica*. The rate of hydrolysis of oligosaccharides were independent of the degree of polymerization (DP) for cellooligosaccharides with DP of 3-6 and laminarioligosaccharides with DP of 3-7, while laminaribiose, cellobiose and sophorose were hydrolysed at lower rates. No activity was detected against curdlan (*A. faecalis*), pachyman (*P. cocos*), CM-(1,3)- $\beta$ -D-glucan, CM-cellulose and schizophyllan (*Schizophyllum commune*). The rates of hydrolysis by the glycosylated and N-deglycosylated forms of rHvExoI were compared for 4NPGlc, laminarin and barley (1,3;1,4)- $\beta$ -D-glucan. The relative activities of the two forms did not differ for polysaccharides, but the hydrolysis of 4NPGlc was lower for N-deglycosylated rHvExoI.

**Table 4.6** Relative activities of rHvExoI on polysaccharides, oligosaccharides and synthetic substrates.

| Substrate                                | Relative activity (%)      |                        |                          |
|--|----------------------------|------------------------|--------------------------|
|  | Native HvExoI <sup>a</sup> | Glycosylated rHvExoI   | N-Deglycosylated rHvExoI |
| <i>Polysaccharides</i>                   |                            |                        |                          |
| Laminarin ( <i>L. digitata</i> )         | 100 <sup>b</sup>           | 100 ± 1.1 <sup>c</sup> | 100 ± 1.2 <sup>c</sup>   |
| Barley (1,3;1,4)-β-D-glucan              | 10                         | 10.0 ± 0.5             | 10.0 ± 0.8               |
| Lichenan ( <i>C. islandica</i> )         | nm <sup>d</sup>            | 1.4 ± 0.1              | nm                       |
| <i>Oligosaccharides</i>                  |                            |                        |                          |
| Sophorose                                | 55                         | 11.0 ± 0.1             | nm                       |
| Laminaribiose                            | 70                         | 38.2 ± 0.6             | nm                       |
| Laminaritriose                           | nm                         | 77.3 ± 1.9             | nm                       |
| Laminaritetraose                         | nm                         | 71.9 ± 3.2             | nm                       |
| Laminaripentaose                         | nm                         | 62.2 ± 2.5             | nm                       |
| Laminarihexose                           | nm                         | 86.2 ± 0.4             | nm                       |
| Laminariheptaose                         | nm                         | 80.8 ± 5.7             | nm                       |
| Cellobiose                               | 14                         | 8.4 ± 0.3              | nm                       |
| Cellotriose                              | nm                         | 16.3 ± 0.8             | nm                       |
| Cellotetraose                            | nm                         | 15.7 ± 1.2             | nm                       |
| Cellopentaose                            | nm                         | 15.4 ± 0.7             | nm                       |
| Cellohexaose                             | nm                         | 16.8 ± 0.4             | nm                       |
| Gentiobiose                              | 36                         | 8.7 ± 0.7              | nm                       |
| <i>Synthetic substrates</i>              |                            |                        |                          |
| 4-nitrophenyl β-D-glucopyranoside        | 10                         | 22.8 ± 1.4             | 16.8 ± 0.8               |
| 4-nitrophenyl β-D-galactopyranoside      | nm                         | nd <sup>e</sup>        | nm                       |
| 4-nitrophenyl β-D-xylopyranoside         | nm                         | nd                     | nm                       |
| 4-nitrophenyl β-D-fucopyranoside         | nm                         | nd                     | nm                       |
| 4-nitrophenyl β-D-lactoside              | nm                         | nd                     | nm                       |
| 4-nitrophenyl β-D-glucosiduronic acid    | nm                         | nd                     | nm                       |
| 4-nitrophenyl N-Acetyl-β-D-glucosaminide | nm                         | nd                     | nm                       |
| 4-nitrophenyl α-L-arabinopyranoside      | nm                         | nd                     | nm                       |
| 4-nitrophenyl β-D-cellobioside           | nm                         | 1.7 ± 0.02             | nm                       |

<sup>a</sup>The data are from Hrmova *et al.*, 1998.

<sup>b</sup>The relative activity of 100% equals to 63 units/mg.

<sup>c</sup>The 100% relative activities toward laminarin were equal to 54.4 and 65.3 units/mg for glycosylated and N-deglycosylated forms of rHvExoI, respectively.

<sup>d</sup>'nm' indicates 'not measured'.

<sup>e</sup>'nd' indicates 'not detectable'.

#### 4.3.3.3 Kinetic parameters of rHvExoI

The kinetic parameters for hydrolysis of laminarin, barley (1,3;1,4)- $\beta$ -D-glucan, laminaribiose, cellobiose and 4NPGlc were determined for both the glycosylated and N-deglycosylated forms of rHvExoI, as shown in Table 4.7. Both forms were highly active on polysaccharides and the most efficient polymeric substrate was barley (1,3;1,4)- $\beta$ -D-glucan, which was hydrolysed approximately 1.5-2 fold more efficiently, in terms of the  $k_{\text{cat}}/K_{\text{M}}$  catalytic efficiency values, than laminarin. Of the disaccharides, laminaribiose was hydrolysed about 12-fold faster than cellobiose by both forms of rHvExoI. The hydrolysis of barley (1,3;1,4)- $\beta$ -D-glucan proceeded about 1.3-fold faster with the N-deglycosylated rHvExoI form, although with the other four substrates, the hydrolytic rates were similar. The  $k_{\text{cat}}/K_{\text{M}}$  catalytic efficiency values of rHvExoI were higher than those of native HvExoI for barley (1,3;1,4)- $\beta$ -D-glucan, laminaribiose, cellobiose and 4NPGlc, while native HvExoI was more efficient at hydrolysing laminarin. Finally, rHvExoI had a slightly higher  $K_{\text{M}}$  value with 4NPGlc than with the disaccharides, although the  $k_{\text{cat}}/K_{\text{M}}$  values were higher for laminaribiose and lower for cellobiose, in agreement with the data for native HvExoI (Hrmova *et al.*, 1998; 2002).

**Table 4.7** Kinetic parameters of rHvExoI on laminarin, barley (1,3;1,4)- $\beta$ -D-glucan, laminaribiose, cellobiose and 4NPGlc.

| Substrate   | Native HvExoI                | Glycosylated rHvExoI | N-Deglycosylated rHvExoI |
|---|------------------------------|----------------------|--------------------------|
| <b>Laminarin</b>                                    |                              |                      |                          |
| $K_M$ (mM)  | 0.098 <sup>a</sup>           | 0.18 $\pm$ 0.01      | 0.22 $\pm$ 0.02          |
| $k_{cat}$ (s <sup>-1</sup> )                        | 73 <sup>a</sup>              | 42.1 $\pm$ 1.6       | 51.7 $\pm$ 2.5           |
| $k_{cat}/K_M$ (mM <sup>-1</sup> ·s <sup>-1</sup> )  | 740 <sup>a</sup>             | 234 $\pm$ 14         | 235 $\pm$ 22             |
| <b>Barley (1,3;1,4)-<math>\beta</math>-D-glucan</b> |                              |                      |                          |
| $K_M$ (mM)  | 0.012 <sup>a</sup>           | 0.04 $\pm$ 0.004     | 0.02 $\pm$ 0.002         |
| $k_{cat}$ (s <sup>-1</sup> )                        | 4 <sup>a</sup>               | 14.1 $\pm$ 0.7       | 9.7 $\pm$ 1.1            |
| $k_{cat}/K_M$ (mM <sup>-1</sup> ·s <sup>-1</sup> )  | 330 <sup>a</sup>             | 365 $\pm$ 57         | 478 $\pm$ 50             |
| <b>Laminaribiose</b>                                |                              |                      |                          |
| $K_M$ (mM)  | 0.37 $\pm$ 0.04 <sup>b</sup> | 1.3 $\pm$ 0.1        | 1.5 $\pm$ 0.1            |
| $k_{cat}$ (s <sup>-1</sup> )                        | 11.7 $\pm$ 0.8 <sup>b</sup>  | 54.2 $\pm$ 2.3       | 66.0 $\pm$ 1.7           |
| $k_{cat}/K_M$ (mM <sup>-1</sup> ·s <sup>-1</sup> )  | 32.0 $\pm$ 1.0 <sup>b</sup>  | 41.2 $\pm$ 2.4       | 43.2 $\pm$ 1.3           |
| <b>Cellobiose</b>                                   |                              |                      |                          |
| $K_M$ (mM)  | 2.7 $\pm$ 0.2 <sup>b</sup>   | 1.2 $\pm$ 0.1        | 1.6 $\pm$ 0.1            |
| $k_{cat}$ (s <sup>-1</sup> )                        | 2.4 $\pm$ 0.2 <sup>b</sup>   | 4.2 $\pm$ 0.2        | 5.4 $\pm$ 0.2            |
| $k_{cat}/K_M$ (mM <sup>-1</sup> ·s <sup>-1</sup> )  | 0.9 $\pm$ 0.01 <sup>b</sup>  | 3.3 $\pm$ 0.2        | 3.3 $\pm$ 0.3            |
| <b>4NPGlc</b>                                       |                              |                      |                          |
| $K_M$ (mM)  | 1.4 <sup>a</sup>             | 2.0 $\pm$ 0.2        | 2.0 $\pm$ 0.1            |
| $k_{cat}$ (s <sup>-1</sup> )                        | 5 <sup>a</sup>               | 27.7 $\pm$ 0.9       | 25.4 $\pm$ 0.7           |
| $k_{cat}/K_M$ (mM <sup>-1</sup> ·s <sup>-1</sup> )  | 3 <sup>a</sup>               | 13.9 $\pm$ 0.6       | 12.8 $\pm$ 0.8           |

<sup>a</sup> Kinetic parameters of HvExoI with laminarin, barley (1,3;1,4)- $\beta$ -D-glucan and 4NPGlc are from Hrmova *et al.*, 1998.

<sup>b</sup> Kinetic parameters of HvExoI with laminaribiose and cellobiose are from Hrmova *et al.*, 2002.

#### 4.3.3.4 Transglycosylation products of rHvExoI

As shown in Figure 4.11, both the glycosylated and N-deglycosylated forms of rHvExoI possessed both hydrolytic and glucosyltransferase activities toward 4NPGlc. The formation of transglycosylation products was detectable within 3 min (0.05 h), and at 4 h and 18 h. The transglycosylation product patterns of N-deglycosylated rHvExoI were very similar to those of glycosylated rHvExoI. During the initial stages of the reaction at 3 min, a small amount of glucose was observed, in addition to 4NP-oligosaccharide products (P<sub>1</sub> and P<sub>2</sub>). As the reaction progressed, after 4 h reaction, the transient transglycosylation products 4NP-glycosides, laminaribiose, cellobiose, gentiobiose and an unknown disaccharide (P<sub>3</sub>) and trisaccharides (P<sub>4</sub>-P<sub>6</sub>) were detected. By 18 h, the 4NP-glycosides, laminaribiose and cellobiose were hydrolysed, and only the major hydrolytic product glucose and traces of gentiobiose were observable. Transglycosylation activity also occurred with barley (1,3;1,4)- $\beta$ -D-glucan (Figure 4.12), from which only the formation of the disaccharide gentiobiose was detected, similar to native HvExoI (Hrmova *et al.*, 1998).

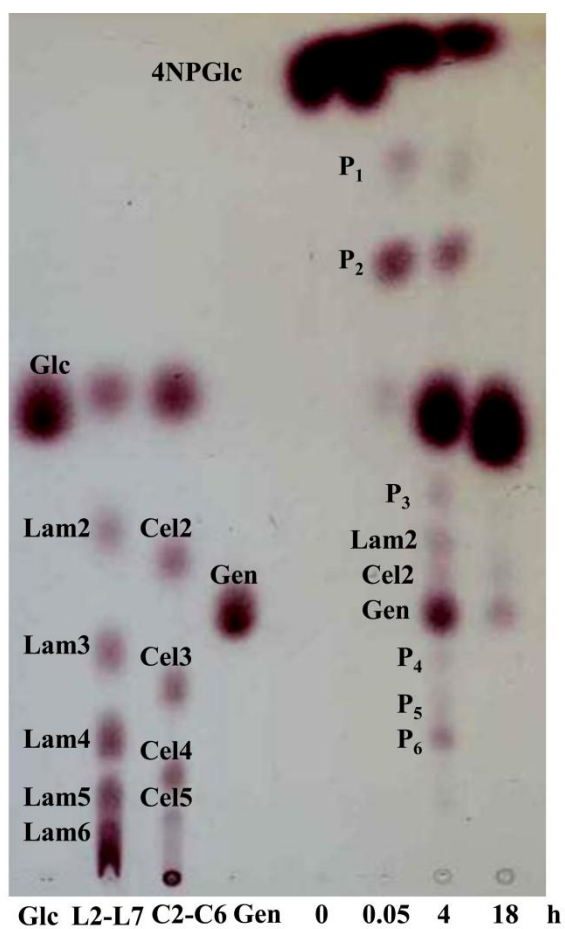


**Figure 4.11** TLC chromatogram of hydrolysis and transglycosylation products formed by glycosylated rHvExoI with 4NPGlc as a substrate. The enzymes were incubated in the presence of 20 mM 4NPGlc at 30°C for 0, 3 min, 4 h and 18 h. Standards are glucose (Glc), laminari-oligosaccharides (L2-L7), cello-oligosaccharides (C2-C6), and gentiobiose (Gen). The presence of oligosaccharide products with unknown structures are indicated as P<sub>1</sub>-P<sub>6</sub>. The reaction times are indicated in hours below the lanes.

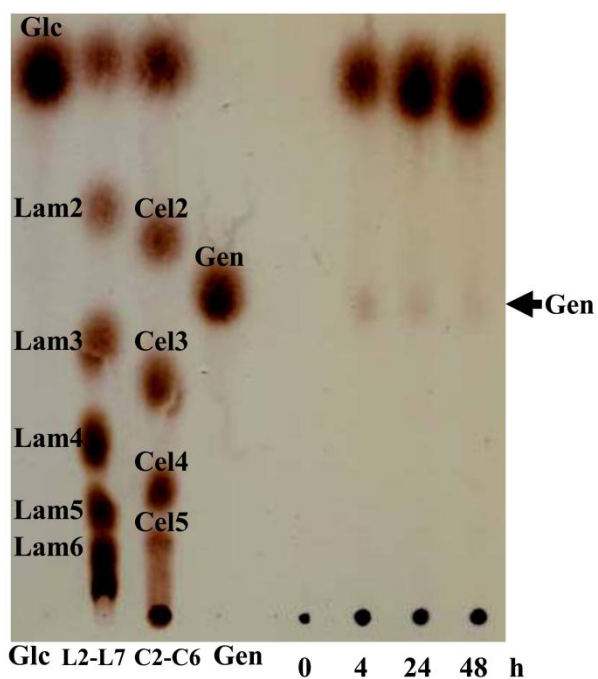


**Figure 4.12** TLC chromatogram of hydrolysis and transglycosylation products formed by glycosylated rHvExoI with barley (1,3;1,4)- $\beta$ -D-glucan as a substrate. The enzyme was incubated in the presence of 1% (w/v) barley (1,3;1,4)- $\beta$ -D-glucan at 30°C for 0, 4, 24 and 48 h. Standards are glucose (Glc), laminari-oligosaccharides (L2-L7), cello-oligosaccharides (C2-C6), and gentiobiose (Gen).

#### 4.3.3.5 Inhibition of rHvExoI

Inhibition of rHvExoI hydrolysis of 4NPGlc by the presence of competitive inhibitors of native HvExoI (Hrmova *et al.*, 1996; 2001; 2002), including methyl-O-thio-gentiobiose (G6sG-OMe), glucono  $\delta$ -lactone (GL) and 2,4-dinitrophenyl 2-fluoro-2-deoxy- $\beta$ -D-glucopyranoside (2F-DNPGlc), was evaluated. The  $K_i$  values of rHvExoI were higher than native HvExoI for G6sG-OMe and GL, and lower for 2F-DNPGlc. For glycosylated rHvExoI, the  $K_i$  values for G6sG-OMe, GL, and 2F-DNPGlc were 109  $\mu$ M, 9.9  $\mu$ M and 0.45  $\mu$ M, respectively, while for N-deglycosylated rHvExoI, these values were 71  $\mu$ M, 8.3  $\mu$ M and 0.59  $\mu$ M, respectively.

**Table 4.8** Inhibition parameters of rHvExoI with methyl-O-thio-gentiobiose (G6sG-OMe), glucono  $\delta$ -lactone (GL) and 2,4-dinitrophenyl 2-fluoro-2-deoxy- $\beta$ -D-glucopyranoside (2F-DNPGlc).

| Inhibitor                                       | Native HvExoI           | Glycosylated rHvExoI | N-deglycosylated rHvExoI |
|---|-------------------------|----------------------|--------------------------|
| <b>G6SG-OMe</b>                                 |                         |                      |                          |
| $K_i$ (M)                                       | $61 \times 10^{-6,a}$   | $109 \times 10^{-6}$ | $71 \times 10^{-6}$      |
| $\Delta G$ (kJ mol <sup>-1</sup> ) <sup>b</sup> | -24.5                   | -23.0                | -24.1                    |
| <b>GL</b>                                       |                         |                      |                          |
| $K_i$ (M)                                       | $2.1 \times 10^{-6,c}$  | $10 \times 10^{-6}$  | $8.3 \times 10^{-6}$     |
| $\Delta G$ (kJ mol <sup>-1</sup> )              | -33.0                   | -29.1                | -29.5                    |
| <b>2F-DNPGlc</b>                                |                         |                      |                          |
| $K_i$ (M)                                       | $25.5 \times 10^{-6,d}$ | $0.5 \times 10^{-6}$ | $0.6 \times 10^{-6}$     |
| $\Delta G$ (kJ mol <sup>-1</sup> )              | -26.7                   | -36.8                | -36.2                    |

<sup>a</sup>  $K_i$  of native HvExoI with G6sG-OMe are from Hrmova *et al.*, 2002.

<sup>b</sup> Gibbs free energy  $\Delta G$  was calculated from  $\Delta G = -RT \ln (K_i)$ .

<sup>c</sup>  $K_i$  of native HvExoI with GL are from Hrmova *et al.*, 1996.

<sup>d</sup>  $K_i$  of native HvExoI with 2F-DNPGlc are from Hrmova *et al.*, 2001.

## 4.4 Discussion

### 4.4.1 Sequence analysis of normal and optimized rHvExoI

The native HvExoI cDNA sequence was analysed for compatibility with *Pichia pastoris* codon usage via the online facility at Genscript Corp (<http://www.genscript.com>). A simple measure of synonymous codon bias (the Codon Adaptation Index, CAI) was used to measure codon bias patterns. Comparing the codon preference of the expression host (*Pichia pastoris*) with the codon usage in the gene via the CAI may be used to predict the gene expression level. A CAI of 1 is considered to be ideal, so if the CAI value of the gene of interest is close to 1, the gene expression level should be high. The native HvExoI cDNA had a CAI value of 0.49, which means that it was likely to be poorly expressed in *P. pastoris*. The sequence of native HvExoI contains a G+C content of approximately 65.5% and most of third positions in each codon were G or C, while *P. pastoris* genes tend to be AT-rich. Therefore, the native HvExoI had several codons that are rarely used in *P. pastoris*, such as CTC (Leu), CCC (Pro), GGG (Gly), ACG/C (Thr) and AGC (Ser), as shown in Table 4.9 (<http://www.kazusa.or.jp/codon/>). In order to improve the expression level of HvExoI, the gene sequence was optimized for *P. pastoris* by GenScript Corp (Piscataway, NJ, USA). The resulting sequence differed from the native cDNA at 547 nucleotide positions and had a G+C content of 39.1%, as shown in Figure 4.1.

**Table 4.9** The codon usage of *Pichai pastoris*. Codon usage was analysed in 137 protein encoding sequences (81,301 codons). Genetic codons are indicated as three capital characters, the frequencies of triplet codon per thousand codons are indicated by the numbers next to the codon and the codon counts out of 81,301 codons are indicated as the number in brackets (<http://www.kazusa.or.jp/codon/>).

|                  |     |                  |                  |                  |      |
|------------------|-----|------------------|------------------|------------------|------|
| TTT 24.1 ( 1963) | Phe | TCT 24.4 ( 1983) | Tyr              | TGT 7.7 ( 626)   | Cys  |
| TTC 20.6 ( 1675) |     | TCC 16.5 ( 1344) |                  | TAC 18.1 ( 1473) |      |
| TTA 15.6 ( 1265) | Leu | TCA 15.2 ( 1234) | Stop             | TGA 0.3 ( 27)    | Stop |
| TTG 31.5 ( 2562) |     | TCG 7.4 ( 598)   |                  | TAG 0.5 ( 40)    |      |
| CTT 15.9 ( 1289) | Leu | CCT 15.8 ( 1282) | His              | CGT 6.9 ( 564)   | Arg  |
| CTC 7.6 ( 620)   |     | CCC 6.8 ( 553)   |                  | CAC 9.1 ( 737)   |      |
| CTA 10.7 ( 873)  |     | CCA 18.9 ( 1540) | CAA 25.4 ( 2069) | CGA 4.2 ( 340)   |      |
| CTG 14.9 ( 1215) |     | CCG 3.9 ( 320)   | CAG 16.3 ( 1323) | CGG 1.9 ( 158)   |      |
| ATT 31.1 ( 2532) | Ile | ACT 22.4 ( 1820) | Asn              | AGT 12.5 ( 1020) | Ser  |
| ATC 19.4 ( 1580) |     | ACC 14.5 ( 1175) |                  | AAC 26.7 ( 2168) |      |
| ATA 11.1 ( 906)  | Met | ACA 13.8 ( 1118) | Lys              | AGA 20.1 ( 1634) | Arg  |
| ATG 18.7 ( 1517) |     | ACG 6.0 ( 491)   |                  | AAG 33.8 ( 2748) |      |
| GTT 26.9 ( 2188) | Val | GCT 28.9 ( 2351) | Asp              | GGT 25.5 ( 2075) | Gly  |
| GTC 14.9 ( 1210) |     | GCC 16.6 ( 1348) |                  | GAC 25.9 ( 2103) |      |
| GTA 9.9 ( 804)   |     | GCA 15.1 ( 1228) | GAA 37.4 ( 3043) | GGA 19.1 ( 1550) |      |
| GTG 12.3 ( 998)  |     | GCG 3.9 ( 314)   | GAG 29.0 ( 2360) | GGG 5.8 ( 468)   |      |

#### 4.4.2 Development of an expression system for active rHvExoI

Bacteria and yeast are common hosts for production of target proteins. Although bacterial expression is convenient, many eukaryotic proteins are produced in low protein yields (Batas *et al.*, 1999; Patra *et al.*, 2000; Ognasyan *et al.*, 2005). Although HvExoI could be expressed in bacteria, it was not able to fold properly, and refolding experiments using various refolding formulations failed to recover active rHvExoI. The reasons why rHvExoI could not be refolded successfully might include its two-domain organisation and the fact that the enzyme contains 10 cysteine residues. From these residues, two disulfide linkages are formed, between Cys151 and C159 in domain 1, and between Cys513 and Cys518 in domain 2 (Varghese *et al.*, 1999). Hence, the probability that the correct disulfide linkages will be formed is low. Therefore, a yeast expression system was introduced that was reported to be able to produce plant enzymes in active forms (e.g. Ketudat Cairns *et al.*, 2000; Hrmova *et al.*, 2009)

Prokaryotic and eukaryotic cells have their own species-specific codon usage patterns. Many target genes from mammals and plants are expressed at low levels in bacteria or yeast, in part because the rate of protein translation is not well correlated to the codon usage and tRNA bias (Brankamp *et al.*, 1995). The HvExoI cDNA amplified from barley seedlings produced low protein yields in *P. pastoris*. Thus, a codon-optimized cDNA was synthesized. Expression of rHvExoI was only successful from the codon-optimized cDNA in a protease-deficient strain of *P. pastoris* and at a low temperature of 20°C. The expressed rHvExoI possessed three post-translationally modified asparaginyl residues, similar to native HvExoI. rHvExoI could be purified by a two-step procedure using a strong cation-exchanger and IMAC with a final yield of 12%, based on the total protein used for purification. The use of selective pooling of the chromatographic fractions, as well as initial contamination with *P. pastoris* exoglucanase (Xu *et al.*, 2006), which was eliminated during the purification, and loss of a small amount of HvExoI that lacked its N-terminal

histidine tag may account for this relatively lower apparent final yield of purified enzyme. Upon N-deglycosylation with endoglycosidase H and purification with a second IMAC step, N-deglycosylated rHvExoI was produced with a yield of 9% and the specific activity of rHvExoI was nearly the same as before N-deglycosylation. Here, the endoglycosidase H was chosen, because it cleaves the chitobiose core of high mannose N-linked glycoproteins, which are commonly observed in yeast, while retaining the first N-acetylglucosamine residue linked to Asn (Maley *et al.*, 1989). A His-tagged form of rHvExoI of 67.2 kDa lacking an EAEA secretion motif was obtained after expression in *P. pastoris* and N-deglycosylation. Thus, secreted rHvExoI was properly processed by the proteases in *Pichia* cells, contrary to previous observations with xyloglucan xyloglucosyl transferase enzymes (Hrmova *et al.*, 2009).

#### **4.4.3 Catalytic properties of rHvExoI**

The pH optimum and thermostability of N-deglycosylated rHvExoI were similar to native HvExoI, although the same parameters of glycosylated rHvExoI were slightly lower. Koseki *et al.* (2006) reported that the N-glycosylation of oligosaccharide chain (2.5 kDa) of asparagines at the catalytic domain increased the thermostability of *Aspergillus kawachii*  $\alpha$ -L-arabinosidase, whereas glycosylated rHvExoI did not exhibit increased stability at elevated temperatures. The molecular mass of glycosylated rHvExoI was higher by approximately 7.7-17.7 kDa than that of N-deglycosylated enzyme due to occupation of three N-glycosylation sites. The calculated molecular mass of the HvExoI polypeptide was 66.8 kDa (Hrmova *et al.*, 1996). Based on the sizes of N-linked carbohydrates at the N-glycosylation sites, we would expect that the presence of these carbohydrates could affect certain enzyme properties, such as pH optimum and thermostability. However, the glycosylated and N-deglycosylated rHvExoI enzymes had pH optima and thermostabilities quite similar to native HvExoI (Hrmova *et al.*, 1998).

A wide variety of substrates with different positional linkages of disaccharides and polysaccharides were hydrolysed by rHvExoI with similar hydrolytic rates, compared to native HvExoI. It has been well documented that this enzyme prefers hydrolysing substrates containing (1,3)- $\beta$ -linked glucoside residues (Hrmova *et al.*, 1996; 1998; 2002). As for the catalytic properties, we found that rHvExoI had  $k_{cat}/K_M$  values very similar to native HvExoI with barley (1,3;1,4)- $\beta$ -D-glucan, although the  $k_{cat}/K_M$  values of rHvExoI were higher with laminaribiose, cellobiose and 4NPGlc, and about 3-fold lower with laminarin (Table 4.7). rHvExoI activity was inhibited with G6sG-OMe, GL and 2F-DNPGlc inhibitors. As seen in Table 4.8, the  $K_i$  values were similar between glycosylated and N-deglycosylated rHvExoI. When these data were compared with native HvExoI, only the  $K_i$  values of G6sG-OMe were in the range of native HvExoI. 2F-DNPGlc could inhibit rHvExoI more strongly than native HvExoI, with  $K_i$  values approximately 46 fold lower, but GL inhibited rHvExoI less strongly than native HvExoI, with  $K_i$  values was approximately 4 fold higher. The only obvious differences between the rHvExoI and native HvExoI enzymes is the presence of the extension of the N-terminus by 11 residues (AHHHHHHHAA) in rHvExoI, and differences in N-glycosylation of both forms produced in *P. pastoris* compared to barley. N-linked sugar chain at Asn498 of native HvExoI consists of a core structure of two  $\beta$ -(1,4)-linked GlcNAc residues followed by two mannosyl residues (Man<sub>2</sub>-GlcNAc<sub>2</sub>-Asn), which has a  $\alpha$ -(1,3)-linked fucosyl residue attached with the first N-linked GlcNAc residue and a (1,2)-xylosyl residue attached with the first branching mannosyl residue, respectively (Varghese *et al.*, 1999). While N-glycosylation of heterologous protein from yeast consists of branching high mannose residues attached to the Man<sub>8</sub>GlcNAc<sub>2</sub>-Asn core (Herscovics and Orlean, 1993; Daly and Hearn, 2004; Jacobs *et al.*, 2009). The 11 residues extension and the Asn600 glycosylation site lie at the N- and C-termini of HvExoI, respectively, distant from the active site, however, the Asn221 and Asn498 N-linked glycosylation sites lie in the proximity of the

active site of HvExoI (Varghes *et al.*, 1999; Hrmova *et al.*, 2001). It is possible that the native barley carbohydrate might help in interaction with a polymeric substrate, such as laminarin, resulting in the tighter binding seen in the native enzyme. However, it appears the high mannose and N-acetyl glucosamine containing carbohydrates affixed to these sites by *P. pastoris* make no significant net interaction with substrates. It is also possible that the differences in N-terminal sequence and posttranslational modification result in differences in protein flexibility or other protein physical properties that might explain the differences in hydrolysis of these substrates.

#### **4.5 Conclusions**

Recombinant rHvExoI could be expressed efficiently in active form from a codon-optimized gene in *P. pastoris*, contrary to expression of the protein from the native HvExoI cDNA sequence and rHvExoI expression in *E. coli*. rHvExoI exhibited mostly  $\beta$ -glucan glucosyl hydrolase activity on a variety of  $\beta$ -linked glucoside substrates and produced a variety  $\beta$ -linked oligosaccharide products from glucosyltransferase activity, similar to native HvExoI. The rHvExoI activity was competitively inhibited by G6sG-OMe, GL and 2F-DNPGlc, similarly to native HvExoI. Thus, the recombinant rHvExoI is an appropriate model to study the molecular basis of catalysis and substrate specificity by site-directed mutagenesis of residues suggested to be involved in catalysis by the X-ray crystal structures of native HvExoI.

## 4.6 References

- Adelsberger, H., Hertel, C., Glawisching, E., Zverlov, V.V., and Schwarz, W.H. (2004). Enzyme system of *Clostridium stercorarium* for hydrolysis of arabinoxylan: reconstitution of the *in vivo* system from recombinant enzymes. **Microbiology** 150: 2257-2266.
- Breves, R., Bronnenmeier, K., Wild, N., Lottspeich, F., Staudenbauer, W.L., and Hofemeister, J. (1997). Genes encoding two different  $\beta$ -glucosidases of *Thermoanaerobacter brockii* are clustered in a common operon. **Appl. Environ. Microbiol.** 63: 3902-3910.
- Cereghino, J.L., and Cregg, J.M. (2000). Heterologous protein expression in the methylotrophic yeast *Pichia pastoris*. **FEMS Microbiol. Rev.** 24: 45-66.
- Chantarangsee, M., Tanthanuch, W., Fujimura, T., Fry, S.C., and Ketudat Cairns, J.R. (2007). Molecular characterization of  $\beta$ -galactosidases from germinating rice (*Oryza sativa*). **Plant Sci.** 173: 118-134.
- Cheng, Q., Li, H., Merdek, K., and Park, J.T. (2000). Molecular characterization of the  $\beta$ -N-acetylglucosaminidase of *Escherichia coli* and its role in cell wall recycling. **J. Bacteriol.** 182: 4836-4840.
- Cregg, J.M., Tolstorukov, I., Kusari, A., Sunga, J., Madden, K., and Chappell, T. (2009). Expression in the yeast *Pichia pastoris*. **Methods Enzymol.** 463: 169-189.
- Crombie, H., Chengappa, S., Helyer, A., and Reid, J.S.G. (1989). A xyloglucan oligosaccharide-active, transglycosylating  $\beta$ -D-glucosidase from the cotyledons of nasturtium (*Tropaeolum majus* L.) seedlings-purification, properties and characterization of a cDNA clone, **Plant J.** 15: 27-38.

- Daly, R., and Wearn, T.W. (2004). Expression of heterologous proteins in *Pichia pastoris*: a useful experimental tool in protein engineering and production. **J. Mol. Recognit.** 18: 119-138.
- Ferrares, L., Trainotti, L, Gattolin, S., and Casadoro, G. (1998). Secretion, purification and activity of two recombinant pepper endo- $\beta$ -1,4-glucanases expressed in the yeast *Pichia pastoris*. **FEBS Lett.** 23: 23-26.
- Harvey, A.J., Hrmova, M., and Fincher, G.B. (2001). Regulation of genes encoding  $\beta$ -D-glucan glucohydrolases in barley (*Hordeum vulgare* L.). **Physiol. Plant** 113: 108-120.
- Herscovics, A., and Orlean, P. (1993). Glycoprotein biosynthesis in yeast. **FASEB J.** 7: 540-550.
- Hrmova, M., Harvey, A.J., Wang, J., Shirley, N.J., Jones, G.P., Stone, B.A., Høj, P.B., and Fincher, G.B. (1996). Barley  $\beta$ -D-glucan exohydrolases with  $\beta$ -D-glucosidase activity: purification, characterization, and determination of primary structure from a cDNA clone. **J. Biol. Chem.** 271: 5277-5286.
- Hrmova, M., and Fincher, G.B. (1998). Barley  $\beta$ -D-glucan exohydrolases. Substrate specificity and kinetic properties. **Carbohydr. Res.** 305: 209-221.
- Hrmova, M., and Fincher, G.B. (2001). Structure-function relationships of  $\beta$ -D-glucan endo- and exohydrolases from higher plants. **Plant. Mol. Biol.** 47: 73-91.
- Hrmova, M., Gori, R.D., Smith, B.J., Fairweather, J.K., Driguez, H., Varghese, J.N., and Fincher, G.B. (2002). Structural basis for broad substrate specificity in higher plant  $\beta$ -D-glucan glucohydrolases. **Plant Cell** 14: 1033-1052.

- Hrmova, M., Gori, R.D., Smith, B.J., Vasela, A., Varghese, J.N., and Fincher, G.B. (2004). Three-dimensional structure of the barley  $\beta$ -D-glucan glucohydrolase in complex with a transition state mimic. **J. Biol. Chem.** 279: 4970-4980.
- Hrmova, M., Streltsov, V.A., Smith, B.J., Vasella, A., Varghese, J.N., and Fincher G.B. (2005). Structural rationale for low-nanomolar binding of transition state mimics to a family GH3  $\beta$ -D-glucan glucohydrolase from barley. **Biochemistry** 44: 16529-16539.
- Hrmova, M., and Fincher, G.B. (2007). Dissecting the catalytic mechanism of a plant  $\beta$ -D-glucan glucohydrolase through structural biology using inhibitors and substrate analogues. **Carbohydr. Res.** 342: 1613-1623.
- Hrmova, M., Farkas, V., Harvey, A.J., Lahnstein, J., Wischmann, B., Kaewthai, N., Ezcurra, I., Teeri, T.T., and Fincher, G.B. (2009). Substrate specificity and catalytic mechanism of a xyloglucan xyloglucosyl transferase HvXET6 from barley (*Hordeum vulgare* L.). **FEBS J.** 276: 437-456.
- Hung, C.Y., Yu, J.J., Lehmann, P.F., and Cole, G.T. (2001). Cloning and expression of the gene which encodes a tube precipitin antigen and wall-associated  $\beta$ -glucosidase of *Cooccidioides immitis*, **Infect. Immun.** 69: 2211-2222.
- Jacobs, P.P., Geysens, S., Vervecken, W., Contreras, R., and Callewaert, N. (2009). Engineering complex-type N-glycosylation in *Pichia pastoris* using Glycoswitch technology. **Nat. Protoc.** 4: 58-70.
- Juge, N., Andersen, J.S., Tull, D., Roepstorff, P., and Svensson, B. (1996). Overexpression, purification, and characterization of recombinant barley  $\alpha$ -amylases 1 and 2 secreted by the methylotrophic yeast *Pichia pastoris*. **Prot. Expr. Purif.** 8: 204-214.

- Kawai, R., Igarashi, K., Kitaoka, M., Ishii, T., and Samejima, M. (2004). Kinetics of substrate transglycosylation by glycoside hydrolase family 3 glucan (1→3)-β-D-glucosidase from the white-rot fungus *Phanerochaete chrysosporium*. **Carbohydr. Res.** 339: 2851-2857.
- Ketudat Cairns, J.R., Champattanachai, V., Srisomsap, C., Wittman-Liebold, B., Thiede, B., and Svasti, J. (2000). Sequence and expression of Thai rosewood β-glucosidase/β-fucosidase, a family 1 glycosyl hydrolase glycoprotein. **J. Biochem.** 128: 999-1008.
- Koseki, T., Miwa, Y., Mese, Y., Miyanaga, A., Fushinobu, S., Wakagi, T., Shoun, H., Matsuzawa, H., and Hashizume, K. (2006). Mutational analysis of *N*-glycosylation recognition sites on the biochemical properties of *Aspergillus kawachii* α-L-arabinofuranosidase 54. **Biochim. Biophys. Acta.** 1760: 1458-1464.
- Kotake, T., Nagawa, N., Takeda, K., and Sakuria, N. (1997). Purification and characterization of wall-bound exo-1,3-β-D-glucanase from barley (*Hordeum vulgare* L.) seedlings. **Plant Cell Physiol.** 38: 194-200.
- Kuntothom, T., Luang, S., Harvey, A.J., Fincher, G.B., Opassiri, R., Hrmova, M., and Ketudat Cairns, J.R. (2009). Rice family GH1 glycoside hydrolases with β-D-glucosidase and β-D-mannosidase activities. **Arch. Biochem. Biophys.** 491: 85-95.
- Li, Y.K., Chir, J., and Chen, F.Y. (2001). Catalytic mechanism of a family 3 β-glucosidase and mutagenesis study on residue Asp-247. **Biochem. J.** 355: 835-840.
- Li, Y.K., Chir, J., Tanaka, S., and Chen, F.Y. (2002). Identification of the general acid/base catalyst of a family 3 β-glucosidase from *Flavobacterium meningosepticum*. **Biochemistry** 41: 2751-2759.
- Maley, F., Trimble, R.B., Tarentino, A.L., and Plummer, T.H. (1989). Characterization of glycoproteins and their associated oligosaccharides through the use of endoglycosidases. **Anal. Biochem.** 180: 195-204.

- Mayer, C., Vocadlo, D.J., Mah, M., Rupitz, K., Stoll, D., Warren, R.A.J., and Withers, S.G. (2006). Characterization of a  $\beta$ -N-acetylhexosaminidase and a  $\beta$ -N-acetylglucosaminidase/ $\beta$ -glucosidase from *Cellulomonas fimi*. **FEBS J.** 271: 2929-2941.
- Opassiri, R., Ketudat Cairns, J.R., Akiyama, T., Wara-Asawapati, O., Svasti, J., and Esen, A. (2003). Characterization of a rice  $\beta$ -glucosidase highly expressed in flower and germinating shoot. **Plant Sci.** 165: 627-638.
- Opassiri, R., Pomthong, B., Onkoksoong, T., Akiyama, T., Esen, A., and Ketudat Cairns, J.R. (2006). Analysis of rice glycosyl hydrolase family 1 and expression of Os4bglu12  $\beta$ -glucosidase. **BMC Plant Biol.** 6.
- Perella, F. (1988). EZ-FIT; A practical curve-fitting microcomputer program for the analysis of the enzyme kinetic data on IBM-PC compatible computers. **Anal. Biochem.** 174: 437-447.
- Seshadri, S., Akiyama, T., Opassiri, R., Kuapasert, B., and Ketudat Cairns, J.R. (2009). Structural and enzymatic characterization of Os3BGlu6, a rice  $\beta$ -glucosidase hydrolyzing hydrophobic glycosides and (1 $\rightarrow$ 3)- and (1 $\rightarrow$ 2)-linked disaccharides. **Plant Physiol.** 151: 47-58.
- Steenbakkens, P.J.M., Harhangi, H.R., Bosscher, M.W., van der Hooft, M.M.C., Keltjens, J.T., van der Drift, C., Vogels, G.D., and Op den Camp, H.J.M. (2003).  $\beta$ -Glucosidase in cellulosome of the anaerobic fungus *Piromyces* sp. strain E2 is a family 3 glycoside hydrolase. **Biochem. J.** 370: 963-970.
- Toonkool, P., Metheenukul, P., Sujiwattanasat, P., Paiboon, P., Tongtubtim, N., Ketudat Cairns, M., Ketudat Cairns, J.R., and Svasti, J. (2006). Expression and purification of dalcochinase, a  $\beta$ -glucosidase from *Dalbergia cochinchinensis* Pierre, in yeast and bacterial hosts. **Prot. Expr. Purif.** 48: 195-204.

- Turner, P., Svensson, D., Adlercreutz, P., and Karlsson, E.N. (2007). A novel variant of *Thermotoga neapolitana*  $\beta$ -glucosidase B is an efficient catalyst for the synthesis of alkyl glucosidases by transglycosylation. **J. Biotechnol.** 130: 67-74.
- Varghese, J.N., Hrmova, M., and Fincher, G.B. (1999). Three-dimensional structure of a barley  $\beta$ -D-glucan exohydrolase, a family 3 glycosyl hydrolase. **Structure** 7: 179-190.
- Xu, Z., Shih, M.C., and Poulton, J.E. (2006). An extracellular *exo*- $\beta$ -(1,3)-glucanase from *Pichia pastoris*: Purification, characterization, molecular cloning, and functional expression. **Prot. Expr. Purif.** 47: 118-127.

# CHAPTER V

## STRUCTURE-FUNCTION STUDIES OF RECOMBINANT BARLEY $\beta$ -D-GLUCAN EXOHYDROLASE I

### Abstract

Based on structural and substrate specificity studies of barley  $\beta$ -D-glucan exohydrolase HvExoI, an in-depth understanding of the structure-function relationships involved in its substrate binding and catalytic mechanism has been established. The essential catalytic residues of rHvExoI identified by these studies were investigated here by site-directed mutagenesis. D95A, D95N, R158A, E161A, E161Q, K206V, E220Q, D285A, D285N, W286A, E491A, E491Q, and R158A/E161A mutations resulted in a lack of detectable  $\beta$ -D-glucosidase/exoglucanase activity. The substitution of W434 (at +1 subsite) by alanine led to the loss of hydrolysis of  $\beta$ -(1,2),  $\beta$ -(1,4), and  $\beta$ -(1,6)-oligosaccharides and loss of inhibition by methyl-O-thio-gentiobiose, which confirmed the role of W434 in mediating the substrate specificity of rHvExoI. Mutation of amino acid residue E220 to alanine appeared to decrease the  $pK_a$  of acid/base residue and decreased the  $k_{cat}$  values for cellobiose and 4NPGlc. Together with previous structural studies, this suggested that this residue might play a role in modulating the pH optimum by coordinating the water molecules around the catalytic acid/base. Overall, the enzymatic properties of the mutants suggest that amino acids at the +1 subsite of GH3 may have more effect on the substrate specificity, while the acidic residue close to the catalytic acid/base may mediate the catalytic mechanism.

## 5.1 Introduction

Among the various glycosyl hydrolases (GH) in the Carbohydrate-Active EnZymes database (CAZy, (<http://www.cazy.org/>), several catalyze the hydrolysis of the glycosidic bond between two glucose residues or a glucose and an aglycone moiety. Barley  $\beta$ -D-glucan exohydrolase I (HvExoI) is a member of GH family 3, which is able to hydrolyse the glycosidic bond at the nonreducing end of  $\beta$ -(1,2)-,  $\beta$ -(1,3)-,  $\beta$ -(1,4)-, and  $\beta$ -(1,6)-gluco-oligosaccharides and polysaccharides. The subsite-binding affinities calculated from the kinetic parameters of HvExoI hydrolysis of  $\beta$ -(1,3)-laminari-oligosaccharides (DP 2-7) and  $\beta$ -(1,4)-cello-oligosaccharides (DP 2-6) suggested that HvExoI has 2-3 subsites for binding glucosyl residues (Hrmova *et al.*, 1998a). The hydrolysis of a variety of  $\beta$ -linkages in polysaccharides and oligosaccharides generated interest in which amino acid residues surround the active site and how they achieve this broad specificity (Hrmova *et al.*, 1996; 1998b).

The structure of HvExoI is the representative of GH3 proteins composed of 2 domains. The N-terminal domain comprise a  $(\beta/\alpha)_8$  triose-isomerase (TIM) barrel structure, while the C-terminal domain is arranged in a six-stranded  $\beta$  sandwich with three  $\alpha$  helices on either side of the sheet (Varghese *et al.*, 1999). The active site of HvExoI lies at the interface between the two domains, with Asp285 in domain 1 acting as the catalytic nucleophile residue and Glu491 in domain 2 as the catalytic acid/base residue (Varghese *et al.*, 1999; Hrmova *et al.*, 2001). To understand the broad specificity of HvExoI to various  $\beta$ -linked gluco-oligosaccharides, the amino acid residues at the -1 and +1 subsites and the different relative orientation of adjacent glucopyranosyl rings bound in the active site has been investigated with enzyme complexes with S-glucoside substrate analogues (Hrmova *et al.*, 2002) and transition state mimics was also studied with inhibitors/enzyme complexes (Hrmova *et al.*, 2004; 2005; 2007). Although the structural basis for the broad specificity of HvExoI has become better understood, in terms of the interactions between active site

amino acid residues and different  $\beta$ -linked substrates, the consequences of each of the observed amino acid residues on hydrolytic rates and catalytic efficiencies could not be determined.

Recently, the expression of heterologous recombinant HvExoI (rHvExoI) has been achieved and the substrate specificity and kinetic parameters of rHvExoI have been compared to native HvExoI (Luang *et al.*, 2010). The substrate preferences of rHvExoI were similar to native HvExoI for  $\beta$ -linked gluco-oligosaccharide hydrolysis. Thus, rHvExoI is available to further identify the roles of amino acid residues around the active site. Here, we constructed a number of mutant rHvExoI proteins with active-site amino acid substitutions by site-directed mutagenesis and characterized their enzymatic properties.

## 5.2 Materials and methods

### 5.2.1 Plasmids and bacterial strains

Plasmid for this work was recombinant pPICZ $\alpha$ BNH<sub>8</sub>\_optimized HvExoI vector (Chapter IV, section 4.2.2.2). The bacteria strain used for DNA cloning was *E. coli* strain XL1 Blue (Stratagene). *Pichia pastoris* strain SMD1168H was used as the expression host.

### 5.2.2 Mutation of the optimized HvExoI cDNA by the QuikChange® Site-Directed Mutagenesis Kit.

Site-directed mutagenesis was performed using a pPICZ $\alpha$ BNH<sub>8</sub> expression vector containing an optimized cDNA fragment that encodes the mature HvExoI (Luang *et al.*, 2010) as the template. Nine amino acid residues were mutated, including the single mutations of the catalytic nucleophile: D285N and D285A; catalytic acid/base: E491Q and E491A; amino acid residues at the -1 subsite: D95N, D95A, R158A, E161Q, E161A, and K206V; E220Q and E220A, which are close to the catalytic acid/base residue; amino acid residues at the +1 subsite: W286A and W434A; and the double mutation R158A/E161A.

Thus, a total of fifteen mutants were generated. The experiments were carried out following the instructions of the QuikChange® Site-Directed Mutagenesis Kit (Stratagene) with the temperature cycling parameters shown in Table 5.1 and the primers shown in Table 5.2.

**Table 5.1** Cycling parameters for mutation of the optimized HvExoI by the QuikChange® Site-Directed Mutagenesis method.

| Segment | Cycles | Temperature | Time   |
|---------|--------|-------------|--------|
| 1       | 1      | 95°C        | 30 s   |
| 2       | 16     | 95°C        | 30 s   |
|         |        | 55°C        | 1 min  |
|         |        | 68°C        | 6 min  |
| 3       | 1      | 68°C        | 10 min |

**Table 5.2** The mutagenic oligonucleotide primers for optimized HvExoI.

| Primer        | Sequence (5'→3')  | T <sub>m</sub> (°C) |
|---------------|---|---------------------|
| D285N Forward | GGGTTTIGTTATTCT <u>A</u> ATTGGGAAGGTATTGATAG                                  | 73.6                |
| Reverse       | CTATCAATACCTTCCAAT <u>T</u> AGAAATAACAAAACCC                                  | 73.6                |
| D285A Forward | GGTTTIGTTATTCTG <u>C</u> TTGGGAAGGTATTGATAG                                   | 74.6                |
| Reverse       | CTATCAATACCTTCCCA <u>A</u> GAGAAATAACAAAACC                                   | 74.6                |
| E491Q Forward | GAACATCCATACT <u>C</u> AAACTAAGGGAGATAAC                                      | 74.2                |
| Reverse       | GTTATCTCCCTTAGTTT <u>G</u> AGTGTATGGATGTTT                                    | 74.2                |
| E491A Forward | GTGAACATCCATACT <u>G</u> CTACTAAGGGAGATAACTTG                                 | 75.7                |
| Reverse       | CAAGTTATCTCCCTTAGTAG <u>C</u> AGTGTATGGATGTTT                                 | 75.7                |
| D95N Forward  | CAATGATCTACGGTATTA <u>A</u> ATGCTGTTTATGGTCAAAC                               | 76.2                |
| Reverse       | GTTTGGACCATGAACAGCAT <u>T</u> AATACCGTAGATCATTG                               | 76.2                |
| D95A Forward  | CAATGATCTACGGTATTG <u>C</u> TGCTGTTTATGGTCAAAC                                | 78.4                |
| Reverse       | GTTTGGACCATGAACAGC <u>A</u> GCAATACCGTAGATCATTG                               | 78.4                |
| R158A Forward | GTAGAGATCCAAGATGGGGT <u>GCT</u> TGTTACGAATCTACTCTGAAG                         | 78.1                |
| Reverse       | CTTCAGAGTAAGATTTCGTAACA <u>AGC</u> ACCCCATCTGGATCTCTAC                        | 78.1                |
| E161Q Forward | CAAGATGGGGTAGATGTTAC <u>A</u> ATCTTACTCTGAAGATAGAAGAATTG                      | 80.7                |
| Reverse       | CAATCTTCTATCTTCAGAGTAAGATT <u>G</u> GTAACATCTACCCCATCTTG                      | 80.7                |
| E161A Forward | CAAGATGGGGTAGATGTTAC <u>G</u> CATCTTACTCTGAAGATAGAAGAATTG                     | 79.5                |
| Reverse       | CAATCTTCTATCTTCAGAGTAAGAT <u>G</u> CGTAACATCTACCCCATCTTG                      | 79.5                |
| K206V Forward | CAAGGTTGCTGCTTGTGCT <u>GTT</u> CATTTTGTGGAGATGGTGGTACTG                       | 79.9                |
| Reverse       | CAGTACCACCATCTCCAACAAAATG <u>AAC</u> AGCACAAAGCAGCAACCTTG                     | 79.9                |
| E220Q Forward | GTACTGTTGATGGTATTAAC <u>C</u> AAAAACAACACTATTATTAAC                           | 74.6                |
| Reverse       | GTTAATAATAGTGTGTTT <u>G</u> GTTAATACCATCAACAGTAC                              | 74.6                |
| E220A Forward | GTACTGTTGATGGTATTAAC <u>C</u> TAAACAACACTATTATTAACAG                          | 74.5                |
| Reverse       | CTGTAAATAATAGTGTGTT <u>AG</u> CGTTAATACCATCAACAGTAC                           | 74.5                |
| W286A Forward | GGGTTTIGTTATTCTGAT <u>GCT</u> GAAAGGTATTGATAGAATTACTAC                        | 73.5                |
| Reverse       | GTAGTAATCTATCAATACCTT <u>AGC</u> ATCAGAAATAACAAAACCC                          | 73.5                |
| W434A Forward | GGTGGTTGGACTATTGA <u>AGCT</u> CAAGGAGATACTGGTAG                               | 75.3                |
| Reverse       | CTACCAGTATCTCCTT <u>AGCT</u> TCAATAGTCCAACCACC                                | 75.3                |
| R158A_E161A   |   |                     |
| Forward       | GAGATCCAAGATGGGGT <u>GCT</u> TGTTACG <u>CT</u> TCTTACTCTGAAGATAGAAGA<br>ATTGT | 76.5                |
| Reverse       | ACAATCTTCTATCTTCAGAGTAAGA <u>AG</u> CGTAACA <u>AGC</u> ACCCCATCTTGGA<br>TCTC  | 76.5                |

\* The mutated nucleotides are underlined.

### **5.2.3 Protein expression and purification of rHvExoI mutants.**

The recombinant pPICZ $\alpha$ BNH<sub>8</sub> plasmids encoding the rHvExoI mutants were linearized and transformed into the *P. pastoris* strain SMD1168H competent cells as described in the section 4.2.2.7. Expression of the rHvExoI mutant proteins was induced in the same expression conditions as wild type rHvExoI, which are described in section 4.2.2.8. The media from cultures induced to secrete mutant proteins were screened for activity against 1 mM 4NPGlc as substrate and for histidine-tagged rHvExoI protein by dot blot with a mouse monoclonal anti-polyhistidine-alkaline phosphatase IgG2a isotype antibody (Sigma). The dot blot membrane was developed with the BCIP/NBT-purple liquid reagent (Sigma).

The E220A and W434A mutant proteins were purified from crude protein cultures by the same procedure described for the glycosylated form of wild type rHvExoI in section 4.2.2.9.

### **5.2.4 Protein characterization of rHvExoI mutants**

The effects of pH on the activities of the glycosylated forms of the E220A and W434A mutant proteins were determined by assaying hydrolysis of 4NPGlc at 30°C for 15 min with the buffers ranging from pH 3.5-10.0 described in section 4.2.2.10. The effect of preincubation at various temperatures on the activities of these mutants was studied similarly to the wild type in section 4.2.2.10, but the activities were measured at the optimum pH in 0.1 M sodium acetate, pH 4.5 for E220A and pH 5.65 for W434A.

Enzyme assays and analyses of substrate specificity, kinetic properties, and inhibition were performed with the glycosylated forms of E220A (2.7-27 pmole) and W434A (0.7-9.3 pmole) in 0.1 M sodium acetate, pH 4.5 and pH 5.65, respectively, as described in section for wild type rHvExoI 4.2.2.11, and 4.2.2.13.

## **5.3 Results**

### **5.3.1 Protein expression and purification of mutants**

The expression of 15 mutants of rHvExoI was screened by activity for 4NPGlc hydrolysis in comparison with the wild type rHvExoI and control construct transformed cultures. No activity could be detected from the D95A, D95N, R158A, E161A, E161Q, K206V, E220Q, D285A, D285N, W286A, E491A, E491Q and R158A/E161A mutants, although the expression could be detected by immunoblotting (data not shown). The activity was clearly observed for the E220A and W434A mutants. Therefore, these two mutants were further purified, in order to test their hydrolysis activity for various substrates. After cation exchange chromatography and IMAC, the yields of about 3.6 mg and 2.3 mg of purified, glycosylated forms of rHvExoI of E220A and W434A mutants were obtained from one liter culture, respectively.

**Table 5.3** Enzyme yields during purification of the rHvExoI E220A mutant.

| Purification step    | Yield     |                       | Specific activity            | Recovery <sup>b</sup> | Purification factor <sup>b</sup> |
|----------------------|-----------|-----------------------|------------------------------|-----------------------|----------------------------------|
|                      | Protein   | Activity <sup>a</sup> |                              |                       |                                  |
|                      | <i>mg</i> | <i>units</i>          | <i>units·mg<sup>-1</sup></i> | <i>%</i>              | <i>-fold</i>                     |
| Crude protein        | 120       | 67.5                  | 0.6                          | 100                   | 1.0                              |
| SP-Sepharose         | 8.0       | 10.8                  | 1.4                          | 16.0                  | 2.4                              |
| 1 <sup>st</sup> IMAC | 3.6       | 6.0                   | 1.7                          | 8.9                   | 3.0                              |

**Table 5.4** Enzyme yields during purification of the rHvExoI W434A mutant.

| Purification step    | Yield     |                       | Specific activity            | Recovery <sup>b</sup> | Purification factor <sup>b</sup> |
|----------------------|-----------|-----------------------|------------------------------|-----------------------|----------------------------------|
|                      | Protein   | Activity <sup>a</sup> |                              |                       |                                  |
|                      | <i>mg</i> | <i>units</i>          | <i>units·mg<sup>-1</sup></i> | <i>%</i>              | <i>-fold</i>                     |
| Crude protein        | 121       | 68.7                  | 0.6                          | 100.0                 | 1.0                              |
| SP-Sepharose         | 7.5       | 10.3                  | 1.4                          | 15.0                  | 2.4                              |
| 1 <sup>st</sup> IMAC | 2.3       | 5.4                   | 2.4                          | 8.0                   | 4.2                              |

<sup>a</sup> Recovered enzyme units assayed on 4NPGlc.

<sup>b</sup> Recoveries are expressed as percentage of enzyme activity in the crude protein, and purification factors are calculated on the basis of specific activities.

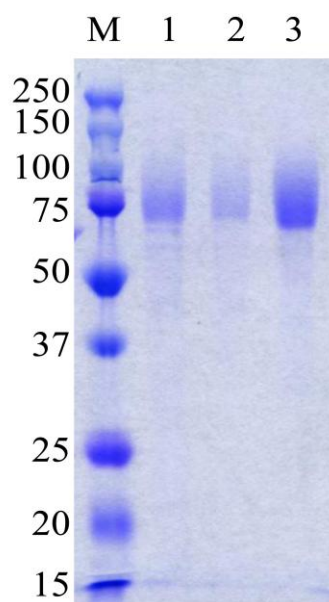


**Figure 5.1** Purification of glycosylated forms of rHvExoI wild type (lane 1), and E220A (lane 2) and W434A (lane 3) mutants by IMAC. Lane M is prestained protein marker.

### **5.3.2 Effect of pH and temperature on rHvExoI mutant enzyme activities**

The pH and thermostability profiles were determined with the purified glycosylated forms of the E220A and W434A mutants. The E220A mutant showed a narrower pH dependence and its optimum (pH 4.5) was slightly lower than that of wild type rHvExoI (pH 5.0) and was projected to have 50% activity at pH 4.0 and 5.3. In contrast, the optimum pH of the W434A mutant (pH 5.7), was slightly higher than wild type rHvExoI and 50% activity was observed at pH 4.6 and 7.1.

The thermostability of the mutant enzymes was similar to wild type, in that the temperature of 50% enzyme inactivation of E22A was approximately 34°C, but it was slightly increased to approximately 41°C for W434A. The presence of BSA could stabilize the enzymes to give approximately 2-fold higher activity under all conditions and it shifted the temperatures of 50% enzyme inactivation to 36 and 43°C for E220A and W434A, respectively.

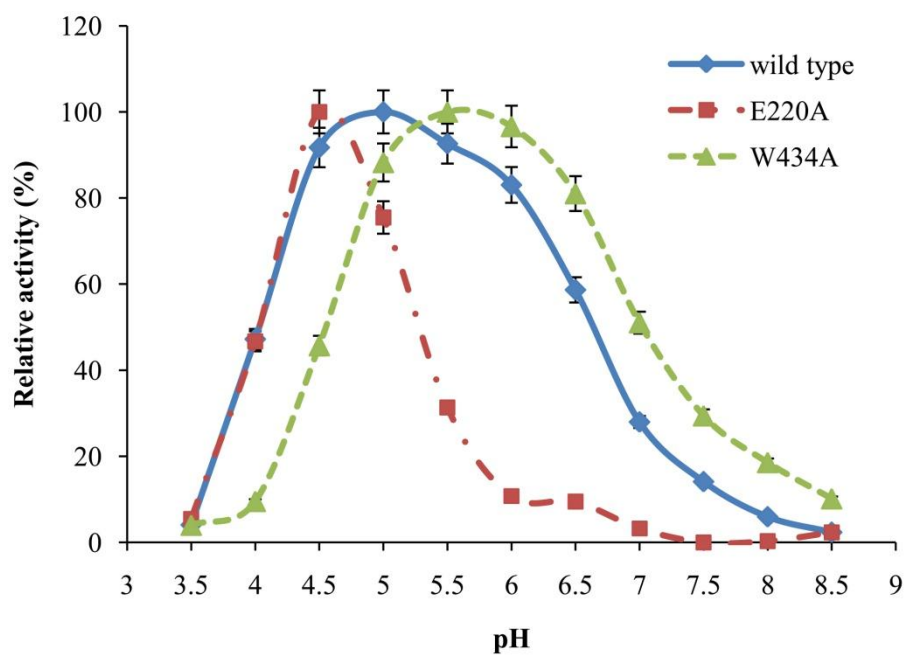


**Figure 5.2** pH profiles of activity for wild type and mutant rHvExoI enzymes. Activity was assayed with 0.2% (w/v) 4NPGlc and 160  $\mu\text{g/ml}$  BSA in 0.1 M citric acid - 0.2 M disodium hydrogen phosphate (McIlvaine buffers) over a pH range 3.0-8.5, at 30°C for 15 min (wild type rHvExoI) or 60 min (E220A and W434A mutants of rHvExoI).

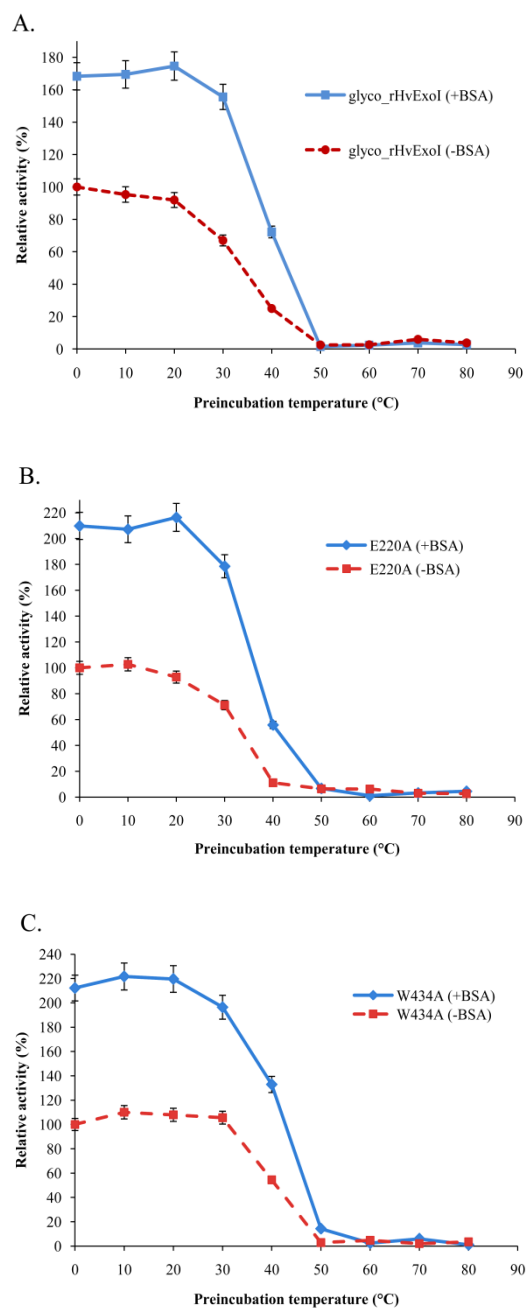


**Figure 5.3** Thermostability of glycosylated forms of wild type and mutant rHvExoI enzymes. (A), wild type; (B), E220A mutant; and (C), W434A mutant. Activity was assayed with 4NPGlc for 15 min at 30°C after preincubation at temperatures range 0-80°C with and without 160 µg/ml BSA for 15 min.

### 5.3.3 Substrate specificity and kinetic analysis of mutant rHvExoI enzymes compared to wild type rHvExoI

The mutations of rHvExoI E220A and W434A decreased its rate of hydrolysis and the range of substrates that it could hydrolyse, as shown in Table 5.5. The rHvExoI E220A mutant retained activity to  $\beta$ -(1,2)-,  $\beta$ -(1,3)-,  $\beta$ -(1,4)-, and  $\beta$ -(1,6)-linked oligosaccharides, though at a lower hydrolytic rate than wild type. However, it had very low activity to laminarin and no activity to barley (1,3;1,4)- $\beta$ -D-glucan. On the other hand, W434A was more affected, in that it could not hydrolyse polysaccharides, the  $\beta$ -(1,2)-linked disaccharide sophorose,  $\beta$ -(1,4)-linked cello-oligosaccharides and the  $\beta$ -(1,6)-linked disaccharide gentiobiose, but only retained activity to 4NPGlc and  $\beta$ -(1,3)-linked laminari-oligosaccharides. The kinetic behavior of the mutants is shown in Table 5.6. The  $k_{\text{cat}}/K_{\text{M}}$  values of E220A were decreased approximately 15-fold for laminaribiose, 16-fold for cellobiose and 11-fold for 4NPGlc compared to wild type rHvExoI. The W434A mutant had a  $K_{\text{M}}$  value for laminaribiose that was increased approximately 1.6-fold and its  $k_{\text{cat}}/K_{\text{M}}$  value was decreased approximately 32-fold compared to wild type. Surprisingly W434 seemed to improve the activity to 4NPGlc, since although both the  $K_{\text{M}}$  and  $k_{\text{cat}}$  values were lower, the  $k_{\text{cat}}/K_{\text{M}}$  value was higher than wild type rHvExoI.

**Table 5.5** Activities of glycosylated rHvExoI E220A and W434A to synthetic and natural substrate.

| Substrate  | Activity<br>( $\mu\text{mole}/\text{min}/\text{mg}$ protein) |                 |       | Relative activity <sup>a</sup><br>(%) |       |
|--|--|-----------------|-------|---------------------------------------|-------|
|  | wild<br>type   | E220A           | W434A | E220A                                 | W434A |
| <b>Polysaccharides</b>                           |  |                 |       |                                       |       |
| Laminarin ( <i>L. digitata</i> )                 | 54.4   | 0.4             | nd    | 0.7                                   | nd    |
| Barley (1,3;1,4)- $\beta$ -D-glucan              | 5.4  | nd <sup>b</sup> | nd    | nd                                    | nd    |
| Lichenan ( <i>C. islandica</i> )                 | 0.8  | nd              | nd    | nd                                    | nd    |
| <b>Oligosaccharides</b>                          |  |                 |       |                                       |       |
| Sophorose  | 6.0  | 1.5             | nd    | 24.8                                  | nd    |
| Laminaribiose                                    | 20.8   | 1.6             | 0.5   | 7.5                                   | 2.4   |
| Laminaritriose                                   | 42.1   | 3.1             | 0.9   | 7.4                                   | 2.0   |
| Laminaritetraose                                 | 39.1   | 3.3             | 1.1   | 8.3                                   | 2.7   |
| Laminaripentose                                  | 33.8   | 3.3             | 1.0   | 9.7                                   | 3.1   |
| Laminarihexaose                                  | 46.9   | 3.3             | 1.0   | 7.0                                   | 2.1   |
| Laminariheptaose                                 | 43.9   | 3.1             | 1.0   | 7.1                                   | 2.2   |
| Cellobiose                                       | 4.6  | 0.3             | nd    | 6.7                                   | nd    |
| Cellotriose                                      | 8.8  | 0.4             | nd    | 5.0                                   | nd    |
| Cellotetraose                                    | 8.6  | 0.5             | nd    | 5.5                                   | nd    |
| Cellopentaose                                    | 8.4  | 0.3             | nd    | 3.8                                   | nd    |
| Cellohexaose                                     | 9.1  | 0.6             | nd    | 6.5                                   | nd    |
| Gentiobiose                                      | 4.7  | 0.6             | nd    | 11.9                                  | nd    |
| <b>Synthetic substrates</b>                      |  |                 |       |                                       |       |
| 4-nitrophenyl $\beta$ -D-glucopyranoside         | 12.4   | 1.6             | 6.1   | 12.5                                  | 48.8  |
| 4-nitrophenyl $\beta$ -D-galactopyranoside       | nd   | nd              | nd    | nd                                    | nd    |
| 4-nitrophenyl $\beta$ -D-xylopyranoside          | nd   | nd              | nd    | nd                                    | nd    |
| 4-nitrophenyl $\beta$ -D-fucopyranoside          | nd   | nd              | nd    | nd                                    | nd    |
| 4-nitrophenyl $\beta$ -D-lactoside               | nd   | nd              | nd    | nd                                    | nd    |
| 4-nitrophenyl $\beta$ -D-glucosiduronic acid     | nd   | nd              | nd    | nd                                    | nd    |
| 4-nitrophenyl N-Acetyl- $\beta$ -D-glucosaminide | nd   | nd              | nd    | nd                                    | nd    |
| 4-nitrophenyl $\alpha$ -L-arabinopyranoside      | nd   | nd              | nd    | nd                                    | nd    |
| 4-nitrophenyl $\beta$ -D-cellobioside            | nd   | nd              | nd    | nd                                    | nd    |
| 4-nitrophenyl $\alpha$ -L-arabinopyranoside      | nd   | nd              | nd    | nd                                    | nd    |
| 4-nitrophenyl $\beta$ -D-cellobioside            | 0.9  | nd              | nd    | nd                                    | nd    |

<sup>a</sup> Relative activity (%) compared to wild type rHvExoI hydrolysis of the same substrate.

<sup>b</sup> 'nd' indicates as 'not detectable'.

**Table 5.6** Kinetic parameters of the rHvExoI E220A and W434A mutants compared with wild type rHvExoI.

| Substrate   | Glycosylated rHvExoI |                 |                |
|---|----------------------|-----------------|----------------|
|   | wild type            | E220A           | W434A          |
| <b>Laminarin</b>                                    |                      |                 |                |
| $K_M$ (mM)  | $0.18 \pm 0.01$      | nm <sup>a</sup> | nm             |
| $k_{cat}$ (s <sup>-1</sup> )                        | $42.1 \pm 1.6$       | nm              | nm             |
| $k_{cat}/K_M$ (mM <sup>-1</sup> .s <sup>-1</sup> )  | $234 \pm 14$         | nm              | nm             |
| <b>Barley (1,3;1,4)-<math>\beta</math>-D-glucan</b> |                      |                 |                |
| $K_M$ (mM)  | $0.04 \pm 0.004$     | nm              | nm             |
| $k_{cat}$ (s <sup>-1</sup> )                        | $14.1 \pm 0.7$       | nm              | nm             |
| $k_{cat}/K_M$ (mM <sup>-1</sup> .s <sup>-1</sup> )  | $365 \pm 57$         | nm              | nm             |
| <b>Laminaribiose</b>                                |                      |                 |                |
| $K_M$ (mM)  | $1.3 \pm 0.1$        | $3.0 \pm 0.2$   | $2.1 \pm 0.2$  |
| $k_{cat}$ (s <sup>-1</sup> )                        | $54.2 \pm 2.3$       | $8.9 \pm 0.3$   | $2.4 \pm 0.1$  |
| $k_{cat}/K_M$ (mM <sup>-1</sup> .s <sup>-1</sup> )  | $41.2 \pm 2.4$       | $2.8 \pm 0.1$   | $1.3 \pm 0.1$  |
| <b>Cellobiose</b>                                   |                      |                 |                |
| $K_M$ (mM)  | $1.2 \pm 0.1$        | $1.7 \pm 0.2$   | nm             |
| $k_{cat}$ (s <sup>-1</sup> )                        | $4.2 \pm 0.2$        | $0.27 \pm 0.01$ | nm             |
| $k_{cat}/K_M$ (mM <sup>-1</sup> .s <sup>-1</sup> )  | $3.3 \pm 0.2$        | $0.16 \pm 0.01$ | nm             |
| <b>4NPGlc</b>                                       |                      |                 |                |
| $K_M$ (mM)  | $2.0 \pm 0.2$        | $1.6 \pm 0.1$   | $0.6 \pm 0.1$  |
| $k_{cat}$ (s <sup>-1</sup> )                        | $27.7 \pm 0.9$       | $2.1 \pm 0.1$   | $9.3 \pm 0.3$  |
| $k_{cat}/K_M$ (mM <sup>-1</sup> .s <sup>-1</sup> )  | $13.9 \pm 0.6$       | $1.3 \pm 0.1$   | $16.7 \pm 1.2$ |

<sup>a</sup> 'nm' indicates as 'not measured'.

### 5.3.4 Inhibition of rHvExoI mutants by inhibitors of wild type rHvExoI

Inhibition of the glycosylated forms of the rHvExoI E220A and W434A mutants was analysed with the competitive inhibitors of wild type rHvExoI methyl-O-thio-gentiobiose (G6sG-OMe), glucono  $\delta$ -lactone (GL) and 2,4-dinitrophenyl 2-fluoro-2-deoxy- $\beta$ -D-glucopyranoside (2F-DNPGlc). The  $K_i$  values for inhibition of the E220A mutant by G6sG-OMe and GL were approximately 2-fold and 10-fold higher than wild type, respectively, while the  $K_i$  of 2F-DNPGlc was the same as wild type. The activity of W434A mutant was inhibited with GL and 2F-DNPGlc with the  $K_i$  values in the same range as those of wild type. Interestingly, activity of the W434A mutant was not inhibited with G6sG-OMe at 20 mM, the maximum concentration that could be tested. This agrees with the fact that rHvExoI W434A could not hydrolyse gentiobiose.

**Table 5.7** Inhibition parameters of rHvExoI E220A and W434A mutants with methyl-O-thio-gentiobiose (G6sG-OMe), glucono  $\delta$ -lactone (GL) and 2,4-dinitrophenyl 2-fluoro-2-deoxy- $\beta$ -D-glucopyranoside (2F-DNPGlc) compared with wild type rHvExoI.

| Inhibitor                                       | rHvExoI                |                            |                      |                       |
|---|------------------------|----------------------------|----------------------|-----------------------|
|   | Glycosylated wild type | N-deglycosylated wild type | Glycosylated E220A   | Glycosylated W434A    |
| <i>G6sG-OMe</i>                                 |                        |                            |                      |                       |
| $K_i$ (M)                                       | $109 \times 10^{-6}$   | $71 \times 10^{-6}$        | $221 \times 10^{-6}$ | $> 0.02$              |
| $\Delta G$ (kJ mol <sup>-1</sup> ) <sup>a</sup> | -23.0                  | -24.1                      | -21.2                | -                     |
| <i>GL</i>                                       |                        |                            |                      |                       |
| $K_i$ (M)                                       | $10 \times 10^{-6}$    | $8.3 \times 10^{-6}$       | $103 \times 10^{-6}$ | $15.3 \times 10^{-6}$ |
| $\Delta G$ (kJ mol <sup>-1</sup> )              | -29.1                  | -29.5                      | -23.1                | -28.0                 |
| <i>2F-DNPGlc</i>                                |                        |                            |                      |                       |
| $K_i$ (M)                                       | $0.5 \times 10^{-6}$   | $0.6 \times 10^{-6}$       | $0.5 \times 10^{-6}$ | $0.6 \times 10^{-6}$  |
| $\Delta G$ (kJ mol <sup>-1</sup> )              | -36.8                  | -36.2                      | -36.5                | -36.3                 |

<sup>a</sup> Gibbs free energy of binding  $\Delta G$  was calculated from  $\Delta G = -RT \ln (K_i)$

## 5.4 Discussion

Varghese *et al.* (1999) solved the structure of native HvExoI and found that it retained a glucose molecule at the -1 subsite by hydrogen bonding interactions with charged amino acids residues. These included D95 (H-bonded to O4 and O6 of glucose), R158 (H-bonded to O2 and O3), K206 (H-bonded to O3 and O4), H207 (H-bonded to O3) and the catalytic nucleophile D285 (H-bonded to O2), as shown in Figure 5.5. This bonding was similar to that seen for the nonreducing end glucosyl residue of S-laminaribiose and S-cellobiose in their complexes (Hrmova *et al.*, 2002). Although the glucose product was fixed in the active site by these noncovalent interactions, it is released when a new substrate comes into the active site. E161, located at the bottom of active site pocket neighboring R158 and interacting with K206 via hydrogen bonding through a water molecule, may be a part of the switch for release of glucose upon entry of a new substrate in the HvExoI catalytic mechanism. The amino acid sequence alignment of GH3 proteins in Figure 5.4 shows that these -1 subsite amino acid residues considered above are conserved, except for D95. The amino acid residues located at the -1 subsite of the active site were mutated in order to test their effects on the activity. No activity was observed from expression of proteins with single mutations of D95, R158, E161 and K206 and double mutation of R158 and E161, based on 4NPGlc hydrolysis.

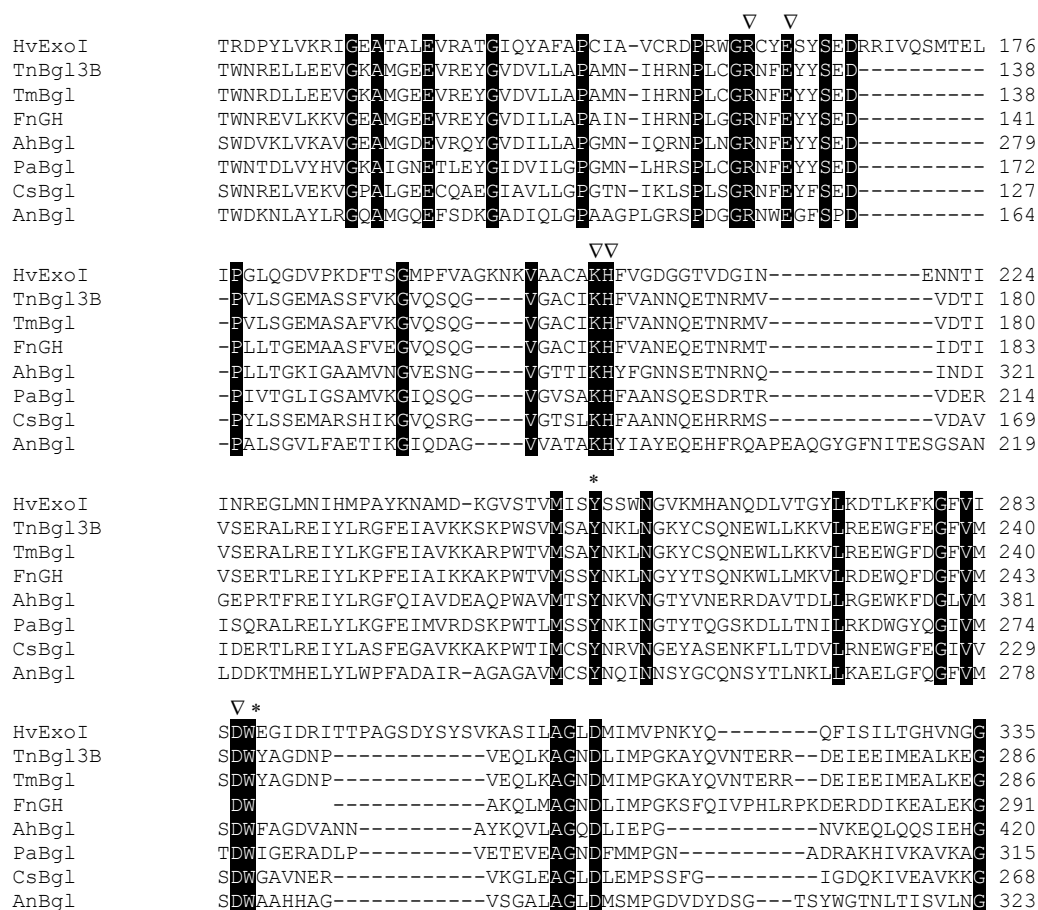


**Figure 5.4** Alignment of the regions of GH3 protein sequences containing amino acid residues at the -1 and +1 subsites. The  $\beta$ -glucosidases from *Thermotoga neapolitana* (TnBgl13B, Genbank accession ABI29899); *Thermotoga maritime* (TmBgl, AAD35119); *Fervidobacterium nodosum* (FnGH, ABS60153); *Aeromonas hydrophila* (AhBgl, ABK38668); *Prevotella albensis* (PaBgl, CAC07184); *Clostridium stercorarium* (CsBgl, CAB08072); and *Aspergillus niger* (AnBgl, ABB29285) were aligned with *Hordeum vulgare*  $\beta$ -D-glucan exohydrolase I (HvExoI, ADC55526). The black highlight indicates identical amino acid residues, triangles indicate conserved amino acid residues found at the -1 subsite, and asterisks indicate conserved amino acid residues at the +1 subsite.

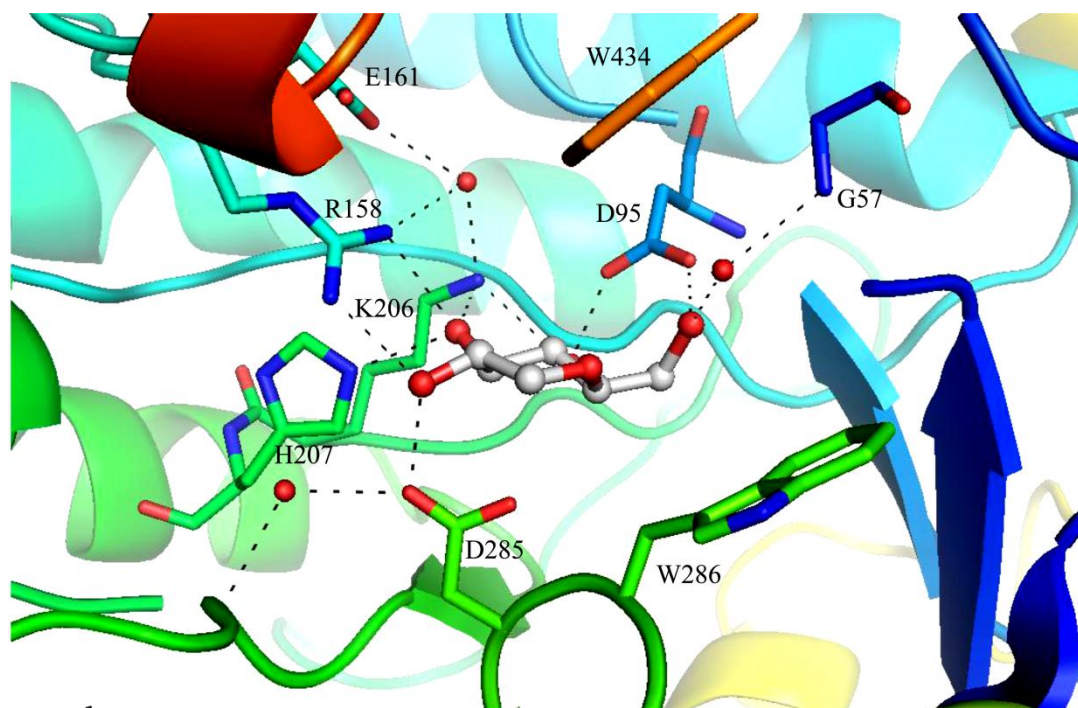


**Figure 5.5** Hydrogen bonding (dashed lines) between glucose (gray carbon), amino acid residues (stick) and water molecules (red balls) around the -1 subsite of HvExoI (PDB code 1IEQ, Varghese *et al.*, 1999).

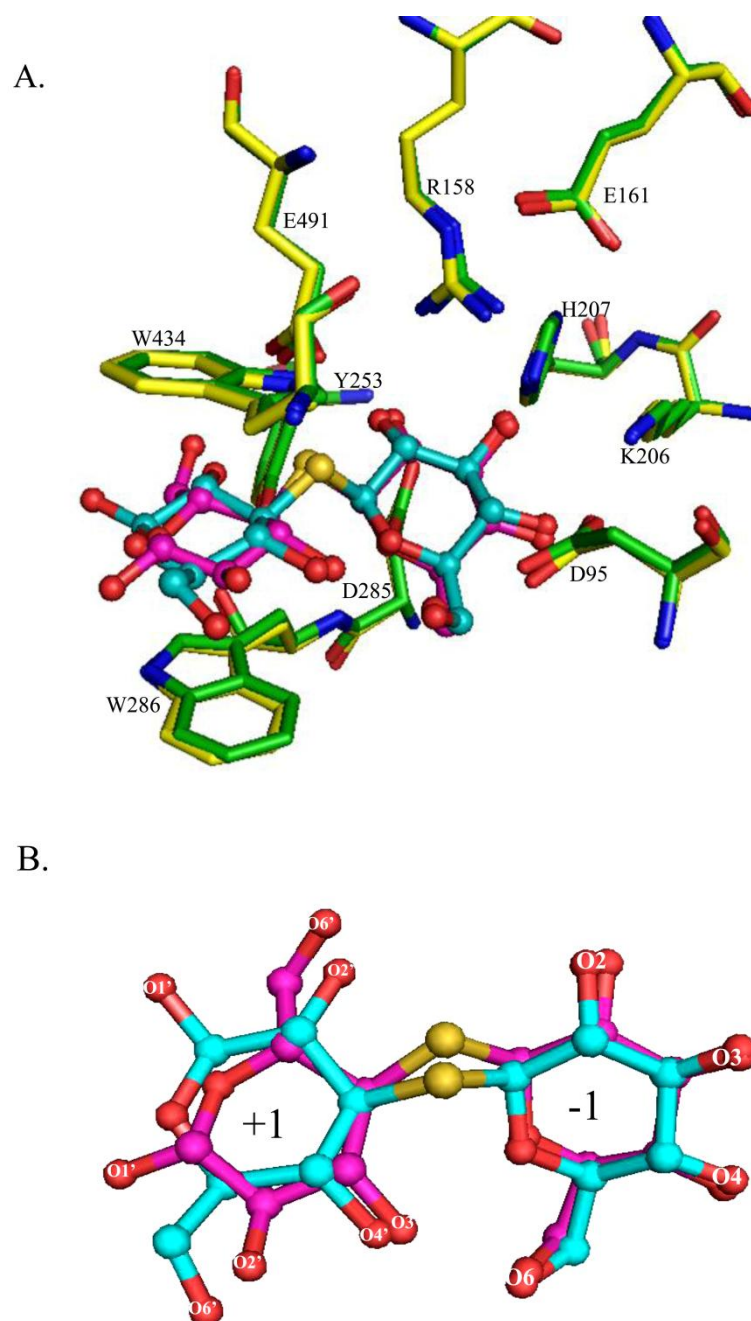


**Figure 5.6** Superimposition of the HvExoI complexes with S-laminaribiose (green carbon of amino acid residues) and S-cellobiose (yellow carbon of amino acid residues) (A) and the relative orientations S-lamaribiose (blue carbons, PDB code 1J8V) and S-cellobiose (pink carbons, PDB code 1IEX) at the -1 and +1 subsites (B) (Hrmova *et al.*, 2002).

The structural basis for the broad specificity of native HvExoI was investigated by Hrmova *et al.* (2001; 2002). The enzyme complexes with the S-substrate analogues S-laminaribiose and S-cellobiose showed that the interactions between amino acid residues and the nonreducing end glucosyl residue at the -1 subsite were identical, but the binding of the glucopyranose moiety was different at the +1 subsite, which lies between W286 and W434A. Here, the W286A mutant rHvExoI had no observable activity. It is likely that W286 is important for rHvExoI substrate binding and activity, since residue W262 of *Aspergillus niger*, which corresponds to W286 (of HvExoI), is a key residue for the enzyme's hydrolytic and transglucosidase activities (Seidle *et al.*, 2005). On the other hand, site-directed mutagenesis used to investigate the role of W434 by changing it to alanine, resulted in an enzyme with  $\beta$ -glucosidase activity, but poor or no exoglucanase activity. Substrate specificity analysis of W434A showed it is a key amino acid residue in generating the relatively broad specificity of rHvExoI. In the W434A mutant, among oligosaccharides only  $\beta$ -(1,3)-oligosaccharides were hydrolysed, and the catalytic efficiency of their hydrolysis was decreased approximately 96%. In addition, the lack of inhibition by G6sG-OMe supports the conclusion that this substitution of W434 caused loss of binding of the  $\beta$ -(1,6)-linked disaccharide. The question is why W434A could hydrolyse only laminari-oligosaccharides but not cello-oligosaccharides. The superimposition of the enzyme complexes with S-laminaribiose and S-cellobiose revealed that E491 (the catalytic acid/base residue) hydrogen bonds to the S-glycosidic bond and the glucopyranose moiety in the +1 subsite is stabilized by interactions with W286 and W434. In addition, the reducing end glucose ring O1' was hydrogen bonded with R291 and O2' was bound with Y253 and R291 for laminaribiose, but S-cellobiose only formed H-bonds between O6' and Y253 and R291. Moreover, the C6'-OH of S-laminaribiose was exposed to the entrance of active site and might interact with E36 in domain 1 via a coordinating water molecule. So, the presence of interactions between laminaribiose and Y253, R291, W286 and E36 might

diminish the effect of losing stacking interactions with W434 in the W434A mutation, so that it retained activity to laminari-oligosaccharides.

Hrmova *et al.* investigated the catalytic mechanism and transition state of native HvExoI. The orientation of E220 interacts with the ligand by coordinating two water molecules in the native HvExoI complexes with 2-deoxy-2-fluoro- $\alpha$ -D-glucopyranosyl (Hrmova *et al.*, 2001) and glucoimidazole inhibitors (Hrmova *et al.*, 2004; 2005). In the E220A mutant, the  $pK_a$  of the catalytic acid/base E491 appeared to have shifted to lower pH (Figure 5.2). For cellobiose and 4NPGlc hydrolysis, the  $k_{cat}$  values were mostly decreased, whereas the  $K_M$  values were affected less (Table 5.6). These results suggest that E220, which is located at the active site had an influence on catalysis by affecting the protonation of the catalytic acid/base E491.

## 5.6 Conclusions

The structural studies of native barley  $\beta$ -D-glucan exohydrolase (HvExoI) have provided many insights into its catalytic mechanism and substrate specificity. However, this is the first work to investigate the role of rHvExoI active site amino acid residues by site-directed mutagenesis. Most amino acid residues at the -1 subsite are involved in binding of the nonreducing sugar residue, the orientation of which is similar for all substrates. The effects of the mutation of W434 at the +1 subsite suggested that it is a key amino acid residue in determining rHvExoI substrate specificity, while E220, which is highly conserved in the plant GH3 exohydrolases (Harvey *et al.*, 2000), is involved in the enzyme catalytic mechanism.

## 5.7 References

- Hrmova, M., Harvey, A.J., Wang, J., Shirley, N.J., Jones, G.P., Stone, B.A., Høj, P.B., and Fincher, G.B. (1996). Barley  $\beta$ -D-glucan exohydrolases with  $\beta$ -D-glucosidase activity: purification, characterization, and determination of primary structure from a cDNA clone. **J. Biol. Chem.** 271: 5277-5286.
- Hrmova, M., MacGregor E.A., Biely, P., Stewart, R.J., and Fincher, G.B. (1998a). Substrate binding and catalytic mechanism of a barley  $\beta$ -D-glucosidase/(1,4)- $\beta$ -D-glucan exohydrolase. **J. Biol. Chem.** 273: 11134-11143.
- Hrmova, M., and Fincher, G.B. (1998b). Barley  $\beta$ -D-glucan exohydrolases. Substrate specificity and kinetic properties. **Carbohydr. Res.** 305: 209-221.
- Hrmova, M., and Fincher, G.B. (2001). Structure-function relationships of  $\beta$ -D-glucan endo- and exohydrolases from higher plants. **Plant Mol. Biol.** 47: 73-91.
- Hrmova, M., Gori, R.D., Smith, B.J., Fairweather, J.K., Driguez, H., Varghese, J.N., and Fincher, G.B. (2002). Structural basis for broad substrate specificity in higher plant  $\beta$ -D-glucan glucohydrolases. **Plant Cell** 14: 1033-1052.
- Hrmova, M., Gori, R.D., Smith, B.J., Vasela, A., Varghese, J.N., and Fincher, G.B. (2004). Three-dimensional structure of the barley  $\beta$ -D-glucan glucohydrolase in complex with a transition state mimic. **J. Biol. Chem.** 279: 4970-4980.
- Hrmova, M., Streltsov, V.A., Smith, B.J., Vasella, A., Varghese, J.N., and Fincher G.B. (2005). Structural rationale for low-nanomolar binding of transition state mimics to a family GH3  $\beta$ -D-glucan glucohydrolase from barley. **Biochemistry** 44: 16529-16539.

- Hrmova, M., and Fincher, G.B. (2007). Dissecting the catalytic mechanism of a plant  $\beta$ -D-glucan glucohydrolase through structural biology using inhibitors and substrate analogues. **Carbohydr. Res.** 342: 1613-1623.
- Luang, S., Hrmova, M., and Ketudat Cairns, J.R. (2010). High-level expression of barley  $\beta$ -D-glucan exohydrolase HvExoI from a codon-optimized cDNA in *Pichia pastoris*. **Protein Expr. Purif.** 73: 90-98.
- Seidle, H.F., McKenzie, K., Marten, I., Shoseyov, O., and Huber, R. (2005). Trp-262 is a key residue for the hydrolytic and transglucosidic reactivity of the *Aspergillus niger* family 3  $\beta$ -glucosidase: Substitution results in enzymes with mainly transglucosidic activity. **Arch. Biochem. Biophys.** 444: 66-75.
- Varghese, J.N., Hrmova, M., and Fincher, G.B. (1999). Three-dimensional structure of a barley  $\beta$ -D-glucan exohydrolase, a family 3 glycosyl hydrolase. **Structure** 7: 179-190.

# CHAPTER VI

## CRYSTALLISATION OF RECOMBINANT BARLEY $\beta$ -D-GLUCAN EXOHYDROLASE I

### Abstract

Recombinant expression of barley  $\beta$ -D-glucan exohydrolase I (HvExoI) in *Pichia pastoris* has allowed investigation of structure-function relationships by site-directed mutagenesis, and structural elucidation of the mutants is useful to fully understand their effects. The rHvExoI expressed in *P. pastoris* was purified by SP-sepharose, immobilized metal ( $\text{Co}^{2+}$ ) affinity chromatography (IMAC), deglycosylation with endoglycosidase H, a second round of IMAC and BioGel-P100 size exclusion chromatography. Many shapes of rHvExoI crystals were obtained in various conditions during screening by the microbatch method. Tetragonal crystals of rHvExoI could be observed in the presence of ammonium sulfate in malate-MES-Tris buffer, pH 5.0, at 95 days. On the other hand, native HvExoI seeds generated from HvExoI purified from barley (Hrmova *et al.*, Carbohydr. Res. 305, 209-221, 1998) served as good nucleants for crystallisation of rHvExoI wild type and its E220A, W434A and R158A/E161A mutants in macroseeding experiments. Thus, although the rHvExoI was different from native HvExoI in the carbohydrate attached to N-glycosylation sites and had eleven extra amino acid residues (AHHHHHHHHAA) at the N-terminus, it could extend the same crystallisation matrix generated by the native protein in the crystal seeds.

## 6.1 Introduction

Barley  $\beta$ -D-glucan exohydrolase I (HvExoI) is a member of glycoside hydrolase family 3 (GH3), which has served as a structural model for this family (Harvey *et al.*, 2000). Crystals of HvExoI were first obtained by vapour diffusion in the presence of ammonium sulfate and polyethylene glycol (Hrmova *et al.*, 1998). The tetragonal crystals were found to form in the buffer of 75 mM HEPES, pH 7.0, containing 7.5 mM sodium acetate, 1.2% (w/v) polyethylene glycol 400 and 0.8 M ammonium sulfate, and belonged to the  $P4_32_12$  space group with cell parameters of  $a = b = 102.1$  and  $c = 184.5$  Å, and there was one molecule in the asymmetric unit. The crystal structure was then solved and the catalytic acid/base and nucleophile residues identified (Varghese *et al.*, 1999; Hrmova *et al.*, 2001). The roles of amino acid residues around the active site have also been investigated by structural investigation of complexes of HvExoI with substrate analogues and inhibitors (Hrmova *et al.*, 2002; 2004; 2005; 2007).

Recently, a codon-optimized HvExoI cDNA was used to express the protein in *Pichia pastoris* and the recombinant rHvExoI properties were found to be quite similar to the native HvExoI (Luang *et al.*, 2010). This has allowed investigation of the roles of active site residues by site-directed mutagenesis (Chapter V). To fully benefit from these analyses, it is necessary to determine the structures of the mutant enzymes, in order to see how they affect the structure of the active site and its interactions with substrates and inhibitors. Here, the preliminary screening for rHvExoI crystallisation by microbatch and macroseeding with native HvExoI seed is described.

## **6.2 Materials and methods**

### **6.2.1 Plasmid and yeast strains**

The generation of the pPICZ $\alpha$ BNH<sub>8</sub> vectors, including barley  $\beta$ -D-glucan exohydrolase I (HvExoI) optimized cDNA (Genbank accession No. GU441535), and those with the mutations E220A, W434A and R158A/E161A was described in Luang *et al.* (2010) and Chapters IV and V. These plasmids were used to express the corresponding proteins in *Pichia pastoris* strain SMD1168H.

### **6.2.2 Expression and purification of wild type rHvExoI and rHvExoI E220A, W434A and R158A/E161A mutants**

The constructs of pPICZ $\alpha$ BNH<sub>8</sub> including the insert gene encoding wild type and mutant rHvExoI proteins were used to express their respective proteins, which were purified as describes previously (Luang *et al.*, 2010; Chapters IV and V). Before protein crystallisation, purified N-deglycosylated rHvExoI was passed through a BioGel-P100 size exclusion column with 50 mM sodium acetate, pH 5.25, containing 200 mM NaCl and 1 mM dithiothreitol at the flow rate of 0.07 ml/min. The elution fractions of wild type, E220A and W434A were monitored by measuring 4NPGlc hydrolysis activity, as described in section 4.2.2.10, but those containing the rHvExoI R158A/E161A mutant were identified by measuring the absorbance at 280 nm and further detecting the protein band on SDS-PAGE. Then, pooled fractions of rHvExoI protein were buffer exchanged to remove NaCl and dithiothreitol with 20 mM sodium acetate, pH 5.25, by 10 kDa molecular-weight cut off Centricon centrifugal filter (Millipore).

### **6.2.3 Preliminary protein crystallisation of wild type rHvExoI**

#### **6.2.3.1 Protein solution preparation**

Purified N-deglycosylated rHvExoI was concentrated to 12.5 mg/ml in 20 mM sodium acetate, pH 5.25., and filtered through a 0.22 µm filter (Millipore).

#### **6.2.3.2 Initial screening of wild type rHvExoI for crystallisation conditions by microbatch and sitting-drop vapour-diffusion techniques**

Microbatch screening was performed in 60 well plastic microbatch plates (Hampton Research). Ten microliters of 100% paraffin oil was pipetted on each well of the plastic plate, then 1 µl of precipitant solution and 1 µl of 12.5 mg/ml wild type rHvExoI were pipetted into the bottom of each well. The precipitant solutions for screening included the Grid Screen Ammonium Sulfate, Crystal Screen Lite, and Crystal Screen2 from Hampton Research. Screening drops were incubated at 277 K and 287 K. Additionally, rHvExoI crystallisation was screened by sitting-drop vapour-diffusion technique at the Bio21 Collaborative Crystallisation Centre (CSIRO, Parkville, Australia, Newman *et al.*, 2008) using the PSS\_1\_Com5 screen formulation from Emerald BioSystems (Bainbridge Island, WA, USA) and the PS gradient-mid range formulation ([http://www.csiro.au/c3/Facility/c3\\_centre\\_robotic\\_crystal.htm](http://www.csiro.au/c3/Facility/c3_centre_robotic_crystal.htm)) with incubation at 281 K and 293 K. The protein crystallisation trials were observed under a microscope to identify those producing crystals.

### **6.2.3.3 rHvExoI crystallisation by macroseeding with native HvExoI seed**

Crystallisation drops of rHvExoI were set up in the same conditions as reported for native HvExoI from seed (Hrmova *et al.*, 1998) by hanging-drop vapour diffusion with small native HvExoI seeds and incubated at 277 K. The crystallisation drop of rHvExoI was prepared by adding 4-6  $\mu$ l of 12.5 mg/ml of wild type, 7.8 mg/ml of E220A, 7.8 mg/ml of W434A, and 4.5 mg/ml of R158A/E161A rHvExoI into 4  $\mu$ l of precipitant solution (100 mM HEPES-NaOH buffer, pH 7.0, 2.4% (w/v) polyethylene glycol 400, 1.6 M ammonium sulfate) and drops (8-10  $\mu$ l) were placed on 22 mm siliconised circular glass cover slips. A few small crystals of native HvExoI were transferred by cat whisker, which was touched to the surface of the parent microcrystal suspension and drawn through the new rHvExoI drop. The cover slips with the crystallisation drops suspended below them were placed over 1 ml reservoirs (1.7 M ammonium sulfate in 50 mM HEPES-NaOH buffer, pH 7.0) with a grease seal between the top of the well and the coverslip, and the coverslip was twisted a few degrees to complete sealing.

## 6.3 Results

### 6.3.1 Protein purification of rHvExoI

The purified N-deglycosylated rHvExoI, which had been submitted to a further purification step of size exclusion chromatography appeared to be over 95% pure (Figure 6.1), so it was used for crystallisation. The final concentration of 12.5 mg/ml of N-deglycosylated rHvExoI wild type was used for crystallisation by microbatch, robotic sitting drop, and macroseeding methods. The mutants of 7.8 mg/ml of E220A and W434A, and 4.5 mg/ml of R158A/E161A were crystallised by macroseeding methods.

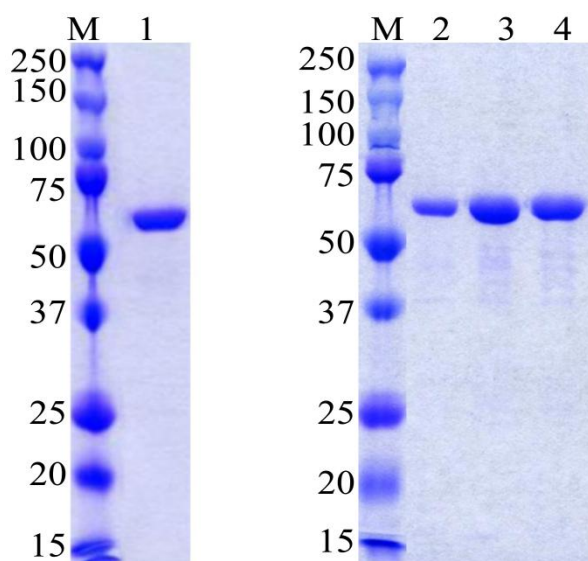


**Figure 6.1** N-deglycosylated wild type and mutant forms of rHvExoI after BioGel-P100 size-exclusion chromatography. Lane M, prestained protein marker; lanes 1-4, the N-deglycosylated forms of wild type rHvExoI, E220A, W434A and R158A/E161A rHvExoI mutants, respectively.

### **6.3.2 rHvExoI crystallisation**

#### **6.3.2.1 Initial screening for crystallisation of rHvExoI by the microbatch and sitting-drop vapour-diffusion techniques**

Many shapes of protein crystal, including needle clusters, spherulite crystals and quasi crystals, were observed from the Hampton kits, the PSS\_1\_Com5 screen formulation and the PS gradient-mid range formulation (Figure 6.2). Surprisingly, tetragonal crystals similar to those of native HvExoI (Hrmova *et al.*, 1998) were observed in two conditions of the PS gradient-mid range formulation (1.8 M ammonium sulfate in 10 mM malate-MES-Tris, pH 5 and 2.2 M ammonium sulfate in 10 mM malate-MES-Tris, pH 5.0) at 95 days, although these conditions were different from those originally used for native HvExoI crystallisation (0.8 M ammonium sulfate, 1.2% (w/v) polyethylene glycol 400, 7.5 mM sodium acetate, 75 mM HEPES, pH 7.0).

**Table 6.1** Conditions yielding crystallisation of wild type rHvExoI in microbatch and sitting-drop vapour-diffusion screening.

| Condition no.                 | Screening kit                | Salt   | Organic Precipitant                                   | Buffer   | Temperature (K) | Day |
|-------------------------------|------------------------------|--|---|--|-----------------|-----|
| Microbatch technique          |                              |  |   |  |                 |     |
| B5                            | Grid Screen ammonium sulfate | 3.2 M ammonium sulfate                           | none  | 0.1 M HEPES, pH 7.0  | 277 K , 287 K   | 3   |
| D2                            | Crystal Screen2              | 20% PEG 10,000                                   | none  | 0.1 M HEPES, pH 7.5  | 277 K , 287 K   | 3   |
| Sitting-drop vapour-diffusion |                              |  |   |  |                 |     |
| A8                            | PSS_1_Com5                   | 0.02% (w/v) sodium azide                         | 5% (v/v) 2-propanol                                   | 2.5 M NaH <sub>2</sub> /K <sub>2</sub> H phosphate, pH 5.5 | 293 K           | 27  |
| A9                            | PSS_1_Com5                   | 0.02% (w/v) sodium azide                         | 2% (v/v) PEG 400                                      | 2 M NaH <sub>2</sub> /K <sub>2</sub> H phosphate, pH 6.5   | 293 K           | 27  |
| B4                            | PS gradient-mid range        | 1.8 M ammonium sulfate                           | none  | 10 mM malate-MES-Tris, pH 5.0                              | 287 K           | 95  |
| B6                            | PS gradient-mid range        | 2.2 M ammonium sulfate                           | none  | 10 mM malate-MES-Tris, pH 5.0                              | 287 K           | 95  |
| C6                            | PSS_1_Com5                   | 0.02% (w/v) sodium azide                         | 4% (w/v) PEG 1500, 30% (v/v) 2-methyl-2,4-pentanediol | 0.1 M HEPES, pH 7.5  | 281 K           | 27  |
| D7                            | PS gradient-mid range        | 1.2 M sodium malonate, pH 7.0                    | none  | 10 mM malate-MES-Tris, pH 9.0                              | 281 K           | 3   |
| D8                            | PS gradient-mid range        | 1.4 M sodium malonate, pH 7.0                    | none  | 10 mM malate-MES-Tris, pH 9.0                              | 281 K           | 3   |
| E1                            | PSS_1_Com5                   | 0.1 M calcium chloride, 0.02% (w/v) sodium azide | 4% (v/v) 2-propanol, 25% (w/v) PEG 3350               | 0.1 M HEPES, pH 7.5  | 281 K           | 3   |

\* Preliminary screening with wild type rHvExoI (12.5 mg/ml) per precipitant ratio of 1:1.

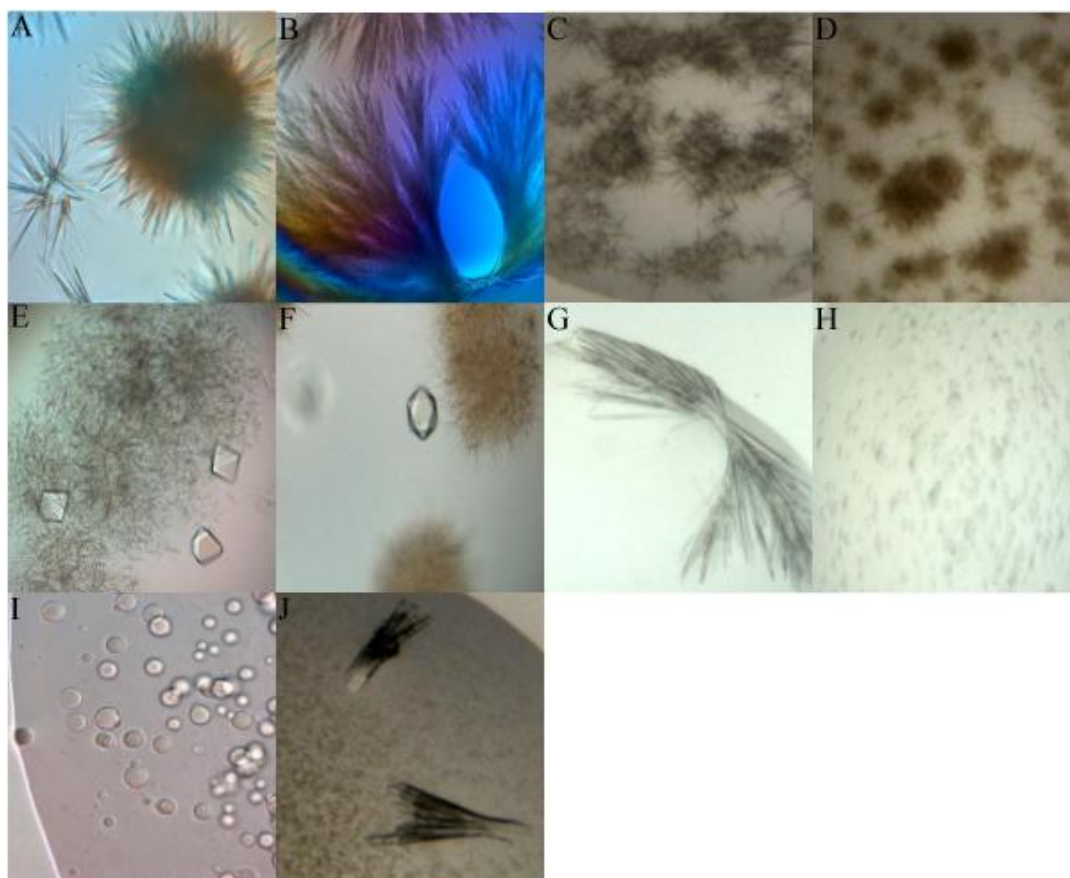


**Figure 6.2** Crystals of wild type rHvExoI from the initial microbatch and sitting-drop vapour-diffusion screening. Conditions are A: 3.2 M ammonium sulfate, 0.1 M HEPES, pH 7.0; B: 20% PEG 10,000, 0.1 M HEPES, pH 7.5; C: 0.02% (w/v) sodium azide, 5% (v/v) 2-propanol, 2.5 M  $\text{NaH}_2\text{PO}_4/\text{K}_2\text{HPO}_4$  phosphate, pH 5.5; D: 0.02% (w/v) sodium azide, 2% (v/v) PEG 400, 2 M  $\text{NaH}_2\text{PO}_4/\text{K}_2\text{HPO}_4$  phosphate, pH 6.5; E: 1.8 M ammonium sulfate, 10 mM malate-MES-Tris, pH 5.0; F: 2.2 M ammonium sulfate, 10 mM malate-MES-Tris, pH 5.0; G: 0.02% (w/v) sodium azide, 4% (w/v) PEG 1500, 30% (v/v) 2-methyl-2,4-pentanediol, 0.1 M HEPES, pH 7.5; H: 1.2 M sodium malonate, pH 7.0, 10 mM malate-MES-Tris, pH 9.0; I: 1.4 M sodium malonate, pH 7.0, 10 mM malate-MES-Tris, pH 9.0; J: 0.1 M calcium chloride, 0.02% (w/v) sodium azide, 4% (v/v) 2-propanol, 25% (w/v) PEG 3350, 0.1 M HEPES, pH 7.5.

### 6.3.2.2 Crystallisation of wild type rHvExoI by macroseeding with native HvExoI

Hrmova *et al.* (1998) could crystallise native HvExoI by hanging drop vapour diffusion over a reservoir of 1.7 M ammonium sulfate after approximately 100 days, but the rHvExoI crystals could not be observed under these conditions. Seeds from these crystals could subsequently be used to seed crystals of HvExoI in order to obtain them in a shorter time. Similarly, rHvExoI crystals could be grown from the small tetragonal native HvExoI seeds, with the crystals appearing to be bigger after 5 days. This indicated that the structures and interacting surfaces of rHvExoI and native HvExoI were similar enough to pack into the same crystal matrix. Moreover, native HvExoI seeds could also be used for rHvExoI E220A, W434A and R158A/E161A mutant crystallisation.

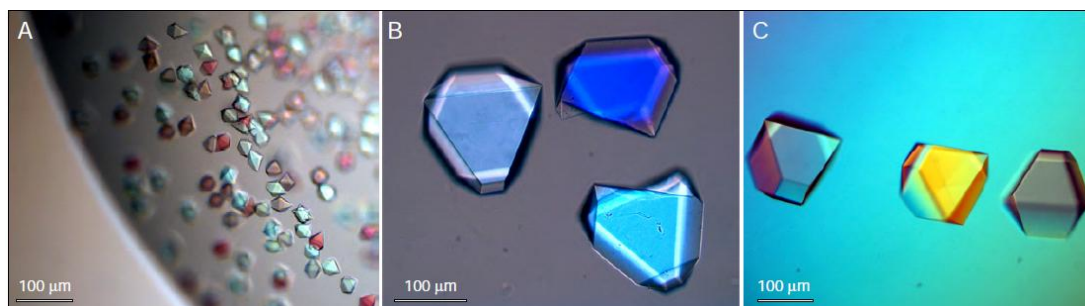


**Figure 6.3** Microcrystals (10 x 5 x 7.5 μm to 20 x 10 x 15 μm) of native HvExoI (A) were used for growing wild type rHvExoI (B), and (C) rHvExoI E220A mutant crystals. The crystals grew in 75 mM HEPES, pH 7.0, containing 0.8 M ammonium sulfate, 7.5 mM sodium acetate and 1.2% (w/v) polyethylene glycol 400, within 5-14 days.

## 6.4 Discussion

Native barley  $\beta$ -D-glucan exohydrolase I (HvExoI) is a glycoprotein with N-glycosylation at Asn221, Asn498 and Asn600 (Varghese *et al.*, 1999). The N-glycosylation increased the molecular mass of native HvExoI to 68.6 kDa (Varghese *et al.*, 1999). The rHvExoI was expressed from *P. pastoris* and the molecular mass of the N-deglycosylated form of rHvExoI determined by MALDI-ToF MS was 67.2 kDa, which is higher than that deduced from the cDNA sequence of 66.8 kDa (Luang *et al.*, 2010). The masses determined by MS of tryptic peptides indicated that the protein appeared to retain one N-acetyl glycosamine (GlcNAc) residue at each of the asparagines glycosylated in the native enzyme (Asn221, Asn498, and Asn600). An oligosaccharide could be observed at Asn498 in native HvExoI, and consisted of two  $\beta$ -(1,4)-linked GlcNAc residues followed by two mannosyl residues, and has  $\alpha$ -(1,3)-linked fucosyl residue linked with the GlcNAc residue that is attached to Asn498 and an (1,2)-linked xylosyl residue attached with the first branching mannosyl residue, respectively (Varghese *et al.*, 1999). Branching mannosyl residues linked on rHvExoI were removed by endoglycosidase H and single GlcNAc residues were retained branching rather than the longer chain of sugar residues seen in native HvExoI. The differences between native HvExoI and rHvExoI, including the extra eleven amino acids at the N-terminus of rHvExoI and the different kinds of sugar at N-glycosylation sites did not prevent production of the rHvExoI crystals using native HvExoI seeds as heterogeneous nucleants. Crystals of wild type rHvExoI and mutants of E220A, W434A and R158A/E161A could crystallise in the condition of native HvExoI by macroseeding.

In addition to those generated with seeding, wild type rHvExoI crystals that appeared to have the same tetragonal shape as those of the native HvExoI and rHvExoI

generated from native HvExoI seeds were observed in the conditions of the PS gradient-mid range screen that contained 1.8 or 2.2 M ammonium sulfate in malate-MES-Tris, pH 5.0. These conditions are significantly different from the 0.8 M ammonium sulfate, 1.2% (w/v) polyethylene glycol 400, 7.5 mM sodium acetate, 75 mM HEPES, pH 7.0, precipitant used to generate the similar native HvExoI crystals in about 95 days.

The crystallisation of rHvExoI mutants may clearly show the interactions between amino acid residues and substrate or inhibitor in the active site that result in dramatic changes in activity upon the mutation of the E220 and W434 residues, which suggest they are important for catalytic mechanism and substrate specificity.

## 6.5 Conclusions

The tetragonal crystals of N-deglycosylated rHvExoI could be observed in 1.8 M and 2.2 M ammonium sulfate in 10 mM malate-MES-Tris, pH 5.0, at 95 days. Moreover, native HvExoI seeds could be used as heterogeneous nucleants to facilitate the crystallisation of wild type and mutant forms of rHvExoI within 5-14 days. So, the structure of rHvExoI may also be nearly identical to that of native HvExoI.

## 6.6 References

- Harvey, A.J., Hrmova, M., Gori, R.D., Varghese, J.N., and Fincher, G.B. (2000). Comparative modeling of the three-dimensional structures of family 3 glycoside hydrolases. **Protein Struct. Funct. Genet.** 41: 257-269.
- Hrmova, M., Varghese, J.N., Høj, P.B., and Fincher, G.B. (1998). Crystallization and preliminary X-ray analysis of  $\beta$ -D-glucan exohydrolase isoenzyme ExoI from barley (*Hordeum vulgare*). **Acta Crystallogr.** D54: 687-698.

- Hrmova, M., and Fincher, G.B. (2001). Structure-function relationships of  $\beta$ -D-glucan endo- and exohydrolases from higher plants. **Plant Mol. Biol.** 47: 73-91.
- Hrmova, M., Gori, R.D., Smith, B.J., Fairweather, J.K., Driguez, H., Varghese, J.N., and Fincher, G.B. (2002). Structural basis for broad substrate specificity in higher plant  $\beta$ -D-glucan glucohydrolases. **Plant Cell** 14: 1033-1052.
- Hrmova, M., Gori, R.D., Smith, B.J., Vasela, A., Varghese, J.N., and Fincher, G.B. (2004). Three-dimensional structure of the barley  $\beta$ -D-glucan glucohydrolase in complex with a transition state mimic. **J. Biol. Chem.** 279: 4970-4980.
- Hrmova, M., Streltsov, V.A., Smith, B.J., Vasella, A., Varghese, J.N., and Fincher G.B. (2005). Structural rationale for low-nanomolar binding of transition state mimics to a family GH3  $\beta$ -D-glucan glucohydrolase from barley. **Biochemistry** 44: 16529-16539.
- Hrmova, M., and Fincher, G.B. (2007). Dissecting the catalytic mechanism of a plant  $\beta$ -D-glucan glucohydrolase through structural biology using inhibitors and substrate analogues. **Carbohydr. Res.** 342: 1613-1623.
- Luang, S., Hrmova, M., and Ketudat Cairns, J.R. (2010). High-level expression of barley  $\beta$ -D-glucan exohydrolase HvExoI from a codon-optimized cDNA in *Pichia pastoris*. **Protein Expr. Purif.** 73: 90-98.
- Newman, J., Pham, T.M., and Peat, T.S. (2008). Phoenito experiments: combining the strengths of commercial crystallization automation. **Acta Cryst.** F64: 991-996.
- Varghese, J.N., Hrmova, M., and Fincher, G.B. (1999). Three-dimensional structure of a barley  $\beta$ -D-glucan exohydrolase, a family 3 glycosyl hydrolase. **Structure** 7: 179-190.

## CHAPTER VII

## CONCLUSION

### 7.1 Rice $\beta$ -glucosidases

Recombinant Os7BGlu26 and Os9BGlu31 were expressed as N-terminal thioredoxin and 6xHistidine tag fusion proteins in *E. coli* strain Origami(DE3). Os7BGlu26 and Os9BGlu31 were both maximally active at pH 4.5 and 40°C. Os7BGlu26 is a  $\beta$ -mannosidase/ $\beta$ -glucosidase that hydrolysed 4NPMAN more efficiently than 4NPGlc and could hydrolyse  $\beta$ -(1,4)-manno-oligosaccharides, similar to rHvBII. Os7BGlu26 hydrolysed  $\beta$ -(1,4)-gluco-oligosaccharides with low cellobiase activity, and increasing hydrolysis efficiency as the DP increased from cellotriose to cellohexose. Os7BGlu26 also hydrolysed the  $\beta$ -(1,3)-linked gluco-oligosaccharides laminaribiose and laminaritriose and the natural plant glycosides *p*-coumaryl alcohol glucoside, sambunigrin, D-amydalin, prunasin, dhurrin and quercetin-3-glucoside. The natural substrates that could be hydrolysed by Os7BGlu26 suggest that its function might be related to cell wall degradation, lignification, and/or defense.

On the other hand, Os9BGlu31, which has the sequence IHENG around the catalytic nucleophile like hydroxyisourate hydrolase (HIUHase) and shares 44% sequence identity with HIUHase, could not hydrolyse oligosaccharides or most glucoside substrates. Os9BGlu31 does not have HIUHase activity, but could hydrolyse 4NPGlc, although the catalytic efficiency was very low ( $k_{\text{cat}}/K_{\text{M}}$  of  $0.02 \pm 0.001 \text{ mM}^{-1}\cdot\text{s}^{-1}$ ). It also hydrolysed 4NP- $\beta$ -D-galactoside, 4NP- $\beta$ -D-fucoside and 4NP- $\beta$ -D-xyloside with 20% relative activity compared to 4NPGlc. Os9BGlu31 hydrolysed the natural cyanogenic glycoside dhurrin

10-fold faster than 4NPGlc and could also hydrolyse phlorizin. However, Os9BGlu31 could not hydrolyse  $\beta$ -(1,2)-,  $\beta$ -(1,3)-,  $\beta$ -(1,4)-, and  $\beta$ -(1,6)-gluco-oligosaccharides, which are the substrates of other rice GH1  $\beta$ -glucosidases (e.g. Os3BGlu7 and Os7BGlu26). HgCl<sub>2</sub> is a strong inhibitor for Os9BGlu31 and the enzyme activity was also slightly inhibited with FeCl<sub>3</sub> and CuSO<sub>4</sub>. The classic  $\beta$ -glucosidase inhibitors glucono  $\delta$ -lactone (GL) and 2,4-dinitrophenyl- $\beta$ -D-2-fluoroglucoside did not inhibit Os9BGlu31 at concentrations that typically lead to near complete inhibition of other GH1  $\beta$ -glucosidases. The function of Os9BGlu31 predicted by a combination its substrate specificity and gene expression (Opassiri *et al.*, 2006) might be to act in the defense response of the plant under stress conditions and infection.

## 7.2 Barley $\beta$ -D-glucan exohydrolase I

The expression of active barley  $\beta$ -D-glucan exohydrolase I (HvExoI) was successful from the optimized HvExoI gene in *Pichia pastoris* (strain SMD1168H). The recombinant HvExoI protein has an eight-histidine tag at the N-terminus (AHHHHHHHHAA) and N-glycosylation was observed at Asn221, Asn498 and Asn600, which resulted in heterogeneous protein size. When nearly all the N-linked carbohydrate was removed by endoglycosidase H, the molecular mass of 67.2 kDa was obtained for N-deglycosylated rHvExoI. rHvExoI preferred to hydrolyse  $\beta$ -(1,3)-linked gluco-oligosaccharides and also hydrolysed  $\beta$ -(1,2),  $\beta$ -(1,4),  $\beta$ -(1,6)-gluco-oligosaccharides, similar to native HvExoI. It hydrolysed the  $\beta$ -D-glucans laminarin and barley (1,3;1,4)- $\beta$ -D-glucan faster than  $\beta$ -linked gluco-oligosaccharides. The activity of rHvExoI was inhibited by methyl-O-thio-gentiobiose (G6sG-OMe), glucono  $\delta$ -lactone (GL) and 2,4-dinitrophenyl 2-fluoro-2-deoxy- $\beta$ -D-glucopyranoside (2F-DNPGlc) in a competitive manner.

The critical amino acid residues at the active site of rHvExoI were investigated by site-directed mutagenesis. No activity could be detected from rHvExoI with the mutations

D95A/N, R158A, E161A/Q, K206V, E220A, D285A/N, W286A, E491A and R158A/E161A. Only two mutants, E220A, which is close to the catalytic acid/base, E491, and W434A, which is in the +1 subsite, were active. The pH optimum of the E220A mutant was 4.5. This E220A mutant hydrolysed  $\beta$ -(1,2)-,  $\beta$ -(1,3)-,  $\beta$ -(1,4)- and  $\beta$ -(1,6)-gluco-oligosaccharides at slower rates than wild type. E220A had a little activity for laminarin, but could not hydrolyse barley (1,3; 1,4)- $\beta$ -D-glucan. The rHvExoI E220A also had a 10-fold higher  $K_i$  value for GL than wildtype, indicating poorer binding of this inhibitor. The mutation of E220 had a significant effect on the catalytic efficiency which, along with its effect on the pH profile might indicate this residue helps maintain the protonation of the catalytic acid/base via its interactions through water molecules. On the other hand, the W434A mutation had more effect on  $\beta$ -linked gluco-oligosaccharide hydrolysis, in that this mutant could hydrolyse only  $\beta$ -(1,3)-gluco-oligosaccharides, for which it had lower catalytic efficiency than wild type. The W434A mutant lost activity to hydrolyse the  $\beta$ -(1,6)-disaccharide gentiobiose and it could not be inhibited with the G6sG-OMe inhibitor, indicating a loss of binding to  $\beta$ -(1,6)-linked disaccharide. So, W434 had a significant effect on the substrate specificity of rHvExoI.

The different kind of carbohydrate at the N-glycosylation sites and the presence of eleven extra amino acid residues at the N-terminus of rHvExoI did not affect its crystallisation. The tetragonal crystals of wild type rHvExoI were observed in two concentrations of ammonium sulfate (1.8 M and 2.2 M) in 10 mM malate-MES-Tris, pH 5.0, at 281 K after 95 days in the sitting-drop vapour-diffusion method. rHvExoI crystals were also produced by macroseeding with tetragonal native HvExoI seeds as heterogeneous nucleants and bigger crystals were obtained within 5-14 days at 281 K. Macroseeding with native HvExoI seeds was further used for crystallisation of the rHvExoI E220A, W434A, and R158A/E161A mutants.

This study showed that amino acid sequence similarity and gene expression analysis (Opassiri *et al.*, 2006) are of some advantage to predict the substrate specificity and biological function of uncharacterised  $\beta$ -glucosidases, but similar enzymes have also diverged to have diverse specificities. Os7BGlu26 activity was similar to the closely related rHvBII and other isoenzymes the  $\beta$ -mannosidase/ $\beta$ -glucosidase cluster in the plant GH1 phylogenetic tree. However, unlike other rice GH1 enzymes studied to date, Os9BGlu31 lacked activity for any  $\beta$ -linked gluco-oligosaccharides and had very low activity to 4NPGlc. It is related to HIUHase, which is not  $\beta$ -glucosidase and cannot hydrolyse 4NPGlc, but Os9BGlu31 displays no HIUHase activity. On the other hand, the GH3 barley  $\beta$ -D-glucan exohydrolase I showed broad specificity similar to the GH1  $\beta$ -glucosidases in the Os7BGlu26 cluster, except that it lacks  $\beta$ -mannosidase activity and can hydrolyse polysaccharides. Therefore the active-site shape and action of amino acids in the active site of rHvExoI assigns the activity, which may converge in enzymes with different primary and tertiary structures.

# **CURRICULUM VITAE**

**NAME** Miss Sukanya Luang  
**DATE OF BIRTH** 5 September, 1981  
**PLACE OF BIRTH** Ubon Ratchathani

## **INSTITUTIONS ATTENDED**

Suranaree University of Technology  
Nakhon Ratchasima, Thailand, 2004-2010  
Doctor of Philosophy (Biochemistry)  
Khon Kaen University  
Khon Kaen, Thailand, 2000-2004  
Bachelor of Science (Biochemistry)

## **AWARDS AND SCHOLARSHIPS**

First Class Honors, Khon Kaen University, 2004  
SUT Outstanding Academic Performance  
Scholarship, 2004-2005  
The Royal Gold Jubilee Ph.D. Scholarship, from  
Thailand Research Fund, Thailand, 2005-2010